平成29年度博士論文
博士（資源学）

Geology and REE Geochemistry of Granitoids and Their Weathered Crusts at The Western Part of North Sumatra, Indonesia.

(インドネシア，北スマトラ西部における花崗岩類とその風化殻の地質と希土類元素地球化学)

2017

イワン セティアワン
Iwan Setiawan
博士工9513251

秋田大学大学院
工学資源学研究科博士後期課程
資源学専攻

GEOLOGY AND REE GEOCHEMISTRY OF GRANITOIDS AND THEIR WEATHERED CRUSTS AT THE WESTERN PART OF NORTH SUMATRA, INDONESIA

by

IWAN SETIAWAN

A thesis submitted to

Department of Geosciences, Geotechnology and Materials Engineering for Resources

Graduate School of Engineering and Resource Science,

Akita University, Japan

As partial fulfillment of the requirement for the degree of

DOCTOR OF ENGINEERING

2017

ABSTRACT

A geological, geochemical and isotopic study on granitoids and their weathered crusts was conducted at Sibolga, Panyabungan, Muarasipongi, and Kotanopan in the western part of North Sumatra, Indonesia. The objectives of this study are to understand the geological occurrences of granitoids, geochemical characteristics of rare earth elements (REE) in granitoids and their behavior in weathered crusts of granitoids. The study was conducted on the basis of microscopic observations, X-ray diffractometry (XRD), scanning electron microscopy (SEM-EDS), X-ray fluorescence spectrometry (XRF), inductively coupled plasma – mass spectrometry (ICP-MS), thermal ionization mass spectrometry (TIMS), and sequential leaching of REE.

Granitoids in Sibolga are, calk-alkaline, ilmenite-series, mainly peraluminous, I-/A-type and are classified into quartz alkali feldspar syenite, quartz syenite, alkali feldspar syenite, alkali feldspar granite, syenogranite, and monzogranite. Cordierite and corundum occur as xenocrysts and inclusions in K-feldspar in syenogranite, quartz alkali feldspar syenite and quartz syenite from Sarudik, Sihobuk and Adian Koting. P_2O_5 contents of the granitoids tend to decrease as ΣREE contents increase. LREE and HREE are enriched in alkali feldspar syenites from Sibolga Julu and Tarutung.

Ganitoids in Panyabungan are calk-alkaline to alkali calcic, ilmenite- and magnetite-series, metaluminous to peraluminous, S- and I-type, and are classified into monzonite, monzodiorite, diorite, syenite, syenogranite, quartz syenite, alkali feldspar granite, quartz alkali feldspar syenite and alkali feldspar syenite. Coexistence of metaluminous, I-type and magnetite-series quartz alkali feldspar syenites and peraluminous, S-type and ilmenite-series granites at Tano Tombangan suggests that those granitoids were derived from different sources. SiO_2 and ΣREE, P_2O_5, and Rb/Sr are positively correlated. P_2O_5 contents of the

granitoids tend to increase as ΣREE contents increase. LREE are enriched in alkali feldspar syenite from Pintu Padang Julu and quartz alkali feldspar syenite from Tanjung Jae. ΣREE contents are high in the S-type and ilmenite-series granitoids than the magnetite-series granitoids, which contain allanite and apatite.

Granitoids in Kotanopan are calk-alkaline, magnetite- and ilmenite-series, peraluminous, and I-type, and are classified into quartz monzonite, monzogranite, syenogranites, tonalites, and granodiorite. Monzogranite, and quartz monzonite from Kotanopan are metaluminous to slightly peraluminous, calcic to alkali-calcic, while a granodiorite from Tanjung Alai is metaluminous and calcic.

The initial Sr isotopic ratio (Sr_i) of syenogranite from Sarudik is high (0.724128), suggesting that the syenogranite magma has resulted from partial melting of granitic crusts and was probably contaminated with metasedimentary rocks in the upper crust. The Sr_i of Sibolga granitoids ranges from 0.710700 to 0.724100, that from Panyabungan ranges from 0.709382 to 0.712104. The Sr_i of granitoids from Sibolga and Panyabungan are lower than those of granitoids from Klabat Suites and Bebulu from Bangka Island. The $^{87}Sr/^{86}Sr$ of quartz alkali feldspar syenite from Pintu Padang Julu (0.710812), and Tukka (0.710700) suggest that most probably they belong to the Main Range granitoids. Metaluminous and I-type granitoids of Sibolga were produced by Paleo-Tethys subduction beneath amalgamated Western Sumatra Block, East Malaya and Indochina in Early Permian, followed possibly by the tectonic translation which resulted in peraluminous, ilmenite-series and A-type granitoids in Sibuluhan Sihaporas, Sibolga Julu, Sarudik and Tarutung. Peraluminous, ilmenite-series and S-type granitoids at Panyabungan, and I-type granitoids from Muara Sipongi and Kotanopan were formed due to the Early Triassic to Early Jurrasic subduction of Meso-Tethys beneath the amalgamated Western Sumatra Block and Sibumasu.

Highly differentiated ilmenite-series I-/A-type granitoids are the parent rocks of the weathered crusts in Sibolga. Allanite and titanite were present in the parent granitoids at Sibuluhan Sihaporas, but they were decomposed in the weathered crusts. Ce was predominantly accumulated in the upper part of weatherd crust due to oxidation of Ce^{3+} to Ce^{4+}, while most of the REE^{3+} moved to the lower part by acidic soil water and they were adsorbed mainly onto halloysite group minerals and gibbsite. The P_2O_5 contents of the weathered crusts of granitoids at the outcrop Sibuluhan Sihaporas A and the outcrop Sibuluhan Sihaporas B tend to be higher than those of the parent rocks, suggesting the occurrence of secondary phosphate minerals in the weathered crusts. ΣREE contents of the weathered crusts in Sibolga are lower than those of their parent rocks indicating that REE were leached out during weathering.

The values of elemental change $(\tau_j)_{(Si,\ Ca,\ Na,\ K)}$ of weathered crusts of Sibuluhan Sihaporas B, Sarudik and Sibolga Julu are -1 suggest losses or removal of these elements. On the other hand, $(\tau_j)_{(Al,\ Fe,\ Mn,\ Ca,\ Na,\ K,\ P)}$ in the Sibuluhan Sihaporas A are +1 suggest addition of these elements. The $\tau_{j(REE)}$ for all weathered crusts of granitoids are -1 suggest losses or removal of these elements. These signatures might be related differential fractionation degree of the REE-bearing minerals (e.g. allanite and titanite) during weathering.

TABLE OF CONTENTS

Page

ABSTRACT i

TABLE OF CONTENTS..... iv

LIST OF FIGURES..... ix

LIST OF TABLES..... xix

LIST OF APPENDICES..... xxi

CHAPTER 1. INTRODUCTION

1.1 Definition of REE..... 1

1.2 Occurrences of REE..... 1

1.2.1 Igneous Rocks..... 2

1.2.2 Hydrothermal Deposits..... 2

1.2.3 Sedimentary Deposits..... 3

1.2.4 Residual Rare Earth Deposits..... 4

1.2.5 Other Rare Earth Deposit Types..... 5

1.3 Main REE ore minerals..... 6

1.4 Use of REE..... 7

1.5 Classifications of Granitoids..... 8

1.5.1 Modal composition/IUGS classification..... 9

1.5.2 S-I-A-M Classification..... 9

1.5.3 Alumina saturation..... 11

1.5.4 Magnetite-ilmenite series..... 11

1.5.5 Tectonic discriminant schemes..... 12

1.5.6 Three-tier chemical scheme..... 12

CHAPTER 2. GEOLOGICAL SETTING

2.1 Regional Geology..... 16

2.2 Southeast Asian Tin Belt..... 20

2.3 Geology of Sumatra Island..... 23

2.4 Local Geology..... 29

.

CHAPTER 3. METHODOLOGY 32

3.1 Geological survey (Fieldwork) 32

3.2 Microscopic Observations 34

3.3 X-ray Diffractometry (XRD) 35

3.3.1 Glycol treatment 37

3.3.2 Hydrochloric acid treatment..... 37

3.3.3 Qualitative analysis 38

3.4 X-ray Fluorescence Spectroscopy (XRF) 39

3.5 Induced Coupled Plasma Mass Spectrometry (ICP-MS) 41

3.6 Scanning Electron Microscope-Energy Dispersive Spectroscopy (SEM-EDS) 41

3.7 Sequential Extraction..... 43

3.8 Thermal Ionization Mass Spectrometry (TIMS) .....

3.8.1 Sr-Nd extraction using double coloumn..... 46

3.8.2 Sr-Nd isotope measurement..... 46

CHAPTER 4. GEOLOGY AND OCCURRENCES OF GRANITIC ROCKS IN THE STUDY AREA 49

4.1 Sibolga and its surrounding areas 49

4.1.1 Occurrence of granitic rocks..... 49

4.1.2.Magnetic susceptibility..... 52

4.1.3 Radioactivity..... 55

4.2 Panyabungan and its surrounding areas 56

4.2.1 Occurrence of granitic rocks..... 56

4.2.2 Magnetic susceptibility..... 57

4.2.3 Radioactivity..... 60

4.3 Muara Sipongi and its surrounding areas 61

4.3.1 Occurrence of granitic rocks..... 61

4.3.2 Magnetic susceptibility..... 64

4.3.3 Radioactivity..... 65

4.4 Kotanopan and its surrounding areas 65

4.4.1 Occurrence of granitic rocks..... 65

4.4.2 Magnetic susceptibility..... 66

4.4.3Radioactivity..... 67

CHAPTER 5. PETROGRAPHY 68

5.1 Petrography of granitoids from Sibolga 68

5.2 Petrography of granitoids from Panyabungan..... 73

5.3 Petrography of granitoids from Muara Sipongi..... 73

5.4 Petrography of granitoids from Kotanopan..... 76

CHAPTER 6.WHOLE-ROCK MAJOR ELEMENTS AND RARE EARTH ELEMENTS GEOCHEMISTRY 82

6.1 Sibolga 82

6.1.1Major elements compositions..... 82

6.1.2 Rare earth elements compositions..... 83

6.2 Panyabungan..... 91

6.2.1 Major elements 91

6.2.2 Rare earth elements 94

6.3 Muara Sipongi..... 97

6.3.1 Major elements 95

6.3.2 Rare earth elements 100

6.4 Kotanopan..... 101

6.4.1 Major elements 101

6.4.2 Rare Earth elements 101

6.5 Type of granitoids..... 104

6.6 Origin of granitoids 109

CHAPTER 7. MINERAL CHEMISTRY AND Sr-Nd ISOTOPES OF GRANITOIDS OF THE STUDY AREAS 111

7.1 Mineral chemistry of granitoids from Sibolga, Panyabungan and Kotanopan... 111

7.2 Sr-Nd isotopic signatures of granitoids in the western part of Sibolga and Panyabungan..... 116

CHAPTER 8. REE GEOCHEMISTRY OF WEATHERED GRANITOIDS IN SIBOLGA AND ITS SURROUNDING AREAS 125

8.1 REE geochemistry of weathered crusts of granitoids at Sibuluhan Sihaporas A 126

8.2 REE geochemistry of weathered crusts of granitoids at Sibuluhan Sihaporas B 130

8.3 REE geochemistry of weathered crusts of granitoids at Sarudik 134

8.4 REE geochemistry of weathered crusts of granitoids at Sibolga Julu..... 137

8.5 Mass Balance..... 144

CHAPTER 9. DISCUSSION 150

9.1 Petrochemistry of granitoids in Sibolga and its surrounding areas, North Sumatra, Indonesia..... 150

9.2 Geochemistry and Sr-Nd isotopic signatures of granitoids in the western part of North Sumatra, Indonesia 158

9.3 Tectonic Evolution and Petrogenetic Model..... 167

9.3.1 Tectonic evolution..... 167

9.3.2 Petrogenetic model..... 170

9.4 REE geochemistry of weathered crusts of granitoids at Sibolga and its surrounding areas..... 173

CHAPTER 10. CONCLUSIONS 176

10.1 Petrochemistry of granitoids in Sibolga and its surrounding areas, North Sumatra, Indonesia..... 177

10.2 Tectonic evolution and petrogenetic model..... 179

10.3 REE geochemistry of weathered crusts of granitoids at Sibolga and its surrounding areas..... 180

REFFERENCES..... 181

ACKNOWLEDGMENTS..... 193

APPENDICES 194

LIST OF FIGURES

Page

Fig. 2.1 Pre-Cenozoic tectonic blocks in Sumatra and Peninsular Malaysia, modified from Hutchison (1994) and Barber and Crow (2003). Sibolga is shown as part of the West Sumatra Block..... 17

Fig. 2.2 Cartoon ilustrating the plate tectonic evolution of Sumatra (Barber & Crow, 2003). 18

Fig. 2.3 Pre-Cenozoic development of arc volcanisme in northern and central Sumatra (modified after Suparka and Asikin, 1981). 19

Fig. 2.4 Map showing granitic provinces of Southeast Asian Tin Belt and the location of the study area (modified after Cobbing et al., 1992; Cobbing 2005). 21

Fig. 2.5 Distribution of granitic rocks and their ages in Sumatra, Malay Peninsula and Tin Islands (modified after Cobbing, 2005) 26

Fig. 3.1 a. hammer, b. magnetic susceptibility meter, c. gamma spectrometer, d. laser range finder, e. Brunton compass, f., g. global positioning system (GPS), and g. loupe. 33

Fig. 3.2 Nikon Eclipse LV 100N POL microscope at Akita University..... 35

Fig. 3.3 Rigaku Multi Flex X-ray Diffractometer at Akita University..... 36

Fig. 3.4 TK-4100 Beads and fuse-sampler for glass beads maker at Akita University..... 40

Fig. 3.5 Rigaku ZSX primus II in Akita University..... 40

Fig. 3.6 a). JEOL 560, b). a JEOL JSM-6610 Scanning Electron Microscope and c). Carbon coater at Akita University..... 42

Fig. 3.7 Procedures of sample preparations for sequential leaching..... 44

Fig. 3.8	Agilent Technologies 7500 Series ICP-MS at Akita University.....	45
Fig. 4.1	Locations and geological map of Sibolga and its surrounding areas (modified after Aspden et al., 1984).	50
Fig. 4.2	Sample location and geological map of Sibolga and its surrounding areas (modified after Rock et al., 1983; Aspden et al., 1982).....	52
Fig. 4.3	Granitoids outcrops at a-b. Sarudik (SR1), c. Sibuluhan Sihaporas (S4), d. Tukka (S8), e. Sihobuk (S24), f. Parombunan-Sibolga Julu (S23), g-h. Adian Koting (SB3 and S21).	53
Fig. 4.4	Weathered rocks at Sibolga and the surrounding areas: a. Sibuluhan Sihaporas A (S1), b. Sibuluhan Sihaporas B (S6), c. Sarudik (S17) and d. Sibolga Julu (S18)	54
Fig. 4.5	Histogram of magnetic susceptibility of granitoids from Sibolga, Panyabungan and Muara Sipongi. (Dashed lines indicate a border line between magnetite- and ilmenite-series)	55
Fig. 4.6	Histogram of radioativity of granitoids from Sibolga and the surrounding areas.	56
Fig. 4.7	Outcrops of granitoids from Tanjung Jae contain a. K-feldspar megacrysts and b. round shape metasedimentary enclaves.....	57
Fig. 4.8	Outcrops of granitoids at Panyabungan and its surrounding areas: a. Parmompang, b. Tebing Pintu Air, c-d. Pintu Padang Julu, e and f. Tano Tombangan.	58
Fig. 4.9	Sample locations of Panyabungan and its surrounding areas (modified after Rock et al., 2012).	59
Fig. 4.10	Histogram of magnetic susceptibility of granitoids from Panyabungan and its surrounding areas.	60

Fig.4.11 Histogram of radioactivity of granitoids from Panyabungan and its surrounding areas. 61

Fig. 4.12 Outcrops of granitoids at Muara Sipongi and its surrounding areas: a-d. Pekantan, e. Muara Sipongi, f-h. Tanjung Alai. 62

Fig. 4.13 Geological and sample locality map of Muara Sipongi and Kotanopan (modified after Rock et al., 2012). 63

Fig. 4.14 Histogram of magnetic susceptibility of granitoids in Muara Sipongi and Tanjung Alai 64

Fig. 4.15 Histogram of radioactivity of granitoids from Muara Sipongi and its surrounding areas. 65

Fig. 4.16 Histogram of radioactivity of granitoids from Muara Sipongi and its surrounding areas 64

Fig 4.17 Outcrops of granitoids from Kotanopan showing gray color and contain mafic nclaves. 66

Fig. 4.18 Magnetic susceptibility of fresh granitoids from Kotanopan 67

Fig. 4.19 Histogram of radioactivity of Kotanopan and its surrounding areas. 67

Fig. 5.1 Photomicrographs under crossed nicols: 70

a. Cordierite (crd) as a xenocryst, with K-feldspar (Kfs), in syenogranite from Sarudik,

b. K feldspar (Kfs) megacrysts showing microperthite texture, in syenogranite from Sarudik. .....

c. Allanite (aln) occurence with K feldspar (Kfs) and biotite (bt), in alkali feldspargranite from Sarudik.....

d. Titanite (ttn) with K-feldspar (Kfs) and quartz (qtz), in alkali feldspar granite from Sarudik.....

e. K feldspar (Kfs) megacryst with plagioclase (plg), in quartz alkali feldspar syenite from Sarudik.....

f. K feldspar (Kfs) in association with biotite (bt) and hornblende (hbl), in syenogranite from Sibuluhan Sihaporas.....

Fig 5.2 Photomicrographs under crossed nicols: 71

a. Megacryst of K-feldspar (Kfs) with biotite (bt) and contain apatite (apt) as inclusions, in syenogranite from Adian Koting,

b. Hornblende (hbl) with biotite (bt) and quartz (qtz), in quartz syenite from Adian Koting,

c. Zircon occurs as inclusion in biotite, and apatite as inclusion in quartz, in quartz syenite from Adian Koting,

d. Cordierite (crd) as xenocryst with K-feldspar, in quartz syenite from Adian Koting,

e. Hornblende (hbl) with biotite (bt) and quartz (qtz), in quartz syenite from Adian Koting,

f. Corundum (crn) as xenocryst in K-feldspar (Kfs), in quartz syenite from Adian Koting

Fig 5.3 Photomicrographs of selected samples from Panyabungan and the surroundings: a. quartz alkali feldspar syenite from Tanjung, b. alkali feldspar granite deformed from Tebing Tinggi, c. Pintu Padang Julu, d. alkali feldspar syenite from Tanjung Jae, e-f.alkali feldspar granite and alkali feldspar syenite from Tano Tombangan..... 74

Fig. 5.4 Photomicrograph of Muara Sipongi granitoids : a-c. quartz syenite and quartz diorite from Muara Sipongi contain plagioclase (pg), quartz (qz), K-feldspar (Kfs), biotite (bt), muscovite (mus), opaque 77

(op), minor chlorite (chl) and epidote (ep) and d. granodorite from Pekantan contains plagioclase (pg), biotite (bt), and chl (chlorite).....

Fig. 5.5 Granitoids from Kotanopan (KNP): a-b. tonalite from Tolung, c-d. syenogranite from tolung, e monzogranite from Kotanopan and f. Tonalite. 79

Fig 5.6 Modal abundance of quartz (Q) alkali feldspar (A) and plagioclase (P) and feldsphatoids (F) of granitoids from Sibolga, Panyabungan, Muara Sipongi and Kotanopan (Le Bas & Streickeisen, 1991; Streickeisen, 1976). 81

Fig. 6.1 Harker diagrams of granitoids from Sibolga and its surrounding areas. 85

Fig. 6.2 Plots of SiO_2 versus (FeO_{tot}/[FeO_{tot}+MgO]), and and Aluminum Saturation Index versus molecular ratio (Al/[Na+K]) (after Frost et al., 2001). 86

Fig. 6.3 Rb-(Y+Nb) and Nb-Y discriminant diagrams of granitoids from Sibolga, Panyabungan, Kotanopan and Muara Sipongi (after Pearce et al., 1984) 87

Fig. 6.4 Chondrite – normalized REE patterns of granitoids from Sibolga and its surrounding areas (values of chondrite are from McDonough & Sun, 1995). 90

Fig. 6.5 Harker diagram of granitoids from Panyabungan and its surrounding areas. 93

Fig. 6.6 Chondrite normalized diagram of granitoids from Panyabungan and its surrounding areas (values of chondrite are from McDonough & Sun, 1995) 96

Fig. 6.7 Harker diagram of granitoids from Muara Sipongi and its surrounding 99

areas. .....

Fig. 6.8 Chondrite-normalized diagram of granitoids from Muara Sipongi and its surronding areas (values of chondrite are from McDonough & Sun, 1995) 100

Fig. 6.9 Harker diagram of granitoids from Kotanopan and Tolung..... 102

Fig. 6.10 Chondrite- normalized REE diagram of granitoids from Kotanopan and Tolung (values of chondrite are from McDonough & Sun, 1995).. 104

Fig. 6.11 Plots of SiO_2 versus (FeO_{tot}/[FeO_{tot}+MgO]) of granitoids from Sibolga, Panyabungan, Muara Sipongi and Kotanopan..... 105

Fig. 6.12 Plots of Aluminium Saturation Index (ASI) versus SiO_2 (wt%) of granitoids from Sibolga, Panyabungan, Muara Sipongi and Kotanopan..... 106

Fig. 6.13 Trace element-normalized patterns show distinct patterns of A- and I-type granitoids. A-type granite from Besar Island area from Ghani et al. (2014). 107

Fig. 6.14 Chondrite normalized trace element patterns show A-, S- and I-type characters of granitoids from Sibolga Panyabungan, and Main Range of Malay Peninsula (Ng et al., 2015) (values of chondrite are from McDonough & Sun, 1995). 109

Fig. 6.15 Y/Nb and (Y+Nb)/Rb discrimination diagram of granitoids from Sibolga and Panyabungan..... 110

Fig. 7.1 Photomicrographs (a and b) which were taken under an optic microscope under crossed nicols and elemental composition mapping by a sanning electron microscope, (c and d) of coarse-grained allanite (aln) crystal in alkali feldspar granite from Sarudik (SR2) are euhedral 112

shape, prismatic and zoning, indicate different proportion of REE contents. The allanite (aln) is associated with K-feldspar, quartz, and biotite. Backscaterred electron by a sanning electron microscopes of REE-bearing minerals of quartz alkali feldspar syenite from Sihobuk consisting of fluorapatite (fl.apt), (e), quartz alkali feldspar syenite and syenogranite from Sarudik (f-g), consisting of allanite (aln) and titanite (ttn). .....

Fig 7.2 Composition mapping of apatite from quartz syenite (SB2) at Tarutung near to Sibolga contains Ce, Nd and Yb. a). Crystal of apatite contains F, P, Ca, Ce, Yb, and Nd, b). A map summary spectrum of apatite shows major composition and contain Ce, Yb, and Nd, c) Ce distribution in the apatite. d). Nd distribution in the apatite. e). Yb distribution in the apatite 113

Fig.7.3 Mineral mapping of titanite and apatite in quartz syenite from Tanjung (PYB 4D). a) Titanite crystal showing its major composition, b) A map summary spectrum of titanite, c) A backscattered image of apatite, and d) spectrum of major composition of apatite..... 114

Fig. 7.4 Zircon in association with U and Th, monzodiorite from Parmompang (PYB 2). a) A backscattered image of zircon, and b). Spectrum of zircon that containing Th and U..... 115

Fig 7.5 Backscatttered electron images of a). Zircon (zr) and b). zircon contain apatite (apt), c-d. apatite and ilmenite (ilm) occurences as inclusion within biotite in granitoids from Kotanopan, and d). apatite and ilmenite as the mineral inclusions in feldspar 115

Fig. 7.6 Photographs of outcrops used for isotope study at Sibolga and Panyabungan and their surrounding areas: a. PYB 4D (Tanjung), b. P4 (Tanjung Jae), P7 (Pintu Padang Julu), d. P8 (Tano Tombangan), e. SB3 (Adian Koting), f. S21 (Adian Koting), g. S8 (Tukka), h. SR1 (Sarudik), and i. S24 (Sihobuk). 117

Fig.8.1 Profile of weathered crust of granitoids of Sibuluhan Sihaporas A..... 126

Fig.8.2 Chondrite normalized REE patterns of the weathered crust of granitoids at Sibuluhan Sihaporas A (SSA) (values of chondrite are from McDonough & Sun, 1995). 128

Fig.8.3 XRD of clay speciations from the weathered crust of granitoids at Sibuluhan Sihaporas A, from level of 310 cm (S3) and level 500 cm (S4). 129

Fig.8.4 Profile of weathered crusts of granitoids at Sibuluhan Sihaporas B 130

Fig.8.5 Chondrite normalized REE patterns of weathered cruts of granitoids at Sibuluhan Sihaporas B (SSB) (values of chondrite are from McDonough & Sun, 1995). 131

Fig.8.6 Backscaterred electron images of allanite (Aln) and xenotime (Xtm) that occur with biotite (Bt) in the weathered crust of granitoids at Sibuluhan Sihaporas B. 132

Fig.8.7 XRD of clay speciations from the weathered crust of granitoids at Sibuluhan Sihaporas B, from the level of 50 cm (S5) and level 450 cm and (S8). 133

Fig.8.8 Profile of weathered crusts of granitoids at Sarudik..... 134

Fig.8.9 Chondrite normalized REE patterms of weathered crust of granitoids at Sarudik (values of chondrite are from McDonough & Sun, 1995)... 135

Fig.8.10	Backscattered electron images of monazite (Mnz) occurs with biotite, and zircon (Zr) in the weathered crust of granitoids from horizon C at Sarudik (SRD).	136
Fig.8.11	XRD of clay speciations from the weathered crust of granitoids at horizon A, level of 50 cm (S9) and horizon B, level of 200cm (S10) from Sarudik.	136
Fig.8.12	Chondrite-normalized REE patterns of weathered crusts of granitoids from Sibolga Julu (SJ) (values of chondrite are from McDonough & Sun, 1995).	138
Fig.8.13	XRD of clay speciations from the weathered crust of granitoids at Sibolga Julu at horizon A, level of 40 cm (S13), and horizon B, from level 200 cm (S14) to 360 cm (S15).	139
Fig.8.14	Backscattered electron images of xenotime (Xtm) occurs in the weathered crust of granitoids from horizon B at Sibolga Julu.....	141
Fig.8.15	Histogram of sequential extraction results showing distribution of ∑REE contents extracted in each step.	141
Fig.8.16	Summary of average LREE, HREE, and Y extracted of Sibuluhan Sihaporas A, Sibuluhan Sihaporas B, Sarudik and Sibolga Julu.....	143
Fig. 9.1	Chondrite normalized REE patterns (normalizing values of chondrite are from McDonough & Sun, 1995).....	151
Fig. 9.2	Plots of a. SiO_2 versus ∑REE b. SiO_2 versus P_2O_5 and c. SiO_2 versus Rb/Sr.	153
Fig. 9.3	SiO_2 and ∑REE , SiO_2 and Rb/Sr, and P_2O_5 and ∑REE of granitoids from Panyabungan.	155
Fig. 9.4	SiO_2 and ∑REE , SiO_2 and Rb/Sr, and P_2O_5 and ∑REE of granitoids	156

at Muara Sipongi

Fig. 9.5 Plots of SiO_2 and ∑REE , b. P_2O_5 and ∑REE , and SiO_2 and Rb/Sr of granitoids at Kotanopan. 157

Fig. 9.6 Correlation diagram of Rb/Sr ratios with the present $^{87}Sr/^{86}Sr$ of Panyabungan and Sibolga granitoids do not have a linier correlation 163

Fig. 9.7 Relation of ∑REE and $^{87}Sr/^{86}Sr$ and P_2O_5 contents of granitoids from Sibolga (SR1, S8, S21, and S24B) and Panyabungan (PYB 4D, P4, and P7). 166

Fig. 9.8 $\varepsilon_i Nd$ initial values vs Sr_i isotopic ratios of granitoids from Sibolga and Panyabungan (modified after DePaolo & Wasserburg, 1979)..... 172

Fig. 9.9 Chemical index of alteration(CIA) of weathered granitoids from Sibuluhan Sihaporas A, Sibuluhan Sihaporas B, Sarudik and Sibolga Julu. 175

LIST OF TABLES

		Page
Table 1.1	Classification of rare earth elements ore deposits.....	3
Table 1.2	REE-bearing minerals of economic or potentially economic deposits	6
Table 1.3	REE uses and applications by industry.....	8
Table 1.4	Characteristics of I- type, S-type and A-type granitoids (Chappel & White, 1974; Winter 2001; Gill, 2010).....	13
Table 1.5	The SIAM Classification of Granitoids (Winter, 2001).....	15
Table 3.1	Procedure of Sr-Rb and Sm-Nd extraction for granitoids of Sibolga and Panyabungan.....	48
Table 5.1	Modal composition of granitoids in Sibolga and its surrounding areas.....	72
Table 5.2	Modal composition of granitoids from Panyabungan and its surrounding areas.....	75
Table 5.3	Modal composition of granitods from Muara Sipongi and its surrounding areas.....	78
Table 5.4	Modal composition of granitoids from Kotanopan and its surrounding areas	80
Table 6.1	Whole rock major elements contents of granitoids in Sibolga and its surrounding areas.....	88
Table 6.2	Rare earth elements concentration of granitoids in Sibolga and its surrounding areas.....	89
Table 6.3	Whole rock major elements contents of granitoids from Panyabungan and its surrounding areas.....	92
Table 6.4	Rare earth elements concentration of granitoids from Panyabungan and its surrounding areas.....	95
Table 6.5	Summary of whole rock major elements, magnetic susceptibilty and radioactivity of granitoids from Muara Sipongi and its surrounding areas.....	98
Table 6.6	Rare earth elements concentration of granitoids from Muara Sipongi and its surrounding areas.....	100
Table 6.7	Summary of whole rock major elements contents, magnetic susceptibility, and radioacivity of granitoids from Kotanopan and its surrounding areas.....	103
Table 6.8	Summary of rare earth elements concentration (unit in ppm), magnetic susceptibility, and radioactivity of granitoids from Kotanopan and its	

surrounding areas..... 103
Table 6.9 Summary of trace and major elements compositions of granitoids in Sibolga and its surrounding areas..... 108
Table 7.1 Summary of Rb, Sr, Sm and Nd contents of selected granitoids from Sibolga and Panyabungan. 117
Table 7.2 Summary of age dating result of Sibolga and Panyabungan area 121
Table 7.3 Result of measurement of Rb/Sr and Sm/Nd of granitoids from Sibolga..... 122
Table 7.4 Result of measurement of Sm/Nd of granitoids from Sibolga and Panyabungan 123
Table 8.1 ∑ REE extracted from the sequential extraction of the weathered crust of granitoids at Sibolga and its surrounding areas..... 142
Table 8.2 TVolumetric change of major elements of weathered crusts of granitoids in Sibolga and its surrounding areas 146
Table 8.3 Elemental changes of major elements of weathered crusts of granitoids in Sibolga and its surrounding areas 147
Table 8.4 Elemental change, τj of REE+Y of weathered crusts of granitoids in Sibolga and its surrounding areas 148
Table 9.1 Summary of initial ratio of SiO_2 contens, Rb/Sr ratio, Rb, Sr, Sm, and Nd contents, 87Sr/86 Sr ratios based on calculation 159
Table 9.2 Summary of age dating result of Sibolga and Panyabungan area 160
Table 9.3 Summary of Rb/Sr and Sm/Nd measurement (TIMS) result of granitoids from Sibolga..... 164
Table 9.4 Summary of ∑ REE and $^{87}Sr/^{86}Sr$ and P_2O_5 contents of granitoids from Sibolga and Panyabungan..... 165

LIST OF APPENDICES

Appendix 1 List of sample from Sibolga and its surrounding areas

Appendix 2 List of weathered rock samples and horizons at Sibolga and its surrounding areas

Appendix 3 Magnetic susceptibility of Sibolga and its surroundings

Appendix 4 Gamma radioactivity of Sibolga and its surroundings

Dedication Letter

I dedicate my efforts to my parents and teachers who guided me until this position. I also dedicate this dissertation to my wife Ani Maliani, Bunga, Putra, Airin and Ryuchi, who have provided much encouragement and support, not only during the last four years, but through out my life.

CHAPTER 1

INTRODUCTION

1.1. Definition of REE

Rare earth elements (REE) include seventeen elements, including fifteen from $_{57}$La to $_{71}$Lu, in addition to $_{21}$Sc and $_{39}$Y (Wilson, 1989, Castor & Hedrick, 2006). The lanthanoids comprise of elements with atomic numbers from 57 to 71 that include the following elements in order of atomic number : lanthanum (La), cerium (Ce), praseodymium (Pr), neodymium (Nd), promethium (Pm), samarium (Sm), europium (Eu), gadolinium (Gd), terbium (Tb), dysprosium (Dy), holmium (Ho), erbium (Er), thulium (Tm), ytterbium (Yb), and lutetium (Lu). In rock-forming minerals, rare earth elements typically occur in compounds as trivalent cations in carbonates, oxides, phosphates, and silicates. Rare earth elements are classified into light rare earth elements (LREE) and heavy rare earth elements (HREE). LREE consists of seven elements from La to Eu (Z = 57 through 63), and HREE consists of eight elements from Gd to Lu (Z = 64 through 71) (Castor & Hedrick, 2006).

1.2 Occurrences of REE

The REE occur in a wide range of rock types: igneous, sedimentary and metamorphic rocks. REE deposits in igneous rocks are commonly associated with alkaline and peralkaline rocks, and they can also be formed in carbonatites (Kamitani, 1991; Long et al., 2010; Castor & Hedrick, 2006). REE can also be enriched in the granitoids through the accumulation of REE-bearing minerals such as apatite, allanite, monazite, titanite and xenotime, since they tend to remain in the melt until the late stages of magmatic differentiation (Wilson, 1989; Castor & Hedrick,

2006). The world distribution of REE deposits corresponding to the classification is shown in Table 1.

1.2.1 Igneous rocks

Carbonatite/alkaline rocks constitute the majority of the world REE resources following the Bayan Obo hydrothermal replacement origin. More than 550 carbonatite/alkaline complexes are distributed in the world (Kamitani et al., 1990). The distribution is restricted to the interior and marginal regions of continents, especially Precambrian cratons and shields, or related to large-scale rift structures. Main concentrated areas of the complexes are the East African rift zones, northern Scandinavia-Kola peninsula, eastern Canada, and southern Brazil. The carbonatites are associated with ultramafic and or alkaline rocks, and in so many cases occur as isolated dikes, cylindrical intrusive bodies and volcanic cones. The ages of complexes vary from Archean to Recent time, and each group of the complexes is closely related to their regional structural events. In East Africa, many carbonatites and alkaline rocks are arranged along the East African rifts and structurally related. The other deposits of hydrothermal and supergene origin in carbonatites also represents a large REE resource and occurs at Araxa and Catalao, Brazil and Mount Weld, Australia.

1.2.2 Hydrothermal Deposits

Bayan Obo, China is the biggest REE deposit in the world. The deposit was formed by hydrothermal replacement of the carbonate rocks of sedimentary origin, but the hydrothermal fluids may be derived from an alkaline–carbonatite intrusive series (Drew et al., 1990; Cao et al., 1995; Bai et al., 1996; Kanazawa et al., 1999).

Table 1.1 Classification of rare earth elements ore deposits

Deposit-type	Mines
(1) Igneous	
a) Carbonatites	Mt. Pass (USA), Weshan, Maoniuping (China), Mount Weld (Australia), Araxa, Catalao (Brazil)
b) Alkaline rocks	Khibiny, Lovozero (Russia), Posos de Caldas (Brazil)
c) Alkaline granites	(Brazil), Strange Lake (Canada)
(2) Hydrothermal	Bayan Obo (China)
(3) Sedimentary	
a) Placer	Kerala (India), Western Australia, Queesland State (Australia), Richards Bay (South Africa)
b) Conglomerate	Elliot Lake (Canada)
(4) Residual	Longnan, Xunwu (China)

1.2.3 Sedimentary Deposits

Weathering of all types of rocks yields sediments that are deposited in a wide variety of environments, such as streams and rivers, shorelines, alluvial fans, and deltas. Depending on the source of the erosion products, certain rare earth elements-bearing minerals, such as monazite and xenotime can be concentrated along with other heavy minerals.

The source need not be an alkaline igneous rock or a related rare-earth deposit. Many common igneous, metamorphic, and even older sedimentary rocks contain enough monazite to produce a monazite-bearing placer deposit. As a result, monazite is almost always found in any placer deposit.

Most placer accumulations with significant amounts of REE minerals are Tertiary or Quaternary deposits, derived from source areas that include granitic rocks or high-grade metamorphic rocks; however, paleo placers deposits that are as old as Precambrian contain REE resources. Orris and Grauch (2002) listed more than 360 REE-bearing placers. Most commercial deposits are in sands of marine origin along or near present coastlines and consist of titanium mineral placers with by-product zircon and monazite; some contain xenotime. In the 1980s,

monazite and xenotime from titania-zircon paleo beach placers in Australia were the third most important source of REEs in the world, but Australia currently exports little or no REE minerals from such sources, owing to their high thorium contents. In addition to Australia, by-product monazite has been extracted from beach deposits in Brazil, India, Malaysia, Thailand, China, Taiwan, New Zealand, Sri Lanka, Indonesia, Zaire, Korea, and the United States. Present-day production is from India, Malaysia, Sri Lanka, Thailand, and Brazil. In Southeast Asia, monazite and xenotime are collected from concentrates produced during placer tin, zircon, and titanium mining.

1.2.4 Residual Rare Earth Deposits

In tropical environments, rocks are deeply weathered to form a unique weathered profile consisting of laterite, an iron- and aluminum-rich weathered rock, as much as tens of meters thick. When a rare-earth deposit undergoes such weathering, it may be enriched in rare earth elements in concentrations of economic interest. A particular type of REE deposit, the ion-absorption type, is formed by extraction of the rare earth elements from seemingly common igneous rocks and fixing the elements onto clays in weathered rocks.

Wu *et al*. (1990) revealed that HREE are mostly concentrated in an adsorption state on clays in the weathered crust of granitic rocks e.g. Longnan, Xing Feng, southern China (Wu et al., 1990), a reported prospect at Takua Pa (Imai et al., 2013) and Phuket in Thailand (Sanematsu et al., 2013), and Madagascar (Berger et al., 2014).

Study on lateritic deposit started since 1980 in China. There are at least 18 prospect areas located in China (Orrisch & Grauch, 2002). REE from these deposits comprise 14% of Chinese production (Wu et al., 1996), and this source has had a substantial impact on yttrium supplies since 1988. The deposits were formed due to the weathering crusts of granite (Ren 1985; Wu et

al., 1996). The ore referred to as REE-bearing ionic absorption clay, mostly comes from two sites in Jiangxi Province - Longnan and Xunwu, the former yielding HREE- and yttrium-rich material and the other, LREE-rich material (O'Driscoll, 2003). Both ores have relatively low cerium content, suggesting deposition from REE-bearing groundwater with depleted cerium that results from the element's insolubility in the oxidized (Ce^{4+}) state. The ore bodies are 3 to 10 m thick and occur mainly in a wholly weathered zone composed of halloysite and kaolinite with residual quartz and feldspar; grades are reported from 0.05% to 0.2% REOs (Wu et al., 1996). There are some prospects of lateritic materials overlying carbonatite in many sites worldwide mostly in the tropical areas, but none has produced significant amounts of REEs (Orris & Grauch, 2002; Berger et al., 2009).

1.2.5 Other Rare Earth Elements Deposit Types

The iron-oxide-copper-gold type of deposit has been recognized as a distinct deposit type only since the discovery of the giant Olympic Dam deposit in South Australia in the 1980s. The Olympic Dam deposit is unusual because it contains a lot of REE and uranium. An economic method for recovering rare earth elements from these deposits has not yet been found (Castor & Hedrick, 2006). Karst bauxites, aluminum-rich weathered rocks that accumulate in cavernous limestone (underlying karst topography) in Montenegro and elsewhere are enriched in rare earth elements, but the resulting concentrations are not of economic interest (Maksimovic & Pantó, 1996). The same can be said for marine phosphate deposits, which can contain as many as 0.1 percent REE oxides (Altschuler et al., 1966). As a result, recovery of REE as a by-product of phosphate fertilizer manufacture has been investigated.

1.3 Main REE ore minerals

Although REE occur as significant variety of minerals, almost all production has come from less than 10 minerals (Castor & Hedrick, 2006). Table 1.2 lists minerals that have yielded REE commercially or have a potential for production in the future.

Table 1.2 REE-bearing minerals of economic or potentially economic deposits

Mineral Name	Mineral Formula*	Rare Earth Oxide (REO) wt % † ‡
Aeschynite	$(Ln,Ca,Fe,Th)(Ti,Nb)_2(O,OH)_6$	36
Allanite (orthite)	$(Ca,Ln)_2(Al,Fe)_3(SiO_4)_3(OH)$	30
Anatase	TiO_2	3
Ancylite	$SrLn(CO_3)_2(OH).H_2O$	46
Apatite	$Ca_5(PO_4)_3(F,Cl,OH)$	19
Bastnasite	$LnCO_3F$	76
Brannerite	$(U,Ca,Ln)(Ti,Fe)_2O_6$	6
Britholite	$(Ln,Ca)_5(SiO4,PO4)_{3(}OH,F)$	62
Cerianite	$(Ce,Th)O_2$	81#
Cheralite	$(Ln,Ca,Th)(P,Si)O_4$	5
Churchite	$YPO_4.{}_2H_2O$	44#
Eudialyte	$Na_{15}Ca_6(Fe,Mn)_3Zr_3(Si,Nb)Si_{25}O_{73}(OH,Cl,H_2O)_5$	10
Euxenite	$(Ln,Ca,U,Th)(Nb,Ta,Ti)_2O_6$	<40#
Fergusonite	$Ln(Nb,Ti)O_4$	47
Florencite	$LnAl_3(PO_4)_{2(}OH)_6$	32#
Gadolinite	$LnFeBe_2Si_2O_{10}$	52
Huanghoite	$BaLn(CO_3)_2F$	38
Hydroxylbastnasite	$LnCO_3(OH,F)$	75
Kainosite	$Ca2(Y,Ln)_2Si_4O_{12}CO_3.H_2O$	38
Loparite	$(Ln,Na,Ca)(Ti,Nb)O_3$	36
Monazite	$(Ln,Th)PO_4$	71
Mosandrite	$(Ca,Na,Ln)_{12}(Ti,Zr)2Si_7O_{31}H_6F_4$	<65#
Parisite	$CaLn_2(CO_3)_3F_2$	64
Samarskite	$(Ln,U,Fe)_3(Nb,Ta,Ti)_5O_{16}$	12
Synchisite	$CaLn(CO_3)_2F$	51
Thalenite	$Y_3Si_3O_{10}(OH)$	63#
Xenotime	YPO_4	61#
Yttrotantalite	$(Y,U,Fe)(Ta,Nb)O_4$	<24#

* Source for mineral formulas: Mandarino (1999), with Ln = lanthanide elements.

† Sources for REO content: Frondel (1958); Overstreet (1967); Anon (1980); Kapustin (1980); Mazzi and Munno (1983); Mariano (1989a).

‡Where more than one analysis is available, the analysis with the highest REO content is reported (e.g., REO for monazite from the Mountain Pass carbonatite is reported; monazite from pegmatites and metamorphic rocks generally has lower REO).

Stoichiometric calculation of REO content.

Extraction of a potentially economic REE resource strongly depends on its REE mineralogy. In the past, producing deposits were limited to those containing REE-bearing minerals that are relatively easy to concentrate because of coarse grain size or other attributes (Castor & Hedrick, 2006).

Minerals that are easily broken down, such as bastnasite, are more desirable than those that are difficult to dissociate, such as allanite. Placer xenotime, once an important source of REE, has been largely abandoned because of its high thorium content. Recently, REE absorbed on clay minerals in laterite have become important sources of REE in China (Castor & Hedrick, 2006).

1.4 Use of REE

Rare earth elements are particularly useful in petrogenetic studies of igneous rocks because all the REE are geochemically similar. All, except Eu and Ce, are trivalent under the most geological conditions. Eu is both trivalent and divalent in igneous systems. The ratio Eu^{2+}/Eu^{3+} depends on oxygen fugacity (fO_2). Geochemical behavior of Eu^{2+} is geochemically very similar to geochemical behavior of Sr. Ce may be tetravalent under highly oxidizing conditions (Wilson, 1989).

The mobility and distribution of REE are used as geochemical tracers for crustal evolution and magma genesis and differentiation (Wilson, 1989). REE are very critical to support the development of future high technology, such as manufacturing catalytic converters, petroleum refining catalyst, magnets, hybrid cars, and electronics, making them economically important worldwide (Pecht et al., 2012; Dickson, 2015). REE uses are indicated in Table 1.2.

1.5 Classifications of Granitoids

Term "granite" is often loosely applied to a broad variety of felsic intrusive rocks. Because granite is a term defined by a restricted range of quartz-plagioclase-alkali feldspar proportions in the IUGS classification, this dual use can be confusing. Meanwhile, term granitoid is adopted for the broader usage. Granitoids are the most abundant plutonic rocks in the upper continental crust. Such a wide spectrum of rock types will have a wide range of sources and genetic processes, and their genesis is not limited to the subduction zone processes (Winter, 2001). There have been numerous attempts to classify the diverse spectrum of granitoids on the basis of their petrography and geochemical compositions.

Table 1.3 REE uses and applications by industry

Automotive	Catalysts for pollution control; catalytic converter catalyst substrate; rechargeable batteries; fuel cells; colored plastics
Ceramics	Oxygen sensors; structural ceramics for bearings; jet engine coatings; investment molds; refractories; pigments
Chemicals	Oil refinery fluid cracking catalysts; pharmaceuticals; water treatment; catalysts; moisture control, dryers, and detection
Defense	Lasers; missile guidance and control; visual displays; radar; electronic countermeasures; communication; shielding
Electronics	Capacitors; cathodes; electrodes; semiconductors; frequency circulators and toroids; yttrium iron (YIG) ferrites garnet thermistors; traveling wave tubes (TWTs); radio
Glass	Polishing compounds; decolorizing; colorizing; increase refraction; decrease dispersion; radiation stabilization; absorber
Illumination	Trichromatic fluorescent lamps; mercury lamps; carbon arc lamps; gas mantles; auto headlamps; long-glow phosphors
Magnets	Speakers and headphones; linear motors; antilock braking systems; tape and disk drives; gauges; electric motors; pumps; ignition
Magnetostrictive	Sonar systems; precise actuators; precision positioning; vibratory screens; speakers; ultrasonics to kill bacteria
Medical	Contrast agents; magnetic resonance imaging (MRI); positron emission tomography (PET); radioisotope tracers and emitters
Metallurgy	Alloying agents in aluminum, magnesium, iron, nickel, and steel alloys; superalloys; pyrophoric alloys; lighter flints; armaments
Phosphors	Cathode-ray tubes (CRTs); fluorescent lighting; radar and cockpit displays; x-ray intensifying screens; temperature sensors
Other refrigeration;	Simulated gemstones; textiles; magnetic refrigeration; hydrogen fuel storage; lubrication; photography; nuclear use

1.5.1 Modal composition/IUGS classification

The International Union of Geological Science (IUGS) classification focuses on differences in abundances and compositions of the feldspar and accounts for a wide variety of granitoids. This scheme is based on measurable parameters. It employs modal proportions of quartz, alkali feldspar, and plagioclase (Streickeisen, 1967). It is simple and truly non-genetic. Besides, the scheme has the major scientific disadvantage of not taking into account the mafic minerals and other minor phases such as muscovite which may be significant for petrogenetic implications. Because of this apparent handicap, geochemical classification schemes flourished.

1.5.2 S-I-A-M Classification

The S-I-A-M classification is based on measured- to inferred parameters. The alphabets of S-I-A-M are the abbreviation of sedimentary, igneous, anorogenic, and mantle, respectively.

Chappel and White (1974) introduced two alphabets, I and S, to denote two distinct types of granitoids. I-type granitoids is metaluminous to weakly peraluminous, relatively sodic and have a wide range of silica content (56-77 wt % SiO_2). It was inferred to have formed from a mafic, meta igneous source, while S-type granitoids is strongy peraluminous, relatively potassic and restricted to higher silica content (64-77 wt % SiO_2), and they are inferred to have formed from melting of metasedimentary rock sources (Mondal & Hussain, 2011; Frost et al., 2001; Chappel & White, 1974).

The I-type granitoids have higher Na, Ca, Sr, Fe^{3+}/Fe^{2+}, $^{87}Sr/^{86}Sr$, and $\delta^{18}O$ and lower $^{143}Nd/^{144}Nd$. The rocks are hornblende-rich, and are either metaluminous or weakly peraluminous. The chemical composition suggests that they are derived by partial melting of a mafic mantle-derived igneous source material (probably of a sub-crustal underplated lithosperic

materials, but subducted crust or older high-level pluton sources cannot be excluded). The S-type granitoids have the opposite chemical trends to those listed above, and is always peraluminous. The rocks are biotite-rich, and typically contain cordierite. They may also contain muscovite, andalusite, sillimanite, and or garnet. The chemical composition suggests that they are produced by partial melting of peraluminous sedimentary source rocks imprinted by weathering at the Earth's surface.

White (1979) thus added an M-type granitoid for both immature arc plutons and the oceanic "plagiogranites" found in the ophiolites-oceanic crust and eroded OIBs, such as Iceland. Whether I-types are two-stage remelts of underplated lithosperic material, and M-type granitoids are melt products of single-stage mantle melts is yet to be confirmed. A-type granitoids (for anorogenic) contain higher SiO_2, alkalis, Fe/Mg, halogens (F and Cl), Ga/Al, Zr, Nb, Ga, Y, and Ce than I-type granitoids (Whalen et al., 1987; Eby, 1990). They have an intra plate trace element signature, commonly lacking the high "decoupled" LIL/HFS ratios associated with subduction zones. I-type and S-type refer to igneous and sedimentary precursor sources respectively, whereas A-type indicates anorogenic setting of emplacement, and not the precursor source. Further, I-type and S-type indicate one-stage origin of the granitoid, derived directly from the igneous or sedimentary sources, whereas M-type may be one-to-more-than-one stage origin, derived directly or indirectly from the mantle (Mondal & Hussain, 2011). The S-I-A-M classification is summarized in Table 1.3 and Table 1 4.

As with most classifications, however, S-I-A-M gives the impression that the types of granitoids are really distinct. In reality, hybrid magmas are common. I-type and S-type hybrids are likely to be produced in orogenic belts by mixing of source reservoirs and/or magmas. In fact, few orogenic belts have shown the I-S distinction as well as the original Lachlan example.

Crustal assimilation is a process that may readily incorporate an S-type component into I-type melts. M-types and I-types are also likely to be mixed in mature island arcs and continental arcs. The reservoirs are so similar that it may be impossible to geochemically or isotopically distinguish them. Magmas that classify geochemically as A-type are not restricted to the original anorogenic setting. Enriched and alkaline magmas may be created in orogenic belts and hybridize with I- and S-types. S-, I-, and M- are based on source chemical characteristics, whereas A- is based on classification (Chappel & White, 2001).

1.5.3 Alumina saturation

This system uses the concept of alumina saturation (Chappel and White, 1974; Frost et al., 2001). A simple parameter A/CNK, defined by molecular Al_2O_3/ (CaO + Na_2O + K_2O), is used to classify the rocks into metaluminous (A/CNK < 1), or peraluminous (A/CNK > 1) or peralkaline A < NK.

1.5.4 Magnetite-series and ilmenite-series

Ishihara (1977) observed that granitoid rocks of magmatic arcs can be conveniently divided into two series based on their magnetic susceptibility: 1) magnetite-series characterized by the occurrence of magnetite and 2) ilmenite-series characterized by the absence of magnetite (Ishihara, 1977). The mineral assemblages imply a higher oxygen fugacity in the magnetite-series granitoids than in the ilmenite-series granitoids during solidification of the granitic magmas.

The magnetite-series granitoids are considered to have been generated in a deep level (upper mantle and lowest crust) and not to have interacted with C-bearing materials; whereas the ilmenite-series granitoids were generated in the middle to lower continental crust and mixed with

C-bearing metamorphic and sedimentary rocks at various stages in their igneous history (Ishihara, 1977).

1.5.5 Tectonic discriminant schemes

Many authors have attempted to establish the links between the chemical composition of the granitoids and the tectonic settings of their emplacement (Mondal & Hussain, 2011). Batchelor and Bowden (1985) and Maniar and Piccoli (1989), have proposed a tectonic discriminant scheme based on a function involving Si–Ti–Fe–Na–K against another function involving Al–Mg–Ca to demonstrate the relationship between chemical composition and tectonic environment of emplacement.

A similar attempt was made by Maniar and Picolli (1989), they classified the granitoids on the basis of major elements into seven tectonic settings: island arc, continental arc, continental collision, post-orogenic, rift, continental epeirogenic uplift, and ocean ridges and islands.

The tectonic classification scheme that has found wide application is the one by Pearce et al. (1984). The scheme is solely based on trace elements, discriminates granitoids into four major tectonic environments: volcanic arc, oceanic ridge, within plate and syn-collision. The major drawback of the tectonic discriminant diagrams is that the elemental composition of the granitoids is a direct manifestation of the sources and the magmatic processes, and not the tectonic environment in which they are emplaced.

1.5.6 Three-tier chemical scheme

Frost et al. (2001) proposed a classification scheme based on three geochemical parameters: Fe-number, modified alkali lime index (MALI) and alumina saturation index (ASI).

Table 1.4 Characteristics of I- type, S-type and A-type granitoids (Chappel & White, 1974; Ishihara, 1977; Winter 2001; Gill, 2010)

	I-types granitoids	S-types granitoids	A-type granitoids
Major element composition	Metaluminous*, Mol. $Al_2O_3/(Na_2O+K_2O+CaO)$ <1.1 Relatively highCaO, Na_2O normally >3.2% in felsic varieties, to >2.2% in more mafic types, and low K_2O	Peraluminous*, Mol. $Al_2O_3/(Na_2O+K_2O+CaO)$ >1.1 Relatively low CaO, Na_2O normally <3.2% in rocks decreasing with approx. 5% K_2O, decreasing to <2.2% in rocks with approx. 2% K_2O	Metaluminous to peralkaline, high ΣFeO/MgO. high contents of FeOt/(FeOt+MgO), SiO_2, Na_2O+K_2O, Ga/Al, REE except Eu, Zr, Nb, and Ta, and low content of Sr, Ba, Eu, CaO and Al_2O_3
Normative minerals	CIPW normative diopside or <1% normative corundum, Normative diopside	>1% CIPW normative corundum, Normative Corundum	Normative diopside + acmite
Range of rock types represented	Broad spectrum of compositions from felsic to mafic. Plutons commonly include a wide range of rock types from basic to acid (SiO_2, 56 to 77 wt%)	Relatively restricted in composition to high SiO_2 types, generally confined to high SiO_2, 64 to 77 wt%. No associated with mafic rocks	Typicaly high SiO_2 granitoids (often associated with syenite)
Xenolith lithologies	Mafic hornblende-bearing xenoliths of igneous appearance	Metasedimentary xenoliths	Various
Associated economic deposits	Porphyry Cu, Mo, sulphides+ Ag, Au, bearing pyrite veins	Sn, W, U (Li, Be, B)	Zr, Hf, Nb, Ta, Y, REE, U, Th,
Range of (87Sr/86Sr)0	Low initial $^{87}Sr/^{86}Sr$ ratios (0.704 to 0.706)	High initial $^{87}Sr/^{86}$ Sr ratios (0.708 to 0.765)	0.702 to 0.717
Type of minerals	Hornblende, sphene, biotite*	Muscovite (ussually with biotite), monazite, cordierite, garnet, apatite	Mafic are Fe-rich biotite or alkali pyroxene or amphibole
Occurence of magnetite/ilmenite	Magnetite and ilmenite	Ilmenite	
Magnetic susceptibility	High magnetic susceptibility and Fe_2O_3/FeO by magnetite	Low magnetis susceptibility and Fe_2O_3/FeO by ilmenite	
Harker diagram	Regular inter-element variations within plutons; linear or near-linear variation diagrams	Variation diagrams more irregular	

- Chappel and White (1974) placed the I-type and S-type boundary at $Al_2O_3/(Na_2O+K_2O+CaO)$mol=1.1 rather than 1

Table 1.5 The SIAM Classification of Granitoids (Winter, 2001)

Type	SiO_2	K_2O/Na_2O	Ca, Sr	A/(C+N+K)*	Fe^{3+}/Fe^{2+}	Cr, Ni	$\delta^{18}O$	$^{87}Sr/^{86}Sr$	Misc	Petrogenesis
S	65-74%	High	Low	High Metaluminous	Low	High	<9/‰	<0.707	Variable LIL/HFS high Rb, Th, U, biotite, cordierite, garnet and ilmenite	Subduction zone, supracrustal sedimentary source
I	53-76%	Low	High in Mafic Rocks	Low: metaluminous to peraluminous	Moderate	low	<9/‰	<0.705	High LIL/HFS, medium Rb, Th, U, hornblende magnetite	Subduction zone, Infra crustal, Mafic to intermed igneous source
A	High >77%	Na_2O high	Low	Variable Peralkaline	Variable	Low	Variable	Variable	Low LIL/HFS, high Fe/Mg, high Ga/Al, high REE, Zr, high F and Cl	Anorogenic, Stable craton and Rift zone
M	46-70%	Low	High	low	Low	Low	<9/‰	<0.705	Low Rb, Th, U, low LIL and HFS	Subduction zone or ocean intra plate mantle-derived

* molar $Al_2O_3/(CaO+NA_2O+K_2O)$

Data from White and Chappel (1983), Clarke (1992) and Whalen (1985)

Based on Fe-number (= FeO/[FeO + MgO]), the granitoids have been divided into two groups: ferroan and magnesian. On the basis of MALI (= $Na_2O + K_2O–CaO$), the granitoids have been divided into four groups: calcic, calc-alkalic, alkali-calcic and alkalic. Based on ASI (molecular Al/(Ca – 1.67P + Na + K), granitoids have been grouped as peraluminous (ASI > 1.0), metaluminous (ASI < 1.0, but [Na + K]< Al) and peralkaline (ASI < 1.0, but [Na + K] > Al).

1.6 Location of Study Area

The study areas are located in Sibolga, Panyabungan, Kotanopan and Muara Sipongi at the western part of North Sumatra province, Indonesia. These areas consist of granitic batholiths of Permian to Cretaceous age, having I-type, S-type and A-type characteristics.

1.7 Objectives

Granitoids in (North) Sumatra are widely distributed, NW-SE direction parallel to the length of the island (Hutchison, 1988). They have a relatively high REE content than the surrounding granites, and associated with the very thick weathered of granitoids crusts. Petrochemical, REE geochemistry on granitoids, and their weathered crusts and the granites source in the western part of Sumatra are of particular importance. Any detailed research on granitic rocks in Sumatra has never been conducted.

The objectives of this study are to understand the geological and REE geochemical characteristics of granitoids and their REE behavior in weathered granitoids crusts, to elucidate the origin and their tectonic evolution, and to elucidate the different types of granitoids in the western part of North Sumatra.

CHAPTER 2

GEOLOGICAL SETTING

2.1 Regional Geology

The Permian was a particularly important period in the geological evolution of Southeast Asia (SE Asia). Sumatra located at the southwestern margin of the Southeast Asia is considered to be composed of fragments of continental plates and magmatic arcs which were derived from Gondwana during the Late Paleozoic and Mesozoicc (Pulunggono & Cameron, 1984; Hutchison, 1994; Nishimura & Suparka, 1997; Metcalfe, 2002; Barber & Crow, 2003; 2005a). Paleomagnetic study of Sumatra Island (Nishimura & Suparka, 1997) suggested that the Sumatra region underwent drift during Triassic through Early Neogene. Sumatra as part of Gondwanaland during the Triassic was located just north of the junction of the Indian and Australian continents (Nishimura & Suparka, 1997).

Sumatra was firmly part of the Sibumasu Block. The Permo-Carboniferous stratigraphy and paleontology of northern Sumatra and Malay Peninsula and Peninsular Thailand were correlated in particular of the occurrence of tilloids. Furthermore, the northern Sumatra compared with the Permo-Carboniferous stratigraphy of Bonaparte Gulf region of northwest Australia has a mirror image relationship, suggesting that Sibumasu Block was separated from this part of the Gondwana margin in the mid-Permian (Hutchison, 1994; Barber & Crow, 2003, 2009).

On the other hand, Permo-Carboniferous rocks in Central Sumatra contain the Cathaysian fauna and flora, suggesting that this area can be correlated to Indochina Block

rather than to Sibumasu (Djambi Nappe). Cathaysialand Block was separated from Gondwana before the Sibumasu Block, and these blocks were successively accreted to the southwest margin of Sundaland (Barber & Crow, 2003). The Cathaysian fauna and flora were associated with an early Permian Volcanic Arc. The existence of Permian arc was also reported by Katili (1973). It has been suggested that this arc was developed on the margin of the Cathaysialand Block and was emplaced in its present position outboard of Sibumasu by strike-slip faulting (Barber & Crow, 2003) (Fig. 2.1).

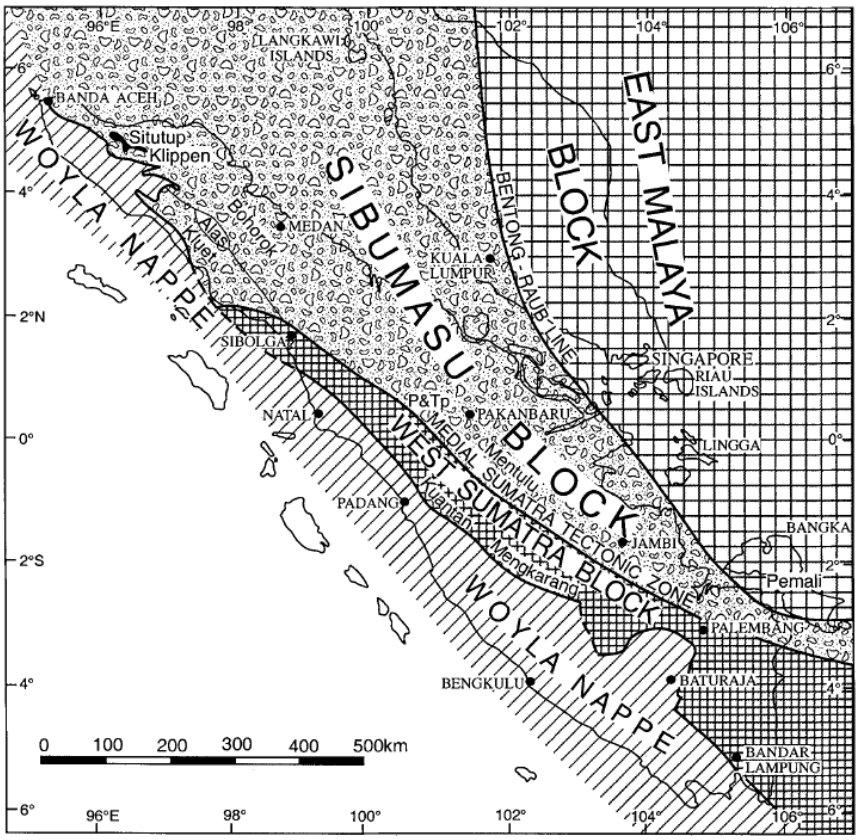

Fig. 2.1 Pre-Cenozoic tectonic blocks in Sumatra and Peninsular Malaysia, modified from Hutchison (1994) and Barber and Crow (2003). Sibolga is shown as part of the West Sumatra Block.

West Sumatra Block was derived from Cathaysia and was emplaced against Sibumasu west margin by dextral transcurrent faulting. East Malaya Block was part of Indochina block. West Burma Block is an extension of West Sumatra Block, from which it was separated by the formation of Andaman Sea in Miocene. The Woyla nappe is correlated with the Mawgyi nappe of Myanmar. The most recently accreted pre-Cenozoic tectonic unit on Sumatra is the Woyla Group, a Jurrasic-Early Cretaceous oceanic volcanic arc. The associated accretionary complex of oceanic crustal material was thrusted over the western margin of Sumatra in the mid-Cretaceous (Barber & Crow, 2009) (Fig. 2.2).

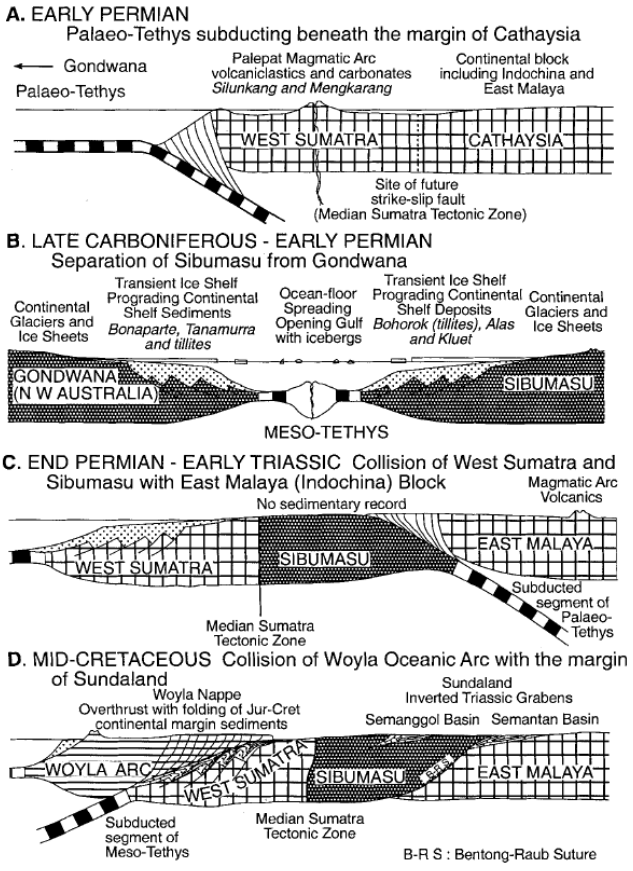

Fig. 2.2 Cartoon ilustrating the plate tectonic evolution of Sumatra (Barber & Crow, 2003).

Pre-Cenozoic tectonic and magmatic development of the mountain ranges of Sumatra were reconstructed by Suparka and Asikin (1981). The development included reversal of the direction of subduction at the end of the Mesozoic because of the northward movement of the Indian continental plate (Fig. 2.3).

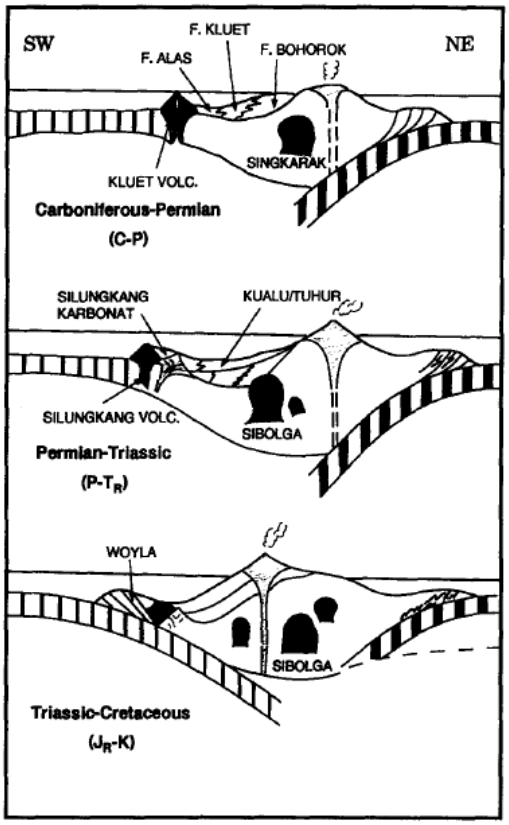

Fig. 2.3 Pre-Cenozoic development of arc volcanisme in northern and central Sumatra (modified after Suparka and Asikin, 1981).

Katili (1973) reported the Permian magmatism on both east and west Sumatra Blocks on the basis of Rb-Sr age determinations on feldspars of Setiti batholiths giving the ages of 298 ± 30 Ma (brecciated granite) and 276 ± 10 Ma (sheared granite). On the Western Block, Lower - Middle Permian volcanic rocks and sedimentary rocks and several

associated granitic plutons crop out and form a discontinuous belt, much disrupted by strike-slip movements along the Sumatra Fault Zone, parallel to the west coast of the island (Crow, 2005).

The products of Permian volcanism on the Western Block are listed as Sibolga granite (Aspden *et al.*, 1982), Silungkang Formation (Katili, 1969; Fontaine & Gafoer, 1989; Silitonga & Kastowo, 1975), Palepat Formation (Fontaine & Gafoer, 1989) and Kuantan Formation (Silitonga & Kastowo, 1975). These events are ultimately resulted in the collision of India with the Asian continental plate during Jurassic through Late Cretaceous, as shown in Fig. 2.2. Suparka and Asikin (1981) assumed that subduction occurred near the Asian plate, based on paleomagnetic and geological data. It is suggested that subduction occurred along the frontal arc of Gondwanaland. The northward drift of the mountain range of Sumatra began at the end of the Triassic, and it collided obliquely with the Asian plate at the beginning of the Cretaceous (Fig. 2.3).

2.2 Southeast Asian Tin Belt

Three main granitoids provinces are identified in Southeast Asia. These are, from west to east; the Western, Main Range, and Eastern Belts, trending broadly from north to south (Cobbing et al., 1986, 1992; Hutchison, 1994; Cobbing, 2005; Searle et al., 2012). Charusiri et al. (1993) reported that the Ar-Ar ages of granitoids from the Western, Main Range and Eastern Belt in Thailand range from 80 to 50 Ma (Late Cretaceous to Paleogene), from 220 to 180 Ma (Late Triassic to Jurassic) and from 245 to 210 Ma (Early to Late Triassic), respectively (Fig. 2.4).

U-Pb ages from Western, Main Range and Eastern Belt from Thailand range from 218 to 71 Ma, 220 to 219 Ma, and 266 Ma, respectively (Gardiner, 2015). The U-Pb ages of granitic rocks in the Main Range, and Eastern Belt from Myanmar range from 220 to 219 Ma, and 266 to 258 Ma, respectively (Gardiner, 2015; Ng et al., 2015).

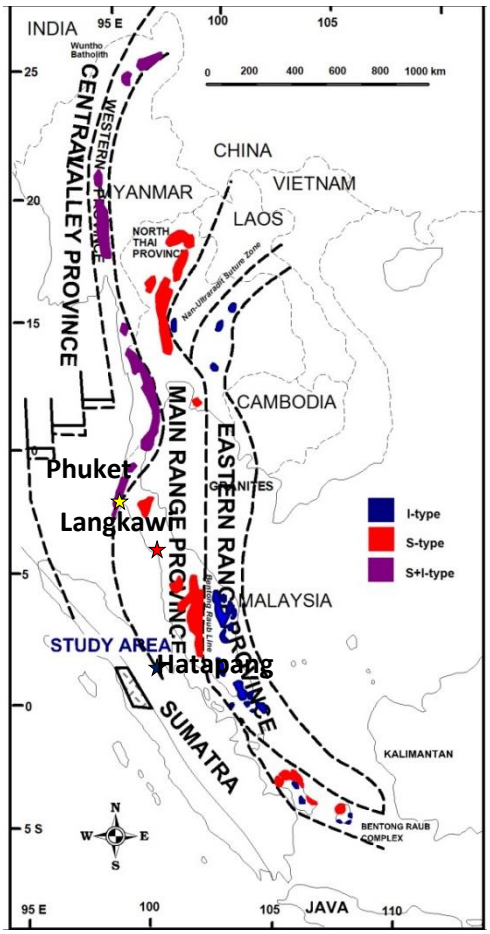

Fig. 2.4 Map showing granitic provinces of Southeast Asian Tin Belt and the location of the study area (modified after Cobbing et al., 1992; Cobbing 2005).

The Eastern Belt and Main Range in Peninsular Malaysia were separated by Bentong-Raub suture (Metcalfe, 2000). The ages of granitoids of Main Range are younger than those of the Eastern Belt. They range from 227 to 198 Ma (Searle et al., 2012; Ghani et al., 2013;

Ng et al., 2015) and 289 to 220 Ma (Gardiner et al., 2015; Ng et al., 2015), respectively. The U-Pb ages of granitic rocks of Main Range from Singapore range from 289 to 201 Ma (Ng et al., 2015), and those of the Eastern Belt range from 254 to 230 Ma (Hotson et al., 2011).

Sumatra Island was formed by collision and suturing of microcontinents during Paleozoic and Mesozoic (Pulunggono & Cameron, 1984; Barber & Crow, 2005a). At present, Indo-Australian Plate is being subducted beneath Eurasian Plate with 20°E direction at a rate from 6 to 7 cm/yr (Pulunggono & Gumilar, 2000). The Middle to Late Paleozoic basement rocks are crustal blocks derived from Gondwana Continent which collided with the eastern margin of Eurasian Plate to form the Sundaland during Late Paleozoic to Early Mesozoic. Pre-Cenozoic basement rocks consist of partially metamorphosed sedimentary rocks and volcanic rocks, which were defomed, intruded by granitoids and later covered by Cenozoic sedimentary rocks and volcanic rocks (Barber & Crow, 2005b).

The granitoids in Sumatra were formed in two geological cycles. The first was the a Carboniferous-Permian cycle of subduction of Paleotethys oceanic floor, and collision of Sibumasu continental plate with the amalgamated East Malay-Indochina Block. The collision was followed by the younger Triassic to Early Jurassic cycle in which a new subduction of Sibumasu and East Malay – Indochina zone was formed along the southwestern margin of the new continent (Sundaland). The second cycle generated granitoids associated with Late Triassic to Early Jurassic volcanic arc along the southern margin of Sundaland, which is the Main Range Belt (Schwartz et al., 1996; Hutchison, 1994, 2014; Cobbing, 2005).

2.3 Geology of Sumatra Island

Sumatra has experienced long magmatic processes during its geological history since Paleozoic up to the present time. The Paleozoic age was indicated by the presence of metavolcanics in the Kuantan Formation (Gafoer & Purbo-Hadiwidjojo, 1986; Silitonga & Kastowo, 1975, 1995), that is Carboniferous in age (Early or Mid to Late Visean) (Fontaine & Gafoer, 1989). The track of the Carboniferous volcanism is also noted by Cameron *et al.* (1982a) through the discovery of green metavolcanics within the Alas Formation, in the Medan Quadrangle that may be of Visean age, like the associated limestone.

A large number of studies on the granitoids were conducted in Sibolga and its surrounding areas, including petrographic descriptions and whole-rock chemical analyses (Cobbing, 2005), tectonics (Nishimura & Suparka, 1997), magmatism and mineralization (Subandrio et al., 2007; Subandrio, 2012).

A subduction may have been initiated at Late Permian at the west coast of Sumatra (Aspden et al., 1984). Muara Sipongi and Kotanopan granitoids were probably formed during the Late Triassic to Early Jurassic, ranging from 197 to 186 Ma (Kanao et al., 1971; Hehuwat & Sopaheluwakan, 1978) and from 182 to 142 Ma (Aspden et al., 1984). During that time, Meso-Tethys oceanic floor was subducted beneath amalgamated West Sumatra Block and Sibumasu continent (Barber et al., 2005). Igneous activities involved the intrusions of granitoids in Muara Sipongi, and Kotanopan lasted from Jurassic through Cretaceous to Neogene.

Granitoids are widely distributed in the Sibolga area and occupy approximately 50x50 km^2 (e.g. Subandrio, 2012). The basement rocks of Sibolga are metasedimentary rocks

composed of Carboniferous metagreywacke and Kluet Formation turbidites (Cameron et al., 1980; Aspden et al., 1982; Pulunggono & Cameron, 1984; and Barber & Crow, 2005b).

Pre-Cenozoic rocks occurred in two different areas of Sumatra. The rocks in the Sibolga area are composed of Early Permian, dioritic to alkali-basalt, and the rocks in the Muarasoma-Natal area composed of sedimentary rocks including alternating layers of quartz-sandstone, claystone, and shale, along with intercalations of limestone (Aspden et al., 1982). These rock assemblages indicate that during Carboniferous through Early Permian, sediments were deposited in shallow marine continental shelf environments. In the Early Permian, magmatic activities which occurred in the western Sibolga area were followed by regional metamorphism. Magmatic activity reached its maximum stage with the intrusion of the Sibolga granite complex during Triassic (Aspden et al., 1982). The distribution of the pre-Cenozoic metamorphic units and granitic intrusions is bounded by WSW-ENE or E-W-striking faults (Nishimura & Suparka, 1997). At northeast of the alkali basalt in the Bonan Dolok Massif, partially metamorphosed andesite-basalt, may have been formed during the Early to Late Permian. Radiometric dating (K-Ar) on an augite-basalt belonging to the calc-alkaline series within a volcanic unit located in the Silungkang area of Sumatra indicates a Permo-Triassic age (248-218 Ma) (Nishimura & Suparka, 1997). Exposures of this massif cover an area to the north of Sibolga, trending almost east-west, and are cut by NNW-SSE-striking faults. The quartz, alkali feldspar and plagioclase (QAP) diagram indicates that the granitoids are classified as quartz-monzodiorite (Nishimura & Suparka, 1997). The granitoids were formed during syn-kinematic orogenesis in the Middle Permian coincident with the breakup of Gondwanaland, which was subsequently followed by subduction of an outer margin sea plate (Nishimura & Suparka, 1997; Barber, 2003).

The granitoids from Bonan Dolok consist of granite, granodiorite and quartz-monzonite (Nishimura & Suparka, 1997). Petrographic analysis reveals that most of these rocks contain hornblende and biotite (Nishimura & Suparka, 1997). Geochemically, about 80% of these rocks belong to the I-type and magnetite-series, whereas the remaining represents S-type granite and ilmenite-series (Nishimura & Suparka, 1997). The occurrence of S-type granitic rocks of Early Permian age suggests that the Sibolga granite complex might have been part of the Late Paleozoic continental crust in this area (Nishimura & Suparka, 1997).

Volcanic-magmatic activities characterized by high-alkali and calc-alkaline rock series occurred in the western Sibolga area during the Permian. The I-type granitoid rocks formed along the east side of the Sibolga granite complex occurred during Late Triassic. Petrographic analysis indicates an association of I-type granitoid with sphenealite, which characterizes the magnetite-series and calc-alkali rock series. This indicates that the granitoids were related to subduction along a paleo-continental margin (Nishimura & Suparka, 1997).

Granite provinces in Sumatra island are divided into two provinces; Western Belt and Main Range (Cobbing, 2005) (Fig. 2.5). The granitic rocks of the Western Belt consist of I-type granitoids and are confined to Barisan Mountains. The Triassic Main Range granite is mainly S-type with subordinate I-type and characterized by tin mineralization (Hutchison & Taylor, 1978; Cobbing, 2005). The oldest rocks in Sumatra have been assigned to the Late Palaeozoic Tapanuli Group which has been divided to Bohorok, Kluet and Alas Formations (Aspden et al., 1982).

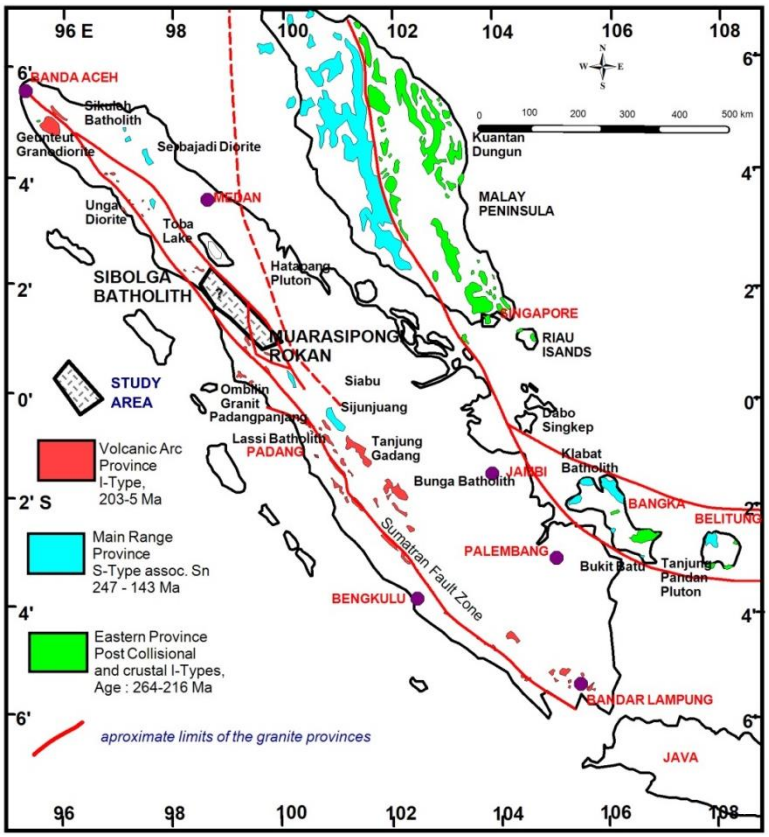

Fig. 2.5 Distribution of granitic rocks and their ages in Sumatra, Malay Peninsula and Tin Islands (modified after Cobbing, 2005).

In Indonesia, tin has been produced mainly from placer deposits both onshore and offshore of Tin Islands such as Bangka, Belitung and Singkep (Sainsburry, 1969). These tin mineralizations are primarily associated with Main Range Belt granitoids, which are distributed in the Southeast Asian Tin Belt, a major metallogenic province of Sn deposits associated with ilmenite-series granitic rocks (Schwartz et al., 1995; Cobbing, 2005). REE deposits in Thailand were classified into primary and secondary deposits. The major primary REE deposits include REE-bearing disseminated tin granitoids and stockworks,

REE-bearing Sn ± W pegmatites, REE-bearing Sn ± W quartz veins and REE-bearing Sn skarns, and these granitoids are of S-type affinity (Charusiri et al., 2006).

The secondary REE deposits are associated with Sn placer deposits derived from granitic rocks by weathering (Charusiri et al., 2006). Wu and Ishihara (1994) reported that total REE contents of granitic rocks in southern Thailand range from 21 to 731 ppm. Sanematsu et al. (2013) reported enrichment and adsorption of REE in the weathered crust of granite in Phuket, Western Belt, southern Thailand. Imai et al. (2013) reported that REEs are concentrated in hydrothermally altered granitic rocks and kaolinite veinlets associated with Sn deposits in the Ranong tin-field and the Takua Pa tin-field in Western Belt, southern Thailand.

In Sumatra Island, tin mineralization associated Main Range Granites occur in the plutons at Sungai Isahan and adjacent areas in the Tiga Puluh region of South Sumatra and the batholith at Sijunjung in the eastern flank of Bukit Barisan to the northeast of Padang (Cobbing, 2005). The Hatapang Granite, located at the south of Lake Toba and to the east of Sibolga associated with a tin prospect, belongs to the S-type Western Belt Granites (Cobbing, 2005; Clarke & Beddo-Stephens, 1987). Uranium prospects are located in Sibolga which are hosted in Cenozoic sediments. The Paleozoic basement on which the sediments were deposited is composed mainly of Permo-Triassic granitic rocks (Tjokrokardono & Ngadenin, 2004; Koesoemadinata & Sastrawiharjo, 1987).

Granitoids in Sumatra are widely distributed in NW-SE direction parallel to the length of the island. They consist of plutons and batholiths up to several hundred km long (Hutchison, 1988). The occurrences of REE-bearing minerals such as allanite and monazite in highly differentiated granitoids have been reported in Sibolga (Subandrio, 2012), while a high concentration of Ce was reported at Parmonangan, north of Sibolga (Suwargi et al.,

2010), Sumatra Island. Therefore, a geological and geochemical study on granitoids in Sibolga are of particular importance.

These granitoids units are equivalent to the Main Range granites of Peninsular Malaysia and Indonesian Tin Islands, which are characterized as S-type granitoids associated with tin and are Triassic in age (Hutchinson & Taylor, 1978; Cobbing, 2005). Bangka and Belitung Islands, well known as the "Tin Islands" were tin producers regions and are located in the region between Peninsular Malaysia (Eastern Province of Tin Belt) and eastern Sumatra (Main Range Province of Tin Belt). Consequently, those two provinces are geographically distinguished by the Bentong-Raub line (Hutchison, 1989). The Tin Islands are characterized by a mixture of both provinces. The Klabat Suite and the Bebulu Suite typify these two areas in Bangka Island. Both of them are associated with tin mineralization. The Klabat Suite of northern Bangka belongs to the S-type granites which is similar to the Main Range Province of Tin Belt. The Klabat Batholith is the largest body and consists of six plutons. There are other tin-mineralized plutons and only the Kelapa Pluton belongs to the I-type granite.

The Bebulu Suite of southern Bangka and Belitung belongs to the S- and IS-type granite. The Bebulu Batholith is the most extensive body and consists of six plutons. Apart from certain samples, the Bebulu Suite has consistently high SiO_2 contents and a restricted range in K_2O-Na_2O-CaO proportions compared to the Klabat plutons (Cobbing et al. 1992). Cobbing et al. (1992) also reported the initial $^{87}Sr/^{86}Sr$ ratios of the S-type Klabat Suite range from 0.7163 to 0.7270, while that of IS-type granite of Bebulu Suite ranges from 0.7123 to 0.7171.

In Sumatra Island, Sungai Isahan - Pegunungan Tiga Puluh regions and Sijunjung Batholith are only examples of the tin mineralizations associated with Main Range Granites (Cobbing, 2005), while the Hatapang Granite, located at the south of Lake Toba and to the east of Sibolga is a reported as a prospect and is associated with S-type granites of the Western Range (Cobbing, 2005; Clarke & Beddo-Stephens, 1987). Sibolga is a uranium prospect area wherein the deposit is hosted in Cenozoic sediments. The Mesozoic basement on which the sediments were deposited is mainly composed of Permo-Triassic Sibolga granites (Koesoemadinata & Sastrawiharjo, 1988).

2.4 Local Geology

The geology of the Sibolga area consists of granitic batholiths which belong to the Sibolga Granite Complex (SGC) and contain several intrusive phases of Permian to Triassic age (Fig. 2) (Aspden et al., 1982). The granitoids are mostly megacrysts coarse-grained biotite granite containing abundant xenoliths of amphibolite and cross cut by the Haporas Granitoids pluton consisting of medium-grained hornblende syenite. The Sibolga granitoids are composed of K-feldspar, quartz, plagioclase, biotite, minor hornblende and accessory minerals including monazite, zircon, allanite, fluorite and uraninite (Subandrio et al., 2007).

Granitoids are widely distributed in the Sibolga area, but they were mostly weathered and covered by very thick soils. Fresh granitoids are mainly exposed along road cuts, rivers, and in the quarries. The granitoids samples were collected from seven different locations from the SGC which are readily accessible and are abundant in fresh outcrops. The plutons do not show clear contact with each other in the field. However, the plutons of

Sarudik, Sibuluhan Sihaporas and Sibolga Julu, Adian Koting and Tarutung, Tukka and Sihobuk exhibit different texture and have different composition, suggesting that they are different intrusive units.

The basement rocks at Sibolga are metasedimentary rocks composed of Carboniferous metagreywacke and Kluet Formation turbidites (Cameron et al., 1980; Aspden et al., 1982; Pulunggono & Cameron, 1984; Barber & Crow, 2005b; Subandrio, 2012). The Kluet Formation represents the distal equivalents of Bohorok Formation and is thought to have been deposited as mass flow and /or turbidity currents on the continental slope/shelf during Late Carboniferous to Earliest Permian (Aspden et al., 1982).

Granitic rocks were identified in Kotanopan, Muara Sipongi, and Panyabungan areas in geological maps by Geological Survey of Indonesia (Rock et al., 1983; Aspden et al., 1982). The Muara Sipongi Granitoids are widely distributed over an area 2 to 5 km wide and 20 km long from Kotanopan to Muara Sipongi (Aspden et al., 1982). Muara Sipongi and Kotanopan Granitoids were identified as magnetite-series (Ishihara, 1977), a calc-alkaline rock of the Jurassic period associated with massive copper, lead, and zinc skarn type deposits (Zulkarnain et.al. 2006; Japan International Cooperation Agency (JICA), 1983). They are mainly of medium-grained holocrystalline hornblende granodiorite and quartz diorite with a small random distribution of diorite. The primary rock-forming minerals are quartz, plagioclase, and hornblende with smaller quantities of biotite and K-feldspar. Fresh rocks are rare, and most minerals are slightly altered; namely, plagioclase has often been altered into sericite and chlorite (Aspden et al., 1982).

Hatapang Granites were identified as a favorable area for the formation of sandstone-type uranium mineralization which is indicated by anomalous radioactivity, uranium

contents of the upper Cretaceous granite intrusions and radioactivity anomalous of Tertiary sedimentary rocks deposited in terrestrial environment (Ngadenin, 2013; Clarke & Beddoe-Stephens, 1987; JICA, 1983). The Hatapang Granite of Cretaceous age is stanniferous, and it may be an outlying representative of the Western Belt (Clarke and Beddoe-Stephens, 1987), developed in Peninsular Thailand and the Shah Scarp region of Burma (Beckinsale, 1979; Mitchell, 1977).

CHAPTER 3

METHODOLOGY

Field geological survey and laboratory analyses were conducted to obtain geological, geochemical and mineralogical data. Fieldwork has been done to observe the granitoids characteristics and their relation with the surrounding rocks and collecting samples while laboratory analyses to obtain mineralogical composition, major elements, rare earth elements, trace elements compositions, and Sr-Nd isotopic ratios.

3.1 Geological Survey (Fieldwork)

The granitoids samples were taken from outcrops. The freshest and representative samples were used for analyses, followed by rock description and measurement of magnetic susceptibility and gamma-ray radioactivity.

Mineralogical identification in the fieldwork was determined using loupe magnification 10x and 20x. Gamma-ray radioactivity values were measured using a Standard Gamma Scout Radiation Detector. The unit of measurement is set to an exposure rate μSv/h (microsievert per hour), which is an internationally accepted unit for tissue dosage. It is important to know whether the granitoids has magnetite-series or ilmenite-series characters. The magnetite-series granites usually accompany sulfide deposits containing Cu, Pb, Zn and Mo, whereas ilmenite-series granites tend to form oxide deposits containing Sn and W (Ishihara, 1977, 1981).

Fig. 3.1 a. hammer, b. magnetic susceptibility meter, c. gamma spectrometer, d. laser range finder, e. Brunton compass, f., g. global positioning system (GPS), and g. loupe.

A geological compass was used for field orientation and to measure geological structure orientation. Laser range finder was used to approximate outcrop dimensions, and a Garmin GPS 60 Csx was used to locate the outcrops position accurately (Fig. 3.1).

Magnetic susceptibility values of the granitoids were measured on site with a Terraplus KT-10 Magnetic Susceptibility Meter (Fig. 3.1b).

3.2 Microscopic Observations

A Nikon Eclipse 100N POL microscope was used to observe properties of minerals under plane polar and crossed polars and to identify mineral and its assemblages. This study has been carried out at Akita University, Japan (Fig. 3.2).

The first step is cutting the rock samples into pieces to form rock chips at about 2 x 3 cm and grind the surface with carborundum size 100/120 mesh, 320 mesh, and 800 mesh, respectively. Put the rock chips into an ultrasonic bath to remove dust and dirt particles for about 15 minutes. The sample were remove from the ultrasonic bath, and grind the chip sample with 1000 mesh of carborundum abrasives powder for more than 30 minutes and put again into the ultrasonic cleaner. The same procedures were repeated with 2000 mesh and 3000 mesh of carborundum abrasives powders before the chips fix on the glass slides. Time required for grinding are 20 minutes and 10 minutes, respectively.

Prepare a preparat glass and the rock chips at 90°C for a night in a hot plate. Make a mix solution of petropoxy 154 with a hardener with ratio 10:1, and put a small portion the solution onto the sample surface and attach the glass preparat on the samples surface carefully to avoid bubbles. Leave for a night. After the samples were mounted correctly and no bubbles content, then leave it again for a night. Next step is using secondary cutter machine to cut the samples into about 1mm in thickness. Followed using prepalap get 100µm in thickness. The samples are ready to grind with 120 mesh, 320 mesh, and 800 mesh of carborundum abrasive to get about 30 µm in thickness, and continue to grind with

1000 mesh, 2000 mesh, and 3000 mesh carborndum abrasives. Samples which are used for SEM analysis are will be followed with a polishing with 3 microns, 1 micron, and 0.25 microns of diamond paste, respectively.

Fig. 3.2 Nikon Eclipse LV 100N POL microscope at Akita University.

3.3 X-ray Diffractometry (XRD)

X-ray diffraction (XRD) analysis was conducted to investigate the mineralogical composition of the rock samples qualitatively. The main purpose of this study is to identify the clay mineralogy of the weathered rocks samples. The measurement was carried out using a Rigaku Multi Flex X-ray Diffractometer at Akita University (Fig. 3.3). Scan ranged from 2° to 60° (2θ) in steps of 0.01° at 2°/min scan speed, using a monochromated Cu Kα (λ= 1.54178 Å) radiation, while for clay scan range from 2° to 40° (2 θ) in step of 0.02° at

2°/min scan speed. The operating conditions were maintained at 30kV operating voltage and 16mA current.

Clay analysis was started with a preparation of 1 gr weathered rocks sample and was disaggregated in distilled water and about 50ml of distilled water was then added into it and was mixed thoroughly for about 5 to 10 minutes. After 1 hour, the upper level solution (4 to 5 cm from surface) was then pipetted and put to another tube and put inside the centrifuge machine at 2000 rpm for 10 minutes. After that step, remove the water and placed the clay materials on the clean glass slide slowly so that the liquid covered the entire surface of the slide and formed oriented mounts.

Fig. 3.3 Rigaku Multi Flex X-ray Diffractometer at Akita University.

Bulk, air-dried, and ethylene glycol (EG) and HCl solvated samples were X-rayed. Quartz, plagioclase, K-feldspar, and biotite are mainly observed in the parent granites. Clay minerals candidates such as illite, montmorillonite, kaolinite, halloysite were observed in the altered or weathered rocks samples. The slide was dried at the room temperature.

3.3.1 Ethylene-Glycol treatment

The sample was exposed to the vapor of the reagent ethylene glycol solvation. It was dried at room temperature for 1 hour and then re-analyzed to determine the presence of montmorillonite, halloysite. Montmorillonite is easily identified by comparing patterns of air-dried and ethylene glycol-solvated preparations. The ethylene glycol-treated preparations give a high 001 reflection at about $2\theta=5.2^{o}$ (d=16.9 Å), which, in the air-dried condition, shifts to about $2\theta=6^{o}$ (d=15 Å) (Moore & Reynolds, 1989). Halloysite response to ethylene glycol solvation involves a decrease in the intensity (peak height) of the peak at d~7.2 Å and an increase in the intensity (peak height) of the peak at ~3.58 Å thus narrowing the d=7.2 Å /d=3.58 Å peak height intensity ratio (Hillier & Ryan, 2002).

3.3.2 Hydrochloric acid treatment

The purpose of this treatment is to destroy the chlorite peaks and to distinguish chlorite from kaolinite. Prepare a glass beaker in the ultrasonic bath and fill both of them with hot water, put inside a 0.2 to 0.5 gr of the weathered sample to the test tube with 30 to 40 ml of concentrated hydrochloric acid (2N HCl) to the test tubes for 1 hours. Remove the acid from the glass beaker, and wash the tubes with distilled water for three times to neutralize the acid using a centrifuge machine. A clay residue remained in the tubes were taken, and put on the surface of preparat glass for a night in the room temperature condition.

3.3.3 Qualitative analysis

The clay minerals were identified using the X-ray diffraction patterns (diffractogram) by the peak's position, intensity, and shape. Peak position is determined using Bragg's law which is written as $n\lambda = 2d\sin\theta$. Most of the clay peaks are at the $2\theta = 40^{o}$ or less. The identification of clay minerals was accomplished by careful consideration of peak positions and intensities. The qualitative identification procedure began by searching for a mineral that explains the strongest peak or peaks, then confirming the choice by finding the positions of weaker peaks for the same mineral. Once a set of peaks was confirmed as belonging to a mineral, these peaks were eliminated from consideration. From the remaining peaks, a mineral that will explain the strongest remaining peak or peaks was searched and then confirmed by looking at its peaks of lesser intensity. This method was repeated until all peaks were identified.

The determinations of clay minerals were based on the treatment results described earlier. Illite profiles are unaffected by ethylene glycol solvation and heating to 550^{o}C (Moore & Reynolds, 1989). Chlorite has a basal series of diffraction peaks based on the first-order reflection of d=14.2 Å. Kaolinite has reflections based on d=7.1 Å structure. Most kaolinites have the 002 peak at $2\theta=24.9°$, and chlorite has its 004 reflections at $2\theta=25.1°$. Identification of chlorite is provided by peaks at $2\theta=6.2$ and $2\theta=18.8^{\circ}$, but these peaks are often weak and may not be detectable if the chlorite abundance is low. The chlorite and kaolinite can be differentiated by treated chemical treatment or heating and then re-examined. Montmorillonite is easily identified by comparing diffraction patterns of air-dried and ethylene glycol-solvated preparations (Moore & Reynolds, 1989).

3.4 X-ray Fluorescence Spectroscopy (XRF)

Analysis was done by a Rigaku ZSX Primus II XRF at Akita University. The samples were crushed to make powder by grinding using an iron mortar and pulverized using agate mortar. An amount of 1.5 to 2 gr of powdered samples were weighted and burn with oven until 110°C to remove moistures of samples (H_2O^+), and then put the samples into a furnace to heat until 900°C for 12 hours to remove the water molecules within the minerals (H_2O^-).

Two silicate rock standards from the Geological Survey of Japan (GSJ) were selected to cover the range of major element compositions of natural igneous rocks. The selected standards were: granite (JG-1a) and rhyolite (JR-2) (GSJ, 1994).

All samples were dried with drying oven and then Loss on Ignition (LOI) was measured with muffle furnace at Akita University. Procedure to obtain LOI is in Appendix 3.1. To calculate LOI, formula is as follows:

a = weight of crucible
b = weight of crucible + weight of sample
c = total mass after combustion
LOI = b-c/b-a*100

Glass beads preparation was prepared by a mix of the powder sample with flux A10 (1 gr) and A 20 (3gr) with a sample/flux ratio 1: 5, with adjustment of fuse-1 = 120 seconds, Fuse-2 = 240 seconds and Fuse-3 = 240 seconds with 1200^{o}C temperature (Fig. 3.4). The samples were analyzed by a Rigaku ZSX Primus II at Akita University (Fig.3.5).

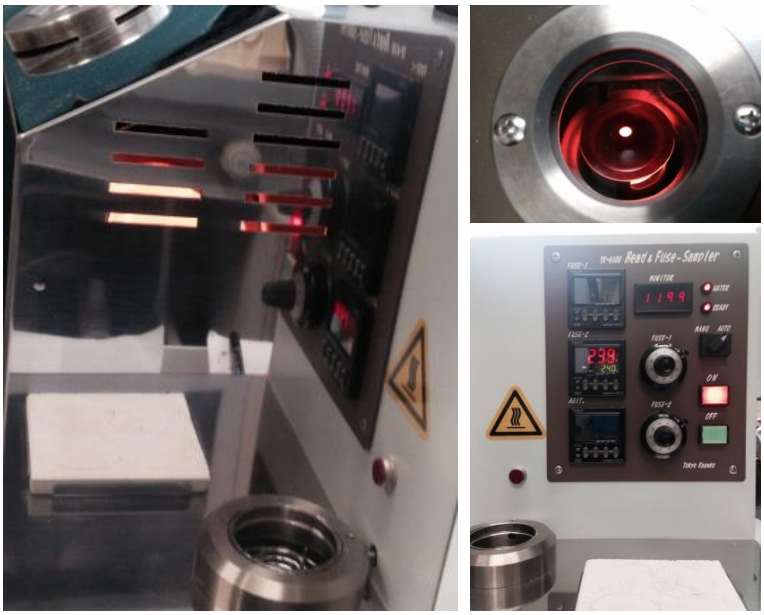

Fig. 3.4 TK-4100 Beads and fuse-sampler for glass beads maker at Akita University.

Fig. 3.5 Rigaku ZSX primus II at Akita University.

3.5 Induced Coupled Plasma Mass Spectrometry (ICP-MS)

To obtain trace elements and rare earth elements compositions, powdered rocks were crushed by an iron mortar and pulverized using an agate mortar. The 0.2 g of sample powder was mixed with lithium metaborate flux of 0.9 gr and fused in a furnace at 1000°C. The sample melt is cooled and dissolved in 100 ml of 4% HNO_3 and or 2% HCl solution. Whole-rock contents of rare earth elements and trace elements were analyzed by ICP-MS at ALS Chemex, North Vancouver, Canada.

3.6 Scanning Electron Microscope-Energy Dispersive Spectroscopy (SEM-EDS)

SEM-EDS analysis was conducted to determine the composition of REE-bearing minerals using a JEOL JSM-6610 LV (Fig. 3.6a) and JEOL IT 300 LV at Akita University. Identification of elements and their concentrations were performed using a program of Oxford Instruments. Selected polished thin samples were carbon coated with a JEOL-560 Auto Carbon Coater (Fig. 3.6b) and then qualitative analysis was conducted for the identification REE-bearing minerals. The condition of measurements are as follow:

1. Accelerating Voltage = 15 kV
2. Filament Load current (L.C.) = 60 µA
3. Spot size = 72
4. Z-axis distance = 10 mm
5. Working distance = 10 mm with good beam stability

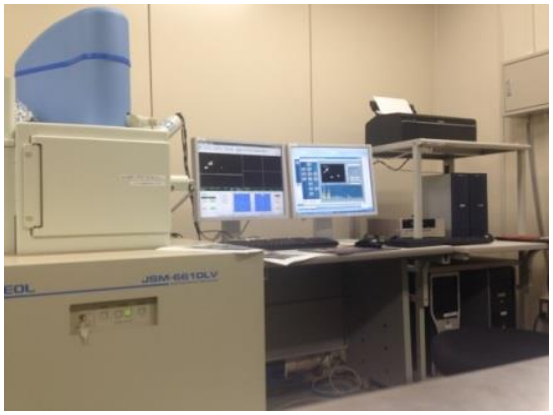

Fig. 3.6 a). JEOL 560, b). a JEOL JSM-6610 Scanning Electron Microscope and c). Carbon coater at Akita University.

3.7. Sequential Extraction

Sequential extraction of trace metals from weathered rocks and sediments is a useful technique for determining chemical form of minerals in weathered materials. Sequential extraction schemes (Miller et al., 1986) which were applied in the analysis of hydrothermally-altered and weathered granitic rocks in Southern Thailand (Imai et al., 2013), are employed in this study. The reagents employed and chemical forms solubilized with 0.5g sample weight are listed below. The procedures are shown in the Fig, 3.7.

(1) Soluble: 20-mL H_2O, shaken 16h,

(2) Exchangeable (neutral salt): 20mL 0.5M $Ca(NO_3)_2$, 16h,

(3) Pb-displaceable: 20mL 0.05M $Pb(NO_3)_2$, 16h,

(4) Acid soluble: 20mL 0.44M CH_3COOH, 8h,

(5) Mn Oxide-occluded: 20mL 0.01M $NH_2OH \cdot HCl$ + 0.1M HNO_3, 30min,

(6) Organically bound: 20mL 0.1M $K_4P_2O_7$, 24h,

(7) Amorphous Fe oxideoccluded: 20mL 0.175M $(NH_4)_2C_2O_4$+ 0.1M $H_2C_2O_4$ (oxalate reagent), in darkness, 4h,

(8) Crystalline Fe oxide occluded: 25-mL oxalate reagent, 85℃, under ultraviolet.

The analysis was using an Agilent Technologies 7500 Series ICP-MS of Akita University (Fig. 3.8).

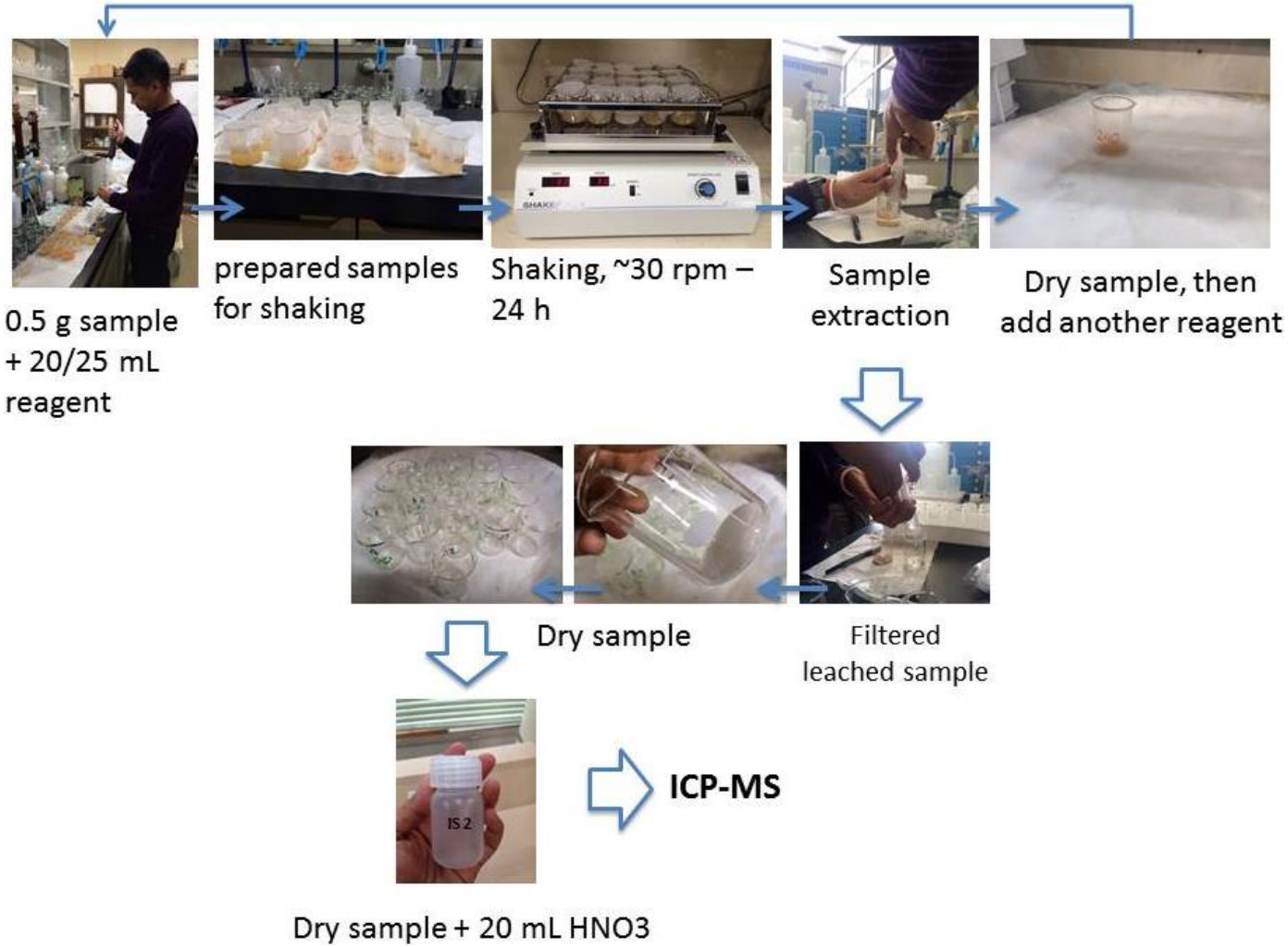

Fig. 3.7 Procedures of sample preparations for sequential leaching.

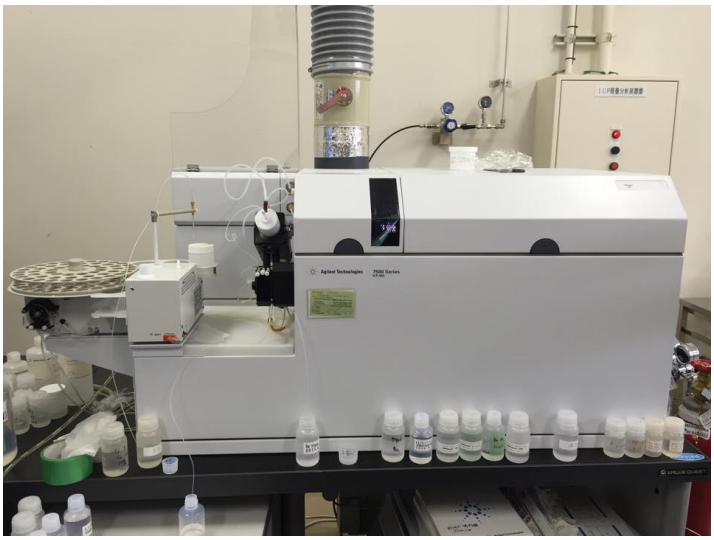

Fig. 3.8 Agilent Technologies 7500 Series ICP-MS at Akita University.

3.8 Thermal Ionization Mass Spectrometry (TIMS)

Sr-Nd isotopic analyses were conducted to elucidate mantle and crustal evolution processes and crustal formation and source of the granitic rocks (De Paolo & Johnson, 1979). Separation of Sr and Nd was undertaken using the procedures described by Yamamoto and Maruyama (1996). Measurement of Sr-Nd isotopic ratio was performed using a Finnigan MAT261 mass spectrometer; $^{87}Sr/^{86}Sr$ and $^{143}Nd/^{144}Nd$ results were normalized to $^{86}Sr/^{88}Sr=0.1194$ and $^{146}Nd/^{144}Nd=0.7219$, respectively. Standard samples of La Jolla, JR-2 and NBS-987, were used. Both separation and measurements were carried at Akita University.

Rb, Sr, Sm, and Nd concentrations were determined by isotope dilution using ^{87}Rb–^{86}Sr and ^{149}Sm–^{150}Nd mixed spikes. Total blanks in the whole procedure were 2.5 ng Rb,

.88 ng Sr, 0.77 ng Sm, and 0.57 ng Nd. Five standards were analyzed for Sr and Nd isotopic ratios, and Rb, Sr, Sm, and Nd concentrations (Yamamoto et al., 2013).

3.8.1 Sr-Nd extraction using double coloumn

An amount of 0.07 g powdered samples were prepared and put into the teflon jar and followed with the addition of ultra pure water and acids (HF and $HClO_4$). Acid digestion using high temperature and fractional evaporation on the hot plate. Separation using column chromatography by ion exchange resin for Sr and REE extraction.

Double column methods to separate Sr and REE, follow the step as follow: 2N HCl, 30 ml to obtain Fe, Rb and Ca, next 2N HCl, 10 ml to recover Rb and Ca. REE are obtained with 6 N HCl, 25 ml addition. Sm and Nd extraction were used small column and using Hydroxyl Isobutyric Acid (HIBA) mixed with superQ water at 4.5 pH. Add 7 ml HIBA to obtain Sm$\pm$Ba, 3.5 ml more to obtain Sm, and to obtain Nd, 6.5 ml HIBA was added. The Procedure of analysis was shown in Table 3.1.

3.8.2 Sr-Nd isotopes measurements and calculation

The procedures of Sr-Rb and Sm-Nd extraction for granitoids are depicted in Table 3.1.

Five standards were analyzed for Sr and Nd isotopic ratios, and Rb, Sr, Sm, and Nd concentrations (Yamamoto et al., 2013).

The calculation of initial Sr isotope ratios are using the present-day (measured) $^{87}Sr/^{86}Sr$ (Sr_p) using the equation :

$^{87}Sr/^{86}Sr\ (Sr_p) - {}^{87}Sr/^{86}Sr\ (Sr_i) = {}^{87}Rb/^{86}Sr\ (Sr_p)\ (e^{\lambda t-1})$ (Rasskazov et al., 2010)

Nicolaysen (1961) used this equation for calculating Sr (i) using isochron method, where

$y = mx + b$

y = measured $^{87}Sr/^{86}Sr$ (Sr_p),

m slope = $e \lambda t-1$, x = $^{87}Rb/^{86}Sr$ p (calculated using the Sr_p)

b= unknown Sr (Sr_i)

Sr_i is a powerful tool to trace the geochemical characteristics of the magma source, since the initial Rb-Sr system of a rock unit with a similar magma source tends to have the same Sr_i. Thus even tough the different rock or mineral samples contain different Sr_p, the melt where these samples came from will inherit the same Sr_i isotopic ratio with the source. The slope m requires time (t) to calculate for the Sr. This time refers to the time after they cooling to a temperature at which they become closed system (Faure, 1986). The $^{87}Sr/^{86}Sr$ and $^{143}Nd/^{144}Nd$ isotopic system of 9 samples were analyzed and they have a very good result and reproducible although two samples did not yielded good results in $^{143}Nd/^{144}Nd$.

The initial Nd isotopic ratios usually do not differ widely for whole-rock samples. This is due to a relatively long half-life of Sm and a very limited fractionation between Sm and Nd caused by their similar geochemical behavior.

The isotopic evolution of Nd in the Earth is described in terms of CHUR (Chondritic Uniform Reservoir: DePaolo, 1988). This model mantle is defined to have initial $^{143}Nd/^{144}Nd$ and Sm/Nd ratios equal to those of chondrites.

Table 3.1 Procedure of Sr-Rb and Sm-Nd extraction for granitoids of Sibolga and Panyabungan

Step	Coloumn volumes	Acid
Column I		
Column I (Ln Spec 2mL ca. 0.8cm×4 cm)		
Preparation	25mL×2 times	6N HCL
Preconditioning	25mL×1 times	6N HCL
	25mL×1 times	6N HCL
	0.75 mLx2	2N HCL
Loading samples	1ml	2N HCL
	1ml	2N HCL
	1ml	2N HCL
	1mlx5	2N HCL
	5mLx6	2N HCL
Rb/Sr extraction	5mLx3	6N HCL
REE extraction	5mLx4	6N HCL
Column II (Ln Spec = as Column I) set in temperature 22C		
Preparation	5mL×1 times	HIBA, pH 4.5
	1mL×1 times	HIBA, pH 4.5
	1mL×1 times	HIBA, pH 4.5
	1mL×1 times	HIBA, pH 4.5
	1mL×1 times	HIBA, pH 4.5
	1mL×1 times	HIBA, pH 4.5
	0.5mL×1 times	HIBA, pH 4.5
	1mL×1 times	HIBA, pH 4.5
	1mL×1 times	HIBA, pH 4.5
	1mL×1 times	HIBA, pH 4.5
	1mL×1 times	HIBA, pH 4.5
	1mL×1 times	HIBA, pH 4.5
Collecting Nd	1mL×1 times	HIBA, pH 4.5

The CHUR is widely used for comparison of initial isotopic compositions of studied rocks with that of primitive mantle at the time of their generation. This is done by the $^{\varepsilon i}$Nd notation: $^{\varepsilon i}Nd = ([^{143}Nd/^{144}Nd]_t^{Sa} / [^{143}Nd/^{144}Nd]_i - 1) \times 10^4$

Where: t= intrusion age, indexes i decipher initial isotopic ratios, Sa = Sample

CHAPTER 4

GEOLOGY AND OCCURRENCES OF GRANITIC ROCKS IN THE STUDY AREA

Field observation on the granitic rocks was conducted at Sibolga, Panyabungan, Muara Sipongi, and Kotanopan, in the western part of North Sumatra, Indonesia. They are located on the west coast of the North Sumatra (Fig. 4.1). Coordinate of samples locations of the study areas are attached in Appendix 1.

4.1 Sibolga and its surrounding areas

4.1.1 Occurrence of granitic rocks

Granitic rocks around Sibolga consist mainly of Sibolga Granitoids Complex (SGC) of Early Permian to Triassic Age. The granitoids are exposed at abandoned quarries, along road cuts and rivers in the Sibolga area. Exposed granitoids in the quarries are usually weathered while those along road cuts and rivers are commonly fresh, Sibolga granitoids are ilmenite-series, and they are generally pinkish to grayish in color and medium to coarse-grained. The minerals presents are pinkish K-feldspar megacrysts and quartz, plagioclase, biotite and minor hornblende. The alteration has occurred at some places at Sibolga Julu, which are indicated by the occurrences of minor chlorite, and clay minerals (Sibolga Julu). The study areas in Sibolga include Sarudik (SRD), Sibuluhan Sihaporas (SS), Sibolga Julu (SJ), Adian Koting (AK), Tukka (TK) and Sihobuk (SHB (Figure 4.2).

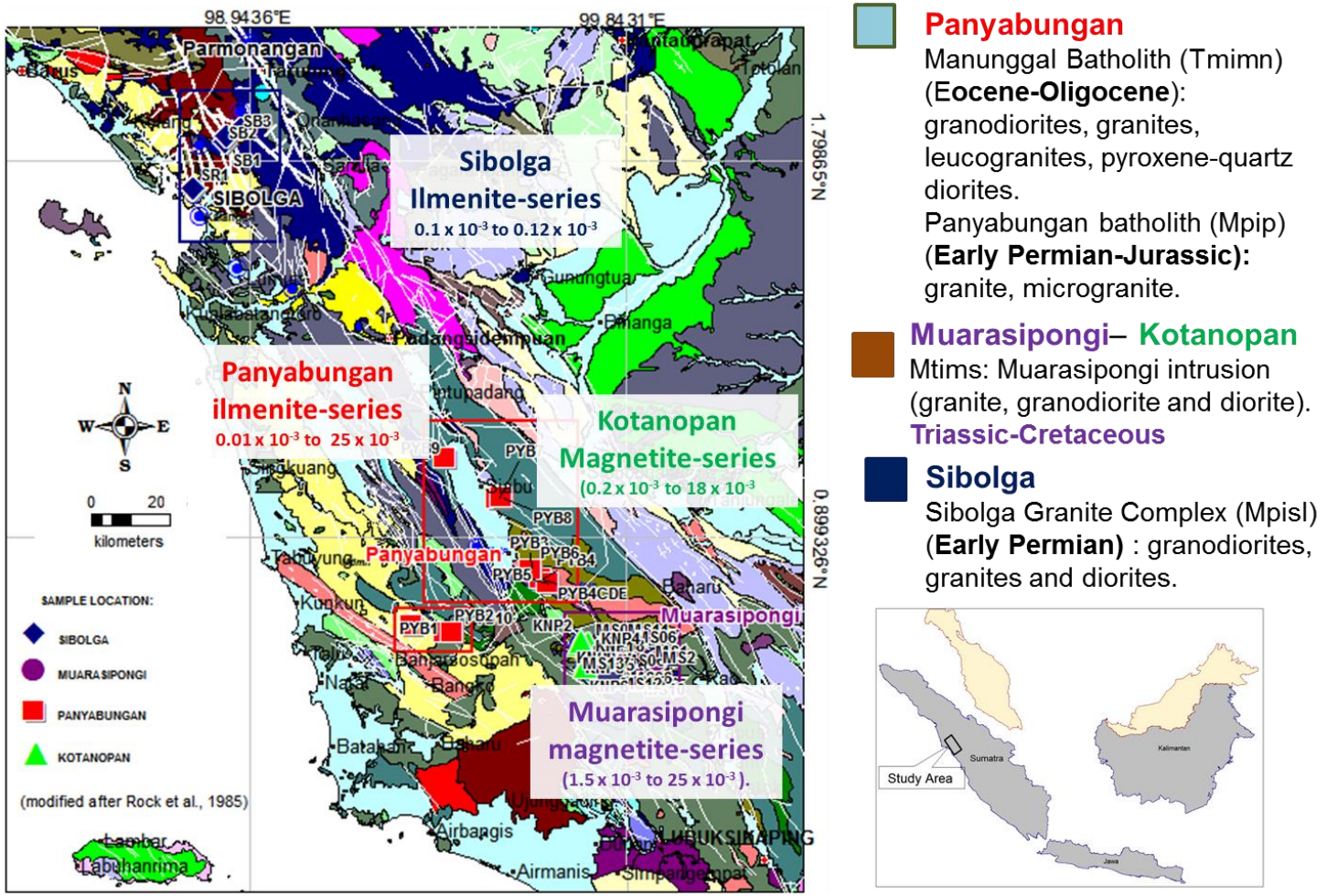

Fig. 4.1 Locations and geological map of Sibolga and its surrounding areas (modified after Aspden et al., 1984).

Observation, sample collections, magnetic susceptibility and radioactivity measurements were carried out mainly on relatively fresh or least altered rocks (Fig. 4.2).

The Sarudik (SRD) Granitoids are pink to brownish in color, coarse-grained, consisting mainly of K-feldspar megacrysts (up to 3 cm), quartz, plagioclase, biotite, hornblende. Basaltic dikes and mafic enclaves were observed in some outcrops.

The Sibuluhan Sihaporas (SS) Granitoids are light gray to pinkish in color, coarse-grained, mainly composed of K-feldspar megacrysts, quartz, plagioclase, and biotite (Fig. 4.3). Similar to that of Sarudik, basaltic dikes and mafic enclaves were observed in some of outcrops at Sibuluhan Sihaporas.

The Sibolga Julu (SBJ) granitoids are pinkish to gray in color, medium to coarse-grained, composed of K-feldspar megacrysts (up to 2 cm), quartz, plagioclase, and biotite.

The Tukka Granitoids are gray to pinkish in color, coarse-grained, composed mainly of K-feldspar megacrysts (up to 2 cm), quartz, plagioclase and biotite. Chlorite occurs as secondary minerals.

The Sihobuk Granitoids are gray to pinkish in color, coarse-grained, composed mainly of K-feldspar megacrysts (up to 1 cm), plagioclase and quartz (Fig. 4.3).

The Tarutung granitoids are pinkish in color, medium to coarse-grained, composed of K-feldspar megacrysts (up to 2 cm), plagioclase, biotite and hornblende.

The granitoids from Adian Koting (AK) are light gray in color, coarse-grained, consisting of megacrysts pinkish K-feldspar, plagioclase, biotite, and hornblende (Fig. 4.3).

Weathered granitoids were observed at many places at Sibuluhan Sihaporas, Sarudik and Sibolga Julu. They mainly exhibit wholly weathered zone, orange to light brown in color, homogeneous and original mineral are less visible (horizon B).The sub-weathered

zone is composed of light brown colored loose weathered crust (horizon C). At some places the horizon B and C were covered by transported materials from upper part by rainfall or landslides (Fig. 4.4). Geochemical characeristics of the weathered will be presented in Chapter 8.

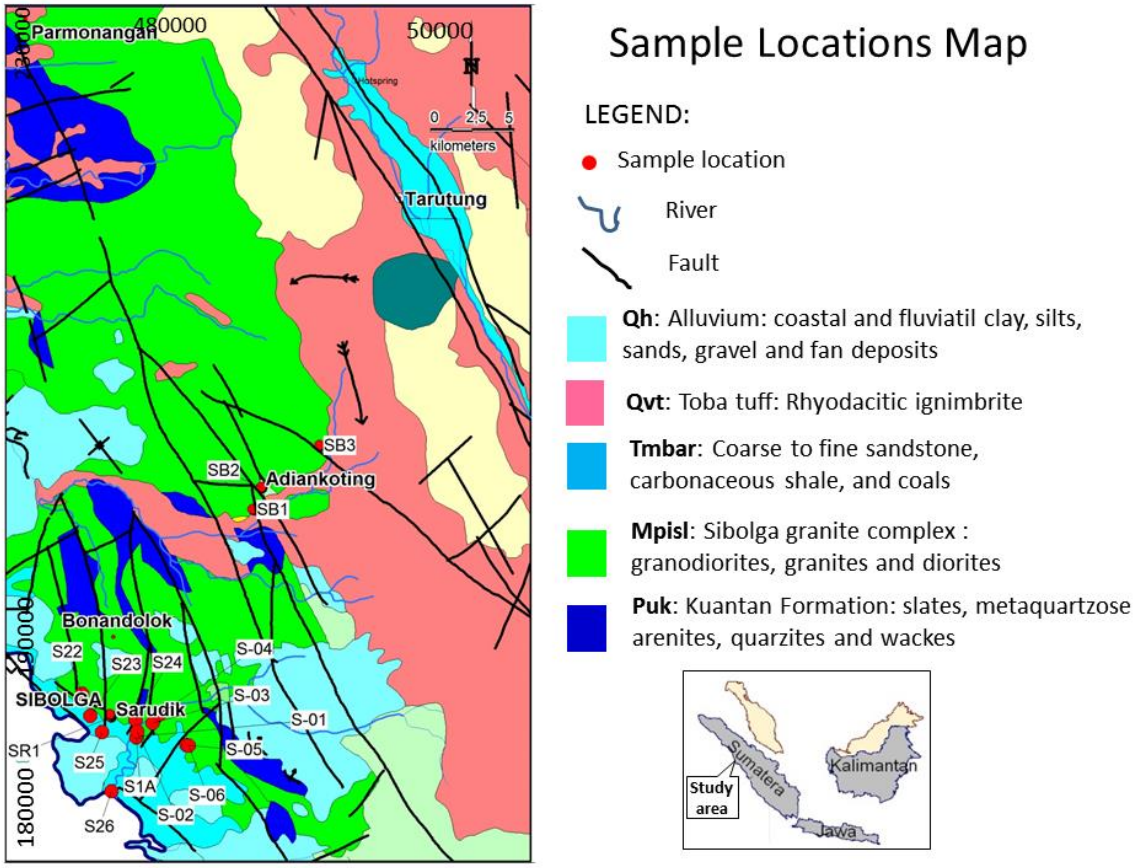

Fig 4.2 Sample location and geological map of Sibolga and its surrounding areas (modified after Rock et al., 1983; Aspden et al., 1982).

4.1.2 Magnetic susceptibility

Magnetic susceptibility of the granitoids of Sibolga is low, ranging from 0.00 to 0.57 $x10^{-3}$ in SI unit, which corresponds to ilmenite-series (Ishihara, 1977).

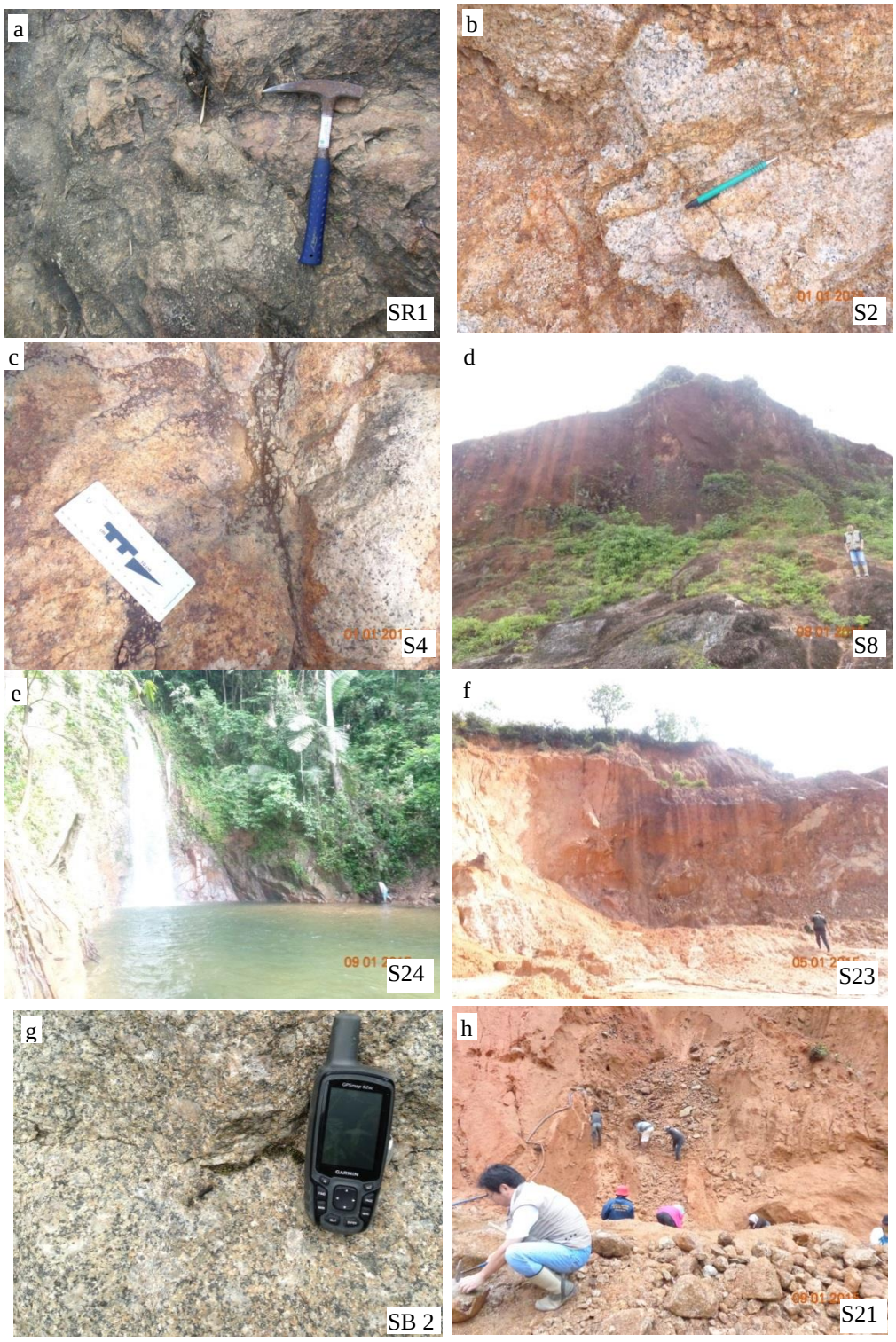

Fig 4.3 Granitoids outcrops at a-b. Sarudik (SR1), c. Sibuluhan Sihaporas(S4), d. Tukka (S8), e. Sihobuk (S24), f. Parombunan-Sibolga Julu (S23), g-h. Adian Koting (SB3 and S21).

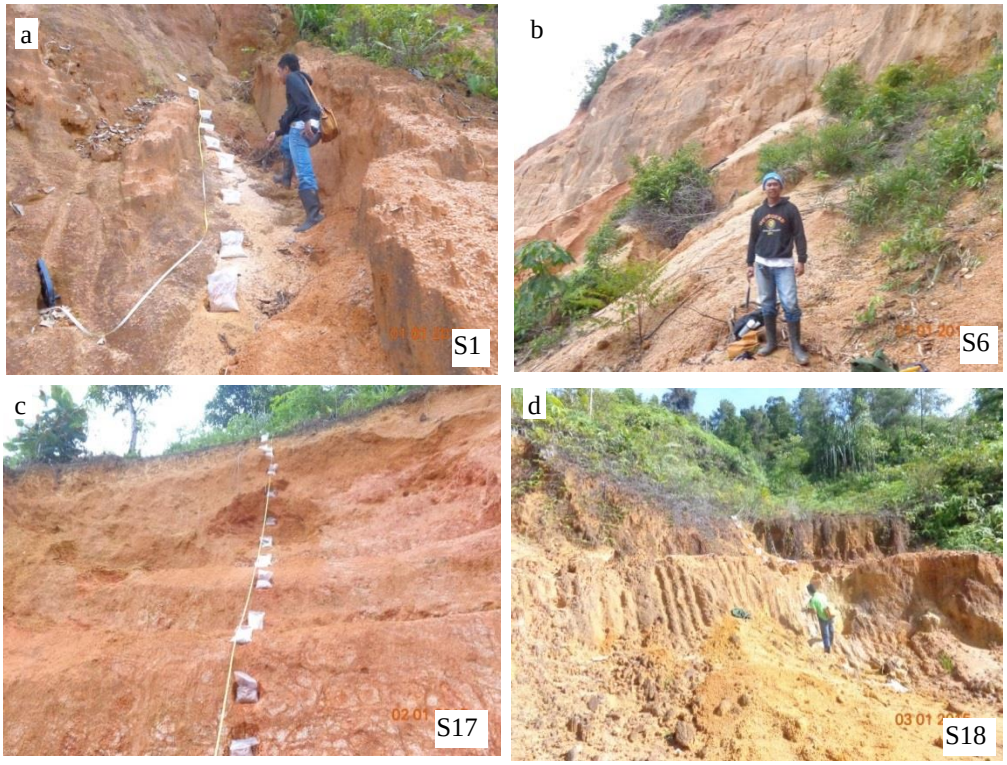

Fig 4.4 Weathered rocks at Sibolga and the surrounding areas: a. Sibuluhan Sihaporas A (S1), b. Sibuluhan Sihaporas B (S6), c. Sarudik (S17) and d. Sibolga Julu (S18).

These values are low compared to those of Muara Sipongi and Kotanopan granitoids ranging from 7.38 to 10.34 x 10^{-3} in SI unit, and 7.93 to 15.78 x 10^{-3} in SI unit, respectively, which correspond to magnetite-series. The magnetic susceptibility of fresh granitoids from Sarudik ranges from 0.01 to 0.57 x10^{-3} in SI unit, that of Sibolga Julu ranges from 0.01 to 0.55 x10^{-3} in SI unit, that of Sibuluhan Sihaporas ranges from 0.00 to 0.16 x10^{-3} SI, that of Tukka ranges from 0.00 to 0.25 x10^{-3} SI, that of Tarutung ranges from 0.02 to 0.24 x10^{-3} SI, and that of Adian Koting ranges from 0.02 to 0.24 x10^{-3} SI. Summary of magnetic susceptibility of fresh granitoids in the study area, in general, is depicted in Figure 4.5 and Appendix 3.

4.1.3 Radioactivity

Radioactivity of granitoids from Sarudik ranges from 0.15 to 0.78 µSv/hr, that of Sibuluhan Sihaporas and Adian Koting ranges from 0.35 to 0.61 µSv/hr, and 0.58 to 0.81 µSv/hr, respectively, while that of Tukka ranges from 0.18 to 0.55 µSv/hr, that of Tarutung ranges from 0.62 to 0.67 µSv/hr, and that of Sibolga Julu ranges from 0.33 to 0.89 µSv/hr (Fig. 4.6). The radioactivity of granitoids from Sibolga is higher than that of Muara Sipongi and Kotanopan, which range from 0.12 to 0.17 and 0.1 to 0.12 µSv/hr, respectively (Appendix 3).

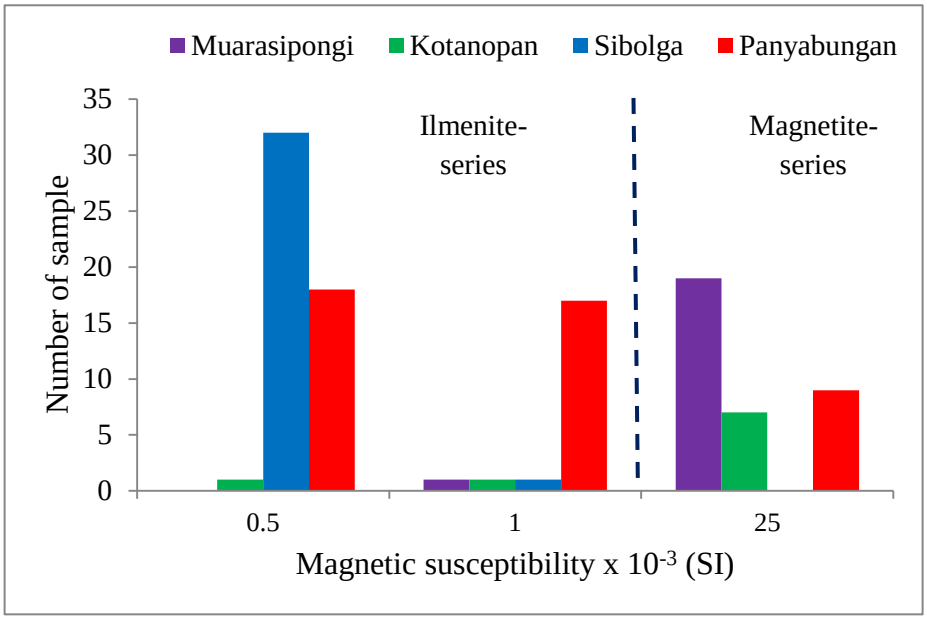

Fig. 4.5 Histogram of magnetic susceptibility of granitoids from Sibolga, Panyabungan and Muara Sipongi. (Dashed lines indicate a border line between magnetite- and ilmenite-series)

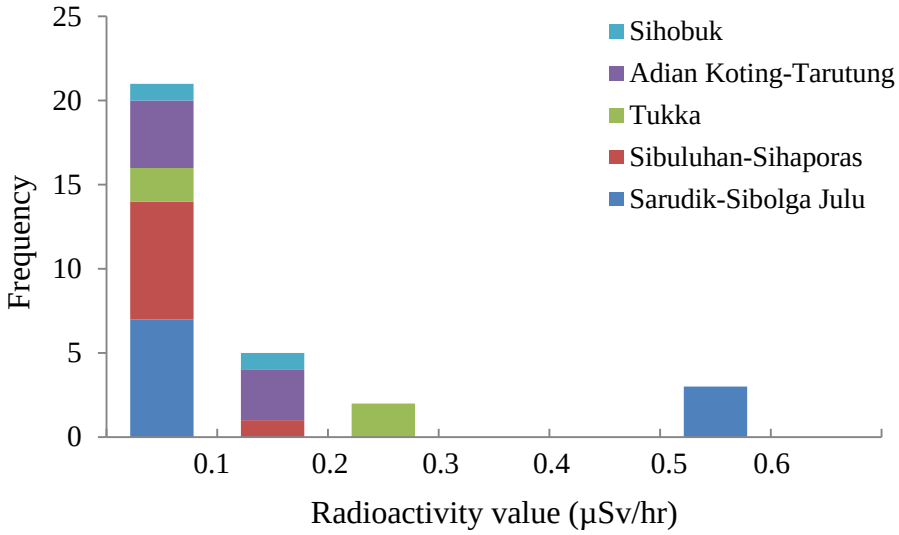

Fig 4.6 Histogram of radioativity of granitoids from Sibolga and the surrounding areas.

4.2 Panyabungan and its surrounding areas

4.2.1 Occurrence of granitic rocks

Granitoids at Panyabungan areas are mainly composed of ilmenite-series in character, and consist of K-feldspar megacrysts, quartz, biotite and muscovite. Mineral segregations were observed, and subangular to angular enclaves were found at Tanjung Jae (Fig. 4.7). A total of 23 samples were collected from Panyabungan areas (Fig. 4.8) (Appendix 1).

Five locations were observed; they are Hutasiantar, Parmompang, Tanjung Jae and Tebing Tinggi and Tano Tombangan (Fig 4.9). Granitoids from Tanjung Julu and Tanjung Jae are less weathered, gray to light brown in color, ilmenite-series, composed of K-feldspar megacrysts (up to 8 cm), quartz, biotite and minor muscovite and iron oxides.

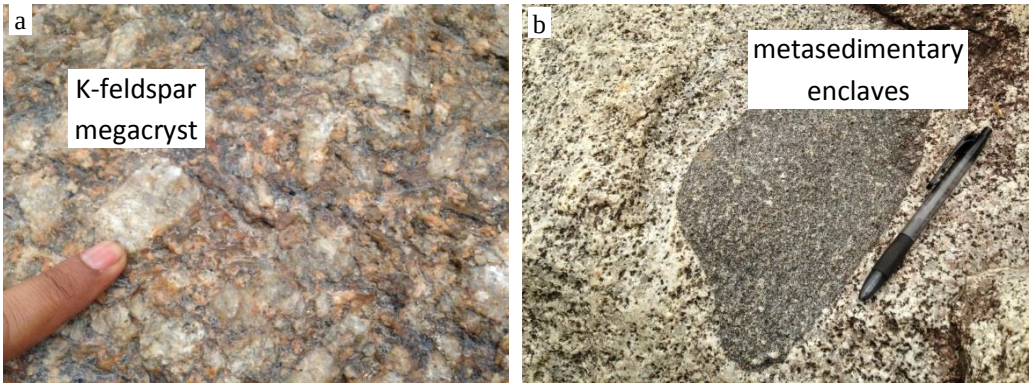

Fig. 4.7 Outcrops of granitoids from Tanjung Jae contain a. K-feldspar megacrysts and b. round shape metasedimentary enclaves.

The granitoids from Pintu Padang Julu (Fig. 4.8c-d) and Tano Tombangan (Fig. 4.8e-f) are ilmenite-series, consisting mainly of K-feldspar, quartz, biotite. A suite of granitoids at Tano Tombangan were mixture of ilmenite-series and magnetite-series granitoids.

Magnetite-series granitoids were indicated by the occurrences of dark green color hornblende and biotite. Alkali feldspar syenites were collected from Tano Tombangan-Si Tumba. They are metamorphosed and brecciated (Fig. 4.8 e-f). Large tourmaline crystals are pegmatitic.

4.2.2 Magnetic susceptibility

Granitoids from Panyabungan are mainly ilmenite-series. Magnetic susceptibility of granitoids from Parmompang, Tebing Tinggi, Tanjung Jae, and Pintu Padang ranges from 0.01 to 0.66 x 10^{-3} in SI unit. Granitoids from Tano Tombangan are mixture of magnetite-series and ilmenite-series (Ishihara, 1977) (Appendix 3).

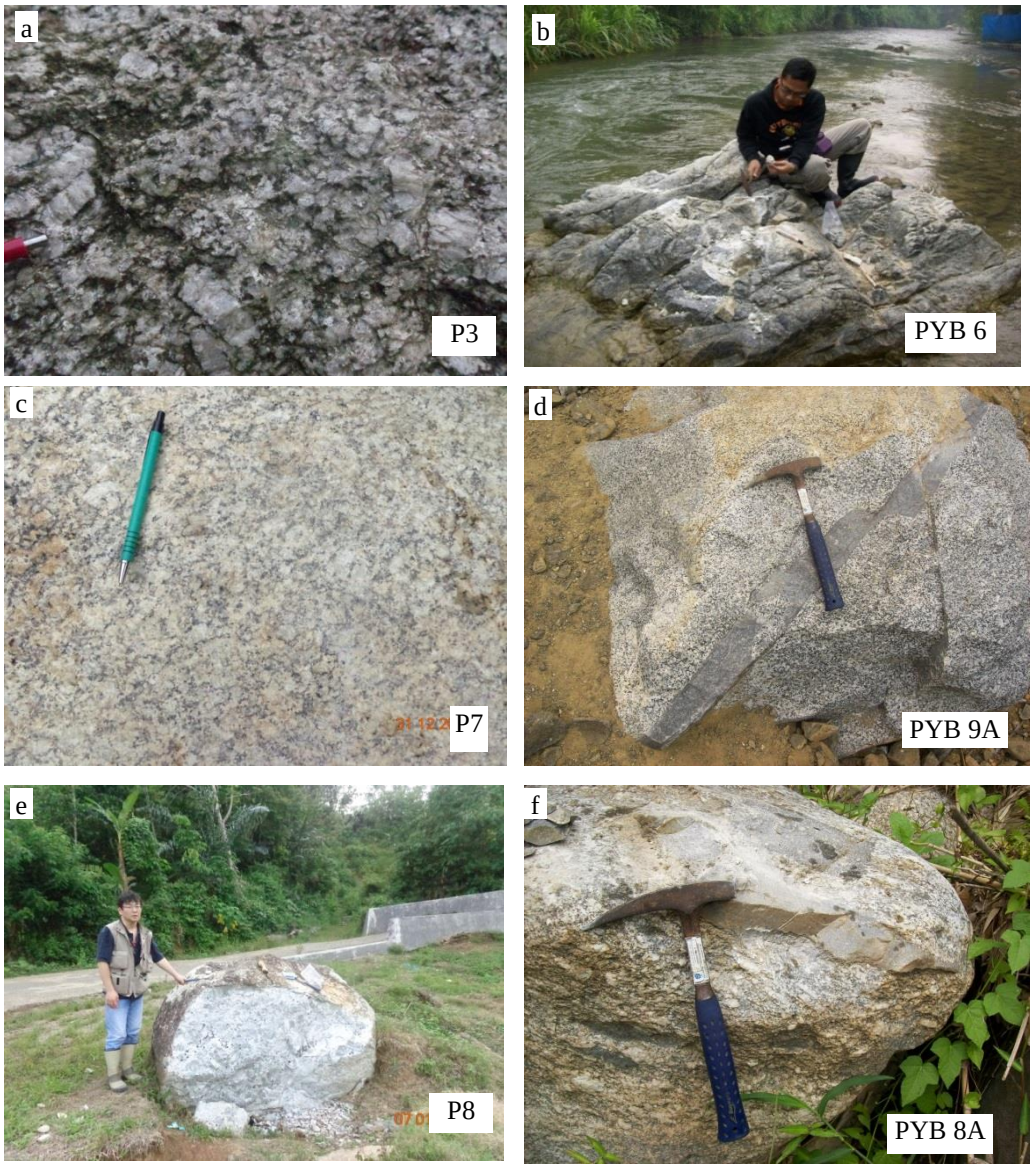

Fig. 4.8 Outcrops of granitoids at Panyabungan and its surrounding areas: a. Parmompang, b. Tebing Pintu Air, c-d. Pintu Padang Julu, e and f. Tano Tombangan.

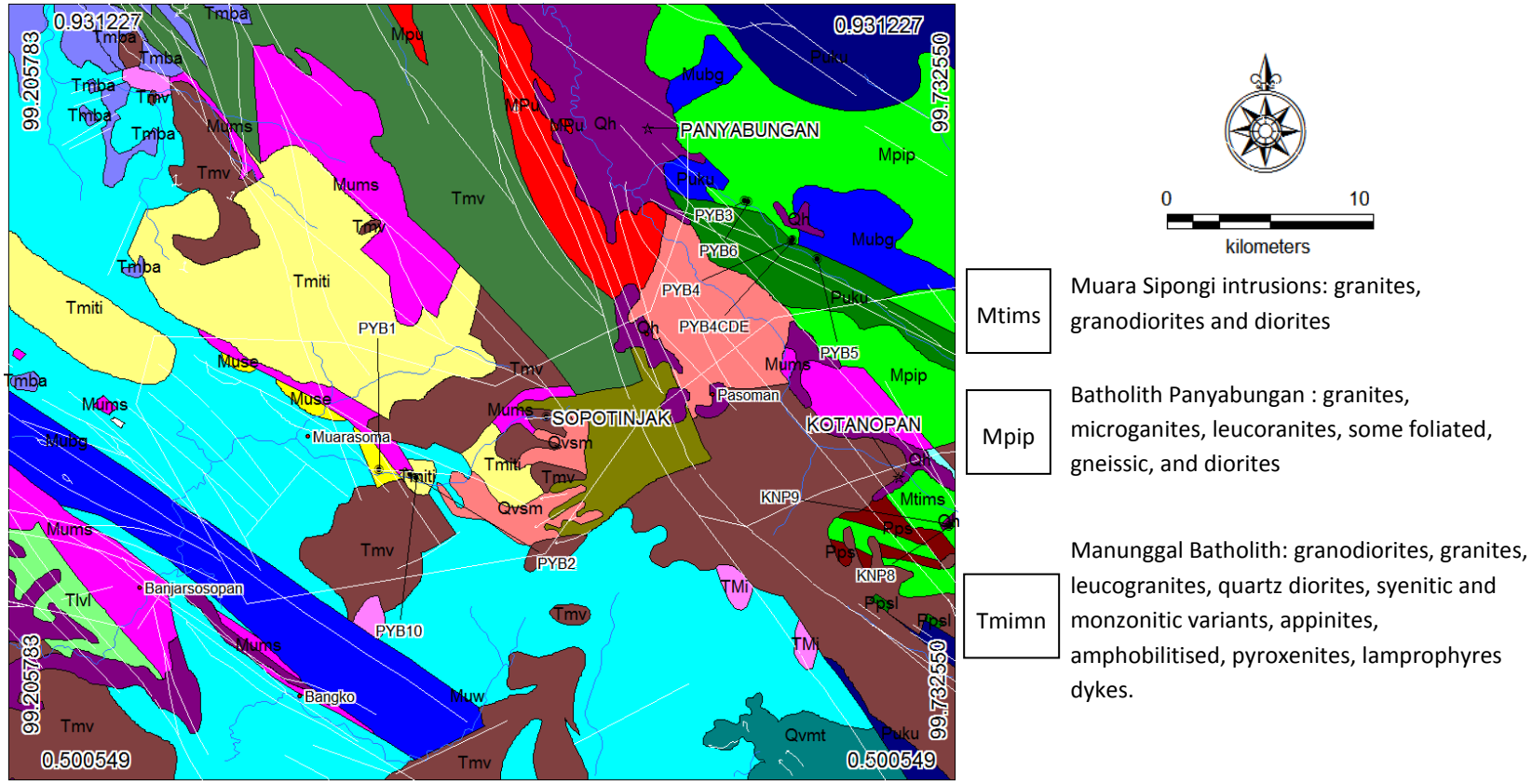

Fig. 4.9 Sample locations of Panyabungan and its surrounding areas (modified after Rock et al., 2012).

Magnetic susceptibility of granitoids from Parmompang ranges from 0.01 to 0.32 x 10^{-3} in SI unit, that of Tebing Tinggi ranges from 0.05 to 0.08 x 10^{-3} SI, that of Tanjung ranges from 0.03 to 0.15 x 10^{-3} in SI unit, and that of Pintu Padang Julu ranges from 0.01 to 0.23 x 10^{-3} in SI unit. The magnetic susceptibility of ilmenite-series and magnetite-series granites from Tano Tombangan ranges from 0.08 to 0.94 x 10^{-3} and 1.53 to 25 x 10^{-3} in SI unit, respectively (Fig 4.10).

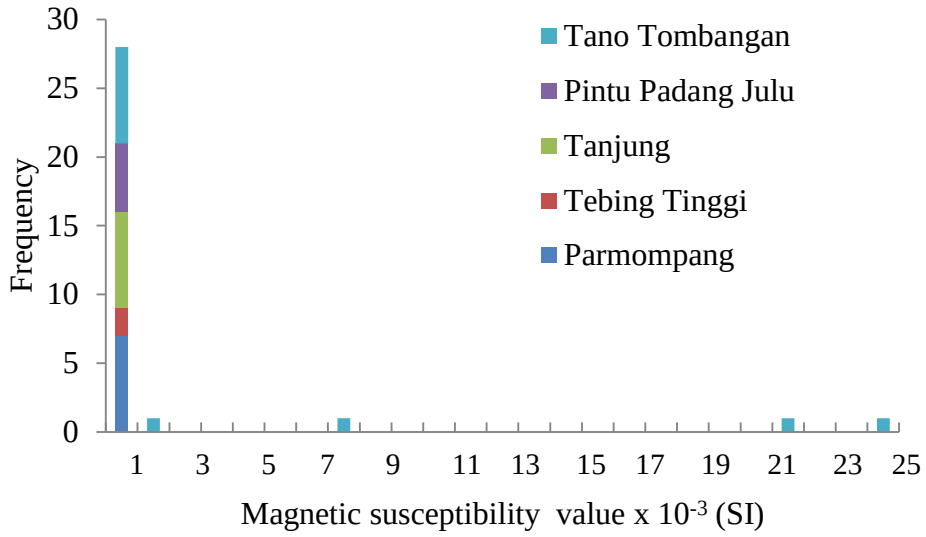

Fig. 4.10 Histogram of magnetic susceptibility of granitoids from Panyabungan and its surrounding areas.

4.2.3 Radioactivity

Radioactivity of Panyabungan Granitoids ranges from 0.18 to 0.47 µSv/hr, and compared to that of Sibolga Granitoids which have maximum radiation at 0.89 µSv/hr, Panyabungan Granitoids has lower radioactivity (Appendix 4). Radioactivity of granitoids from Parmompang ranges from 0.18 to 0.28 µSv/hr, that of Tebing Tinggi is 0.34 µSv/hr,

that of Tanjung Jae ranges from 021 to 0.37 µSv/hr, that of Pintu Padang Julu is 0.47 µSv/hr, while that of Tano Tombangan ranges from 0.21 to 0.41 µSv/hr (Fig. 4.11).

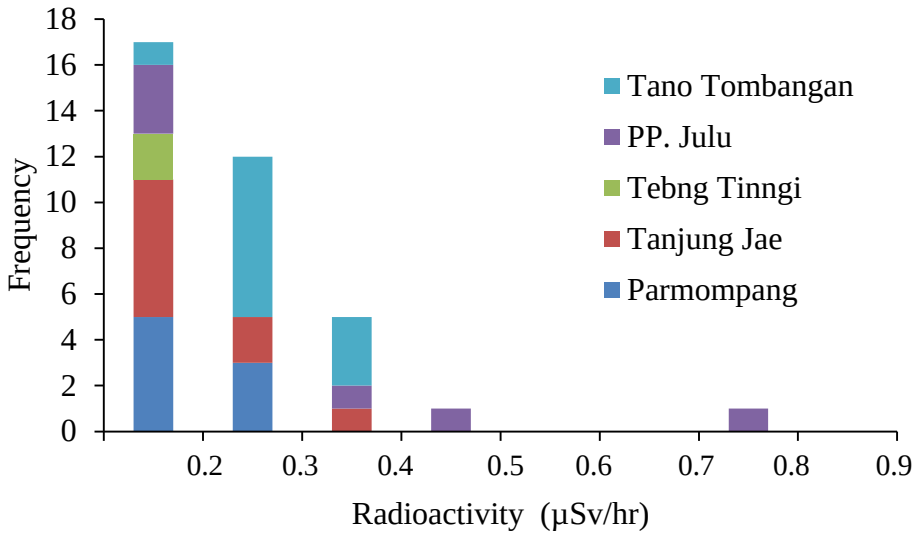

Fig. 4.11 Histogram of radioactivity of granitoids from Panyabungan and its surrounding areas.

4.3 Muara Sipongi and its surrounding areas

4.3.1 Occurrence of granitic rocks

The granitoids at Muara Sipongi and the surroundings areas are usually altered. Seventeen samples were collected from Muara Sipongi (Fig. 4.12e), Sungai Cibadak, Hutadangka, Pekantan (Fig. 4.12a-d) and Tanjung Alai (Fig.4.12f-h) (Fig. 4.13) (Appendix 1). Ten out of seventeen granitoids samples from Muara Sipongi and Tanjung Alai were relatively fresh, while the rest of granitoids samples collected from Pekantan and Sungai Cibadak were altered. Granitoids from Muara Sipongi contained mafic enclaves and mafic intrusions (Fig 4.12b).

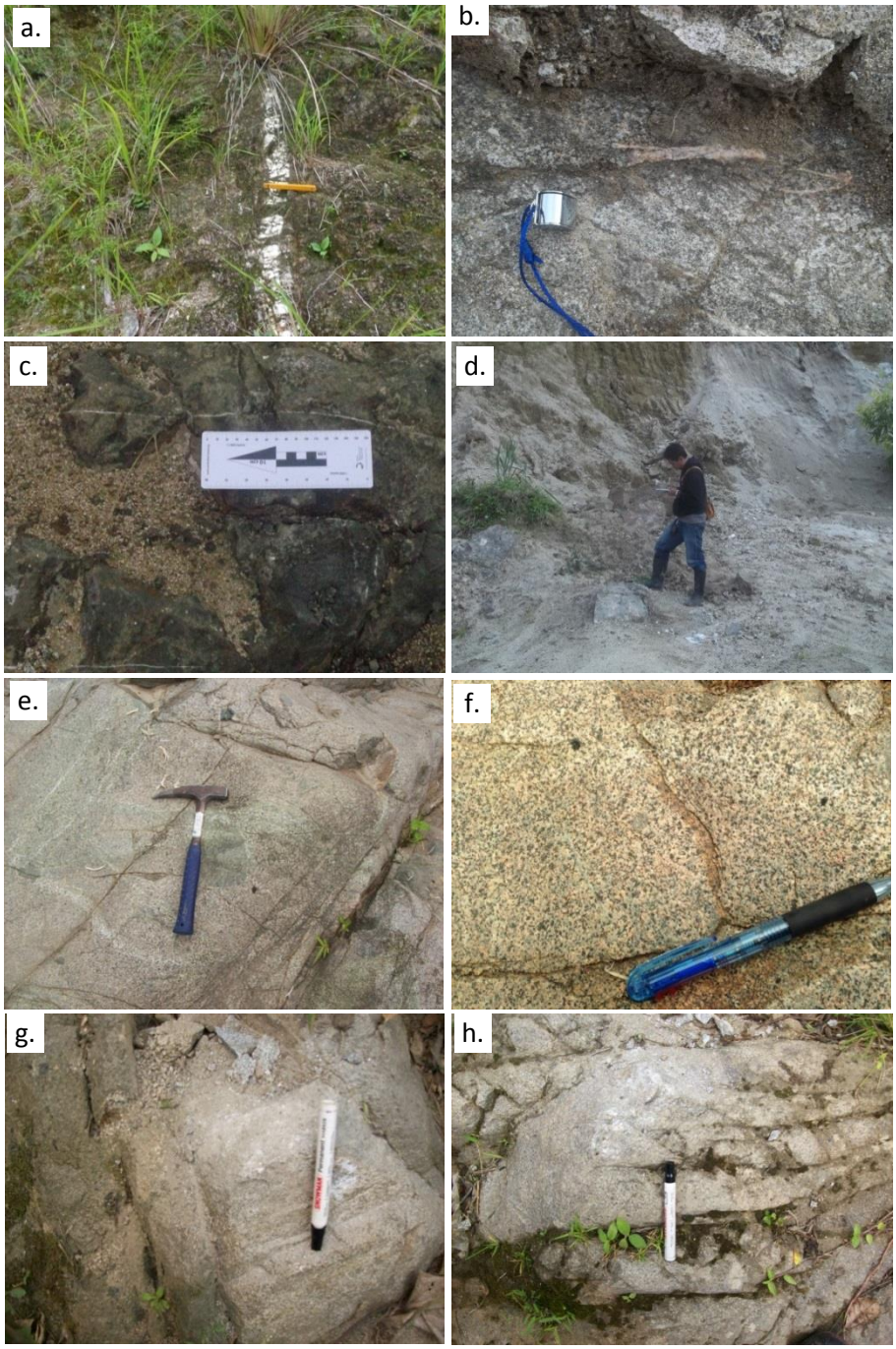

Fig. 4.12 Outcrops of granitoids at Muara Sipongi and its surrounding areas: a-d. Pekantan, e. Muara Sipongi, f-h. Tanjung Alai.

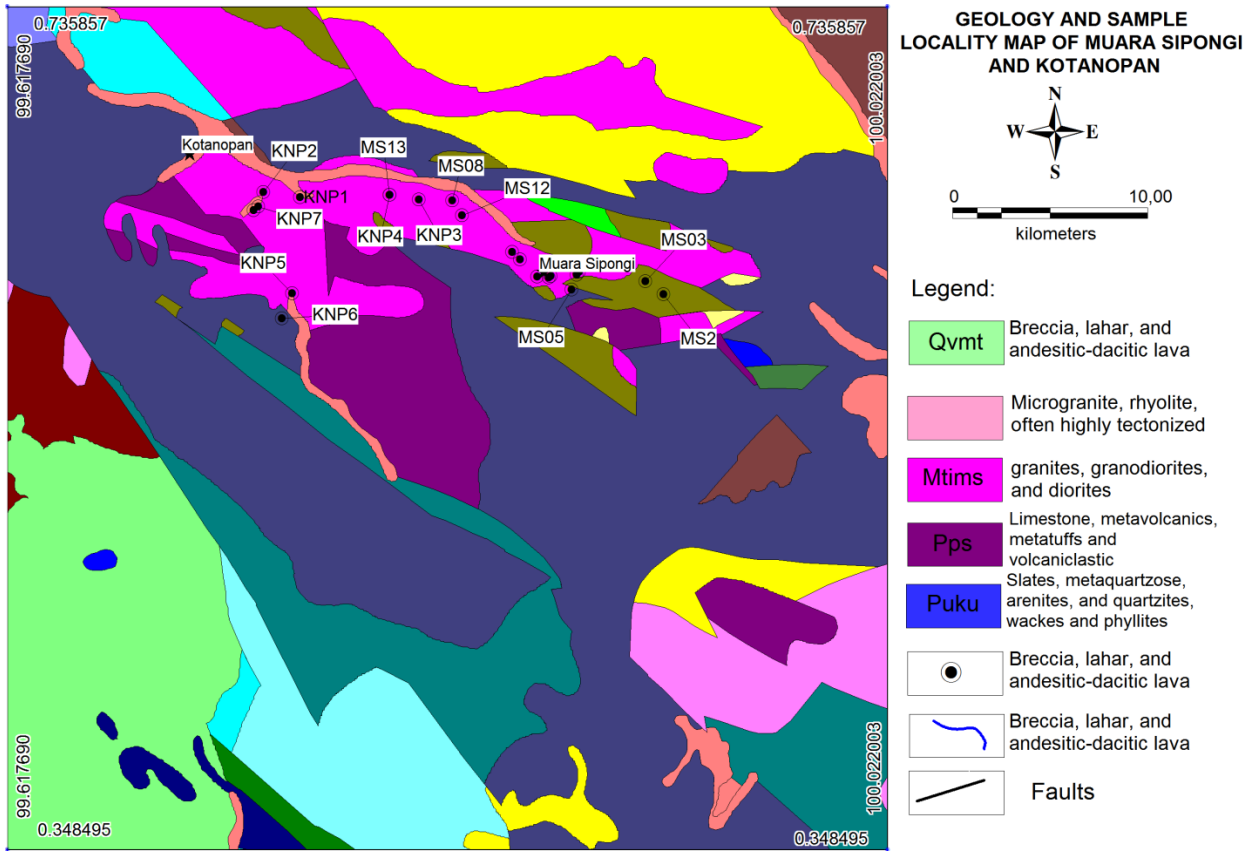

Fig. 4.13 Geological and sample locality map of Muara Sipongi and Kotanopan (modified after Rock et al., 2012).

Granitoids at Muara Sipongi are light gray in color, coarse to medium grained, and granodioritic to granitic in composition. Minerals present are plagioclase, K-feldspar, quartz, biotite, and hornblende. At Pekantan (M4) location, granitoids contain a quartz vein, present in a structure zone which is indicated by the existences of fractures and slicken sides. A meter size block of ultramafic rocks has been found within the granitoids.

4.3.2 Magnetic susceptibility

Summary of magnetic susceptibility is attached in Appendix 3.

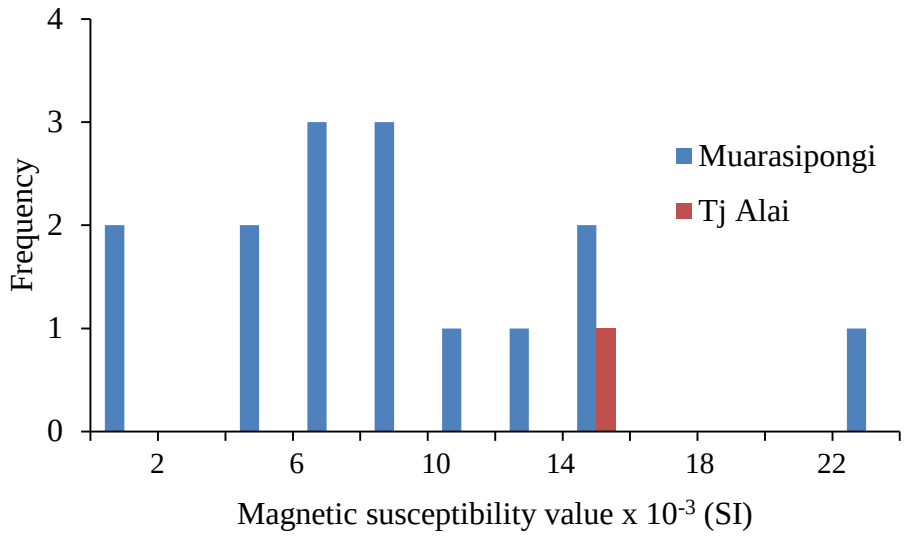

Fig. 4.14 Histogram of magnetic susceptibility of granitoids in Muara Sipongi and Tanjung Alai.

Granitoids from Muara Sipongi are magnetite-series. The magnetic susceptibility ranges from 7.4 to 10.3 x 10^{-3} in SI unit (Fig. 4.14). Granitoids from Tanjung Alai is magnetite-series, and its magnetic susceptibility is 7.9 x 10^{-3} in SI unit.

4.3.3 Radioactivity

Radioactivity of granitoids from Muara Sipongi ranges from 0.1 to 0.22 µSv/hr while that of Pekantan is 0.1 µSv/hr (Fig.4.15). This radioactivity of granitoids from Muara Sipongi is lower compared to those of Sibolga and Panyabungan (Appendix 4).

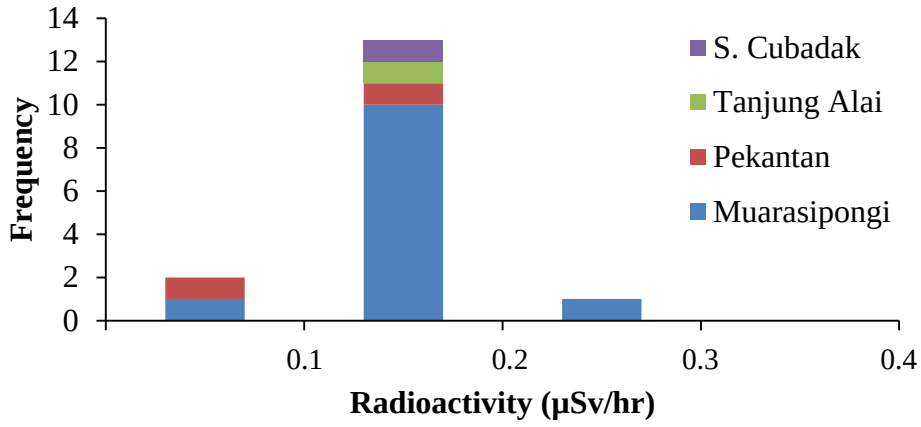

Fig 4.15 Histogram of radioactivity of granitoids from Muara Sipongi and its surrounding areas.

4.4 Kotanopan and its surrounding areas

4.4.1 Occurrence of granitic rocks

Outcrops of granitoids in Kotanopan are similar with those in Muara Sipongi. The granitoids in Kotanopan are mainly altered, and only those at few outcrops were relatively fresh (Figs. 4.13, 4.16) (Appendix 1). The granitoids outcrops are granodioritic in compositions, mainly composed of plagioclase, quartz, K-feldspar, biotite and hornblende. Mafic enclaves exist in some granitoids (Fig. 4.17). A total of nine samples of granitoids were collected from Kotanopan, but only two samples are relatively fresh.

Fig. 4.16 Outcrops of altered and least altered granitoids.

Fig. 4.17 Outcrops of granitoids from Kotanopan showing gray color and contain mafic enclaves.

4.4.2 Magnetic susceptibility

Magnetic susceptibility measurements were conducted on relatively fresh or least altered granitoids (Appendix 3). The magnetic susceptibility corresponds to magnetite-series granites, and they range from 2.3 to 13.6 x 10^{-3} in SI unit (Fig. 4.18).

4.4.3 Radioactivity

Radioactivity of granitoids from Kotanopan is lower contrasted to those of Muara Sipongi, Panyabungan, and Sibolga (Appendix 4). The radioactivity ranges from 0.1 to 0.12 µSv/hr. Summary of radioactivity value depicted in Fig. 4.19.

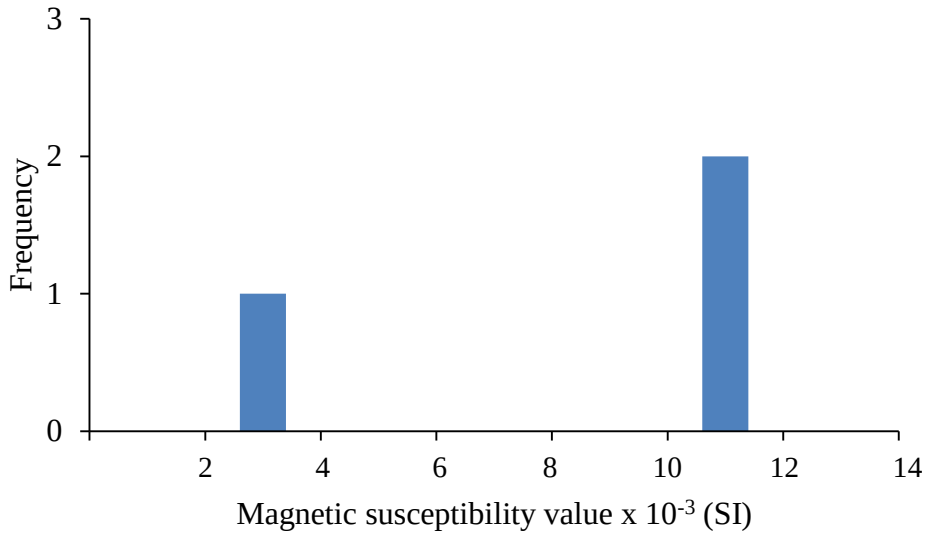

Fig. 4.18 Magnetic susceptibility of fresh granitoids from Kotanopan.

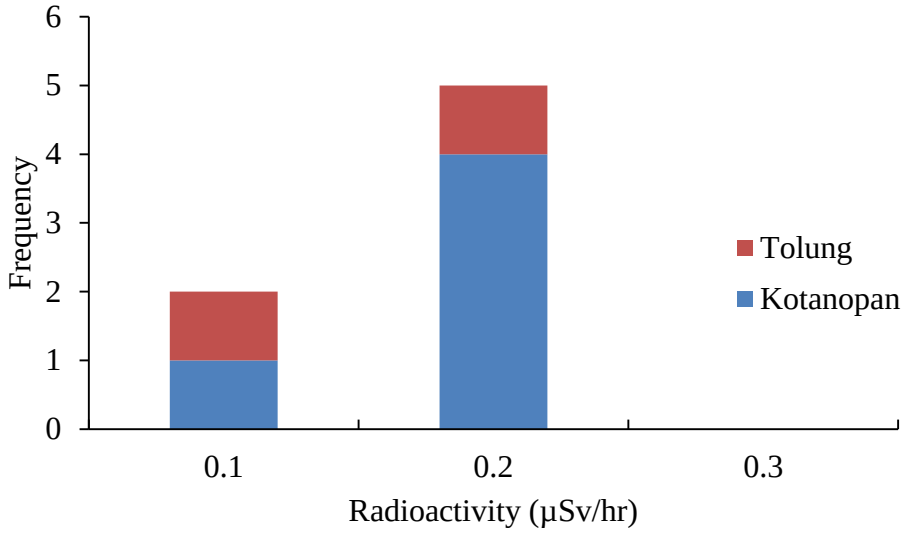

Fig. 4.19 Histogram of radioactivity of Kotanopan and its surrounding areas.

CHAPTER 5

PETROGRAPHY

Mineral assemblages of the granitoids in Sibolga, Panyabungan, Muara Sipongi and Kotanopan were studied on the basis of petrography.

5.1 Petrography of granitoids from Sibolga

Granitoids from Sibolga are classified into quartz alkali feldspar syenite, syenogranite, alkali feldspar granite, alkali feldspar syenite and quartz syenite on the basis of modal abundance of quartz, alkali feldspar, and plagioclase (after Le Bas & Streckeisen, 1991; Streickeisen, 1976). The granitoids from Sibolga contain REE-bearing minerals such as apatite, allanite, and titanite. Summary of mineralogical composition of the samples is shown in Table 5.1 and Figure 5.1.

Syenogranite from Sarudik (SR1) is composed mainly of K-feldspar megacrysts, quartz, plagioclase, hornblende, biotite and cordierite (Figs. 5.1a, 5.1b). Cordierite occurs as xenocrysts included in K-feldspar. Zircon, apatite, allanite, titanite and ilmenite are accessory minerals. Alkali feldspar granite from Sarudik (SR2 and S25) is composed mainly of K-feldspar megacrysts, plagioclase, quartz, biotite and minor muscovite. Titanite, zircon, allanite, magnetite and ilmenite are accessory minerals. K-feldspar is present as perthite, microperthite and microcline. K-feldspar, plagioclase and biotite are partly altered to chlorite and sericite (Table 5.1, Figs. 5.1c, 5.1d). Quartz alkali feldspar syenite from Sarudik (S14) is composed chiefly of K-feldspar megacrysts, plagioclase, quartz and biotite. Apatite and allanite are accessory minerals (Table 5.1, Fig. 5.1e). Garnet is present

in the quartz alkali feldspar syenite at Tarutung (S18A) (Table 5.1). K-feldspar commonly shows microcline twinning. Quartz exhibits undulose extinction. K-feldspar, plagioclase and biotite are partly altered to chlorite and sericite. Corundum occurs as xenocrysts and inclusions in K-feldspar in the quartz alkali feldspar syenite at Sihobuk (S24) (Table 5.1).

Syenogranite at Sibuluhan Sihaporas (S5) is composed chiefly of K-feldspar, plagioclase, biotite, hornblende and quartz (Table 5.1, Fig. 5.1f).

Monzogranite from Sibolga Julu is composed mainly of K-feldspar megacrysts, quartz, plagioclase and biotite. Plagioclase is twinned and intergrown with K-feldspar which exhibits microcline twinning. Zircon and apatite are accessory minerals (Table 5.1).

Syenogranite at Adian Koting (SB1) is composed mainly of K-feldspar megacryst, plagioclase, biotite and hornblende. Apatite is present as an accessory mineral. K-feldspar, plagioclase and biotite are partly altered to chlorite and sericite (Table 5.1, Fig. 5.2a). Quartz syenites from Adian Koting (SB2 and SB3) are composed mainly of K-feldspar megacrysts, quartz, plagioclase, hornblende, biotite and minor corundum and cordierite (Table 5.1, Figs. 5.2b, 5.2c). Allanite, apatite, and ilmenite are present as accessory minerals (Table 5.1, Figs. 5.2a, 5.2c). Corundum and cordierite occur as xenocrysts and inclusions in K-feldspar (Table 5.1, Figs. 5.2d, 5.2f). Alkali feldspar syenites from Tukka have almost the same mineral composition with quartz alkali feldspar syenite, but the proportion between K-feldspar megacrysts and quartz is different. They are mainly composed of K-feldspar megacrysts, quartz, plagioclase, hornblende, and biotite. Zircon and ilmenite are accessory minerals (Table 5.1).

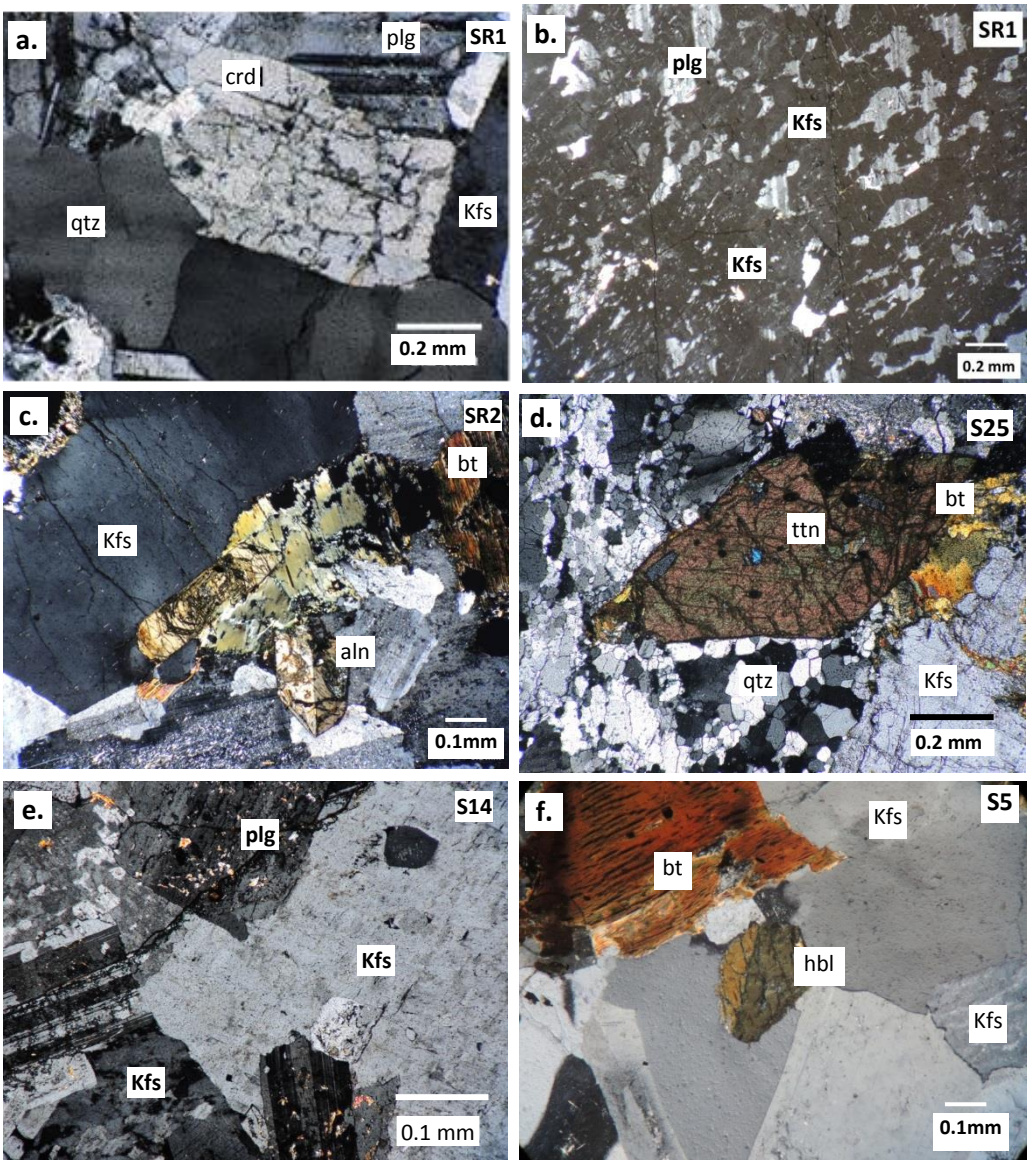

Fig. 5.1 Photomicrographs under crossed nicols:
a. Cordierite (crd) as a xenocryst, with K-feldspar (Kfs), in syenogranite from Sarudik,
b. K feldspar (Kfs) megacrysts showing microperthite texture, in syenogranite from Sarudik,
c. Allanite (aln) occurence with K feldspar (Kfs) and biotite (bt), in alkali feldspar granite from Sarudik,
d. Titanite (ttn) with K-feldspar (Kfs) and quartz (qtz), in alkali feldspar granite from Sarudik,
e. K feldspar (Kfs) megacryst with plagioclase (plg), in quartz alkali feldspar syenite from Sarudik.
f. K feldspar (Kfs) in association with biotite (bt) and hornblende (hbl), in syenogranite from Sibuluhan Sihaporas.

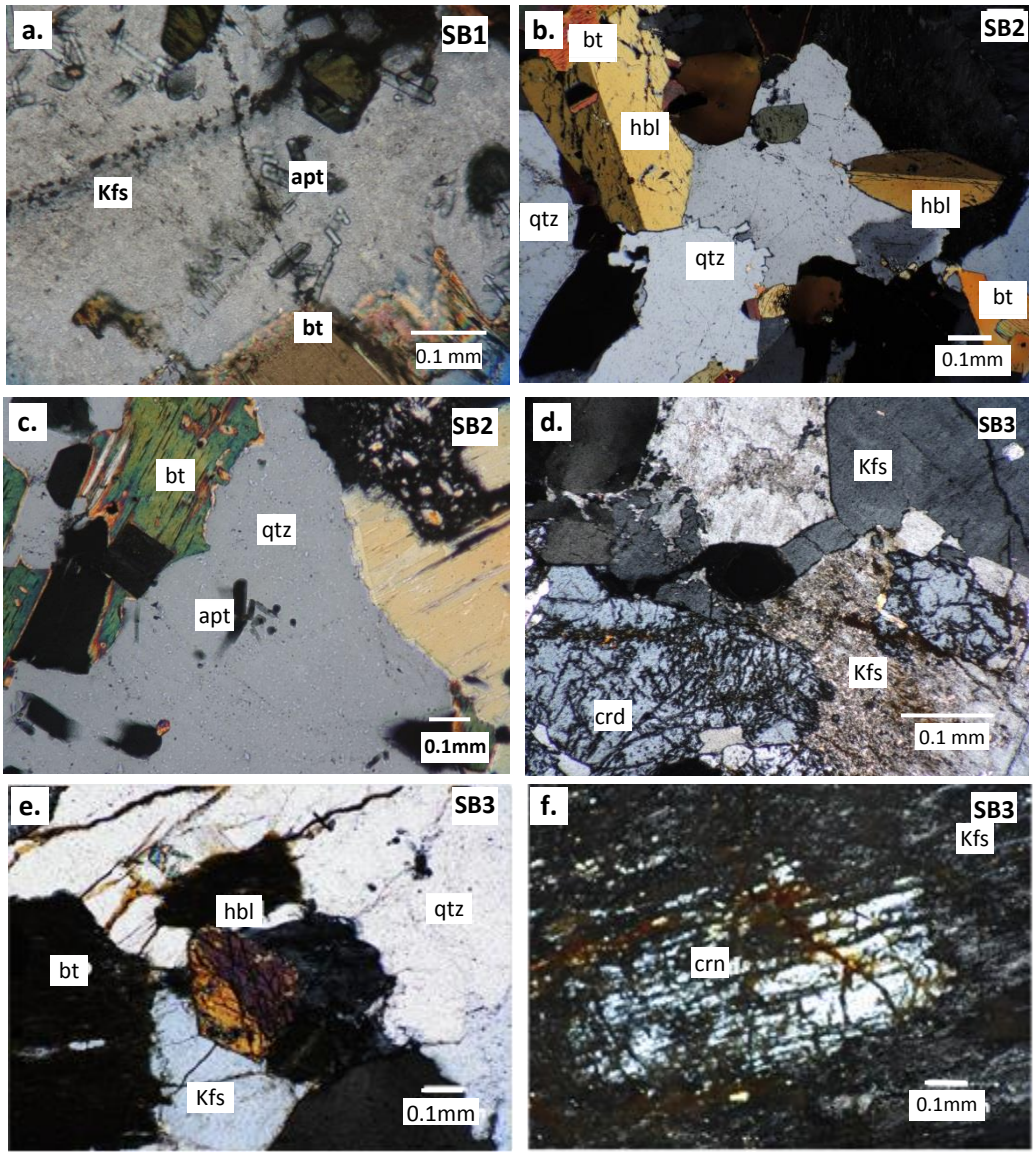

Fig. 5.2 Photomicrographs under crossed nicols:

a. Megacryst of K-feldspar (Kfs) with biotite (bt) and contain apatite (apt) as inclusions, in syenogranite from Adian Koting,
b. Hornblende (hbl) with biotite (bt) and quartz (qtz), in quartz syenite from Adian Koting,
c. Zircon occurs as inclusion in biotite, and apatite as inclusion in quartz, in quartz syenite from Adian Koting,
d. Cordierite (crd) as xenocryst with K-feldspar, in quartz syenite from Adian Koting,
e. Hornblende (hbl) with biotite (bt) and quartz (qtz), in quartz syenite from Adian Koting,
f. Corundum (crn) as xenocryst in K-feldspar (Kfs), in quartz syenite from Adian Koting.

Table 5.1 Modal composition of granitoids in Sibolga and its surrounding areas

No	Locality	Sample	Rock Name	Primary mineral														Secondary minerals					Ore Minerals			Total
		code		Kfs	plg	hbl	bt	qtz	crn	crd	px	gt	mv	ttn	zr	apt	aln	qzs	chl	ep	cal	ser	op	mt	ilm	
1	Sarudik	SR 1	syenogranite	56	14			20	2				4	*	*	*			2			2	*			100
2	Sarudik	SR2	alkali feldspar granite	62	5		6	20			*		3	*	*		*		3			1		*	*	100
3	Sarudik	S14	alkali feldspar syenite	81	4		9	3								*	*		2				1	*		100
5	Sarudik	S16	syenogranite	65	10		2	20					3	*			*									100
6	Sarudik	S25	alkali feldspar granite	58	5		9	26						*	*				2							100
7	Sibuluhan Sihaporas	S1A	syenogranite	65	8			25					2		*		*									100
8	Sibuluhan Sihaporas	S3	quartz syenite	56	9	1	4	10					4		*	*	1		7	1		6	1	*		100
9	Sibuluhan Sihaporas	S4	syenogranite	57	15			20					5		*	*			2			1				100
10	Sibuluhan Sihaporas	S5	syenogranite	50	14	2	4	25					2		*				1			2	1	*	*	100
11	Sibuluhan Sihaporas	S6	quartz alkali feldspar syenite	71	5		5	15					2		*				2							100
12	Sibuluhan Sihaporas	S7	quartz syenite	70	9			11					4		*	*	*		4			1	1			100
13	Tukka	S8	quartz alkali feldspar syenite	62	5		15	8					1		*	*	*		5			4				100
14	Tukka	S9	quartz alkali feldspar syenite	81	6			7											5				1	*		100
15	Tukka	S10	quartz alkali feldspar syenite	89	3			5					2		*								1	*		100
16	Sibolga Julu	S17	quartz syenite	66	20			5				2							4			2	1			100
17	Sibolga Jul	S22	quartz alkali feldspar syenite	67	6		5	12					3		*	*			6				1			100
18	Sibolga Julu	S23(a)	syenogranite	46	20			18					8						2			5	1			100
19	Sibolga Julu	S23(b)	monzogranite	39	27		4	25					2		*				1		1		1			100
20	Tarutung	S18A	quartz alkali feldspar syenite	80				10				5										4	1			100
21	Tarutung	18B	quartz monzonite	41	28	9	10	12			*				*	*	*									100
22	Tarutung	S19	quartz syenite	70	8		10	5							*				4			3				100
24	Adian Koting	S20	quartz syenite	52	14	6	10	15							*		*		3							100
25	Adian Koting	S21	quartz syenite	50	15	6	15	9	*						*	*			3			1	*	*		100
26	Adian Koting	SB 1	syenogranite	28	5		9	21											4			32	1			100
27	Adian Koting	SB2	quartz syenite	58	8	1	15	10		2			2	*					3			1		*	*	100
28	Adian Koting	SB 3	quartz syenite	52	6	4	11	12	1						*	*			4	2		8	1	*	*	100
29	Sihobuk	S24	quartz syenite	56	8			6		*		2			*	*		20	1	1	5	1				100

Abbreviation: Kfs: K-feldspar, plg: plagioclase, hbl: hornblende, bt: biotite, qtz: quartz, crn: corundum, crd: cordierite, px: pyroxene,gt: granet, mv: muscovite, ttn: titanite, zr: zircon, apt: apatite, aln: allanite, qzs: secondary quartz, chl: chlorite, ep: epidote, cal: calcite, ser: sericite,op: opaque minerals, mt: magnetite, ilm: ilmenite. (*) : accessory minerals, minor amounts (<1% vol.)

Granitoids which are fresh or have suffered from low intensity of alteration (least altered) are used for chemical analysis of whole-rock major elements and rare earth elements.

5. 2 Petrography of granitoids from Panyabungan

Granitoids from Panyabungan are classified to monzodiorite, syenite, alkali feldspar syenite, quartz syenite, quartz alkali feldspar syenite, alkali feldspar syenite, alkali feldspar granite, and quartz alkali feldspar granite (Le Bas & Streickeisen, 1991). Summary of petrographic result is depicted in Table 5.2.

Granitic rocks at Tanjung Jae consist of alkali feldspar syenite, quartz syenite, and quartz alkali feldspar syenite. Alkali feldspar syenite is composed of abundant K-feldspar megacrysts, plagioclase, quartz, ± biotite, minor muscovite and ± cordierite, while zircon is an accessory mineral. Quartz alkali feldspar syenite is composed of K-feldspar megacrysts, plagioclase, quartz and biotite with zircon and apatite as accessory minerals (Fig. 5.3). Tano Tombangan Granitoids are mainly alkali feldspar syenite, mainly consist of abundant of K-feldspar megacrysts, ± quartz, ±biotite, ±muscovite, ±hornblende, ±tourmaline (?). Zircon and apatite are accessory minerals. Granitic rocks at Pintu Padang Julu consist of alkali feldspar syenite and quartz alkali feldspar syenite and alkali feldspar syenite. Quartz alkali feldspar syenite is composed of K-feldspar, plagioclase, quartz and biotite. Zircon and apatite are accessory minerals while alkali feldspar syenite is composed of K-feldspar, plagioclase, biotite, ±muscovite, ±hornblende, and ±quartz. Zircon and apatite are accessory minerals.

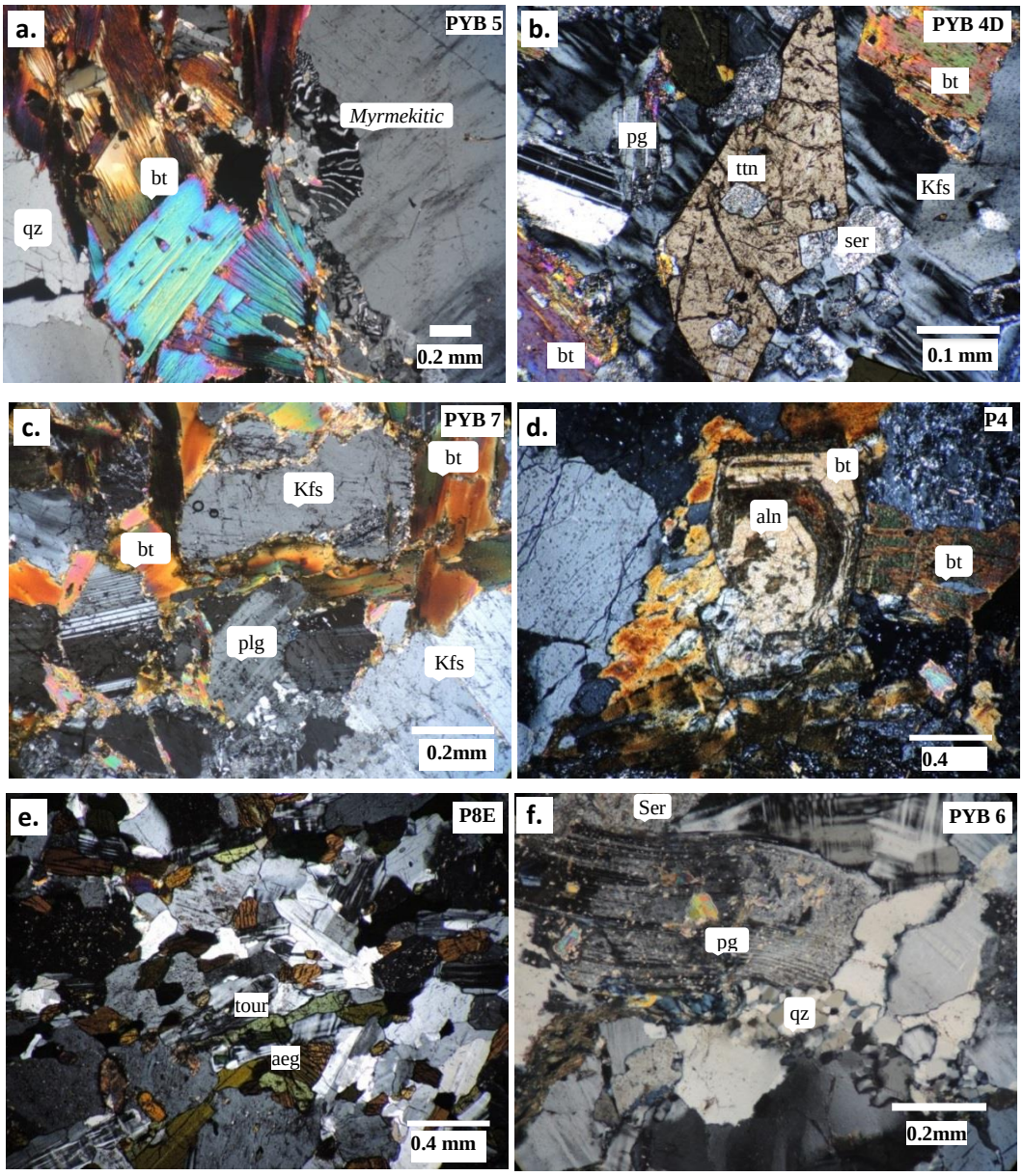

Fig 5.3 Photomicrographs of selected samples from Panyabungan and the surroundings: a. quartz alkali feldspar syenite from Tanjung, b. alkali feldspar granite deformed from Tebing Tinggi, c. Pintu Padang Julu, d. alkali feldspar syenite from Tanjung Jae, e-f.alkali feldspar granite and alkali feldspar syenite from Tano Tombangan.

Abbreviation: Kfs: K-feldspar, plg: plagioclase, hbl: hornblende, bt: biotite, qtz: quartz, aeg: aegerine, ttn: titanite, aln: allanite, tou: tourmaline, ser: sericite.

Table 5.2 Modal composition of granitoids from Panyabungan and its surrounding areas

	Locality	Sample	Rock	Primary Mineral														Alteration Minerals				Opaque minerals					
		Code	Name	Kfs	pg	hbl	bt	qz	crd	ne	mv	zr	mnz	ap	aln	tour	qz	chl	ep	cal	ms	ser	op	py	cpy	gal	mt	ilm
1	Parmompang-timur	PYB 2	Mzd	12	44	5	10	10				*	*					10	2	1	5			*	*	*	*	*
2	Tanjung	PYB 4D	QS	53	15		10	15			1	*						2	2			2		*	*			
3	Tanjung Jae	P4	AFS	76	2		6	11			3	*		*	*			4				2	1					
4	Tanjung jae	PYB 5	QAFS	69	5		14	15			2	*		*	*			4				1						
5	Tanjung Jae	P5	AFS	52	30	5	2	4	2		10												2					
6	Tanjung	PYB 4E	AFS	70	3		8	2			5	*		*			8	3				1						
7	Tebing Pintu Air	PYB 6	AFG	49	6		1	20	12		8							2		1		1						
8	Tebing Tinggi	P6	AFG	67	3			20			7											2	1					
9	Si Tumba, tanotumbangan	P8B	AFS	70	5	10	7	5			2	*		*									1					
10	Tano Tombangan	P8C	AFS	80	3	6	2									6						1	2					
11	Tano Tombangan	P8E	AFS	63	3	18		5		8			1	*					1	1								
12	Tano Tombangan	P8A	AFS	79	2		6	5			1									5			1					
13	Tano Tombangan	P9	QAFS	62	2		20	5						*		8				1		2						
14	Tano Tombangan	PYB 9A	AFS	47	4	8	15				1	*					3			2	20	10		*	*			
15	Pintu padang julu	P7	QAFS	68	5		10	10				*		*	*			5					2				*	*
16	Pintupadang Julu	PYB 8A	QAFS	67	4		12	15				*		*				2										
17	Pintupadang Julu	PYB 8B	AFS	41	6		10	6			19	*						8				10						1
18	Pintupadang Julu	PYB 8C	AFG	53		2	10	15				*		*				4	1			14	1					
19	Pintupadang Julu	P8D	AFS	65	18	6	3	5		3		*		*						1			1					

Abbreviation : Kf: K-feldspar, Pg: Plagioclase, Hb: Hornblende, Bi: Biotite, Qz: Quartz, Crd: Cordierite, Tour: Tourmaline, Zr: Zircon, Mnz: Monazite; Ap: Apatite; Ms: Muscovite; Si:Secondary quartz, Chl: Chlorite, Ep: Epidote, Cal: Calcite, Mu: Secondary Muscovite; Ser: Sericte; Op: Opaque, Py: Pyrite, Cpy: Chalcopyrite, Gal: Galena, Mt: Magnetite, ilm: ilmenite.

Rock Name: Mzd: Monzodiorite; QS: Quartz syenite; AFS: Alkali Feldspar Syenite; QAFS: Quartz Alkali Feldspar Syenite; AFG: Alkali Feldspar Granite

Granitic rocks at Parmompang are monzodiorite composed mainly of plagioclase, K-feldspar, quartz, biotite, and hornblende. Zircon and monazite are accessory minerals. Tebing Granitoids are alkali feldspar granite, consisting mainly of K-feldspar, quartz, ± biotite and ± cordierite. Photomicrographs of selected samples are shown in Fig. 5.3.

5.3 Petrography of granitoids from Muara Sipongi

Seventeen granitoids samples were collected from Muara Sipongi and are mostly altered. Only four samples are relatively fresh while the remaining samples are weakly to moderately altered. The granitoids from Muara Sipongi are classified to quartz diorite, granodiorite, monzogranite, and quartz monzonite, those from Pekantan are granodiorites, that from Sungai Cibadak is monzodiorite and that from Tanjung Alai is diorite. Summary of petrography is depicted in Table 5.3 and Fig. 5.4.

5.4 Petrography of granitoids from Kotanopan

Granitoids from Kotanopan and Tolung are classified to quartz monzonite, tonalite, monzogranite, granodiorite, and syenogranite, based on modal abundance of quartz (Q), alkali feldspar (A) and plagioclase (P) (Streickeisen, 1976). Quartz monzonite and granodiorite are mainly composed of plagioclase, K-feldspar, quartz, hornblende. Zircon and apatite are accessories minerals. Tonalite is composed of plagioclase, quartz and K-feldspar and zircon as an accessory mineral. Monzogranite consists mainly of K-feldspar, plagioclase, quartz, biotite with zircon as an accessory mineral.

Syenogranite from Tolung is mainly composed of K-felspar, plagioclase, quartz and biotite. Titanite, zircon, allanite, ±monazite, and ±apatite are accessory minerals. Tonalite consists of mainly plagioclase, K-feldspar, quartz and hornblende, and zircon as an accessory mineral. Summary of mineralogical composition of the samples is depicted in Table 5.4 and Fig. 5.5.

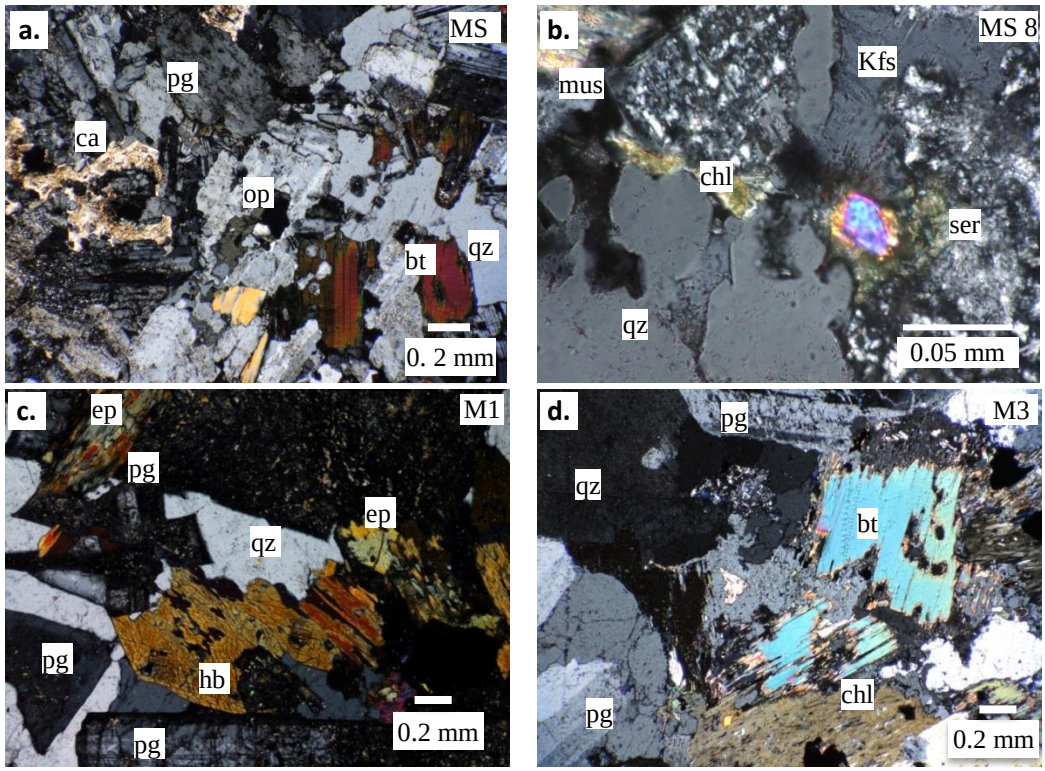

Fig 5.4 Photomicrograph of Muara Sipongi granitoids : a-c. quartz syenite and quartz diorite from Muara Sipongi contain plagioclase (pg), quartz (qz), K-feldspar (Kfs), biotite (bt), muscovite (mus), opaque (op), minor chlorite (chl) and epidote (ep) and d. granodorite from Pekantan contains plagioclase (pg), biotite (bt), and chl (chlorite).

Table 5.3 Modal composition of granitods from Muara Sipongi and its surrounding areas

No	Locality	Sample Code	Rock Name	Primary Mineral										Alteration mineral			Opaque minerals						
				Kf	pg	hbl	bt	qz	grt	px	ms	zr	ap	chl	ep	ser	py	cp	sl	mr	asp	mt	ilm
1	M	M1	quartz diorite	5	50	25		9		4					3	4						*	
2	M	MS 5	Granodiorite	12	42	8	2	28						2		5						*	
3	M	MS 6	Monzogranite	18	20	16		38				*	*	3	1	4						*	
4	M	MS8	quartz syenite	32	15	2	7	6			12	1		10	5	9	1	*	*	*	*	*	*
5	M	MS 11	Quartz monzonite	45	36			18	*			*										*	
6	M	MS 12	monzogranite	20	27	8	9	31						5								*	
7	P	M4	Granodiorite	20	34	14		22						3	1	6						*	
8	P	M6	granodiorite	12	42	10	4	22				*	*	6		4						*	
9	Cb	MS 7	Monzodiorite	19	42	1		12		1				10	5	10						*	
10	Tj	MS 9	Diorite	5	59		10				5			5	8	4	*					*	*

Abbreviation : pg: plagioclase, Kfs: K-feldspar, hbl: hornblende, bt: Biotite, qz: quartz, grt: garnet, px: pyroxene, ms: muscovite, chl: chlorite, ep: epidote, ser: sericite, py: pyrite, cp: Chalcopyrite, sl: Sphalerite, mr: Marcasite, asp: arsenopyrite, mt: magnetite, ilm: ilmenite. Locality : M: Muara Sipongi, P: Pekantan, Cb: Sungai Cibadak, Tj: Tanjung.

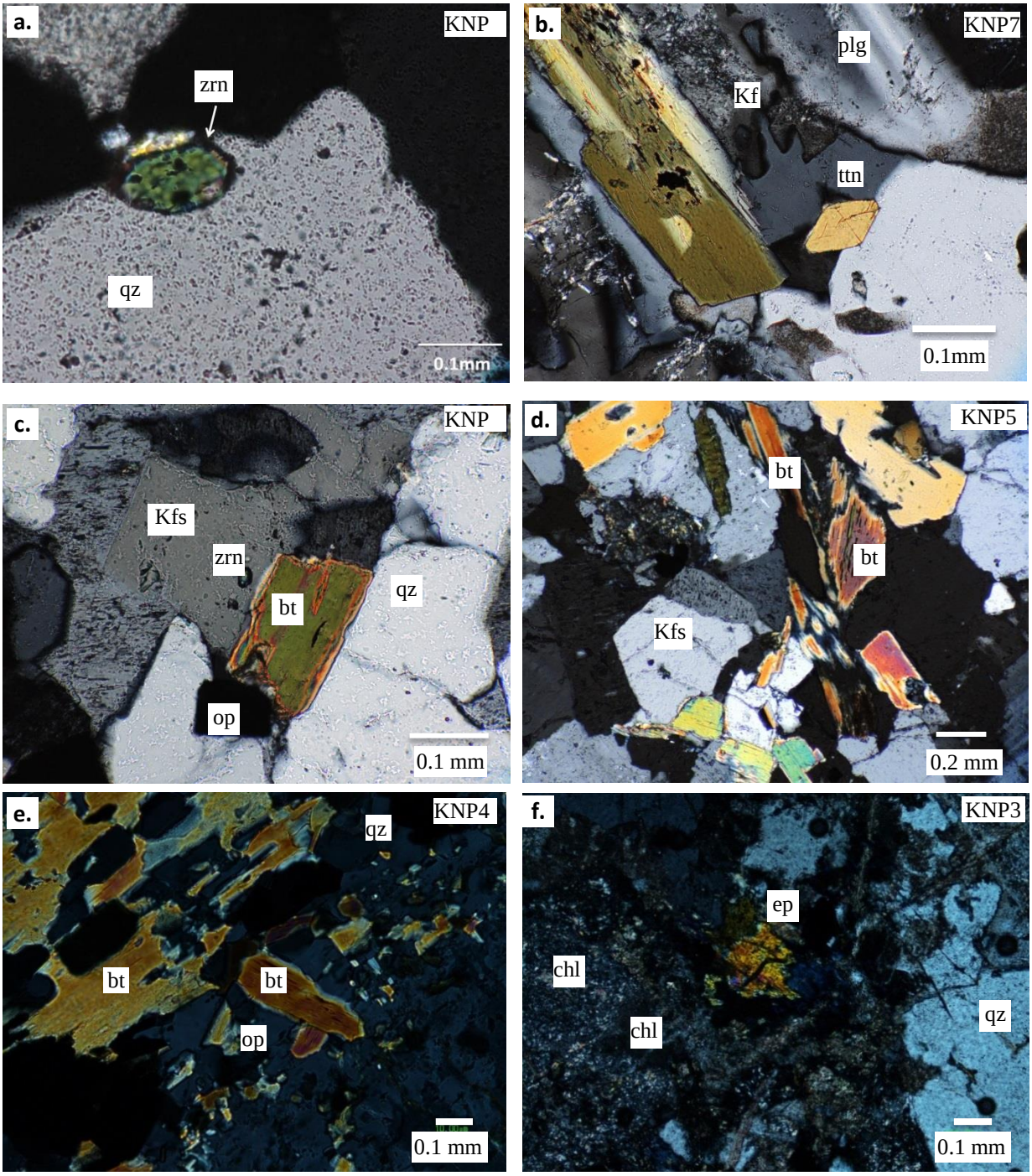

Fig. 5.5 Granitoids from Kotanopan (KNP): a-b. tonalite from Tolung, c-d. syenogranite from tolung, e monzogranite from Kotanopan and f. Tonalite.

Abbreviation : Kfs: K-feldspar, qz: quartz, plg: plagioclase, bt: biotite, zrn: zircon, chl: chlorite, ttn: titanite, ep: epidote, op: opaque mineral

Table 5.4 Modal composition of granitoids from Kotanopan and its surrounding areas

	Locality	Sample code	Rock name	Kf	pg	hbl	bt	qz	mv	ttn	zr	mnz	ap	aln	tre	chl	ep	cal	mu	ser	cly	op	py	cpy	sf	mt
1	Kotanopan	KNP2	Qmz	22	40	3		14			*		*			8	2			6	3	1				
2	Kotanopan	KNP3	Tn	4	42			25			*					3	3	6		14		3				
3	Kotanopan	KNP4	Mzg	38	24		9	25			*					3				5			*	*	*	
4	Kotanopan	KNP8	Gd	6	40	15		25			*		*			3	2			6		4				*
5	Tolung	KNP 5	Syg	44	15		10	20	7	*	*	*		*									1	*		*
6	Tolung	KNP 6	Syg	55	10		3	20	5	*	*		*	*		2				1	1		*			*
7	Tolung	KNP 7	Tn	5	49	1		15			*				1	5	3		5	10	3					

Abrreviation :

Kfs: K-feldspar, Pg: plagioclase, Hb: hornblende, Bi: biotite, Qz: quartz, Mv: muscovite, Ti: titanite, Zr, zircon, Mo: monazite, Ap: apatite,Chl: Chlorite, Ep: epidote, Cal: calcite, Mu= muscovite, Ser: sericite, Op: opaque, Py: pyrite, Cpy: chalcopyrite, Sf: sphalerite, Mg: magnetite.

Rocks name: Qmz: quartz monzonite, Tn: Tonalite, Mzg: monzogranite, Gdr: granodiorite, Syg: syenogranite

The summary of modal abundance of quartz (Q) alkali feldspar (A) and plagioclase (P) and feldsphatoid (F) of granitoids from Sibolga, Panyabungan, Muara Sipongi and Kotanopan were plotted in the QAPF discrimination diagram (Le Bas & Streickeisen, 1991; Streickeisen, 1976) (Fig. 5.6).

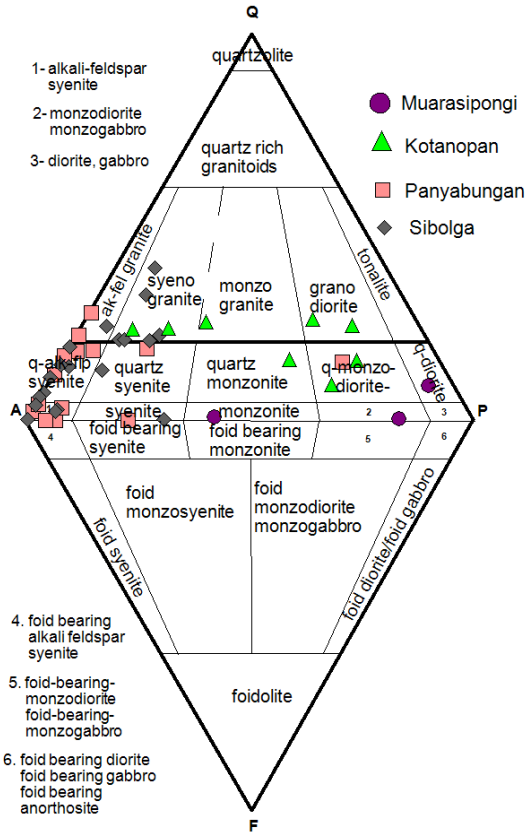

Fig. 5.6 Modal abundance of quartz (Q) alkali feldspar (A) and plagioclase (P) and feldsphatoids (F) of granitoids from Sibolga, Panyabungan, Muara Sipongi and Kotanopan (Le Bas & Streickeisen, 1991; Streickeisen, 1976).

Granitoids from Sibolga and Panyabungan were mainly fall in the field of quartz alkali feldspar syenite and syenogranite. Whereas granitoids from Muara Sipongi and Kotanopan were mainly fall in the field of syenogranite, granodiorite and quartz monzodiorite, monzodiorite and quartz diorite (Fig. 5.6).

CHAPTER 6

WHOLE-ROCK MAJOR ELEMENTS AND RARE EARTH ELEMENTS GEOCHEMISTRY

6.1 Sibolga

6.1.1Major elements compositions

Whole rock chemical compositions of 22 samples were analyzed (Table 6.1). The SiO_2 contents widely range from 63 to 80 wt.%. Loss on ignition (LOI) of the fresh samples ranges from 0.01 to 1.59 wt.%. Altered rock samples were not plotted in the Harker diagrams.

The SiO_2 content of quartz alkali feldspar syenite, and syenogranites from Sarudik ranges from 73 to 80 wt.%, that of alkali feldspar syenite and quartz syenite from Sibolga Julu ranges from 65 to 76 wt.%, while that of alkali feldspar syenite and quartz alkali feldspar syenite from Tarutung ranges from 72 to 77 wt.%. The P_2O_5 contents of quartz alkali feldspar syenite, and syenogranites from Sarudik ranges from 0.01 to 0.06 wt.%, that of alkali feldspar syenite and quartz syenite from Sibolga Julu ranges from 0.01 to 0.08 wt.%, while P_2O_5 contents of alkali feldspar syenite and quartz alkali feldspar syenite from Tarutung range from 0.03 to 0.04 wt.% (Table 6.1).

The quartz alkali feldspar syenites from Sarudik and alkali feldspar syenites from Sibolga Julu and Tarutung contain low P_2O_5 compared to the rest of samples. The SiO_2 contents of quartz alkali feldspar syenite, quartz syenite and syenogranite from Sibuluhan

Sihaporas range from 71 to 77 wt.%, P_2O_5 contents from 0.01 to 0.07 wt.%. The SiO_2 contents of quartz alkali feldspar syenite and quartz syenite of the Tukka range from 63 to 73 wt.% and P_2O_5 contents from 0.08 to 0.23 wt.%. SiO_2 contents of quartz alkali feldspar syenite from Sihobuk granitoids range from 66 to 73 wt.% and P_2O_5 contents from 0.04 to 0.14 wt.%, while SiO_2 contents of syenogranite and monzogranite from Adian Koting range from 68 to 69 wt.% and P_2O_5 contents from 0.12 to 0.16 wt.%. P_2O_5 contents of quartz alkali feldspar syenite, monzogranite, syenogranite and of the Tukka, the Sihobuk and the Adian Koting are relatively high (Fig. 6.1 and Table 6.1).

Harker Diagrams indicate that most of the major elements (TiO_2, Al_2O_3, FeO, MnO, MgO, CaO, and P_2O_5) decrease with increasing SiO_2 while K_2O and Na_2O, are unclear and slightly increase, respectively (Fig. 6.1).

Plots of SiO_2 versus (FeO_{tot}/[FeO_{tot}+MgO]), SiO_2 versus (Na_2O+K_2O+CaO) and Aluminium Saturation Index (ASI) versus molecular ratio Al/(Na+K) discrimination diagrams show that most of the granitoids fall within ferroan and peraluminous-type granites based on the classification diagram of Frost et al. (2001) (Fig. 6.2). Rb-(Y+Nb) and Nb-Y discriminant diagrams (Pearce et al, 1984) of granitoids from Sibolga fall in the within plate environment (Fig. 6.3).

6.1.2 Rare earth elements compositions

Whole-rock rare earth elements and trace elements contents of 25 samples were analyzed, but only 14 samples fresh and least altered were presented (Table 6.2). Chondrite normalized REE patterns of alkali feldspar syenite from Sibolga Julu, syenogranite from

Sibuluhan Sihaporas, alkali feldspar syenite from Tarutung, quartz syenite from Tukka, and quartz alkali feldspar from Sihobuk show that REE, particularly LREE are enriched (Fig. 6.4).

REE patterns normalized to chondrite show that REE of syenogranites and quartz alkali feldspar syenites from Sarudik are similar to that of quartz syenite from Sibolga Julu, where relatively flat patterns of both LREE and HREE and significant depletion of Eu were observed (Fig. 6.4).

ΣREE contents of alkali feldspar syenites from Sibolga Julu and Tarutung, quartz alkali feldspar syenite from Sarudik, syenogranite, quartz syenite and quartz alkali feldspar syenite from Sibuluhan Sihaporas, and quartz syenite from Tukka are higher compared to those of quartz syenite from Adian Koting and quartz alkali feldspar syenite from Tukka.

ΣLREE contents of alkali feldspar syenite and quartz syenite from Sibolga Julu range from 241 to 914 ppm, ΣHREE from 240 to 389 ppm, and Rb/Sr ranges from 1 to 121. ΣLREE contents of quartz alkali feldspar syenite and alkali feldspar syenite from Tarutung range from 445 to 1023 ppm, ΣHREE contents from 86 to 206 ppm, and Rb/Sr ranges from 5.3 to 5.4.

ΣLREE contents of quartz alkali feldspar syenite and syenogranite from Sarudik range from 212 to 533 ppm, ΣHREE contents from 109 to 309 ppm, and Rb/Sr ranges from 3.9 to 70. ΣLREE contents of quartz alkali feldspar syenite, syenogranite and quartz syenite from Sibuluhan Sihaporas range from 388 to 487 ppm, ΣHREE contents range from 63 to 462 ppm, and Rb/Sr ranges from 4 to 50. ΣLREE contents of quartz alkali feldspar syenite and quartz syenite from Tukka range from 203 to 626 ppm,

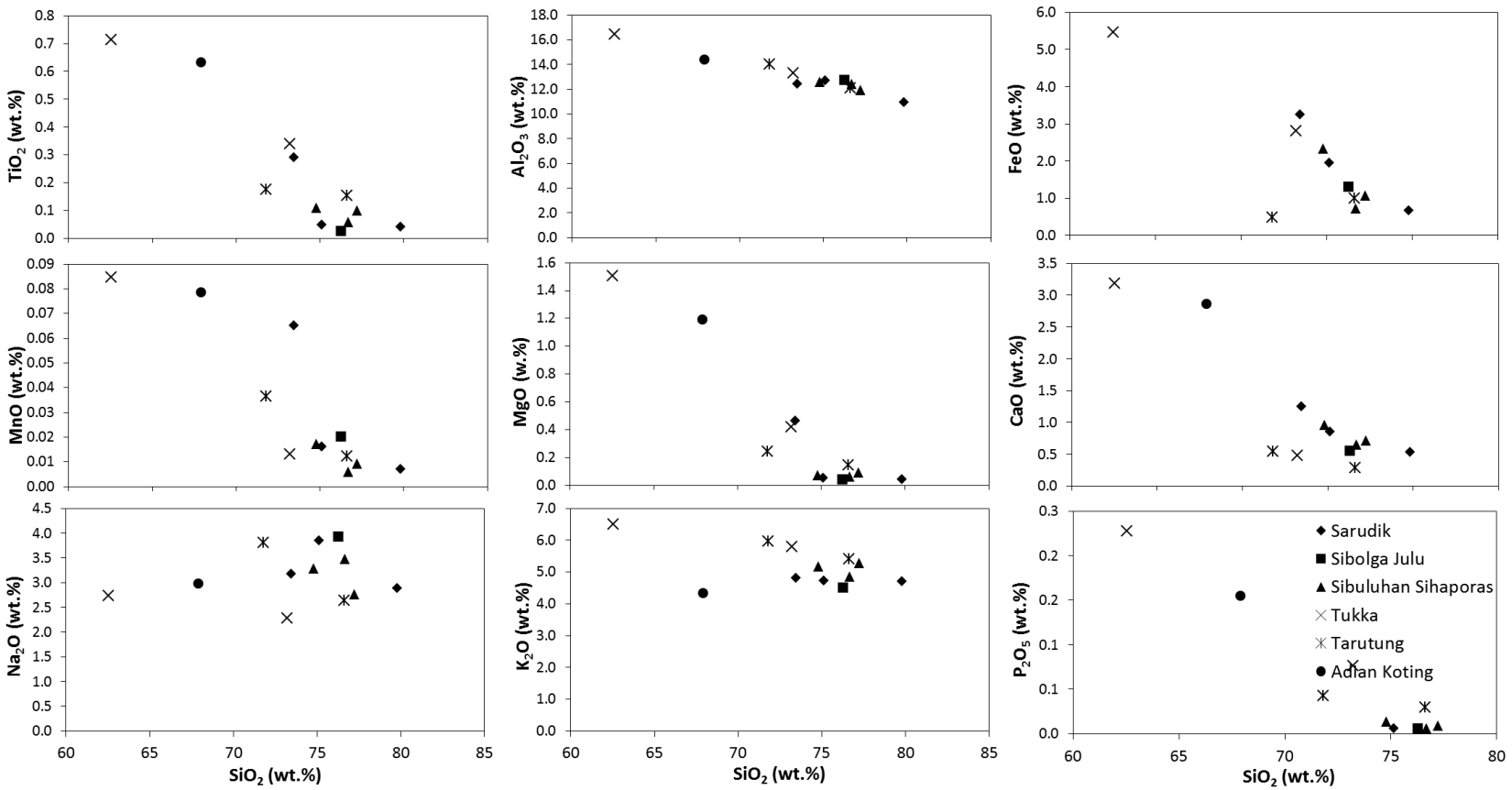

Fig. 6.1 Harker diagrams of granitoids from Sibolga and its surrounding areas.

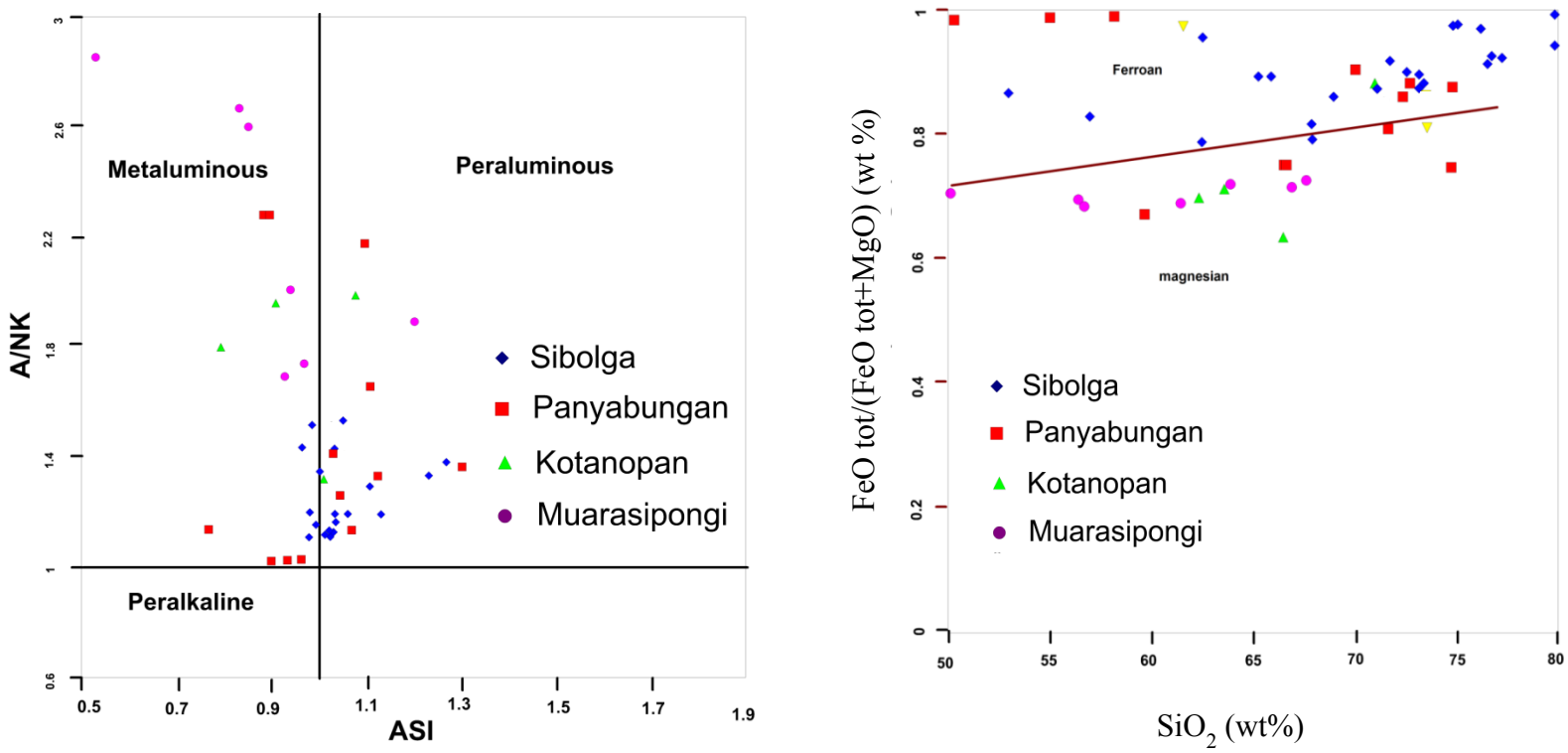

Fig. 6.2 Plots of SiO_2 versus (FeO_{tot}/[FeO_{tot}+MgO]), and and Aluminum Saturation Index versus molecular ratio (Al/[Na+K]) (after Frost et al., 2001).

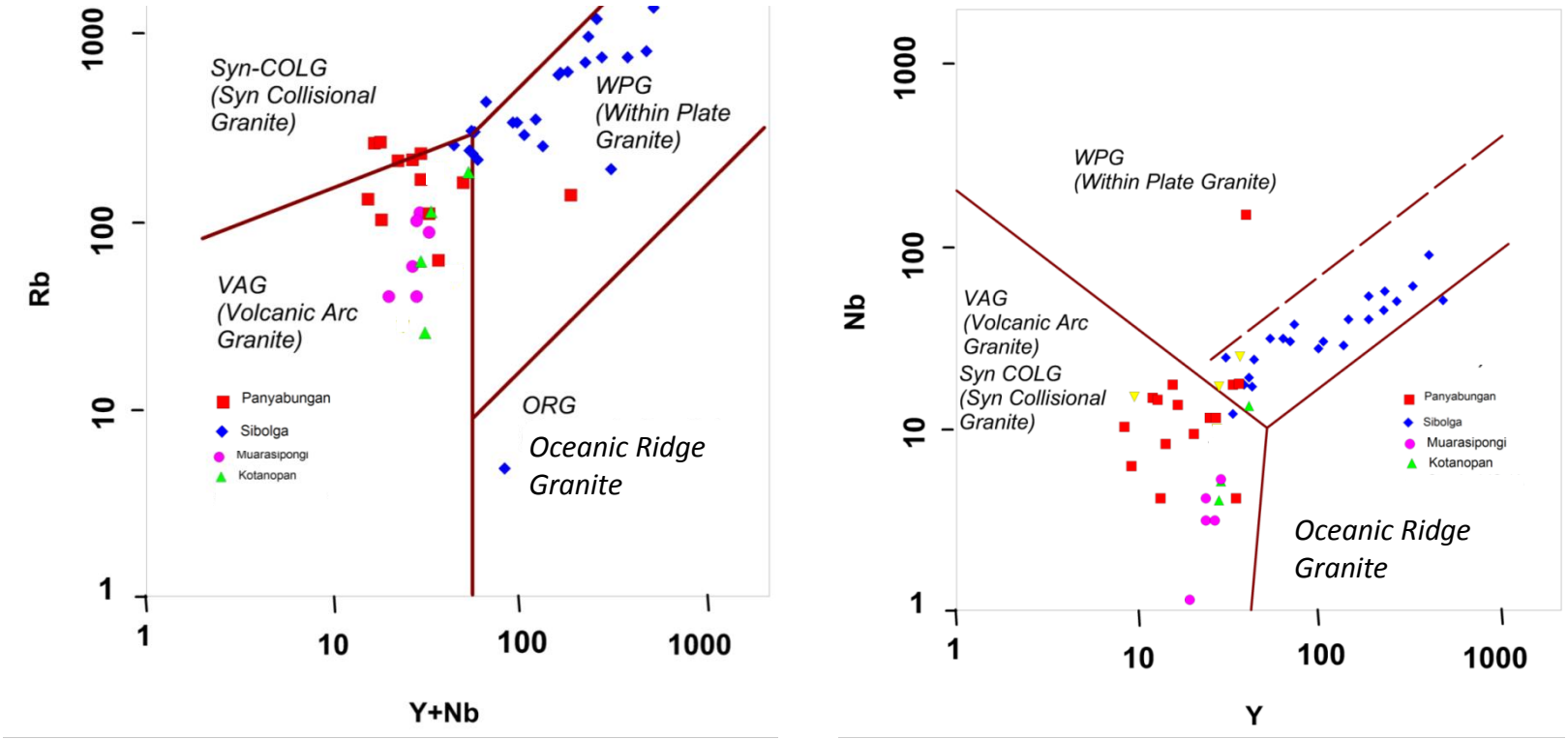

Fig. 6.3 Rb-(Y+Nb) and Nb-Y discriminant diagrams of granitoids from Sibolga, Panyabungan, Kotanopan and Muara Sipongi (after Pearce et al., 1984).

Table 6.1. Whole rock major elements contents of granitoids in Sibolga and its surrounding areas

Sample code	Locality	Rock name	Magnetic susceptibility x 10^{-3} (SI)	Radioactivity µSv/hr	Major elements (wt.%)											
					SiO_2	TiO_2	Al_2O_3	FeO	MnO	MgO	CaO	Na_2O	K_2O	P_2O_5	LOI	Total
SR1	Sarudik	Syenogranite	0.01	0.12	75.14	0.05	12.69	1.94	0.02	0.05	0.86	3.85	4.72	0.01	0.46	100.01
S14	Sarudik	Alkali feldspar syenite	0.57	0.60	73.46	0.29	12.42	3.25	0.07	0.46	1.25	3.17	4.80	0.06	0.41	100.00
S16	Sarudik	Syenogranite	0.01	0.70	79.80	0.04	10.92	0.66	0.01	0.04	0.53	2.88	4.70	0.01	0.33	99.99
S29*	Sarudik	-	-	-	71.15	0.36	14.30	3.10	0.02	0.47	0.55	2.55	5.67	0.07	1.41	99.65
S17	Sibolga Julu	Quartz syenite	0.01	0.89	65.25	0.24	19.06	1.88	0.01	0.23	1.36	8.91	1.24	0.08	1.54	100.01
S23	Sibolga Julu	Monzogranite	0.01	0.33	76.27	0.03	12.75	1.30	0.02	0.04	0.55	3.94	4.50	0.01	0.45	100.01
S1*	Sibuluhan-	-	0.04	0.47	75.01	0.09	15.15	0.62	0.00	0.10	0.00	0.17	5.01	0.01	3.75	99.93
S2*	Sihaporas	-	0.02	0.48	62.56	0.08	20.75	0.68	0.00	0.03	0.03	2.39	10.97	0.02	2.40	99.92
S5	Sibuluhan-	Syenogranite	0.01	0.55	77.24	0.10	11.94	1.06	0.01	0.09	0.71	2.77	5.27	0.01	0.67	99.99
S5B*	Sihaporas	-	0.16	0.05	79.94	0.08	10.97	7.24	0.03	0.09	0.03	0.80	0.07	0.01	0.07	99.32
S6	Sibuluhan-	Quartz alkali feldspar syenite	0.07	0.47	74.79	0.11	12.61	2.34	0.02	0.07	0.96	3.28	5.16	0.01	0.39	100.00
S7	Sihaporas	Quartz syenite	0.01	0.61	76.68	0.06	12.44	0.73	0.01	0.06	0.65	3.48	4.85	0.01	0.96	100.01
S8	Tukka	Quartz alkali feldspar syenite	0.06	0.55	72.50	0.42	12.86	3.12	0.03	0.36	0.92	2.83	4.93	0.08	1.59	99.99
S9	Tukka	Quartz alkali feldspar syenite	0.09	0.34	73.22	0.34	13.32	2.80	0.01	0.42	0.48	2.29	5.79	0.08	0.94	100.01
S10B	Tukka	Quartz alkali feldspar syenite	0.20	0.18	62.53	0.71	16.43	5.46	0.08	1.51	3.18	2.74	6.51	0.23	0.01	100.00
S18B	Tarutung	Quartz monzonite	0.03	0.62	76.61	0.15	12.10	1.46	0.01	0.14	0.28	2.64	5.41	0.03	1.00	99.99
S19	Tarutung	Quartz syenite	0.24	0.70	71.80	0.18	14.04	2.57	0.04	0.24	0.54	3.80	5.96	0.04	0.49	99.99
S21	Adian Koting	Quartz syenite	0.10	0.58	67.90	0.63	14.43	4.49	0.08	1.19	2.86	2.98	4.33	0.16	0.46	100.01
SB1*	Adian Koting	Syenogranite	0.12	0.14	69.04	0.48	14.20	4.67	0.06	0.79	2.14	2.86	4.87	0.12	0.26	99.48
SB3*	Adian Koting	Quartzsyenite	0.11	0.08	67.92	0.61	14.25	5.00	0.08	1.16	2.43	2.79	4.38	0.16	0.65	99.44
S24*	Sihobuk	Quartz alkali feldspar syenite	0.09	0.56	73.25	0.21	13.36	2.39	0.03	0.29	0.75	3.15	5.60	0.04	0.66	99.73
S24B*	Sihobuk	Quartz syenite	0.17	0.61	65.96	0.53	15.51	4.95	0.09	0.61	2.24	2.92	6.27	0.14	0.22	99.44

Explanation:
FeO = The expression of total Fe content. **LOI** = Lost on Ingnition

Table 6.2 Rare earth elements concentration of granitoids in Sibolga and its surrounding areas

	Sample	Rare Earth Elements (REE) (ppm)																			
Locality	code	La	Ce	Pr	Nd	Sm	Eu	Gd	Tb	Dy	Ho	Tm	Er	Yb	Lu	∑REE	LREE	HREE	Ce/Ce*	Eu/Eu*	$(La/Yb)_N$	$(Gd/Yb)_N$
Sarudik	SR-01	48.5	112.0	16.6	65.5	23.4	0.2	26.6	5.2	33.2	6.7	2.6	18.7	16.7	2.2	378.1	266	112	1.0	0.0	2.0	1.3
Sarudik	SR 02*	165.0	279.0	29.2	101.0	18.8	0.8	14.9	2.2	12.0	2.2	0.8	6.2	5.4	0.8	638.1	594	44	1.0	0.1	21.0	2.3
Sarudik	S14	131.5	257.0	28.1	97.2	18.8	0.6	15.0	2.1	12.0	2.2	1.0	7.2	6.5	0.9	580.0	533	47	1.0	0.1	13.7	1.9
Sarudik	S.16*	41.6	92.7	12.5	48.7	16.5	0.1	18.1	3.4	20.6	3.9	1.5	10.7	9.2	1.2	280.5	212	68	1.0	0.0	3.1	1.6
Sibuluhan	S.1*	117.5	34.7	29.9	108.5	37.3	0.5	48.1	9.6	61.2	11.4	4.9	35.2	31.0	4.1	533.8	328	205	0.1	0.0	2.6	1.3
Sihaporas	S.2*	68.4	118.0	16.7	59.0	15.5	0.3	15.5	3.1	23.9	5.0	2.9	17.9	18.9	2.6	367.5	278	90	0.8	0.1	2.5	0.7
Sibuluhan	S5	89.3	187.5	21.6	72.7	16.9	0.2	16.3	2.7	17.8	3.6	1.7	11.8	11.6	1.6	455.2	388	67	1.0	0.0	5.3	1.1
Sibuluhan	S5B*	38.2	67.0	11.4	40.9	12.2	0.2	11.9	2.4	16.7	3.3	1.6	10.1	10.7	1.4	227.8	170	58	0.8	0.0	2.4	0.9
Sihaporas	S6	116.0	246.0	28.0	95.3	23.5	0.2	21.5	3.9	24.8	4.9	2.5	16.0	15.9	2.2	600.6	509	92	1.0	0.0	5.0	1.1
Sibuluhan	S7	102.0	128.5	28.5	109.0	35.6	0.2	41.6	7.4	45.2	8.5	3.5	25.1	21.9	2.9	559.9	404	156	0.6	0.0	3.2	1.5
Sihaporas	S27/S1*	66.7	74.2	13.8	45.8	9.3	0.9	7.7	1.2	6.8	1.4	0.7	4.3	4.5	0.7	238.0	211	27	0.6	0.3	10.0	1.4
Sibuluhan	S29*	126.0	239.0	25.5	81.8	13.9	0.9	9.5	1.3	7.0	1.3	0.5	3.5	3.1	0.5	513.5	487	26	1.0	0.2	28.0	2.5
Tukka	S8	183.0	271.0	34.0	116.0	20.7	1.4	18.5	2.8	16.4	2.9	1.1	8.4	6.9	0.9	684.0	626	58	0.8	0.2	18.0	2.2
Tukka	S9	52.9	96.8	10.3	35.0	6.9	0.7	5.3	0.8	5.5	0.9	0.4	3.1	2.5	0.4	221.5	203	19	1.0	0.4	14.5	1.7
Tukka	S10	49.4	95.2	11.2	39.4	7.4	2.5	5.3	0.7	4.1	0.8	0.3	2.3	2.3	0.3	221.2	205	16	1.0	1.2	14.5	1.9
Adian Koting	S21	67.8	126.5	13.7	48.6	9.7	1.4	7.4	1.1	6.6	1.2	0.5	3.8	3.6	0.5	292.4	268	25	1.0	0.5	12.8	1.7
Adian Koting	SB-01*	74.1	135.0	14.6	48.4	7.8	1.4	5.9	0.8	4.5	0.9	0.4	2.3	2.9	0.4	299.3	281	18	1.0	0.6	17.5	1.7
Adian Koting	SB 02 *	73.6	132.0	14.2	49.5	9.4	1.4	7.5	1.2	6.5	1.2	0.5	3.5	3.6	0.5	304.5	280	24	1.0	0.5	13.9	1.7
Adian Koting	SB-03 *	66.0	123.0	13.8	47.8	8.5	1.4	6.4	1.1	6.3	1.2	0.5	3.3	3.5	0.6	283.2	260	23	1.0	0.6	12.9	1.5
Sibolga Julu	S17	368.0	222.0	57.5	219.0	45.0	2.6	52.9	7.5	43.7	8.6	3.2	25.0	18.1	2.5	1075.5	914	161	0.4	0.2	13.8	2.4
Sibolga Julu	S23	44.6	114.5	14.2	50.8	16.6	0.1	18.8	3.8	25.5	5.1	2.5	16.9	17.5	2.4	333.0	241	92	1.1	0.0	1.7	0.9
Tarutung	S18B	404.0	231.0	78.1	258.0	49.6	2.2	35.2	4.7	23.9	3.9	1.4	10.6	8.4	1.1	1112.1	1023	89	0.3	0.2	32.7	3.4
Tarutung	S19	116.0	216.0	22.9	75.2	14.1	0.6	11.1	1.6	9.4	1.7	0.8	5.6	5.3	0.8	481.1	445	36	1.0	0.1	14.9	1.7
Sihobuk	S24A*	137.5	261.0	28.2	95.9	17.8	0.7	13.5	2.0	11.3	2.1	0.8	6.3	5.3	0.8	583.2	541	42	1.0	0.1	17.6	2.1
Sihobuk	S24B*	103.0	183.0	19.2	61.6	10.5	2.3	7.8	1.0	5.5	1.0	0.5	2.9	3.1	0.5	401.8	380	22	1.0	0.8	22.7	2.1

Explanation :
LREE is the summary of Light Rare Earth Elements (La to Eu). HREE is the summary of Heavy Rare Earth Elements (Gd to Lu).
∑REE Total summary of LREE. $Ce/Ce^* = Ce_N/(La_N x Pr_N)^{1/2}$, $Eu/Eu^* = Eu_N/(Sm_N x Gd_N)^{1/2}$ (Mc Donough and Sun, 1995).

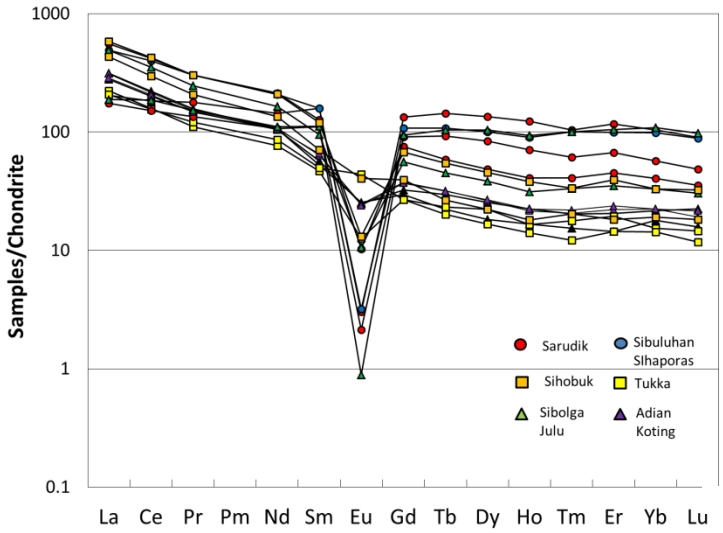

Fig. 6.4 Chondrite – normalized REE patterns of granitoids from Sibolga and its surrounding areas (values of chondrite are from McDonough & Sun, 1995).

ΣHREE contents range from 37 to 147 ppm, and with a Rb/Sr ranging from 0.4 to 4. ΣLREE content of quartz syenite from Adian Koting is 292 ppm, ΣHREE contents range from 44 to 60 ppm, and Rb/Sr is 0.7.

Quartz syenite and quartz alkali feldspar syenite from Tarutung and Tukka, quartz syenite from Sibuluhan Sihaporas, and quartz alkali feldspar syenite from Sarudik contain allanite and apatite, thus their chondrite normalized REE patterns show enrichment in both of LREE and HREE, while quartz syenite from Adian Koting and quartz alkali feldspar and alkali feldspar syenite from Tukka contain only zircon and they show relatively depleted both in LREE and HREE compared to those of quartz syenite and alkali feldspar syenite from Tarutung, that of quartz syenite from Sibuluhan Sihaporas, and that of quartz alkali feldspar syenite from Sarudik.

6.2 Panyabungan

6.2.1 Major elements

Major elements analysis of twelve granitoids from Panyabungan and its surrounding areas was conducted. They include of Tanjung Hutasiantar (PYB3), Tanjung Tebing Pintu Air (PYB 6) and Aek Nangali (PYB 10). Three samples are collected from Tanjung Jae (PYB 4D, PYB 5, and P4), Pintu Padang Julu ((PYB 7, PYB 8C and P7) and Tano Tombangan (P8A, P8D and P8C) (Table 6.3).

SiO_2 content of alkali feldspar granite from Tebing Pintu Air is 72.3 wt.%, those of quartz syenite, alkali feldspar syenite and quartz alkali feldspar syenite from Tanjung range from 70 to 74.7 wt.%, while SiO_2 contents of alkali feldspar granite and quartz alkali feldspar syenite from Padang Julu range from 66.4 to 71.6 wt. % and those of alkali feldspar syenites from Tano Tombangan range from 55.0 to 58.2 wt.% (Table 6.3).

The SiO_2 content of alkali feldspar syenite from Tano Tombangan are low compared to that of alkali feldspar syenite from Pintu Padang Julu, Tanjung Jae and Pintu Air suggest removal of SiO_2 to form K-feldspar in pegmatitic rocks (e.g. alkali feldspar syenite). Quartz alkali feldspar syenite from Pintu Padang Julu (P7) has a relatively high radioactivity value and high contents of TiO_2, FeO, MgO, CaO, and P_2O_5 (Table 6.3 and Fig. 6.5). They are calcic, peraluminous and formed in volcanic arc environment.

Harker diagrams of selected fresh or least altered samples are shown in the Figure. 6.5. TiO_2 Al_2O_3, MnO, CaO, MgO, K_2O and P_2O_5 are negatively correlated with SiO_2 and Fe_2O_3 and Na_2O are positively trends correlated with SiO_2 at Tano Tombangan.

Table 6.3 Whole rock major elements contents of granitoids from Panyabungan and its surrounding areas

No	Sample Code	Locality	Magnetic Susceptibility	Radio-Activity	Major elements (wt.%)											
			(x 10^{-3} SI)	(µSv/hr)	SiO_2	TiO_2	Al_2O_3	FeO	MnO	MgO	CaO	Na_2O	K_2O	P_2O_5	LOI	Total
1	PYB3	Tj. Hutasiantar	0.05	0.12	74.85	0.16	12.25	2.45	0.05	0.33	0.38	3.02	5.44	0.06	0.74	99.73
2	PYB6	Tj. Tebing Pintu Air	0.04	0.12	72.30	0.22	13.48	3.09	0.08	0.49	1.97	3.56	3.46	0.08	0.92	99.65
3	PYB4D	Tanjung	0.18	0.15	74.74	0.28	12.30	2.58	0.02	0.88	0.25	1.33	6.37	0.08	0.87	99.70
4	PYB5		0.07	0.07	70.00	0.26	14.31	3.19	0.02	0.35	1.35	1.84	7.73	0.08	0.51	99.64
5	P4		0.076	1.63	72.80	0.37	13.38	2.83	0.02	0.40	1.03	1.81	6.61	0.10	0.35	99.70
6	PYB7	Pintu Padang Julu	0.01	0.01	71.52	0.37	13.19	4.01	0.04	0.71	2.32	1.84	5.31	0.12	0.11	99.54
7	PYB8C		0.07	0.07	71.62	0.52	13.18	4.06	0.04	0.97	2.25	1.81	4.63	0.15	0.31	99.54
8	P7		0.23	1.88	66.37	0.84	14.65	5.92	0.08	1.98	3.87	2.15	2.97	0.33	0.18	99.34
9	P8A	Tano Tombangan	25	0.33	55.04	0.21	21.87	3.40	0.07	0.05	1.55	8.21	7.46	0.02	1.74	99.62
10	P8D		1.65	1.40	58.16	0.11	21.46	4.31	0.06	0.03	0.70	9.27	5.25	0.01	0.16	99.52

Explanation:
FeO = Total Fe expressed as FeO. **LOI** = Lost on Ignition

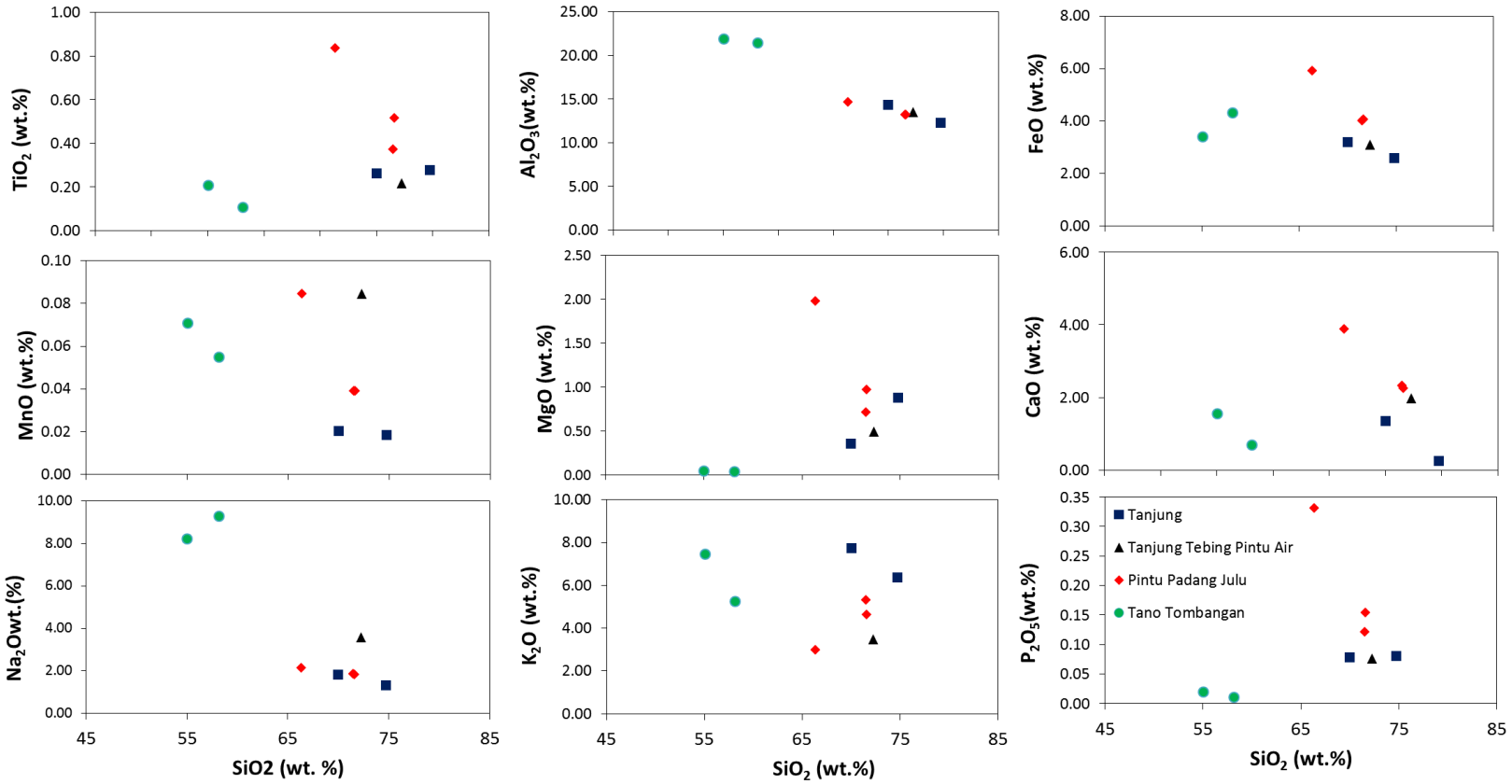

Fig. 6.5 Harker diagram of granitoids from Panyabungan and its surrounding areas.

Al_2O_3, FeO, MnO, MgO, CaO and P_2O_5 are negatively correlated with SiO_2 while SiO_2 and K_2O are positively correlated at Pintu Padang Julu. Al_2O_3, MnO, CaO, K_2O and P_2O_5 are negatively correlated with SiO_2, while SiO_2 and MgO are positively correlated, while relation between SiO_2 and TiO_2, Na_2O and P_2O_5 are unclear.

Plots of SiO_2 versus (FeO_{tot}/[FeO_{tot}+MgO]) and SiO_2 versus (Na_2O+K_2O-CaO) and Aluminium Saturation Index (ASI) versus molecular ratio (Al/[Na+K]) discrimination diagrams show that most of the granitoids fall within ferroan and peraluminous-type granites based on the classification diagram of Frost et al. (2001) (Fig. 6.2). Two metaluminous alkali feldspar granites show ferroan characters. On the other hand quartz syenite from Tanjung Jae and quartz alkali feldspar syenite from Pintu Padang Julu are peraluminous and magnesian characters. Rb-(Y+Nb) and Nb-Y discriminant diagrams (Pearce et al, 1984) of granitoids from Panyabungan fall in the volcanic arc environment (Fig. 6.3)

6.2.2 Rare earth elements

The rare earth elements compositions of eight whole-rock samples out of sixteen including the granitoids from Tanjung Jae PYB 4D, PYB 5 and PYB 6, that from Pintu Padang Julu P7, PYB 7, PYB8C, and that Tano Tombangan P8A, P8D were selected. LREE in granitoids from Pintu Padang Julu are more enriched than the granitoids from Tano Tombangan and Tanjung Jae (Table 6.4, Fig. 6.6).

ΣREE contents of quartz syenite, quartz alkali feldspar syenite, and alkali feldspar granite from Tanjung jae range from 85 to 356 ppm, those of quartz alkali feldspar granite and alkali feldspar granite range from 200 to 535 ppm while those of alkali feldspar syenite from Tano Tombangan range from 31 to 81 ppm.

Table 6.4 Rare earth elements concentration of granitoids from Panyabungan and its surrounding areas

	Sample code	Locality	Rock Name	Mag. Susc.	Rad.	Rare earth elements (REE)													
						La	Ce	Pr	Nd	Sm	Eu	Gd	Tb	Dy	Ho	Tm	Er	Yb	Lu	∑REE
1	PYB04D	Tanjung	Quartz syenite	0.18	0.15	13.5	29.4	3.83	17	4.66	1.49	4.94	0.71	3.97	0.81	0.29	2.07	2.09	0.33	85.09
2	PYB-05	Tanjung Jae	Quartz alkali feldspar syenite	0.07	0.07	85.2	167.5	18.85	64.9	8.76	2.19	4.39	0.47	2	0.31	0.1	0.77	0.69	0.07	356.2
3	PYB-06	Tanjung Tebing Pintu Air	Alkali feldspar granite	0.04	0.12	45.7	85.4	9.72	33	6.72	0.83	5.09	0.73	4.62	0.82	0.38	2.38	2.34	0.38	198.11
4	PYB-07	Pintu Padang Julu		0.01	0.097	132.5	247	27.2	92.1	13.95	2.81	8.2	1.02	5.23	0.91	0.23	2.36	1.56	0.21	535.28
5	P7/PYB 9	Pintu Padang Julu	Quartz alkali feldspar syenite	0.23	1.88	42.8	85.3	9.77	36.8	7.28	1.97	5.5	0.75	4.13	0.73	0.3	2.06	1.87	0.26	199.52
6	PYB-08C	Pintu Padang Julu	Alkali feldspar granite	0.07	0.07	104.5	195	22.6	77.5	10.85	3.41	6.5	0.7	2.94	0.52	0.13	1.14	0.76	0.13	426.68
7	P8A/PYB 9	Tano Tombangan	Alkali feldspar syenite	25	0.33	21.1	35.7	3.54	11.6	1.85	0.57	1.61	0.27	1.6	0.3	0.15	1.15	1.03	0.12	80.59
8	P8D/PYB 9	Tano Tombangan	Alkali feldspar syenite	1.65	1.4	6.6	13.2	1.45	4.9	1.04	0.66	0.92	0.13	0.79	0.13	0.06	0.52	0.48	0.09	30.97

Explanation :
∑REE Total summary of REE
Mag. Susc. = magnetic susceptibility (x 10^{-3} SI), Rad.=Radioactivity (µSv/hr)

Chondrite-normalized REE patterns of granitoids from Panyabungan are different among the various samples. They showed various patterns, but in general, all patterns show LREE enrichment and depletion of HREE, those of Tano Tombangan show relatively similar pattern but they have different Eu behavior that are probably resulted by different degree of fractionation of feldspar. The chondrite normalized REE patterns from Tanjung Jae were very different with those two areas. The REE patterns show three different patterns. The first pattern is similar to that of Pintu Padang Julu, the second is enriched in LREE and depleted in HREE, and the third is relatively flat. These various patterns indicate that quartz syenite, quartz alkali feldspar syenite, and alkali feldspar granite at Panyabungan were derived from different sources, therefore they have different and various degree of feldspar fractionation.

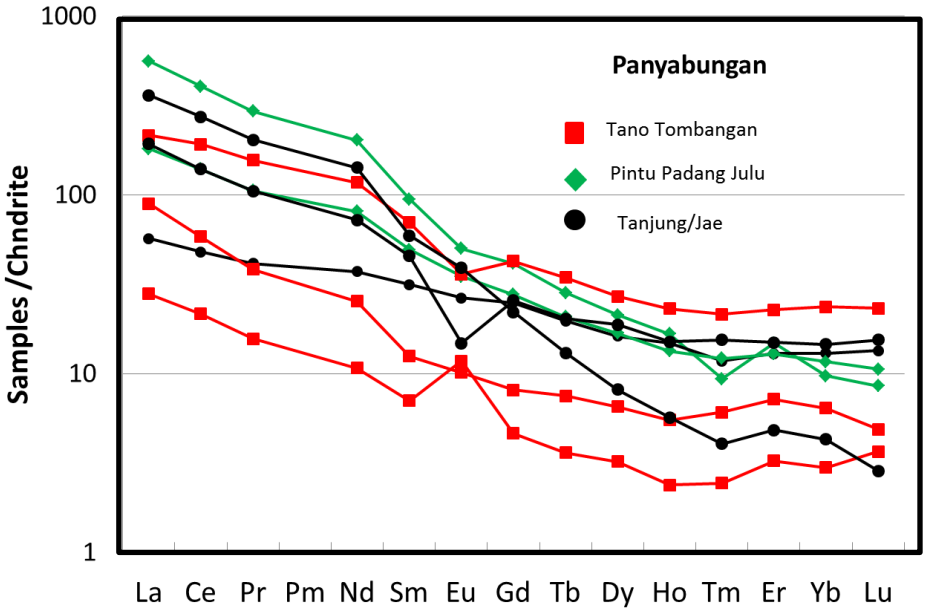

Fig. 6.6 Chondrite normalized diagram of granitoids from Panyabungan and its surrounding areas (values of chondrite are from McDonough & Sun, 1995).

6.3 Muara Sipongi

6.3.1 Major elements

Major elements compositions of eight granitoids samples were analyzed including six samples from Muara Sipongi (MS2-MS6, MS11-MS12), one sample collected from Sungai Cubadak (MS7) and Tanjung Alai (MS10) (Table 6.5). Four out of eight samples are fresh and least altered samples (MS6, MS 10, MS11 and MS 12). While rest of the samples were altered, and will not be discussed. SiO_2 contents of granitoids from Muara Sipongi range from 61.5 to 67.6 wt.%. That of granitoids from Tanjung Alai is 64.8 wt%. P_2O_5 contents of granitoids from Muara Sipongi range from 0.09 to 0.14 wt.%, while that of granitoids from Tanjung Alai is 0.11 wt.%. P_2O_5 contents are positively correlated with ΣREE. The characters of P_2O_5 and REE in granitoids from Muara Sipongi are different with those from Panyabungan and Sibolga, in which P_2O_5 is negatively correlated with ΣREE

TiO_2, Al_2O_3, FeO, MnO, MgO, Na_2O and P_2O_5 are negatively correlated with SiO_2 while CaO and K_2O are positively correlated with SiO_2. These plots showing parallel patterns to each other suggest they have a genetic relationship (Fig. 6.7).

Plots of SiO_2 versus (FeO_{tot}/[FeO_{tot}+MgO]) (Fig. 6.2), and SiO_2 versus (Na_2O+K_2O-CaO) and Aluminium Saturation Index (ASI) versus molecular ratio (Al/[Na+K]) discrimination diagrams show that most of the granitoids fall within magnesian, calcic-alkali and metaluminous affinity based on the classification diagram of Frost et al. (2001) (Fig. 6.2). Rb-(Y+Nb) and Nb-Y discriminant diagrams (Pearce et al, 1984) of granitoids from Muara Sipongi fall in the volcanic arc environment (Fig. 6.3)

Table 6.5 Summary of whole rock major elements, magnetic susceptibilty and radioactivity of granitoids from Muara Sipongi and its surrounding areas

No.	Sample	Locality	Rock	Mag.	Rad.	Major elements (wt.%)											
	code		name	Susc		SiO_2	TiO_2	Al_2O_3	FeO	MnO	MgO	CaO	Na_2O	K_2O	P_2O_5	LOI	Total
1	MS2	Muarasipongi				50.10	0.54	15.30	7.46	0.12	3.17	13.18	2.40	1.34	0.12	5.42	99.16
2	MS3	Muarasipongi	Granodiorite	15.31	0.12	56.75	0.79	16.61	7.96	0.16	3.73	7.33	2.98	1.39	0.20	1.21	99.11
3	MS5	Muarasipongi	Monzogranite	15.17	0.18	56.43	0.78	16.39	8.64	0.15	3.90	7.55	2.90	1.30	0.20	0.78	99.02
4	MS6	Muarasipongi	Monzodiorite	10.34	0.16	63.89	0.50	15.12	5.75	0.11	2.31	4.77	3.25	2.06	0.12	1.49	99.37
5	MS7	Sungai Cibadak	quartz syenite	9.60	0.14	67.01	0.45	14.59	4.53	0.08	1.84	3.72	3.00	3.21	0.09	0.96	99.48
6	MS10	Tanjung Alai	Quartz monzonite	7.93	0.19	64.80	0.52	14.50	5.79	0.09	2.23	4.40	3.25	2.46	0.11	1.20	99.35
7	MS11	Muarasipongi	monzogranite	9.36	0.12	61.53	0.58	15.96	6.77	0.11	3.08	2.73	3.50	2.49	0.14	2.35	99.24
8	MS12	Muarasipongi	Quartz monzonite	7.38	0.17	67.61	0.46	13.98	5.34	0.09	1.86	3.76	2.91	3.23	0.09	0.67	100.00

Explanation:
FeO = The expression of total Fe content.
LOI = Lost on Ingnition; Mag. Susc. = magnetic susceptibility (x 10^{-3} SI), Rad.=Radioactivity (µSv/hr)
MS= Muara Sipongi; SC= Sungai Cibadak; TA: Tanjung Alai

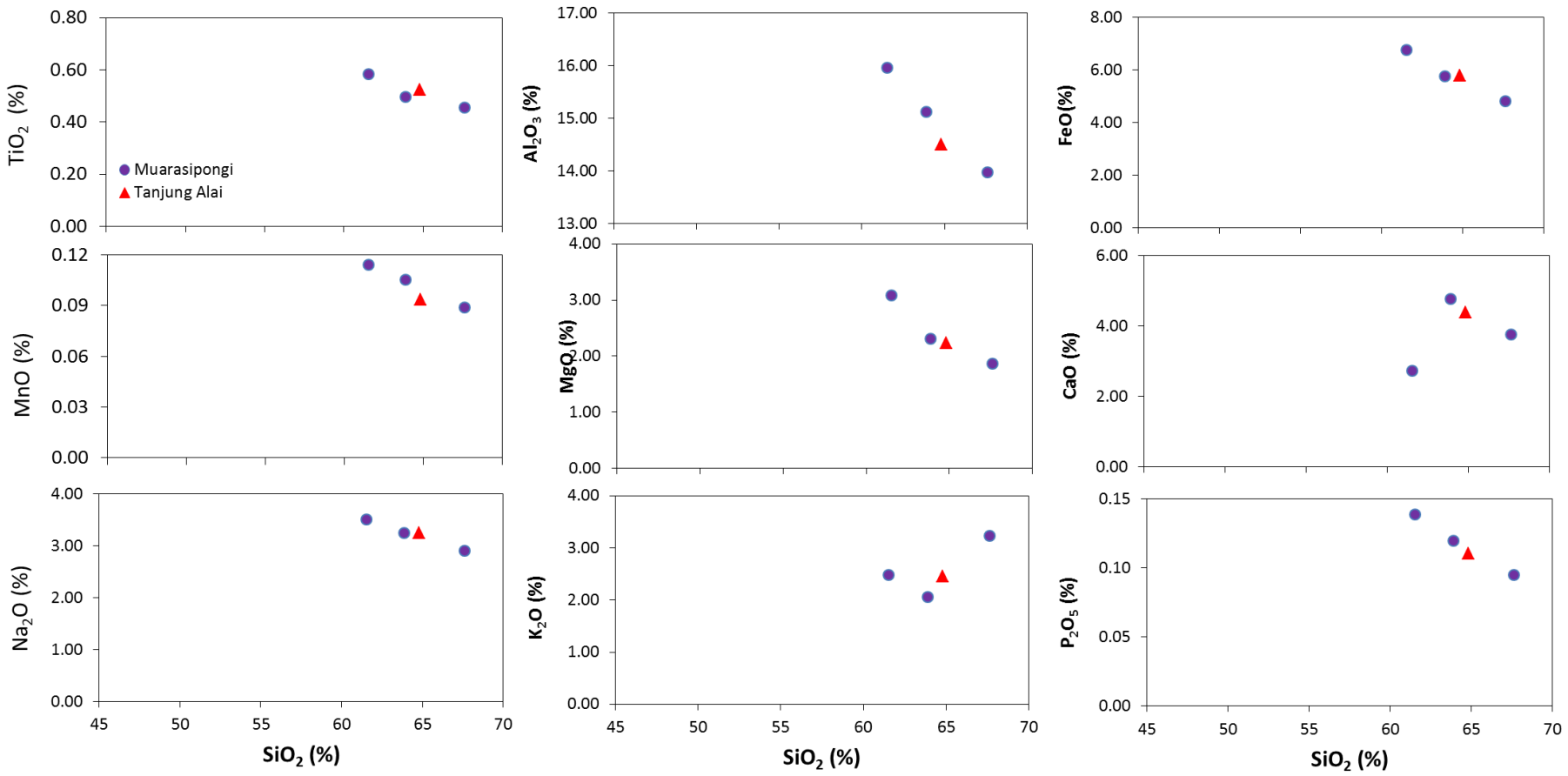

Fig 6.7 Harker diagram of granitoids from Muara Sipongi and its surrounding areas.

6.3.2 Rare earth elements

A total of ten samples were analyzed, but only three fresh and least altered samples were presented, because of (Table 6.6). These are monzogranite, and quartz monzonite from Muara Sipongi (MS6, MS 11, and MS 12). ΣREE of monzogranite ranges from 66 to 75 ppm while that of quartz monzonite is 71 ppm. Chondrite-normalized REE patterns show relatively similar patterns (Fig. 6.8).

Table 6.6 Rare earth elements concentration of granitoids from Muara Sipongi and its surrounding areas

No	Sample code	La	Ce	Pr	Nd	Sm	Eu	Gd	Tb	Dy	Ho	Tm	Er	Yb	Lu	ΣREE
1	MS-02	7.5	15	2.12	9.6	2.54	0.82	2.88	0.42	2.74	0.63	0.32	1.69	1.82	0.3	48.4
2	MS-03	10.8	22.6	3.19	12.8	3.48	1.06	3.4	0.46	3.41	0.76	0.32	2.32	2.21	0.38	67.2
3	MS-05	9.1	20.3	2.73	12.2	3.55	0.88	3.86	0.64	3.99	0.8	0.35	2.6	2.47	0.32	63.8
4	MS-06	10.7	22.9	3.11	11.4	2.75	0.72	3.7	0.53	3.66	0.73	0.36	2.26	2.43	0.34	65.6
5	MS-07	11.1	24.3	3.26	13	3.34	0.73	3.57	0.67	3.75	0.85	0.41	2.74	2.67	0.45	70.8
6	MS08	9	15.9	2.06	8.5	2.15	0.9	2.46	0.38	2.42	0.49	0.23	1.55	1.56	0.24	47.8
7	MS09	14.1	27.3	3.42	13.8	3.26	0.75	3.43	0.59	3.64	0.73	0.34	2.06	2.44	0.41	76.3
8	MS-10	10.4	23.1	2.83	12.3	3.08	0.66	3.28	0.53	3.6	0.7	0.3	2.35	2.29	0.37	65.8
9	MS-11	10.9	24.5	3.06	13.3	3.47	0.64	3.73	0.56	3.92	0.92	0.37	2.56	2.81	0.38	71.1
10	MS-12	11.9	26.4	3.46	13.5	3.76	0.63	3.85	0.58	3.59	0.8	0.44	2.8	2.9	0.43	75.0

Explanation : ∑REE Total summary of REE.

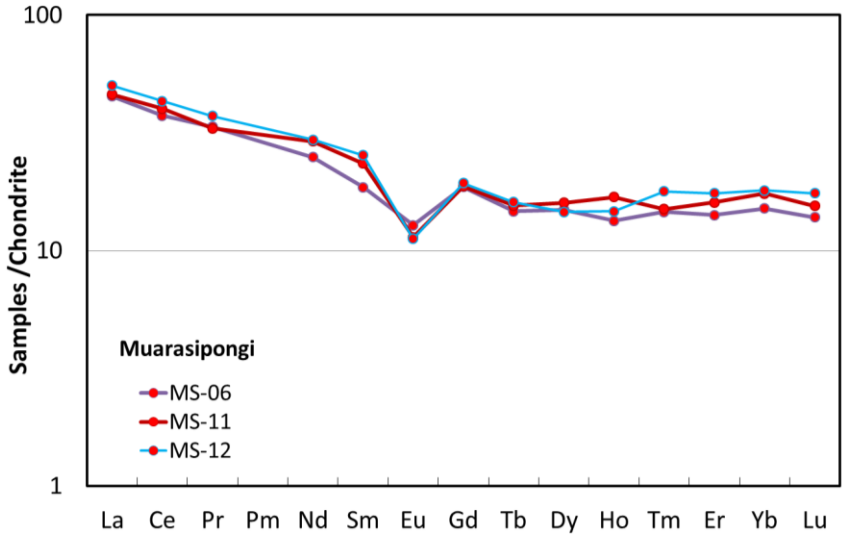

Fig. 6.8 Chondrite-normalized diagram of granitoids from Muara Sipongi and its surronding areas (values of chondrite are from McDonough & Sun, 1995).

6.4 Kotanopan

6.4.1 Major elements

A total of eight samples were collected from Kotanopan (KNP2 – KNP4 and KNP 8) and Tolung (KNP 5- KNP 7 and KNP 9). Four out of eight samples relatively fresh (KNP2, KNP3, KNP 4 and KNP 9). The major elements, trace elements, and rare earth elements contents of them are analyzed (Table 6.7).

SiO_2 contents of quartz monzonite, tonalite, and monzogranite from Kotanopan range from 62.4 to 71.0 wt. %. The SiO_2 content of monzodiorite is 66.5% wt.%. TiO_2, Al_2O_3, FeO, Na_2O, MnO, K_2O and P_2O_5 are negatively correlated with SiO_2 while CaO and Na_2O are positively correlated with SiO_2 (Fig. 6.9).

Plots of SiO_2 versus (FeO_{tot}/[FeO_{tot}+MgO]), and SiO_2 versus (Na_2O+K_2O-CaO) (Fig.) and Aluminium Saturation Index (ASI) versus molecular ratio (Al/[Na+K]) (Fig.) discrimination diagrams show that most of the granitoids fall within magnesian and metaluminous based on the classification diagram of Frost et al. (2001) (Fig. 6.1). Rb-(Y+Nb) and Nb-Y discriminant diagrams (Pearce et al, 1984) of granitoids from Kotanopan fall in the volcanic arc environment (Fig. 6.3)

6.4.2 Rare Earth Elements

Eight representative samples were selected, but only three samples were used for the geochemical analyses, because of these selected samples are fresh or least altered. KNP2 and KNP 9 from Kotanopan, KNP 4 from Tolung.

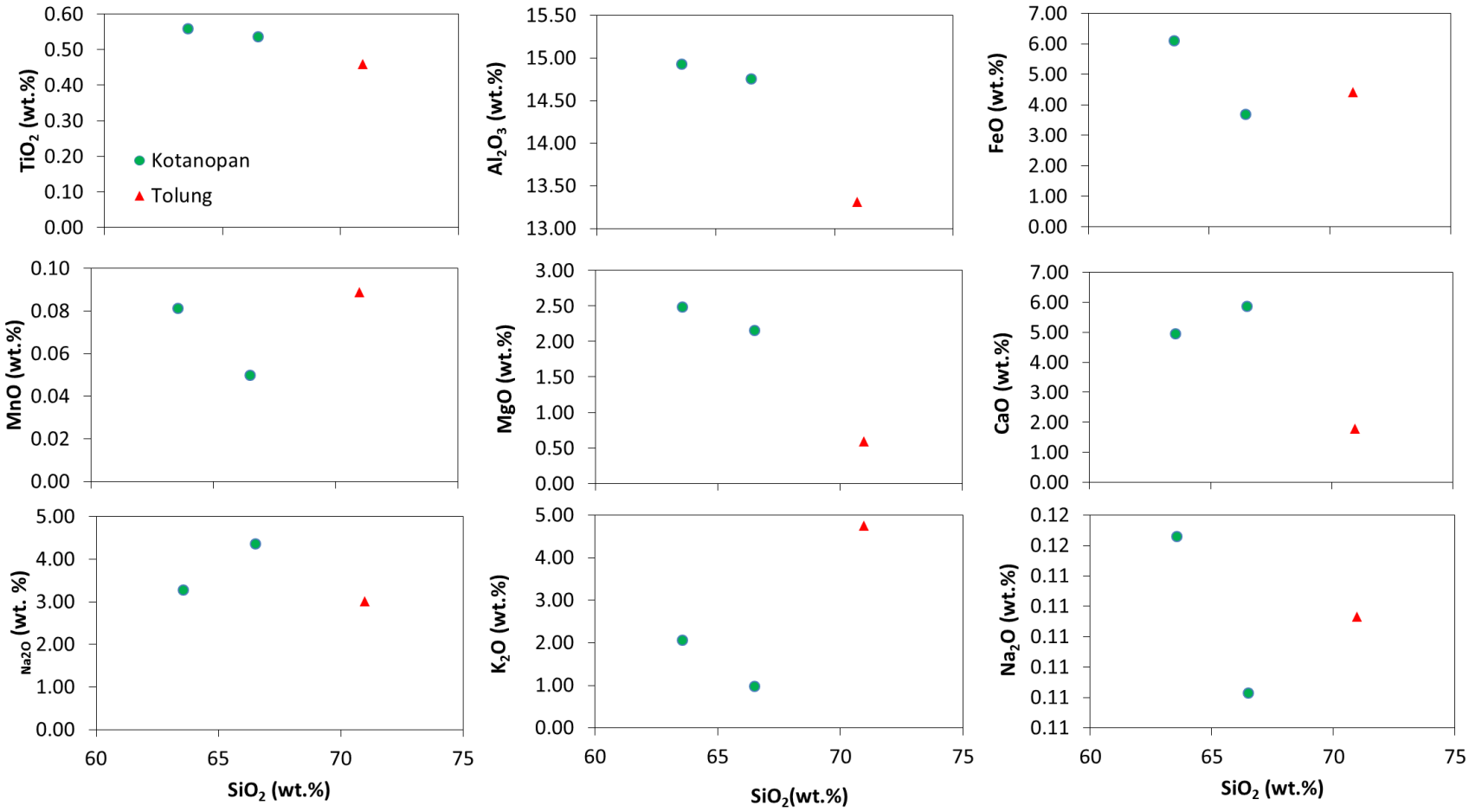

Fig. 6.9 Harker diagram of granitoids from Kotanopan and Tolung.

Table 6.7 Summary of whole rock major elements contents, magnetic susceptibility, and radioacivity of granitoids from Kotanopan and its surrounding areas

Sample	Locality	Mag. Susc.	Rad.	Rock	Major Elements (Wt %)											
code				name	SiO_2	TiO_2	Al_2O_3	FeO	MnO	MgO	CaO	Na_2O	K_2O	P_2O_5	LOI	Total
KNP2	Kotanopan	7.93	0.12	Quartz monzonite	63.55	0.56	14.93	6.10	0.08	2.49	4.96	3.28	2.07	0.12	1.19	99.32
KNP9	Kotanopan	15.78	0.10	monzodiorite	66.50	0.54	14.76	3.68	0.05	2.15	5.86	4.35	0.98	0.11	0.59	99.59
KNP4	Tolung	11.91	0.12	monzogranite	70.97	0.46	13.31	4.42	0.09	0.59	1.78	3.01	4.75	0.11	0.01	99.50

Explanation : Mag. Susc.= Magnetic susceptibility (x 10^{-3} SI unit); Rad. = Radioactivity (μsV/hr). **FeO** = Total Fe expressed as FeO **LOI** = Lost on Ingnition

Table 6.8 Summary of rare earth elements concentration (unit in ppm), magnetic susceptibility, and radioactivity of granitoids from Kotanopan and its surrounding areas

Sample code	Locality	Rock name	Mag. Susc	Rad.	La	Ce	Pr	Nd	Sm	Eu	Gd	Tb	Dy	Ho	Tm	Er	Yb	Lu	∑REE
KNP-02	Kotanopan	Quartz monzonite	7.93	0.12	8.8	21.4	3.0	12.0	2.9	0.8	3.7	0.6	4.0	0.8	0.4	2.7	2.5	0.4	63.8
KNP-04	Tolung	monzogranite	11.91	0.12	89.1	162.0	17.0	55.8	9.0	1.6	7.9	1.2	6.4	1.3	0.5	3.6	3.2	0.5	358.9
KNP-09	Kotanopan	monzodiorite	15.78	0.10	8.0	20.2	3.0	13.4	3.1	0.7	3.8	0.6	3.7	0.9	0.4	2.6	2.8	0.4	63.6

Explanation :
∑REE Total summary of REE.
Mag. Susc. = magnetic susceptibility, Rad.=Radioactivity

ΣREE contents of quartz monzonite and monzodiorite from Kotanopan range from 62 to 63 ppm, while that of monzogranite from Tolung is 359 ppm (Table 6.8).

Chondrite-normalized REE patterns of Kotanopan show relatively flat and overlapped each other, and showing a variation of Eu anomaly (Fig. 6.10), which suggests removal of feldspars. Granitoids from Tolung show enriched in LREE but depleted in HREE. Quartz monzonite and monzodiorite in Kotanopan and monzogranite from Tolung granitoids are possibly derived from different sources.

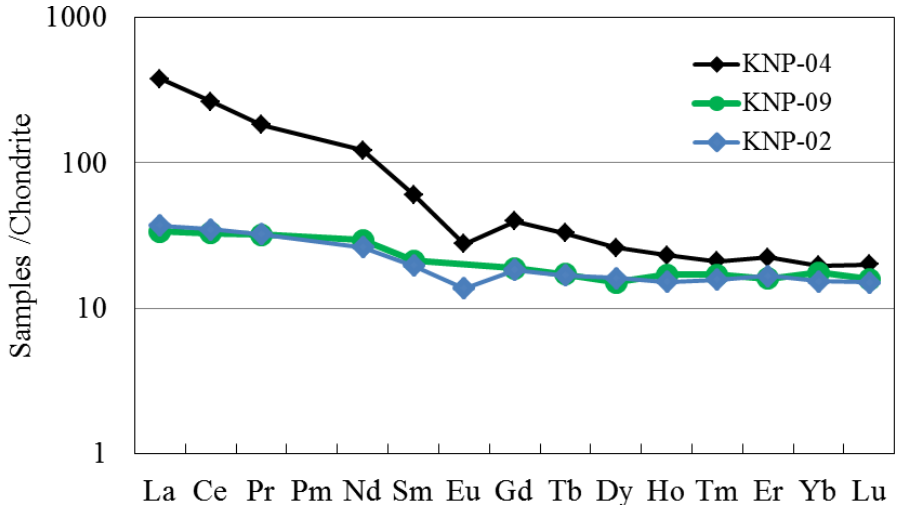

Fig. 6.10 Chondrite- normalized REE diagram of granitoids from Kotanopan and Tolung (values of chondrite are from McDonough & Sun, 1995).

6.5 Type of granitoids

Plots of dicrimination diagram of granitoids from Sibolga were mainly fall in the peraluminous and ferroan (Frost et al., 2001) and they were formed within plate environment (Pearce et al., 1984). According to discrimination diagram of molar $Al_2O_3/(Na_2O+K_2O+CaO)>1.1$, relatively high CaO content, which is typically 3.2 wt%, and low K_2O content (White and Chappell, 1983),

granitoids from Sibolga are I-type in characters. Plots of SiO_2 versus (FeO_{tot}/[FeO_{tot}+MgO]), SiO_2 versus (Na_2O+K_2O+CaO) (Fig. 6.11) and Aluminium Saturation Index (ASI) versus molecular ratio Al/(Na+K) discrimination diagrams (Fig. 6.12) (Frost et al., 2001) show that most of the granitoids from Sibolga are ferroan and peraluminous-granites. However based on other geochemical characteristics which is proposed by Loiselle and Wones (1979), granitoids from Sibolga also have A-type granites characters (Fig. 6.13). The granitoids were characterized by high SiO_2 and (Na_2O+K_2O) contents, Zr, Nb, and Ta contents, and REE contents except Eu, Ga/Al and (FeO_{tot}/[FeO_{tot}+MgO]) ratios, and low Sr, Ba, Eu, CaO and Al_2O_3 contents (Loiselle & Wones, 1979; Collins et al., 1982; White & Chappell, 1983).

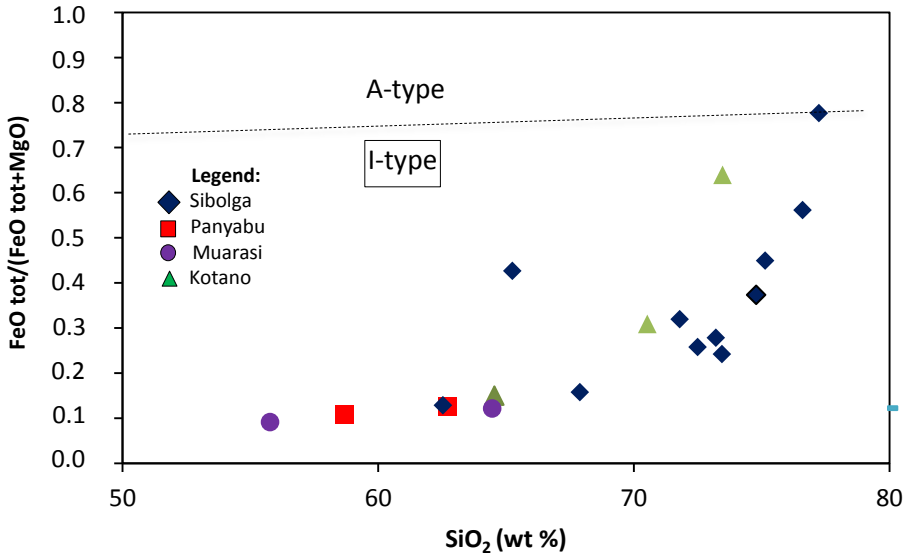

Fig. 6.11 Plots of SiO_2 versus (FeO_{tot}/[FeO_{tot}+MgO]) of granitoids from Sibolga, Panyabungan, Muara Sipongi and Kotanopan.

Spider diagram of Zr, Ta, Rb, Th, Ba, Sr, Nb, Ta and HREE contents (Fig. 6.11 and Table 6.7), and based on other geochemical characteristics as mentioned above, the granitoids from

Sibolga can be classified as I-/A-type granitoids. The granitoids from Sarudik (SR 1 and S16), Sibuluhan Sihaporas (S5, S6, and S7), Sibolga Julu (S23) and Tarutung (S18 and S19) are classified into A-type granitoids, while the granitoids from Sarudik (S14), Tukka (S8, S9, and S10), Sibolga Julu (S17) and Adian Koting (S21) are classified into I-type.

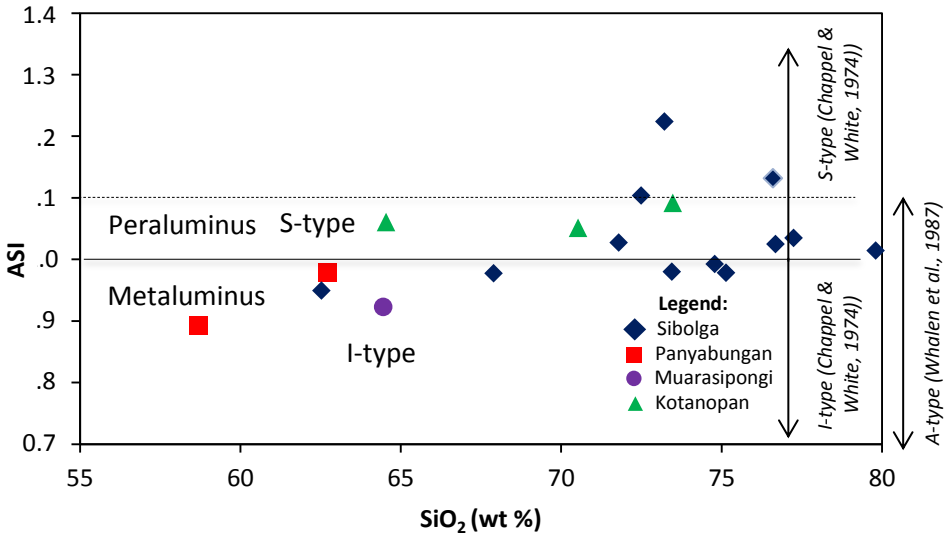

Fig. 6.12 Plots of Aluminium Saturation Index (ASI) versus SiO_2 (wt%) of granitoids from Sibolga, Panyabungan, Muara Sipongi and Kotanopan.

Compared to the A-type granitoids in Besar Island, Malaysia, the A-type granitoids of Sibolga are highly differentiated and their ΣREE contents are higher.

There are three possibilities for the source of A-type granitoids: 1) partial melting of the residue that remained after the production of an I-type granite, 2) partial melting of upper crustal igneous source of tonalitic to granodioritic composition (Creaser et al., 1991), and 3) fractionational crystallization of alkaline magma that forms alkaline igneous complexes (Salvi &

William-Jones, 2005). The granitoids from Sibolga are most probably resulted from partial melting of igneous source of tonalitic to granodioritic composition.

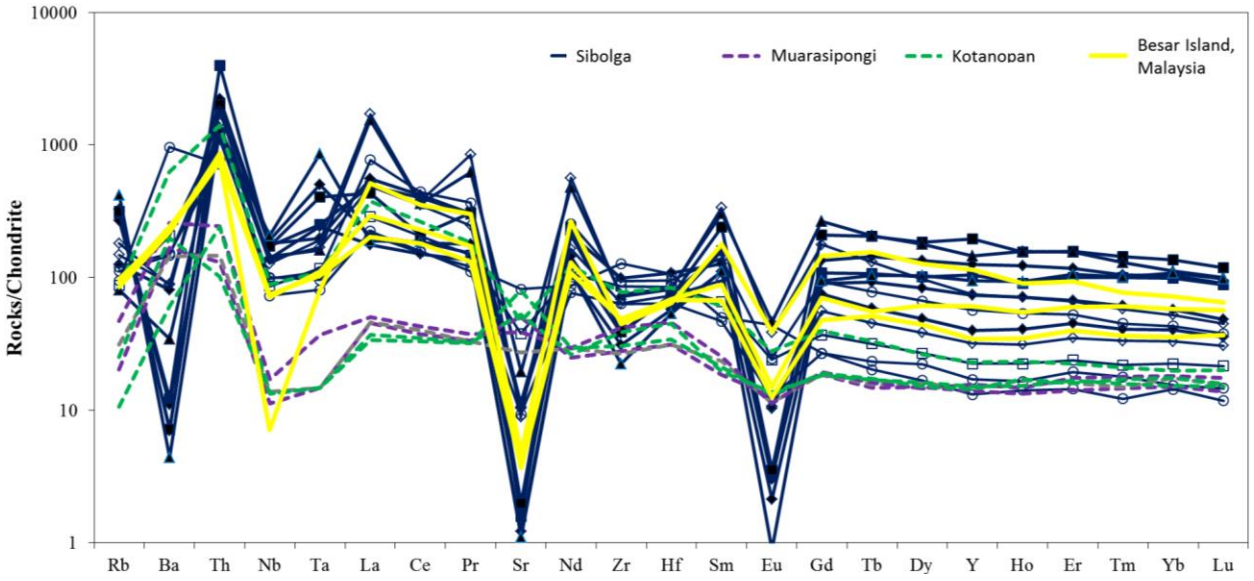

Fig. 6.13 Trace element-normalized patterns show distinct patterns of A- and I-type granitoids. A-type granite from Besar Island area from Ghani et al. (2014).

The granitoids from Muara Sipongi and Kotanopan, are metaluminous, thus I-type, and magnetite-series. Their incompatible elements and high field strength elements (HFSE) contents are high (Table 6.9).

Table 6.9 Summary of trace and major elements compositions of granitoids in Sibolga and its surrounding areas

No	Code	Locality	Rb	Ba	Sr	Zr	Yb	SiO_2	CaO	Al_2O_3	FeO/	Na_2O	ΣREE	LREE	HREY	Granite	Rock Name
			(unit in ppm)					(unit in wt %)			MgO	$+K_2O$	(unit in ppm)			Type	
1	SR1	SRD	752.0	16.9	13.0	145.0	16.7	75.1	0.9	12.7	39.6	8.6	378.1	266.2	309.4	A	Syenogranite
2	S14	SRD	289.0	193.5	75.0	378.0	6.5	73.5	1.3	12.4	7.8	8.0	580.0	533.1	109.2	I	Alkali feldspar syenite
3	S16	SRD	616.0	26.6	8.8	118.0	9.2	79.8	0.5	10.9	16.7	7.6	280.5	212.1	183.5	A	Syenogranite
4	S5	SS	587.0	36.5	15.0	202.0	11.6	77.2	0.7	11.9	12.8	8.0	455.2	388.1	134.4	A	Syenogranite
5	S6	SS	699.0	29.3	11.0	174.0	15.9	74.8	1.0	12.6	35.9	8.4	600.6	509.0	255.1	A	Quartz alkali feldspar syenite
6	S7	SS	723.0	17.2	14.0	149.0	21.9	76.7	0.7	12.4	13.5	8.3	559.9	403.8	462.1	A	Quartz syenite
7	S8	TK	257.0	353.0	84.0	358.0	6.9	72.5	0.9	12.9	9.7	7.8	684.0	626.1	147.1	I	Quartz alkali feldspar syenite
8	S9	TK	276.0	365.0	68.0	241.0	2.5	73.2	0.5	13.3	7.4	8.1	221.5	202.6	45.7	I	Quartz alkali feldspar syenite
9	S10B	TK	218.0	2320.0	591.0	485.0	2.3	62.5	3.2	16.4	4.0	9.3	221.2	205.1	36.8	I	Quartz alkali feldspar syenite
10	S17	SJ	184.5	82.6	142.0	283.0	18.1	65.3	1.4	19.1	9.3	10.2	1075.5	914.1	389.4	I	Quartz syenite
11	S23	SJ	966.0	10.6	8.0	85.0	17.5	76.3	0.6	12.8	33.8	8.4	333.0	240.7	240.4	A	Monzogranite
12	S18B	TR	342.0	216.0	64.0	272.0	8.4	76.6	0.3	12.1	11.2	8.1	1112.1	1022.9	206.2	A	Quartz monzonite
13	S19	TR	417.0	212.0	77.0	244.0	5.3	71.8	0.5	14.0	11.9	9.8	481.1	444.8	86.2	A	Quartz syenite
14	S21	AK	200.0	496.0	274.0	329.0	3.6	67.9	2.9	14.4	4.2	7.3	292.4	267.6	59.9	I	Quartz syenite
Muara Sipongi																	
15	MS 6	MS	46.8	404.0	366.0	2.4	106.0	63.9	4.8	15.1	2.5	5.3	65.6	29.8	35.8	I	Monzogranite
16	MS 11	MS	72.1	348.0	197.0	2.8	102.0	61.5	2.7	16.0	2.2	6.0	71.1	33.2	38.0	I	Quartz monzonite
17	MS 12	MS	108.0	619.0	280.0	2.9	160.0	67.6	3.8	14.0	2.6	6.1	75.0	35.3	39.8	I	monzogranite
Kotanopan																	
18	KNP2	KNP	58.1	478.0	381.0	2.5	148.0	63.6	5.0	14.9	2.5	5.3	63.8	48.9	40.0	I	Quartz monzonite
19	KNP4	KNP	193.0	1500.0	337.0	3.2	297.0	71.0	1.8	13.3	7.5	7.8	358.9	334.4	63.5	I	monzogranite
Besar Islanda, Malaysia (Ghani et al., 2014)																	
20	BH2	Hujung	212.0	585.0	34.0	171.0	11.6	75.7	0.5	12.1	27.7	8.4	615.3	514.6	131.8	A	Syenogranite
21	BT10	Tengah	196.0	534.0	27.0	186.0	5.7	77.9	0.2	12.2	20.4	8.5	268.3	230.3	48.8	A	Syenogranite
22	BES6	Besar	225.0	548.0	26.6	181.0	9.3	77.3	0.4	12.1	42.6	4.0	354.7	298.8	70.8	A	Syenogranite

Explanation :
LREE = Summary of Light Rare Earth Elements (La to Eu). HREE is the summary of Heavy Rare Earth Elements (Gd to Lu).
∑REE Total summary of LREE and HREE. HREY= HREE + Y;
SRD= Sarudik, SS= Sibuluhan Sihaporas, TK=Tukka, SJ=Sibolga Julu, TR= Tarutung, AK= Adian Koting

6.6 Origin of granitoids

Syenogranite from Sarudik (SR1) exhibits negative Ba and Sr anomalies and is enriched in Rb, Th, and REE (Fig. 6.14). These features are comparable to those of typical crustal melts, e.g. granitoids of the Lachlan Fold Belt (Chappell & White, 1992). The Ba and LREE contents of quartz alkali feldspar syenite from Tukka, quartz syenite from Adian Koting and quartz syenite from Sihobuk are higher, but HREE contents are lower compared to the syenogranite from Sarudik. These patterns are the characteristics of I-type granites. On the other hand, quartz syenite and alkali feldspar syenite from Tanjung Jae and quartz alkali feldspar syenite from Pintu Padang Julu show quite similar patterns with the I-type granitoids but Th, Nb, LREE and HREE contents are lower (Fig. 6.14).

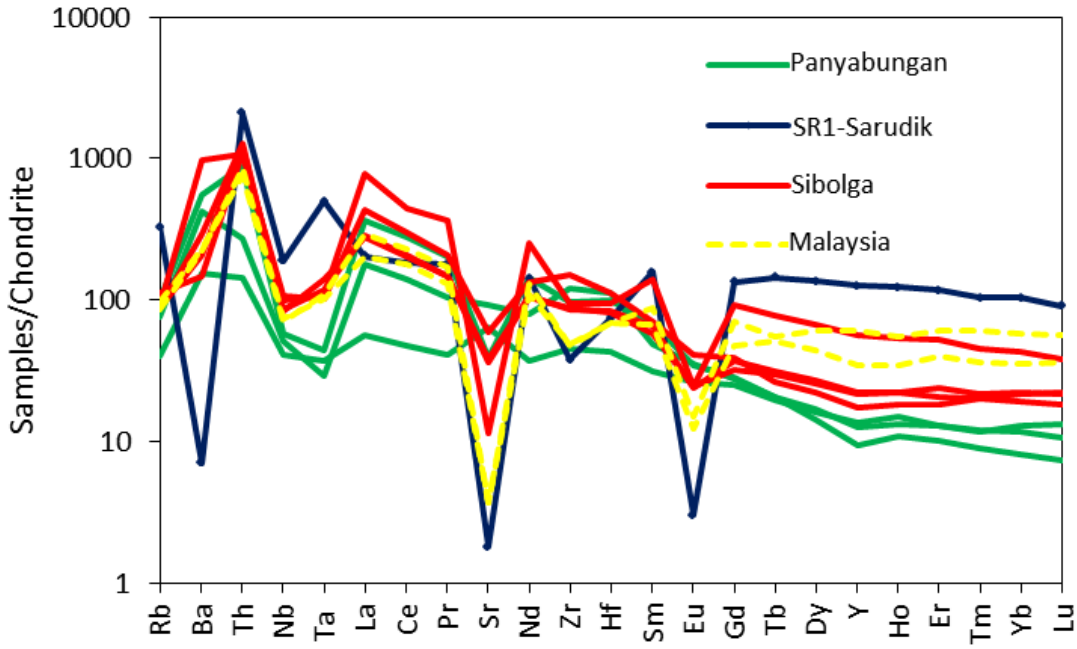

Fig. 6.14. Chondrite normalized trace element patterns show A-, S- and I-type characters of granitoids from Sibolga Panyabungan, and Main Range of Malay Peninsula (Ng et al., 2015) (values of chondrite are from McDonough & Sun, 1995).

HREE contents of A-type granites from Main Range of Malay Peninsula are lower, and Ba, Th, and Eu contents are higher (Ng et al., 2015) than those of A-type syenogranite from Sarudik (Fig. 6.13). Rb contents with respect to Y+Nb contents and Nb contents with respect to Y contents of quartz alkali feldspar syenites and quartz syenites from Tukka, Sihobuk, Adian Koting were plotted in the field of within plate setting (WPG) (Fig. 9.11).

Syenogranite from Sarudik, quartz syenite, and alkali feldspar syenite from Tanjung, and quartz alkali feldspar syenite from Pintu Padang Julu, were plotted in the field of volcanic arc environment (VAG) (Pearce et al., 1984) (Fig. 6.15).

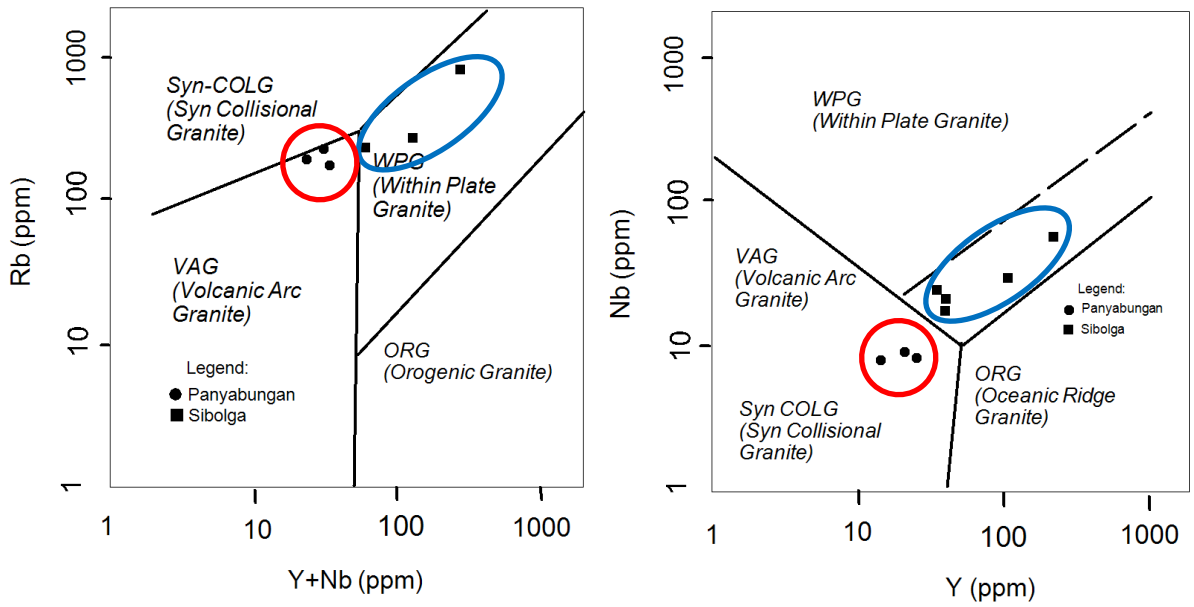

Fig. 6.15. Y/Nb and (Y+Nb)/Rb discrimination diagram of granitoids from Sibolga and Panyabungan.

CHAPTER 7

MINERAL CHEMISTRY AND Sr-Nd ISOTOPES OF GRANITOIDS OF THE STUDY AREAS

7.1 Mineral chemistry of granitoids from Sibolga, Panyabungan and Kotanopan

Titanite, zircon, apatite, and allanite in three fresh granitoids from Sibolga were identified. The mode of occurrences of zircon, apatite and allanite are almost similar in all the observed samples, while titanite was found only in the syenogranite and alkali feldspar granite from Sarudik. Allanite and titanite found in syenogranite and alkali feldspar granite from Sarudik are primary in origin and exhibit euhedral shape (Fig 7.1). Size of allanite ranges from 0.1 to 1.4 mm across. Zoning and metamict textures indicate the presence of radioactive elements. Titanite exhibits euhedral shape, from 100 to 300 μm in size, and contains La, Ce, and Nd. Large prismatic allanite crystals associated with quartz, K-feldspar and biotite showing zoning in the syenogranite from Sarudik indicate different REE proportions (Fig. 5.8). Whereas whole-rock P_2O_5 content of quartz alkali feldspar syenite from Sibuluhan Sihaporas and quartz monzonite from Tarutung tends to be low ranging from 0.01 to 0.03 wt.%, the whole-rock ΣREE contents are high ranging from 601 to 1112 ppm, presumably due to the occurrences of allanite. Apatite is not abundant in the quartz alkali feldspar syenite from Tukka and Tarutung, syenogranite and alkali feldspar granite from Sarudik and quartz syenite from Sibuluhan Sihaporas.

Compositions of the REE-bearing mineral of quartz syenite from Adian Koting and that of syenogranite (SR1), alkali feldspar granite (SR2) and quartz alkali feldspar syenite from Adian Koting were analyzed. REE-bearing minerals are titanite, zircon, apatite, and allanite, and the results are summarized in Chapter 5, Table 5.1, Figure 7.1.

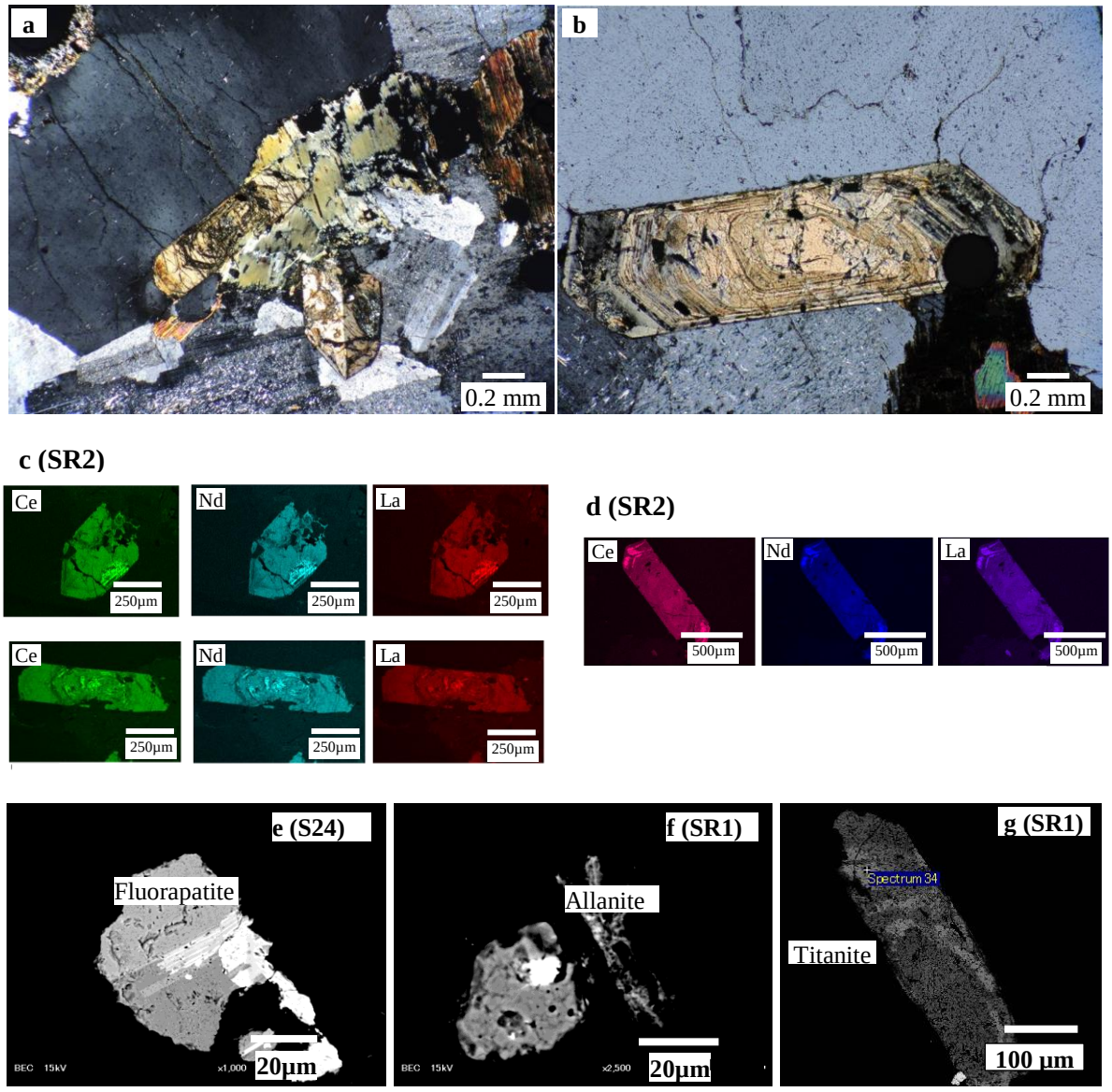

Fig. 7.1 Photomicrographs (a and b) which were taken under an optic microscope under crossed nicols and elemental composition mapping by a sanning electron microscope (c and d) of coarse-grained allanite (aln) crystal in alkali feldspar granite from Sarudik (SR2) are euhedral shape, prismatic and zoning, indicate different proportion of REE contents. The allanite (aln) is associated with K-feldspar, quartz, and biotite. Backscaterred electron by a sanning electron microscopes of REE-bearing minerals of quartz alkali feldspar syenite from Sihobuk consisting of fluorapatite (fl.apt) (e), quartz alkali feldspar syenite and syenogranite from Sarudik (f-g), consisting of allanite (aln) and titanite (ttn).

REE-bearing apatite was identified at Adian Koting (SB2). The apatite contains cerium (Ce), neodymium (Nd), and ytterbium (Yb) (Fig 7.2). Zircon, apatite, and allanite occurred in all samples with exceptions of titanite, which were only found in the syenogranite and alkali feldspar granite from Sarudik area (Fig 7.1). Large prismatic crystals of allanite associated with quartz, K-feldspar and biotite, showing zoning texture in the syenogranite from Sarudik area indicate different REE proportions.

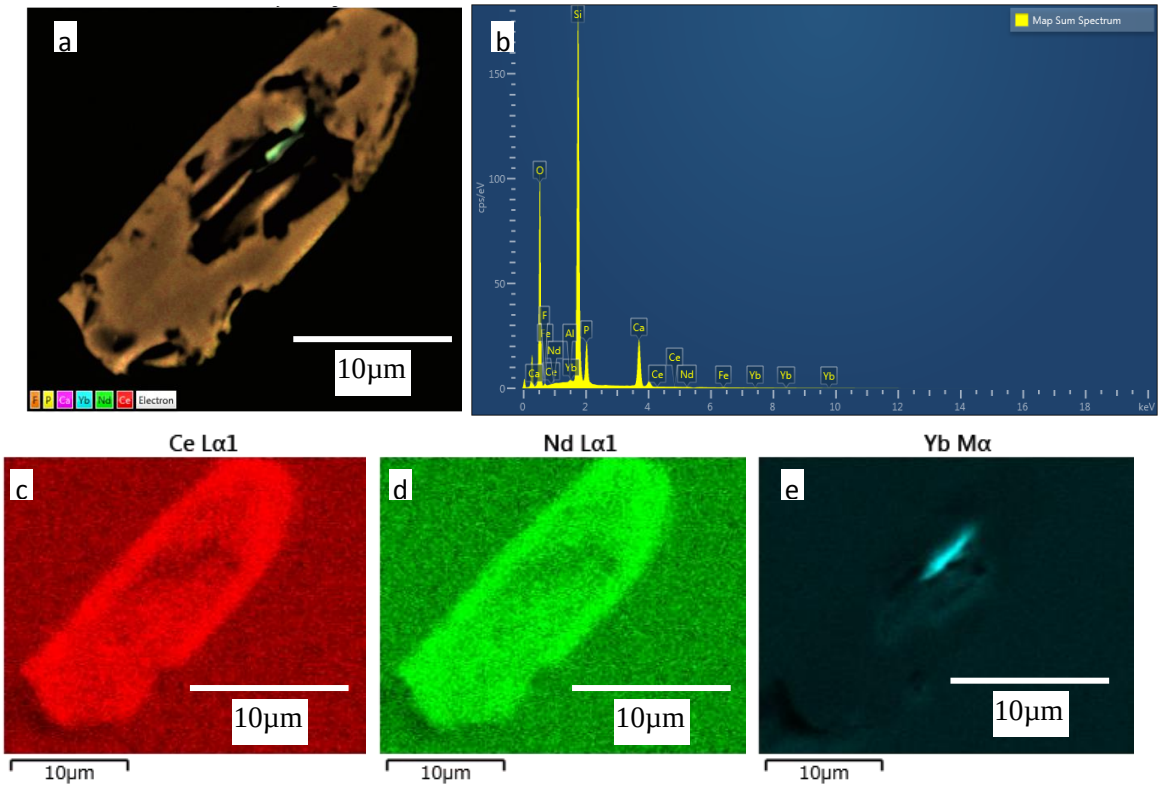

Fig 7.2 Composition mapping of apatite from quartz syenite (SB2) at Tarutung near to Sibolga contains Ce, Nd and Yb. a). Crystal of apatite contains F, P, Ca, Ce, Yb, and Nd, b). A map summary spectrum of apatite shows major composition and contain Ce, Yb, and Nd, c) Ce distribution in the apatite. d). Nd distribution in the apatite. e). Yb distribution in the apatite

In Panyabungan, quartz syenite from Tanjung (PYB 4D) and monzodiorite from Parmompang (PYB 2) were selected for SEM-EDS analysis. The result shows that quartz syenite

contains zircon and apatite, and titanite. Titanite contains Ce, Nd, and Yb (Fig. 7.3). Monzodiorite contains zircon. SEM-EDS photomicrograph is shown in Figure 7.4.

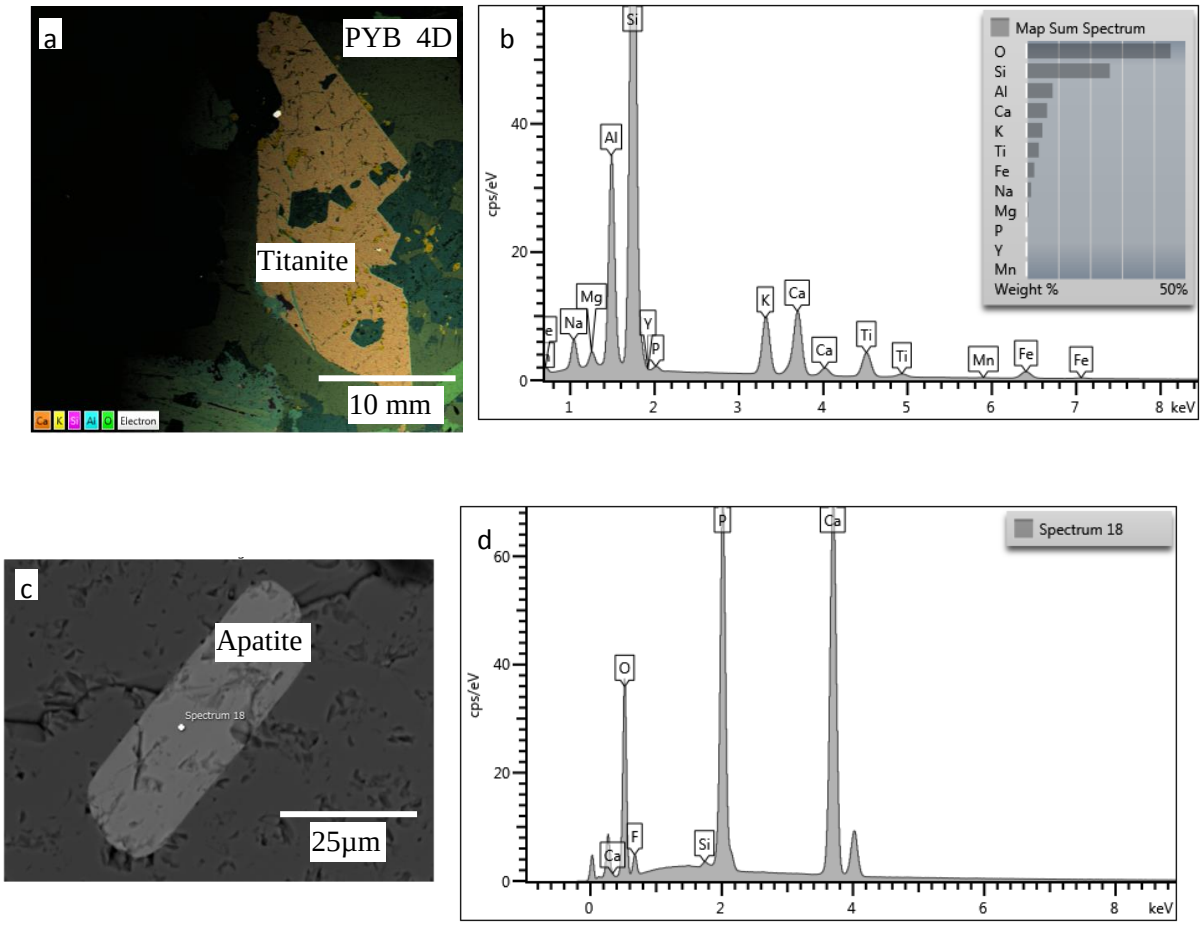

Fig.7.3 Mineral mapping of titanite and apatite in quartz syenite from Tanjung (PYB 4D). a) Titanite crystal showing its major composition, b) A map summary spectrum of titanite, c) A backscattered image of apatite, and d) spectrum of major composition of apatite.

There are no samples selected from Muara Sipongi for SEM-EDS because occurrences of REE-bearing minerals were scarce. Granitoids from Kotanopan and Muara Sipongi contain less REE-bearing minerals compared to that of granitoids from Sibolga. Only zircon was observed in granitoids from Kotanopan (KNP 7) (Fig. 7.5).

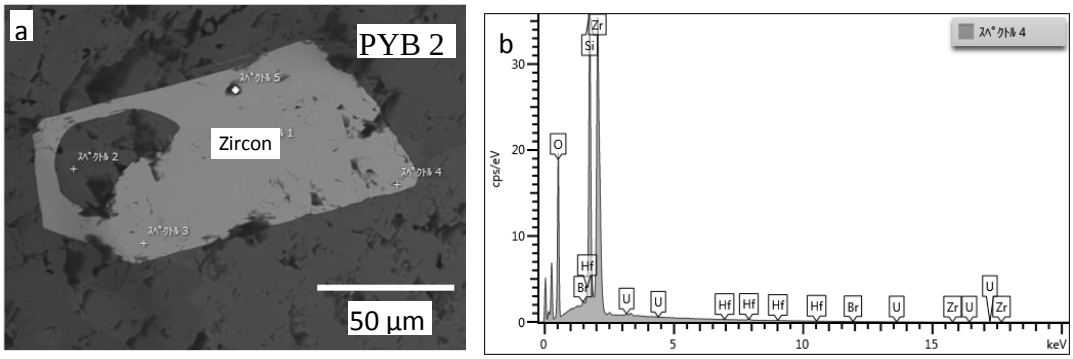

Fig. 7.4 Zircon in association with U and Th, monzodiorite from Parmompang (PYB 2). a) A backscattered image of zircon, and b). Spectrum of zircon that containing Th and U.

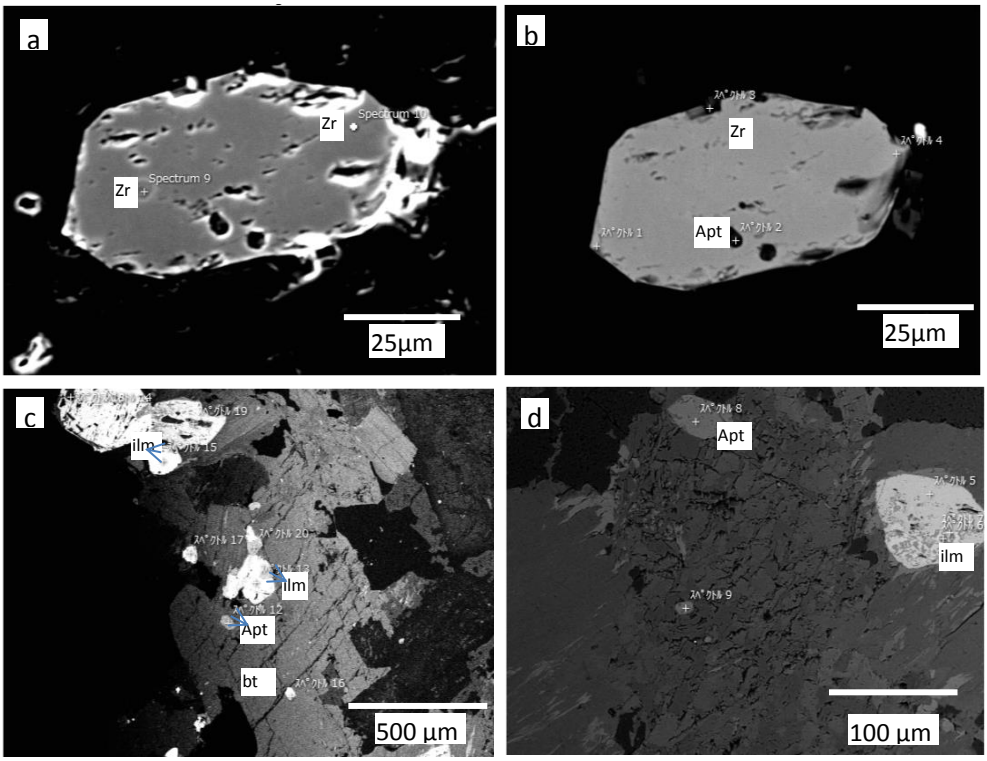

Fig 7.5 Backscatttered electron images of a). Zircon (zr) and b). zircon contain apatite (apt), c-d. apatite and ilmenite (ilm) occurences as inclusion within biotite in granitoids from Kotanopan, and d). apatite and ilmenite as the mineral inclusions in feldspar .

7.2 Sr-Nd isotopic signatures of granitoids in the western part of Sibolga and Panyabungan

Granitic rocks in Sumatra island are divided into two provinces, namely the Western and Main Range granites (Cobbing, 2005). The granitic rocks of the Western Belt consist of I-type granitoids and are confined to Barisan Mountains in Sumatra. The Main Range granitic rocks are mainly S-type with subordinate I-type and characterized by tin mineralization (Hutchison & Taylor, 1978; Cobbing, 2005).

A study of Sr-Nd isotopic characters of granitods was focused on granitoids from Sibolga and Panyabungan which have high ΣREE contents compared to those of Muara Sipongi and Kotanopan (Chapter 6).

Granitoids at Sibolga were identified as I-, and A-type ilmenite-series, and those at Panyabungan as S-type ilmenite-series (Chapter 6) (Loiselle & Wones, 1989; Chappell & White, 1992; Frost et al., 2001). Granitoids from Sibolga are quartz syenite, quartz alkali feldspar syenite and syenogranite, while Panyabungan granitoids consist of alkali feldspar syenite, quartz alkali feldspar syenites and quartz syenite. The granitoids at Sibolga are composed of biotite – hornblende granite and granodiorite with pink K-feldspar megacrysts, mafic enclaves, and dikes. These characteristics are typical of the Eastern Granite Province of Peninsular Malaysia and the Tin Islands of Indonesia (Cobbing, 2005). However, granitic rocks of the Main Range and Western Granite Provinces exist in Sumatra island (Figure 7.6).

The Panyabungan Granitoids are mainly coarse-grained, light gray color, consist of K-feldspar megacrysts, muscovite, contain metasedimentary rocks enclaves and are slightly deformed. The photographs of outcrops show in the Figure 7.6. The summary of locality, tectonic environments and geochemical characteristcs of the granitoids from Sibolga and Panyabungan is depicted in Table 7.1.

Figure 7.6 Photographs of outcrops used for isotope study at Sibolga and Panyabungan and their surrounding areas: a. PYB 4D (Tanjung), b. P4 (Tanjung Jae), P7 (Pintu Padang Julu), d. P8 (Tano Tombangan), e. SB3 (Adian Koting), f. S21 (Adian Koting), g. S8 (Tukka), h. SR1 (Sarudik), and i. S24 (Sihobuk).

A total of nine samples from different locations including from Sibolga (Sarudik, Sihobuk, Tukka, Adian Koting) and Panyabungan (Tanjung and Pintu Padang Julu) were studied to reveal their Sr and Nd isotopic compositions. The granitoids from the former represent the Sibolga Granite Complex and those from the latter are Panyabungan Batholith.

Table 7.1 Summary of Rb, Sr, Sm and Nd contents of selected granitoids from Sibolga and Panyabungan.

No.	Location	Sample code	SiO_2 (wt %)	Rb (ppm)	Sr (ppm)	Rb/Sr	Sm (ppm)	Nd (ppm)	Sm/Nd
1.	Tanjung Jae	PYB4D	74.74	92.6	457	0.20	4.66	17.0	0.27
2.	Tanjung Jae	P4	72.80	226	283	0.80	10.15	65.2	0.16
3.	Pintu Padang Julu	P7	66.37	173	668	0.26	7.28	36.8	0.20
4.	Tano Tombangan	P8C PEG	54.97	117	262	0.45	10.35	53.6	0.19
5.	Sarudik	SR1	75.14	752	13.1	57.4	23.40	65.5	0.36
6.	Adian Koting	SB3	67.92	204	264	0.77	8.47	47.8	0.18
7.	Tukka	S8	72.50	257	83.5	3.08	20.70	116.0	0.18
8.	Adian Koting	S21_2	67.90	200	274	0.73	9.72	48.6	0.20
9.	Sihobuk	S24B	65.96	208	427	0.49	10.45	61.6	0.17

To examine analytical precision and reproducibility for the isotopic measurement of Sr and Nd, we repeatedly analyzed standard solutions of ARMS and NBS 987 for Sr, and those La Jolla, and DEWA standard solution for Nd. The mean values for ARMS is 0.710191 ± 0.00001 (2σ, n=20), those for NBS 987 is 0.710230 ± 0.000005(2σ, n=20), those for La Jolla 0.511839 ± 0.000008, and those for DEWA were 0.512131 ± 0.000004. These values are consistent with published data. Comparing the results the mean values for the standard solutions show good agreement for the isotope measurement.

Three silicate rock standards from te Geological Survey of Japan (GSJ) were selected to cover the range of major elements compositions of natural igneous rocks. The selected standards

are JR2, JB-2, JA1. The measured of Sr isotope ratios are 0.705423±0.000003, 0.513119+ 0.705482±11, and 0.513059 ± 0.000014, respectively (Table 7.3).

Sr isotopic ratios ($^{87}Sr/^{86}Sr$) were calculated from 20 to 23 measurement blocks for granitoids from Panyabungan and 14 to 40 blocks for granitoids from Sibolga. Final decision values were decided after offline and standard corrections. The $^{87}Sr/^{86}Sr$ (p) of granitoids from Tanjung Jae ranges from 0.720814 to 0.718746, those from Pintu Padang Julu ranges from 0.711523 to 0.711536, and that from Tano Tombangan ranges from 0.715757. The $^{87}Sr/^{86}Sr$ (p) of granitoids from Sarudik, 1.223221 to 1.222425, are the highest among all the samples even with those from Panyabungan. Those from Adian Koting ranges from0.717345 to 0.717691, and those from Sibolga Julu ranges from 0.744167 to 0.720253. The $^{87}Sr/^{86}Sr$ (p) of granitoids from Sarudik is the highest, calculated value average is 1.222823 (Table 7.3).

The calculation of initial Sr isotope ratios are using the present-day (measured) $^{87}Sr/^{86}Sr$ (Sr_p) using the equation :

$^{87}Sr/^{86}Sr\ (Sr_p) - {}^{87}Sr/^{86}Sr\ (Sr_i) = {}^{87}Rb/^{86}Sr\ (Sr_p)\ (e^{\lambda t-1})$ (Rasskazov et al., 2010)

Nicolaysen (1961) used this equation for calculating Sr (i) using isochron method,

where

$y = mx + b$

y = measured $^{87}Sr/^{86}Sr\ (Sr_p)$,

m slope = $e\ \lambda t-1$, x = $^{87}Rb/^{86}Sr$ p (calculated using the Sr_p)

b= unknown Sr (Sr_i)

For slope measurement, the age (t) is referring to the age obtained by the previous study (Table 7.2). The assumed age of the granitoids were taken from at the closest of the collected granitoids sample.

The $^{143}Nd/^{144}Nd$ isotopic ratios of 9 samples were analyzed and they have a very good result and reproducible. Two samples did not yield good results in $^{143}Nd/^{144}Nd$ because the recovered Nd is very low. Hence there are relatively large analytical uncertainties. In addition, we could not obtain Nd isotope analysis of Tano Tombangan (Panyabungan) and Sarudik (Sibolga) granitoids. The initial Nd isotopic ratios usually do not differ widely for whole-rock samples. This is due to a relatively long half-life of Sm and a very limited fractionation between Sm and Nd caused by their similar geochemical behavior.

The $^{143}Nd/^{144}$ Nd isotopic ratios were calculated from 10 to 28 measurement blocks for granitoids from Panyabungan and 11 to 20 blocks for granitoids from Sibolga. Final decision values were decided after offline and standard corrections. The $^{143}Nd/^{144}$ Nd (p) of granitoids from Tanjung Jae ranges from 0.512214 to 0.512220, those from Pintu Padang Julu ranges from 0.512251 to 0.512274. The average of $^{143}Nd/^{144}$ Nd (p) of granitoids from Adian Koting ranges from 0.512205 to 0.512217 and those from Tukka and Sihobuk at Sibolga ranges from 0.512014 to 0.512018, and 0.512007 to 0.512025. The summary of Sm/Nd depicted in Table 7.4.

The $\varepsilon^{143}Nd$ value is estimated approximately -8.2 and -7.5 assuming an age of 202 Ma for granitoids from Tanjung Jae and Pintu Padang Julu, respectively. The $\varepsilon^{143}Nd$ value is estimated approximately -8.7 and -8.2 assuming an age of 219 Ma for the granitoids from Adian Koting, that of -12.1 and -12.3 assuming an age of 264 Ma for granitoids from Tukka and Sihobuk (Sibolga), respectively.

The isotopic evolution of Nd in the Earth is described in terms of CHUR (Chondritic Uniform Reservoir: DePaolo, 1988). This model mantle is defined to have initial $^{143}Nd/^{144}Nd$ and Sm/Nd ratios equal to those of chondrites.

Table 7.2 Summary of age dating result of Sibolga and Panyabungan area

Location	Inferred location	Isotopic method mineral	Age (Ma)	References
Sibolga granite complex	Unspecified area	K/Ar on biotite	206.1+2.5	Hehuwat, 1975
Sibolga	Unspecified area	K-Ar, biotit	211±3	Hehuwat, 1976
Sibolga	Unspecified area	K-Ar, hornblenda	219±4	Hehuwat, 1976
Sibolga	Unspecified area	Sr-Rb	257±24	Hehuwat, 1977
Sibolga (near city)	Sarudik (?)		264	Aspden et al., 1982
	Unspecified area	K-Ar on biotite	211+5	Beckinsale (in Aspden 1982)
Sibolga	Unspecified area	Rb-Sr, biotit	211,5±2,6	Wikarno dkk. (1988)
Sibolga	Unspecified area	Rb-Sr, biotit	217,4±4,4	Wikarno dkk. (1988)
Padang Sidempuan	Panyabungan (?)	K-Ar, biotite	202±2	Wikarno dkk. (1993)
Sibolga granite complex (Mpisl)	Unspecified area	Rb/Sr whole rock	264+6	Wikarno dkk. (1993)
Tarutung	Adian Koting (?)	Rb-Sr, hornblenda	206,1±2,5	Wikarno dkk. (1988)
Tarutung	Tarutung	Rb-Sr, biotit	218,8±3,9	Wikarno dkk. (1988)
Sibolga	Unspecified area	K-Ar, biotit	206±2	Fontaine & Gafoer (1989)
Satelit Sibolga	Unspecified area	K-Ar, biotit	212±3	Fontaine & Gafoer (1989)
Sibolga	Unspecified area	K-Ar, biotit	216±3	Fontaine & Gafoer (1989)
Satelit Sibolga	Unspecified area	K-Ar, biotit	217±4	Fontaine & Gafoer (1989)
Sibolga	Unspecified area	K/Ar on Hbd	144+2.4	Fontaine & Gafoer (1989)
Sibolga	Unspecified area	K/Ar on biotite	147+2.4	Fontaine & Gafoer (1989)
Sibolga	Unspecified area	K/Ar on biotite	211+2.6	Fontaine & Gafoer (1989)
Sibolga	Unspecified area	K/Ar on biotite	217.4+4	Fontaine & Gafoer (1989)
Sibolga	Unspecified area	K/Ar on Hbd	218.8+3.9	Fontaine & Gafoer (1989)

Table 7.3 Result of measurement of Rb/Sr and Sm/Nd of granitoids from Sibolga

No	Location	Sample code	Obs	Block	Offline correction	**C**-obs-ARMS corr	**D**-offline corr-ARMS corr	Final Decision
1		ARMS 5	0.710154 ± 0.000004		0.710155 ± 0.000003			
2		ARMS 6	0.710146 ± 0.000004		0.710149 ± 0.000004			
3		ARMS 7	0.710151 ± 0.000004		0.710148 ± 0.000003			
4		ARMS 8	0.710160 ± 0.000004		0.710158 ± 0.000003			
5		ARMS 2	0.710140 ± 0.000004		0.71014 ± 00.000005			
	average+std dev		0.710150 ± 0.000004		0.710150 ± 0.000004			
	true isotopic ratio		0.710191 ± 0.00001		0.710191 ± 0.00001			
1	Tanjung Jae	PYB4D	0.720777 ± 0.000005	20	0.720772 ± 0.000004	0.720819 ± 0.000005	0.720814 ± 0.000004	0.720814 ± 0.000004
2	Tanjung Jae	P4	0.718704 ± 0.000004	20	0.718704 ± 0.000004	0.718746 ± 0.000004	0.718746 ± 0.000004	0.718746 ±0.000004
3	Pintu Padan Julu	P7	0.721368 ± 0.001473	20	0.711482 ± 0.000004	0.721410 ± 0.001473	0.711523 ± 0.000004	0.711523 ± 0.000004
			0.711494 ± 0.000003	20	0.711495 ± 0.000003	0.711535 ± 0.000003	0.711536 ± 0.000003	0.711536 ± 0.000003
4	Tano Tombangan	P8C PEG	0.715715 ± 0.000004	23	0.715716 ± 0.000004	0.715757 ± 0.000004	0.715758 ± 0.000004	0.715757 ± 0.000004
5	Sibolga	SR1	1.215637 ± 0.056081	19	1.22315 ± 0.000009	1.215708 ± 0.056081	1.223221 ± 0.000009	1.223221 ± 0.000009
			1.223094 ± 0.000696	40	1.222354 ± 0.000008	1.223165 ± 0.000696	1.222425 ± 0.000008	1.222425 ± 0.000008
6	Adian Koting	S21_2	0.717401 ± 0.000083	14	0.717303 ± 0.000005	0.717443 ± 0.000083	0.717345 ± 0.000005	0.717345 ± 0.000005
7	Adian Koting	SB3	0.717648 ± 0.000005	20	0.717649 ± 0.000004	0.717690 ± 0.000005	0.717691 ± 0.000004	0.717691 ± 0.000004
1		ARMS 6	0.710146 ± 0.000004		0.710149 ± 0.000004			
2		ARMS 7	0.710151 ± 0.000004		0.710148 ± 0.000003			
3		ARMS 8	0.710160 ±		0.710158 ± 0.000003			
4		ARMS2	0.710140 ± 0.000004		0.710140 ± 0.000005			
5		ARMS 3	0.710169 ± 0.000006		0.710168 ± 0.000006			
6		ARMS 4	0.710165 ± 0.000008		0.71017 ± 0.000004			
			4.260931 ± 0.000030		4.260933 ± 0.000025			
	average+std dev		0.71015517 ± 0.000011		0.710156 ± 0.000012			
	true isotopic ratio		0.710191 ± 0.000010		0.710191 ± 0.000010			
	average+std dev	NBS _987	0.710227 ± 0.000007	20	0.710230 ± 0.000005	0.710263 ± 0.000007	0.710266 ± 0.000005	0.71026622 ± 0.000005
	true isotopic ratio	JR-2	0.705383 ± 0.000006	20	0.705387 ± 0.000003	0.705419 ± 0.000006	0.705423± 0.000003	0.70542297 ± 0.000003
8	Sibolga	S8	0.774123 ± 0.000005	20	0.744129 ± 0.000004	0.774162 ± 0.000005	0.744167± 0.000004	0.744167 ± 0.000004
9	Sibolga	S24B	0.720215 ± 0.000005	20	0.720216 ± 0.000005	0.720252 ± 0.000005	0.720253±0.000005	0.720253 ± 0.000005

Explanation :
factor : 1,000058
Obs : original measurement result
Block : number of measured data
Offline correction : corrected result
C-obs-ARMS corr : observation result x factor
D-offline corr-ARMS corr : offline correction x factor
Final Decision : final result
Standard reference : ARMS, NBS 987, and JR-2

Table 7.4 Result of measurement of Sm/Nd of granitoids from Sibolga and Panyabungan

No	Sample code	Location	Obs	2 sigma	Block	offline correction	2 sigma	**C**-obs-ARMS Corr	2 sigma	**D**-offline corr-ARMS corr	2 sigma	Final Decision		ε_{Nd}
	La Jolla		0.511712	0.000009	13	0.511758	0.000008	0.511833	0.000009	0.511839	0.000008	0.511839	0.000008	
	JB-2		0.513018	0.000026	24	0.5113038	0.000014	0.513140	0.000026	0.513119	0.000014	0.513119	0.00014	
	JA-1		0.513060	0.000093	12	0.512979	0.000014	0.513182	0.000093	0.513059	0.000014	0.513059	0.000014	
	DEWA		0.512011	0.000005	20	0.512053	0.000004	0.512131	0.000005	0.512131	0.000004	0.512131	0.000004	
1	PYB4D	Tanjung Jae	-	-	-	-	-	-	-	-	-	-	-	
2	P4	Tanjung Jae	0.511847	0.000833	28	0.512133	0.000017	0.511968	0.000833	0.512214	0.000017	0.512217	0.000017	-8.2
			0.423314	0.081645	19	0.512139	0.000016	0.423414	0.081645	0.512220	0.000016			-8.2
3	P7	Pintu Padan Julu	0.512133	0.000016	10	0.512170	0.000013	0.512255	0.000016	0.512251	0.000013	0.512251	0.000013	-7.5
			0.512130	0.00004	1	0.512193	0.000030	0.512252	0.00004	0.512274	0.000030			-7.5
4	P8C PEG	Tano Tombangan	-	-	-	-	-	-	-	-	-	-	-	
5	SR1	Sibolga	-	-	-	-	-	-	-	-	-	-	-	
6	S21_2	Adian Koting	0.512048	0.000014	20	0.512102	0.000011	0.51217	0.000014	0.512182	0.000011	0.512194	0.000011	-8.7
			0.512067	0.000015	20	0.512125	0.00001	0.512189	0.000015	0.512205	0.00001			
7	SB3	Adian Koting	0.512097	0.000006	20	0.512137	0.00005	0.512219	0.000006	0.512217	0.000005	0.512216	0.000007	-8.2
			0.512092	0.00001	20	0.512134	0.000008	0.512214	0.00001	0.512214	0.000008			
8	S8	Sibolga	0.511897	0.000008	20	0.511938	0.000007	0.512019	0.000008	0.512018	0.000007	0.512018	0.000007	-12.1
			0.511897	0.000009	20	0.511934	0.000008	0.512019	0.000009	0.512014	0.000008			
9	S24B	Sibolga	0.511889	0.000004	20	0.511929	0.000003	0.512009	0.000004	0.512007	0.000003	0.512007	0.000003	-12.3
			0.511960	0.000087	11	0.511947	0.000007	0.512080	0.000087	0.512025	0.000007			

Explanation :
factor : 1,000058
Obs : original measurement result
Block : number of measured data
Offline correction : corrected result
C-obs-ARMS corr : observation result x factor
D-offline corr-ARMS corr : offline correction x factor
Final Decision : final result
Standard reference : La Jolla, JB-2, JA-1 and DEWA

The CHUR is widely used for comparison of initial isotopic compositions of studied rocks with that of the primitive mantle at the time of their generation. This is done by the $^{\varepsilon i}$Nd notation:

$^{\varepsilon i}Nd = ([^{143}Nd/^{144}Nd]_t^{Sa} / [^{143}Nd/^{144}Nd]_i - 1) \times 10^4$

Where: t= intrusion age, indexes i decipher initial isotopic ratios, Sa = Sample

CHAPTER 8

REE GEOCHEMISTRY OF WEATHERED CRUSTS OF GRANITOIDS AT SIBOLGA AND ITS SURROUNDING AREAS

Weathered crusts of granitoids typically consist of different layers which differ in physical and geochemical characteristics (Wu et al., 1990; Sanematsu et al., 2013; Sanematsu & Watanabe, 2016). Four weathered profiles of four different locations at Sibolga were studied, two representative outcrops from Sibuluhan Sihaporas (SS), one representative outcrop from Sarudik (SRD) and one representative outcrop from Sibolga Julu (SJ). The weathering profiles were divided into four different layers, i.e. horizon A, B, C and D, based on the classification by Wu et al. (1990). Horizon A is top most surface layer, dark brown in color, contains plant roots and organic substances. Horizon B is wholly weathered zone, very loose, and porous in structure, yellow, gray and pink in color, clay is developed along fissures of parent rocks in network of the upper zone, quartz, feldspar and mica were present in the lower zone. Horizon C is sub-weathered zone, this layer is gradually transformed from the above zone without distinct boundary. Clay is further less abundant, while mica, feldspar, mica and quartz increase. Horizon D is slightly weathered zone, very less content of clay, and the rocks keep to some extent their original forms except that some feldspar begin to be weather and mica is hydrated partially.

Description of the weathered profile of Sibuluhan Sihaporas, Sarudik and Sibolga Julu are outlined below. The mode of occurrence of (REE + Y) is elucidated using the sequential extraction experiment.

8.1 REE geochemistry of weathered crusts of granitoids at Sibuluhan Sihaporas A

At Sibuluhan Sihaporas, located at the east of Sibolga, quartz syenite and quartz alkali feldspar syenite of ilmenite-series, peraluminous and calk-alkaline affinity are exposed. Two (2) locations were selected for observation and samples collections. Both of the two areas are easy to access, and they are abandoned quarry site. The first location at the Sibuluhan Sihaporas is a reddish color weathered rock profile with 23 meters height by laser distance meter (Appendix 2). The slope is approximately 45°, but 10 meters below the top surface, the slope changes very gentle. Some parts of the lower surface were covered by transported materials from the upper surface (Fig 8.1).

Fig. 8.1 Profile of weathered crust of granitoids of Sibuluhan Sihaporas A.

The profile consists of horizon A with 0.5 to 1 meter in thickness located on the top surface, it has brown in color, containing black to brown roots and organic matters. Horizon B is 3 to 8 meters thick and rich in clay minerals with sometimes associated with carbonic materials. Quartz and a little feldspar are present in brownish to reddish and partly white to yellowish and soft-weathered crust. The horizon C is 2 to 3 meters in thickness, pinkish to

grayish and partly white in color, including clay minerals. Quartz and feldspar are present in red-brown, yellow-brown and inherently-brittle weathered crust. This horizon still maintains the original texture of granite. The horizon D is the freshest and least weathered rock, where quartz, feldspars, and biotite are present. Eleven samples were collected from B and C horizon of 5 meters profile for each 50 cm interval. A sample of horizon D was obtained from the lowermost part of the profile.

A total of 4 weathered rock were selected from total of 11 samples from Sibuluhan Sihaporas A (S1) for the sequential extraction. The analyzed samples were taken from level of 50 cm (S1), 240 cm (S2), and 310 cm (S3) of the horizon B, and that taken from 500 cm (S4) of the horizon C. Horizon D was taken from the lower part of profile.

The sequential extraction result shows that Total REE (ΣREE) from Sibuluhan Sihaporas A range from 196 to 263 ppm, with an average of 204 ppm. while Y contents range from 55 to 113 ppm, respectively (Table 8.1, Fig. 8.15).

REE are mainly extracted from step 2 and step 8. These suggest that significant fraction of the REE occurs as ion exchangeable (step 2), and crystalline Fe-oxide occluded forms (step 8) (Fig. 8.16). ΣREE obtained from step 2 ranges from 32 to 154 ppm, while that of step 8 ranges from 27 to 87 ppm (Fig. 8.2). Extracted Yttrium (Y) contents range from 20 to 60 ppm.

The behavior of REE leaching of those four samples from Sibuluhan Sihaporas A are slightly similar except for Ce. Negative Ce- and Eu anomalies in the leachate are the common characteristics, except for the leachate of S2 and S4 which have positive Ce-

anomaly and suggest an accumulation of Ce in the oxidation zone. The leachate from S2 and S4 showing more HREE enrichment than S1 and S3 (Fig. 8.2).

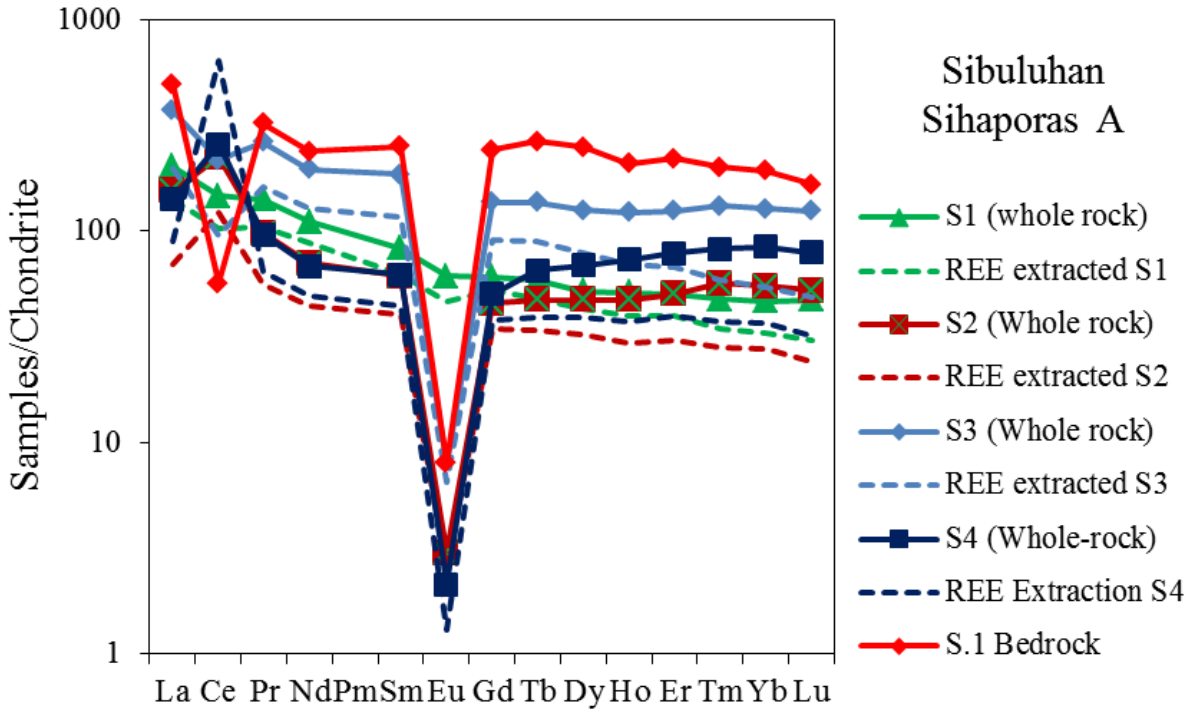

Fig. 8.2 Chondrite normalized REE patterns of the weathered crust of granitoids at Sibuluhan Sihaporas A (SSA) (values of chondrite are from McDonough & Sun, 1995).

Clay speciation were conducted by orientation, ethylene glicolated and HCl treatment methods. The result of XRD is depicted in Figure 8.3. Halloysite group and gibbsite were identified in the horizon B. Total REE (ΣREE) extracted using step 2 is the highest suggesting that REE are dominantly present as ion exchangeable form and are most possibly adsorbed on to surface of halloysite and gibbsite in the horizon B.

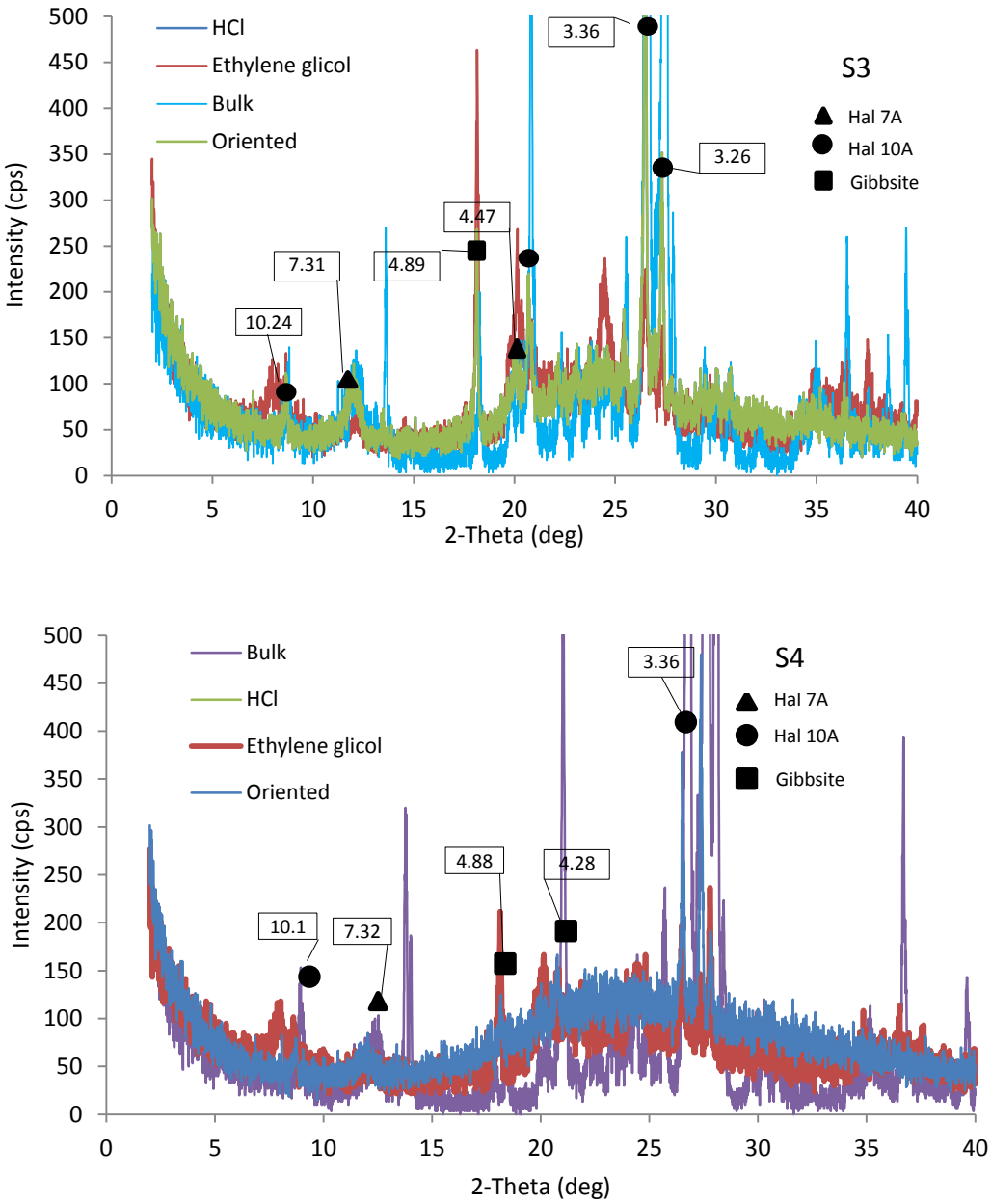

Fig. 8.3 XRD of clay speciations from the weathered crust of granitoids at Sibuluhan Sihaporas A, from level of 310 cm (S3) and level 500 cm (S4).

8.2 REE geochemistry of weathered crusts of granitoids at Sibuluhan Sihaporas B

Sibuluhan Sihaporas B is located approximately 4 km to the north of the Sibuluhan Sihaporas A. A gentle slope of 6 to 6.5 meters weathered granites profile was observed, and 12 samples were collected for every 50 cm interval (Appendix 2). The profile consist of A horizon with 20 to 30 cm from the top surface, dark brown in color, containing organic matters such as roots. B horizon is 5.5 meters in thickness and rich in brown to yellowish clay minerals (Fig. 8.4). The C horizon was not clearly identified because the surface was covered by transported materials from the upper horizon, while the D horizon was observed at the bottom of the profile. This horizon still maintains the original texture of granite. Quartz, feldspar, and oxidized biotite weathered crust were identified.

Fig. 8.4 Profile of weathered crusts of granitoids at Sibuluhan Sihaporas B.

A total of 4 representative samples were selected from the total of 12 samples from Sibuluhan Sihaporas B. They were taken from level of 50 cm from the top (S5), 200 cm (S6),

350 cm (S7) and 450 cm (S8). ΣREE from Sibuluhan Sihaporas B range from 82 to 198 ppm, with an average of 152 ppm (Table 8.1). The REE is mainly extracted by step 2, 6, and 8, suggesting that significant fraction of REE was in the ion exchangeable, organically bounded, and crystalline Fe-oxide occluded forms (Fig. 8.5). ΣREE extracted from step 2 ranges from 32 to 52 ppm, that of step 6 ranges from 7 to 52 ppm, and that of step 8 ranges from 40 to 91 ppm (Fig. 8.15). Y is contained mainly as ion exchangeable, crystalline Fe-oxide occluded, and bounded in organic materials forms, which range from 31 to 60 ppm, 6.7 to 40 ppm, and 0.8 to 3.40 ppm, respectively (Figs. 8.15, 8.16).

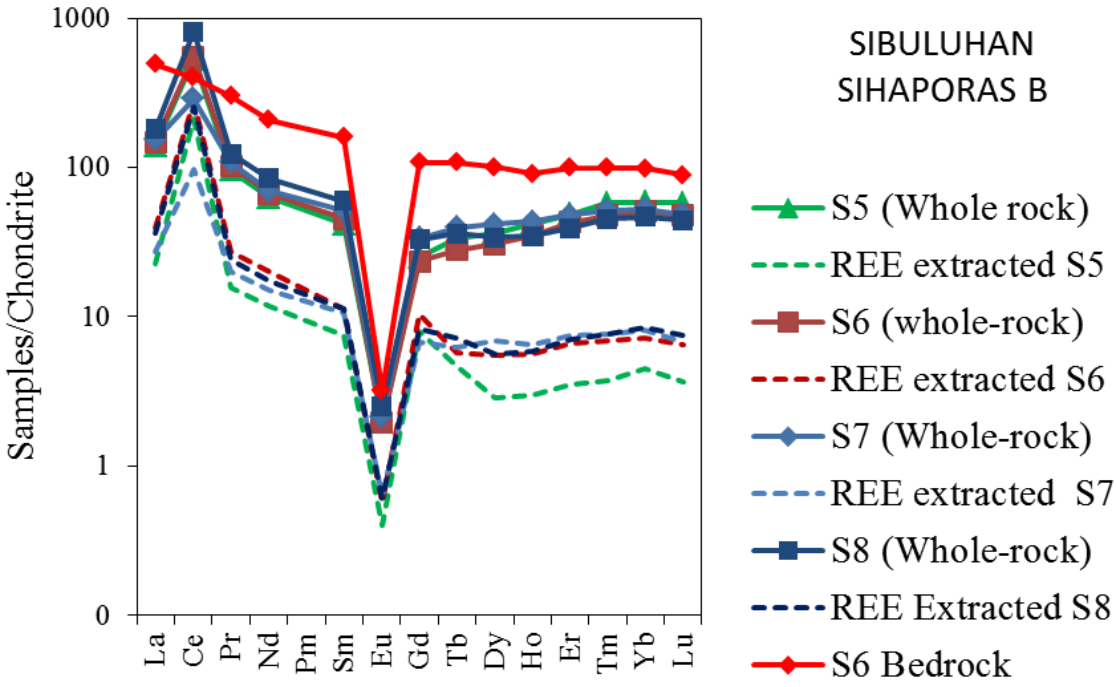

Fig 8.5 Chondrite normalized REE patterns of weathered cruts of granitoids at Sibuluhan Sihaporas B (SSB) (values of chondrite are from McDonough & Sun, 1995).

The behavior of REE during leaching is slightly similar with those four samples from Sibuluhan Sihaporas B. Positive Ce anomaly and Eu negative anomaly in the leachate are the

common characteristics. In the weathered crust of granitoids of S5 the behavior of leaching is different wherein HREE are more depleted compared with those fom the lower horizon.

Allanite and xenotime occur in the C horizon and were associated with biotite. Xenotime ranges from 2 to 20 μm in size, irregular to angular in shape. Large xenotime crystal showing metamict texture associated with U and Th, euhedral in shape, range from 40 to 80 μm in size (Fig. 8.6). Halloysite and gibbsite were identified from the horizon C (Fig. 8.7).

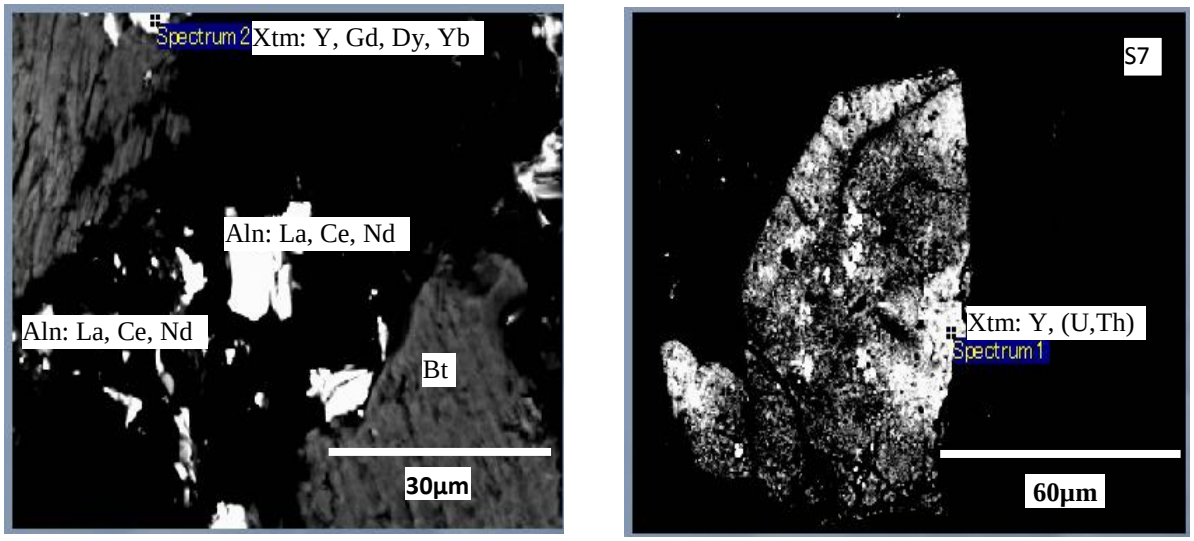

Fig 8.6 Backscaterred electron images of allanite (Aln) and xenotime (Xtm) that occur with biotite (Bt) in the weathered crust of granitoids at Sibuluhan Sihaporas B.

Clay speciation were conducted by orientation, glicolated and HCl treatment methods. The result of XRD is depicted in Figure 8.7. Halloysite group mineral and gibbsite were identified. The ΣREE extracted using step 8 is the highest suggesting that REE are dominantly present as crystalline Fe-oxide occluded form, while the remaining REE are mainly present as ion exchangeable and bound in organic materials. The REE of ion exchangeable form are the most possibly adsorbed on to surface of halloysite and gibbsite.

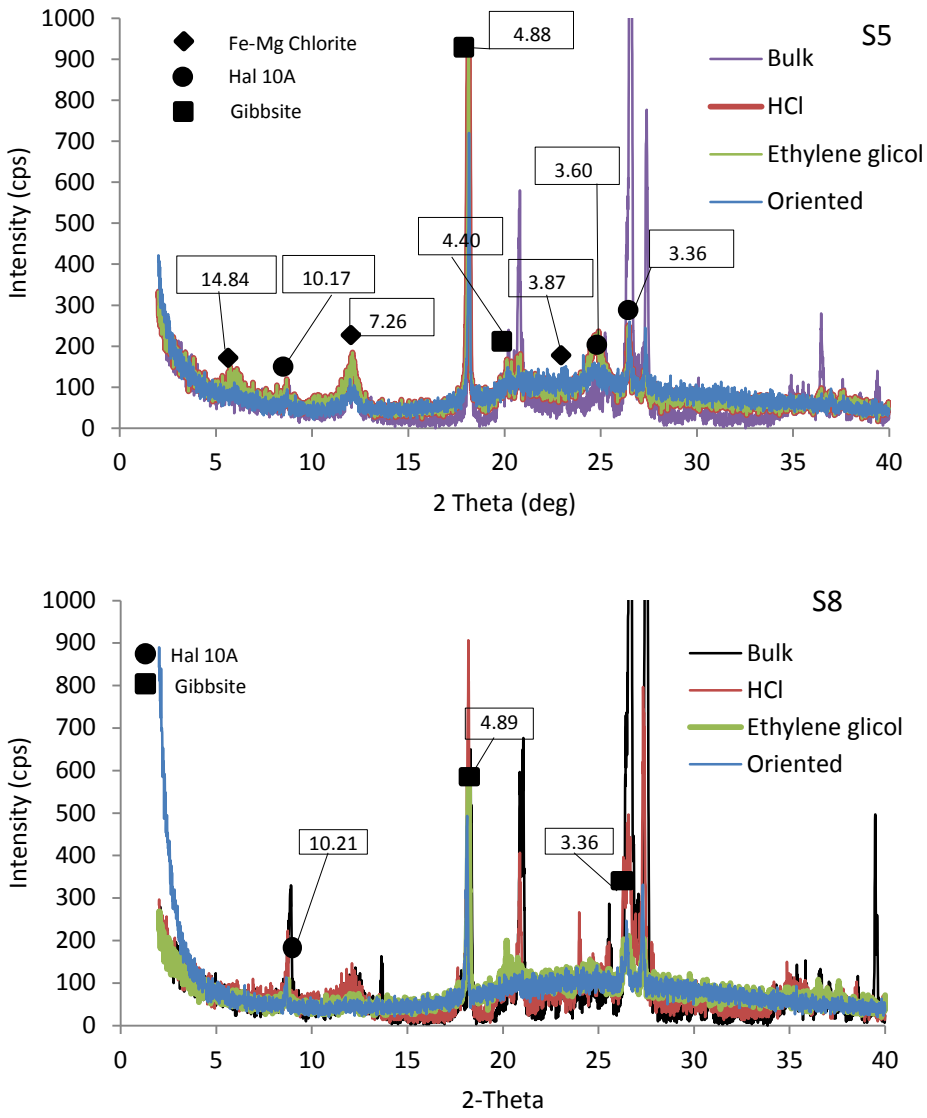

Fig. 8.7 XRD of clay speciations from the weathered crust of granitoids at Sibuluhan Sihaporas B, from the level of 50 cm (S5) and level 450 cm and (S8).

8.3 REE geochemistry of weathered crusts of granitoids at Sarudik

A twelve (12) meters profile of weathered granites was observed, and 24 samples were collected for every 50 cm interval. The profile consists of horizon A, B, C, and D. The horizon A is 15 to 20 cm in thickness from top of the surface (Appendix 2), horizon B is 3.5 meters in thickness and rich in brown and gray clay minerals, horizon C is 8 meters thickness, pinkish to grayish and partly white in color, including clay minerals. Quartz, feldspars, and biotite are present in yellowish to brownish and inherently-brittle weathered crust of horizon C. The horizon D is least weathered horizon of granite, consists mainly of quartz and feldspars (Fig. 8.8).

Fig. 8.8 Profile of weathered crusts of granitoids at Sarudik.

A total of 4 out of 12 samples were selected from the weathered profile of Sarudik. They were collected from level is 50 cm (S9), 200 cm (S10), 500 cm (S11) and 950 cm (S12). Total of REE (ΣREE) from Sarudik ranges from 21 to 82 ppm, with an average 52 ppm, respectively (Table 8.1). ΣREE are extracted mainly from step 8, 2, 7 and 6, suggesting that significant fraction of the REE occur as crystalline Fe-oxide occluded, ion exchangeable, amorphous Fe oxide occluded, and bounded in organic forms (Fig. 8.9). The behavior of REE during leaching is similar with those four samples from Sarudik. Positive Ce anomaly and Eu negative anomaly

in the leachate are the common characteristics. The leachates were mostly enriched in HREE (Fig. 8.9). ΣREE extracted from step 8 ranges from 6 to 41 ppm, that of step 2 range from 10 to 13 ppm, that of step 7 range from 1 to 19 ppm while that of step 6 range from 3 to 9 ppm, respectively (Fig. 8.15). Y contents were extracted mainly in the step 8, ranging from 0.4 to 1.3 ppm (Fig. 8.16).

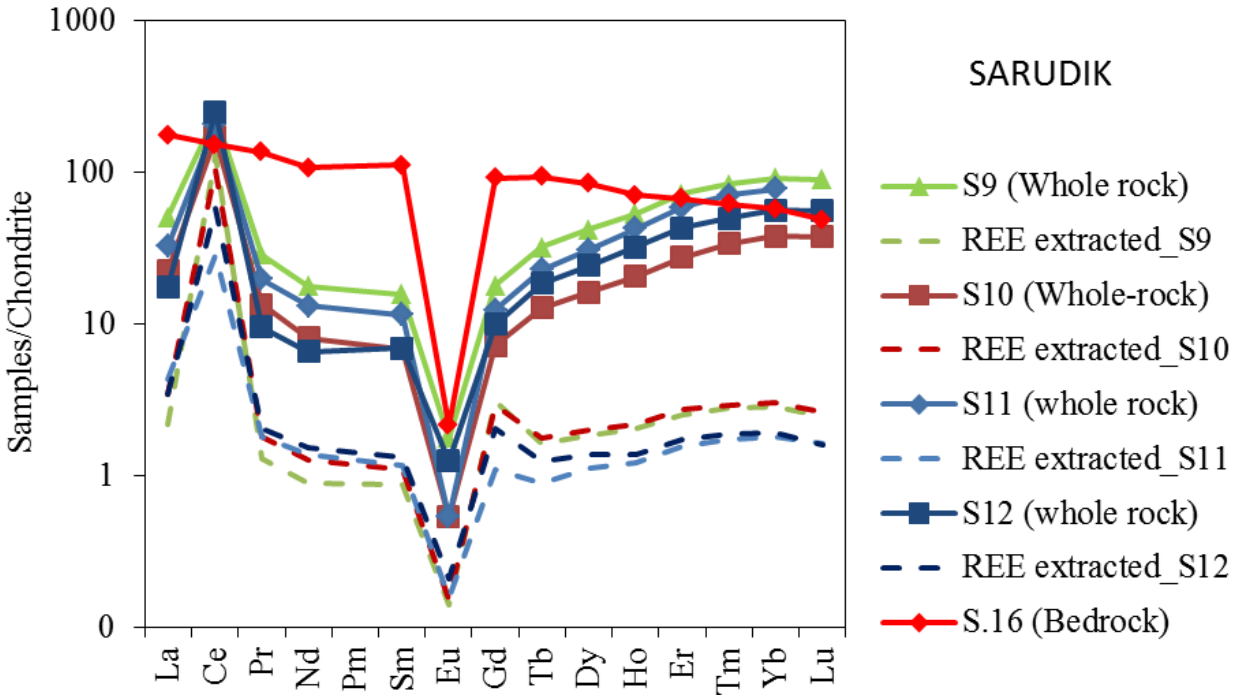

Fig. 8.9 Chondrite normalized REE patterms of weathered crust of granitoids at Sarudik (values of chondrite are from McDonough & Sun, 1995).

Kaolinite and gibbsite were identified from the horizon A and B (Fig. 8.11). Clay speciation were conducted by orientation, ethylene glicolated and HCl treatment methods. The result of XRD is depicted in Figure 8.7. Kaolinite and gibbsite were identified in the transition from horizon A to B, and horizon B, respectively. The ΣREE extracted using step 8 is the highest suggesting that REE are dominantly present as crystalline Fe-oxide occluded form in the lower part of horizon A and upper part of horizon B,

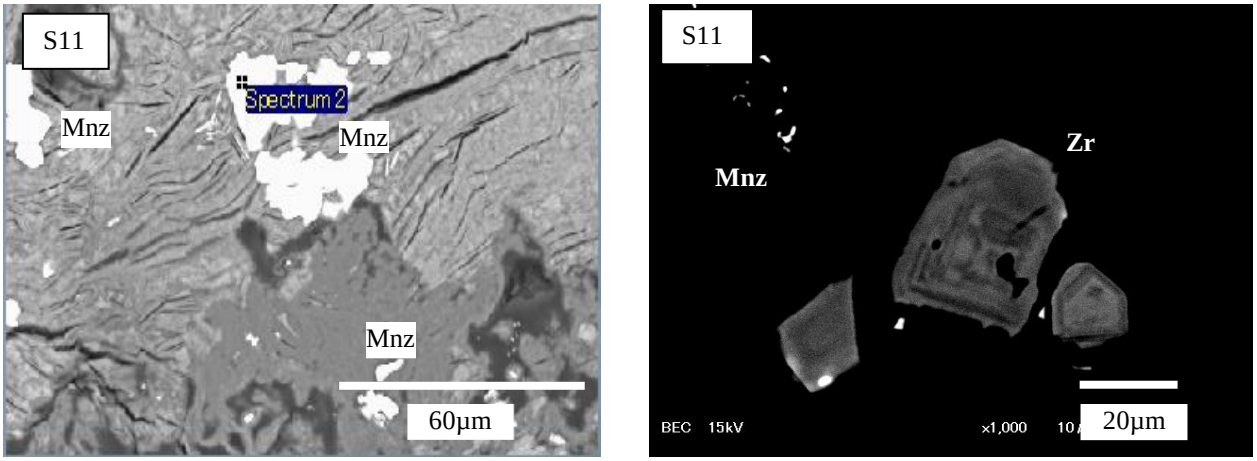

Fig 8.10 Backscattered electron images of monazite (Mnz) occurs with biotite, and zircon (Zr) in the weathered crust of granitoids from horizon C at Sarudik (SRD).

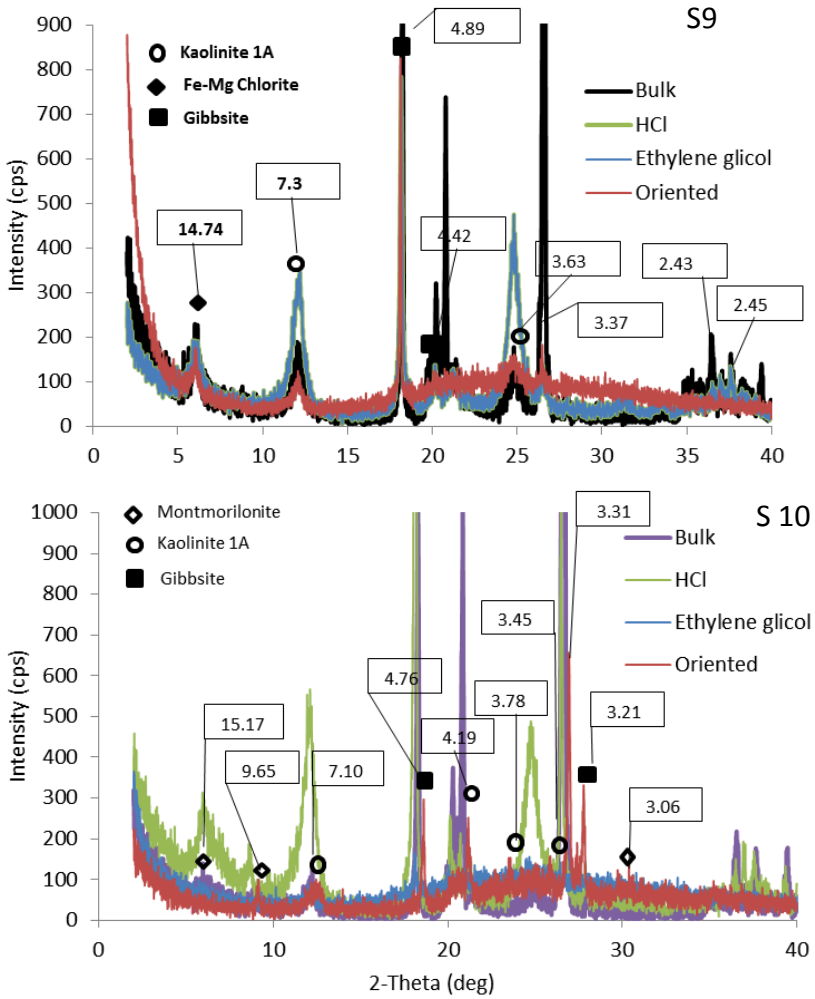

Fig. 8.11 XRD of clay speciations from the weathered crust of granitoids at horizon A, level of 50 cm (S9) and horizon B, level of 200cm (S10) from Sarudik.

while the remaining are also present as ion exchangeable, amorphous Fe oxide occluded, and bounded in organic forms. Crystalline Fe-oxide minerals are ilmenite, hematite and goethite, which can take a role in containing REE in the weathering samples (Braun et al., 1990). The REE of ion exchangeable form are the most possibly adsorbed on to surface of kaolinite group mineral and gibbsite in the lower part of horizon A and upper part of horizon B.

8.4 REE geochemistry of weathered crusts of granitoids at Sibolga Julu

Fiveteen (15) samples were collected from six meters weathered crust of granitoids at each 50 cm interval (Appendix 2). The profile consists of horizon A, B, C, and D. The horizon A is 40 cm in thickness from the top surface and it has brown in color, containing black to brown roots and organic matters. Horizon B is 3 meters in thickness, brown to yellow clay minerals. Horizon C is 3 meters in thickness, brown to yellow and gray to white in color at some parts. Gray and white are the color of clay mineral as identified as a kaolinite-rich layer with 90 cm in thickness within horizon C. Quartz, and feldspars are present in the brown to yellow and inherently-brittle weathered crust. Horizon D is the freshest and least weathered horizon which contain quartz and feldspars.

A total of 3 out of 12 samples from Sibolga Julu were selected. They were taken from level of 40 cm (S13), 200 cm (S14), and 360 cm (S15). Total REE contents (ΣREE) from Sibolga Julu range from 114 to 138 ppm respectively, with an average 121 ppm. REE are mainly extracted from step 2, 8, 7 and 6, suggesting that significant fraction of the REE occurs as ion exchangeable (step 2), crystalline Fe-oxide occluded (step 8), and organically bounded forms. ΣREE extracted from step 2, 8, 7, and 6 ranges from 21 to 102 ppm, 3 to 75 ppm, 0.5 to 17 ppm,

and 0.8 to 17 ppm, respectively. Y is present as crystalline Fe-oxide occluded which ranges from 0.3 to 1. 7 ppm.

ΣREE content of bulk weathered granitoids crust ranges from 135 to 636 ppm while the result of the sequential extraction correspond a range from 22 to 534 ppm. ΣREE concentrated within kaolin-dominant horizons of the weathered crust ranges from 1,229 to 1,586 ppm while ΣREE in the bedrock ranges from 281 to 1,076 ppm (Table 7.1). Chondrite normalized REE patterns of the parent granites show enrichment of both LREE and HREE.

The REE behavior of leaching is slightly similar among those three samples from Sibolga Julu. Negative Ce and Eu anomalies in the leachate are the common characteristics, and Dy-negative anomaly was present (Fig. 8.2).

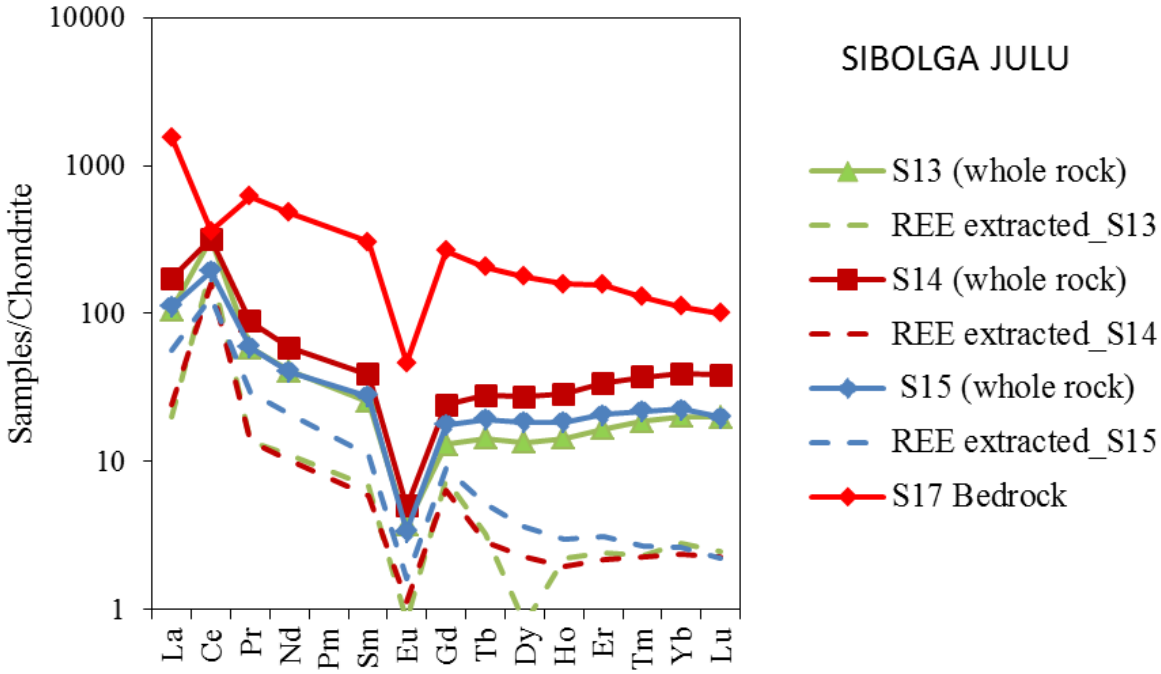

Fig. 8.12 Chondrite-normalized REE patterns of weathered crusts of granitoids from Sibolga Julu (SJ) (values of chondrite are from McDonough & Sun, 1995).

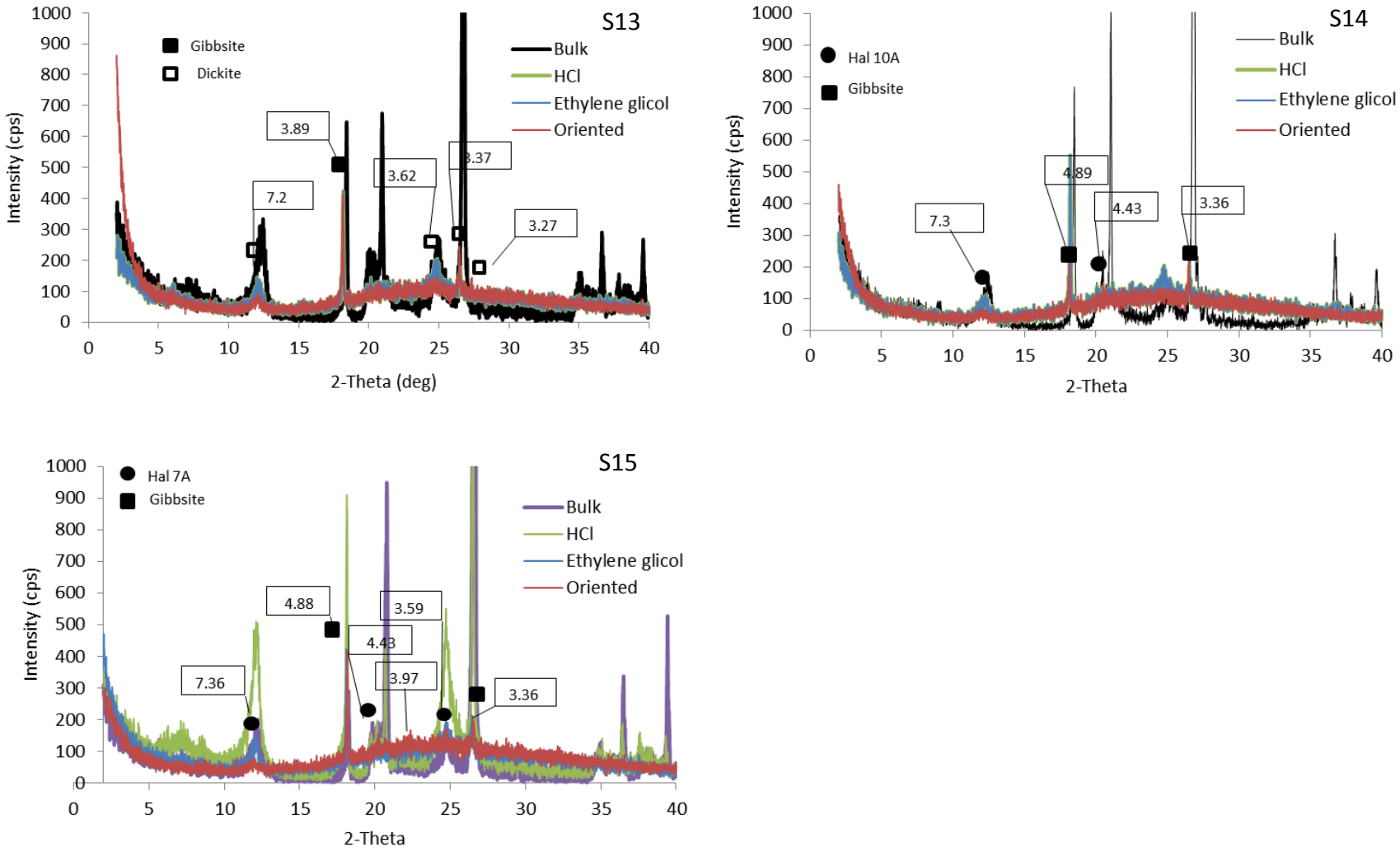

Fig. 8.13 XRD of clay speciations from the weathered crust of granitoids at Sibolga Julu at horizon A, level of 40 cm (S13), and horizon B, from level 200 cm (S14) to 360 cm (S15).

Halloysite and gibbsite were identified from the horizon B (Fig. 8.11). Clay speciation were conducted by orientation, ethylene glicolated and HCl treatment methods. The result of XRD is depicted in Figure 8.7. The ΣREE extracted using step 2 is the highest suggesting that REE are dominantly present as ion exchangeable form in the horizon B, while the remaining REE are also present as crystalline Fe-oxide occluded, and organically bound forms in the the horizon A and upper part of horizon B. The ion exchangeable are the most possibly adsorbed on to surface of halloysite and gibbsite (Fig. 8.13).

The enrichment of REE in the granitoids from Sibolga was caused by crystallization of allanite and titanite, which contain Ce, La, Pr, Nd, Yb, Gd, and Y. The proportion of ΣREE extracted by sequential extraction of the weathered crust from Sibuluhan Sihaporas ranges from 55% to 74% while that from Sarudik and Sibolga Julu ranges from 11% to 58%. ΣREE contents in the weathered crust are lower than that of the parent granitoids. Low content of ΣREE contents in the weathered crust suggests that part of REEs was leached out during weathering (Fig. 8.14). Summary of LREE and HREE (REE) extracted in each step of sequential extraction depicted in Figures 7.14 and 7.15.

The ΣREE extracted from the weathered crusts of granitoids from Sibuluhan Sihaporas A and Sibuluhan Sihaporas B are higher than those from Sarudik and Sibolga Julu. REE extracted from Sibuluhan Sihaporas A and Sibolga Julu are dominantly present as ion exchangeable (step 2), crystalline Fe-oxide occluded (step 8), organically bound (step 6), and Fe-oxide occluded forms (step 7). While those at Sibuluhan Sihaporas B and Sarudik are dominantly present as crystalline Fe-oxide occluded (step 8), ion exchangeable (step 2), organically bound (step 6), and Fe-oxide occluded forms (step 7) (Fig. 8.15, Table 8.1).

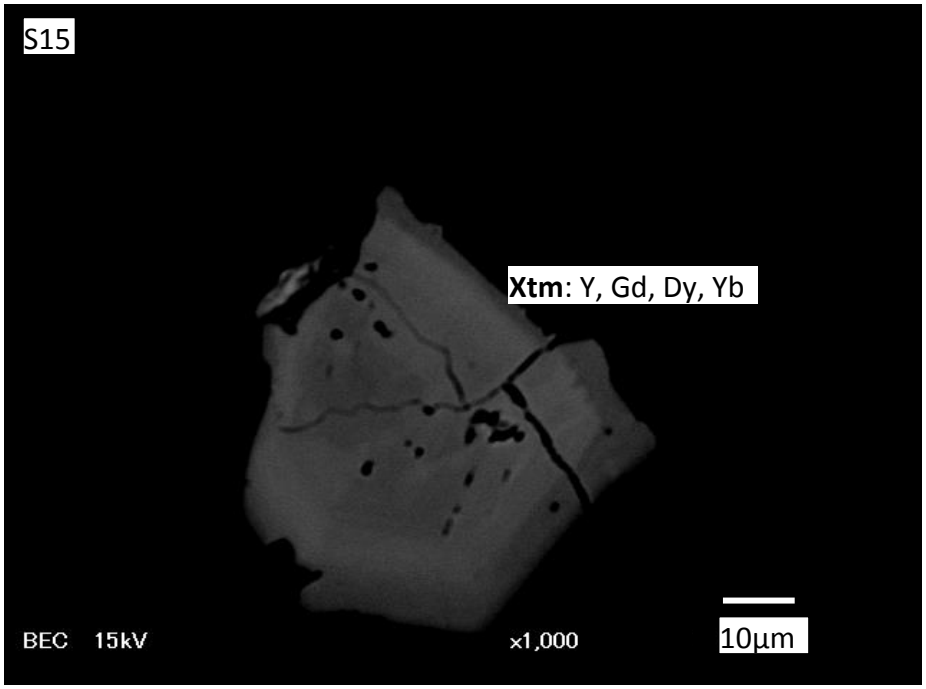

Fig. 8.14 Backscattered electron images of xenotime (Xtm) occurs in the weathered crust of granitoids from horizon B at Sibolga Julu.

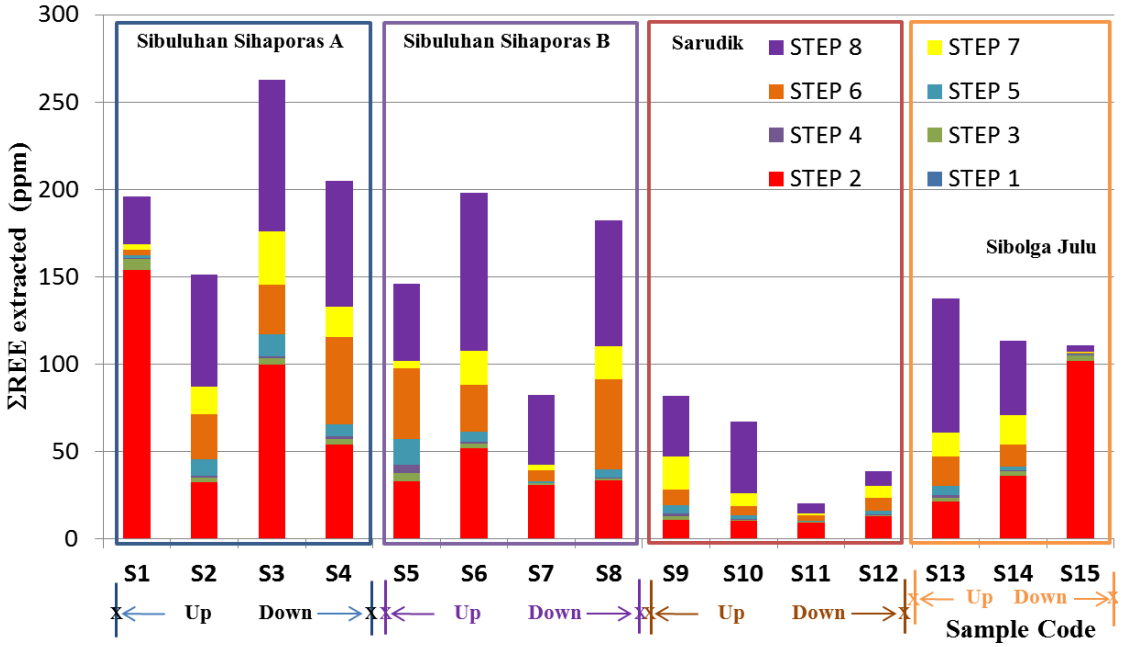

Fig. 8.15 Histogram of sequential extraction results showing distribution of ΣREE contents extracted in each step.

Table 8.1 ΣREE extracted from the sequential extraction of the weathered crust of granitoids at Sibolga and its surrounding areas

Locality	Sibuluhan Sihaporas				Sibuluhan Sihaporas B				Sarudik				Sibolga Julu		
	S1	S2	S3	S4	S5	S6	S7	S8	S9	S10	S11	S12	S13	S14	S15
Reagant								(REE)							
water		0.00	0.01	0.00	0.01	0.01	0.00	0.02	0.02	0.02	0.01	0.01	0.07	0.01	0.01
exchangeable salts	154.05	32.36	99.82	54.36	32.84	51.98	31.04	33.62	11.08	10.38	9.57	12.91	21.38	36.00	102.19
Pb displaceable	6.50	2.74	3.68	2.95	4.86	2.65	0.77	1.27	2.12	0.86	0.46	0.76	2.25	2.73	3.05
acid soluble	0.28	1.38	0.84	1.50	4.72	1.21	0.22	0.43	1.62	0.50	0.08	0.38	1.59	0.46	0.18
Mn-oxide occluded	1.54	9.44	13.00	6.97	15.07	5.48	0.89	4.55	4.40	2.10	0.37	1.98	5.12	2.33	0.61
organically bound	3.06	25.53	28.49	49.78	40.07	26.99	6.73	51.52	9.11	4.95	2.91	7.45	17.13	12.59	0.81
amorphous Fe-oxide occluded	3.37	15.57	30.20	17.40	4.33	19.27	3.02	18.70	18.92	7.70	1.49	6.88	13.73	16.98	0.53
crystalline Fe-oxide occluded	27.13	64.19	87.02	72.00	44.13	90.55	39.61	72.41	34.87	40.56	5.71	8.58	76.45	42.44	3.31
ΣTotal REE	195.93	151.22	263.06	204.95	146.03	198.14	82.29	182.53	82.14	67.05	20.61	38.95	137.71	113.53	110.69
(Y)	S1	S2	S3	S4	S5	S6	S7	S8	S9	S10	S11	S12	S13	S14	S15
water	0.00	0.00	0.00	0.00	0.00	0.00	0.00	0.00	0.00	0.00	0.00	0.00	0.00	0.00	0.00
exchangeable salts	49.00	18.93	62.40	28.99	2.31	4.18	3.91	5.12	0.29	0.47	0.57	0.94	0.41	1.51	3.83
Pb displaceable	0.72	0.50	0.83	0.63	0.25	0.07	0.06	0.07	0.05	0.03	0.04	0.04	0.04	0.07	0.11
acid soluble	0.08	0.41	0.39	0.42	0.10	0.04	0.04	0.03	0.02	0.01	0.02	0.02	0.03	0.01	0.01
Mn-oxide occluded	0.32	1.84	3.90	0.34	0.13	0.10	0.09	0.11	0.06	0.02	0.05	0.04	0.05	0.02	0.03
organically bound	0.60	1.87	7.57	0.89	0.01	0.17	0.17	0.17	0.06	0.04	0.05	0.01	0.07	0.00	0.03
amorphous Fe-oxide occluded	0.34	16.18	6.94	0.47	0.01	0.06	0.06	0.06	0.04	0.03	0.05	0.03	0.05	0.03	0.01
crystalline Fe-oxide occluded	6.64	18.94	30.53	23.65	0.78	2.37	3.40	1.55	1.27	1.39	0.38	0.31	1.70	0.04	0.25
ΣY	57.71	58.67	112.57	55.38	3.59	7.00	7.72	7.12	1.79	1.99	1.17	1.38	2.36	1.68	4.27
ΣREE+Y	253.64	209.88	375.63	260.33	149.62	205.14	90.01	189.65	83.94	69.04	21.77	40.33	140.08	115.22	114.96

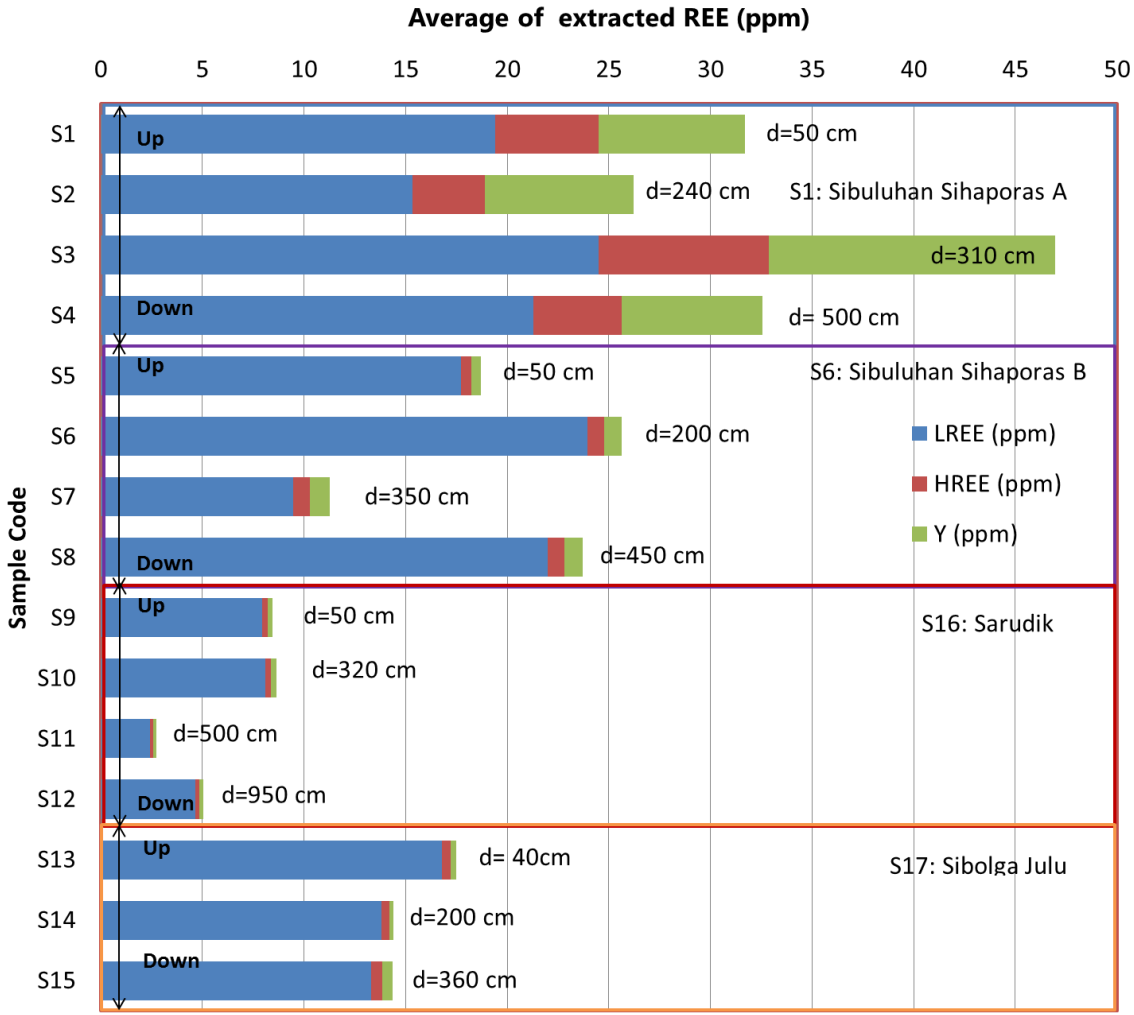

Fig. 8.16 Summary of average LREE, HREE, and Y extracted of Sibuluhan Sihaporas A, Sibuluhan Sihaporas B, Sarudik and Sibolga Julu.

(REE + Y) are mainly present as ion exchangeable in Sibuluhan Sihaporas A and Sibolga Julu, which range from 51 to 203 and 22 to 106 ppm, respectively. The remaining REE are presesent as crystalline Fe-oxide occluded, organically bound, amorphous Fe-oxide occluded, Mn-oxide occluded, Pb-displaceable, and acid soluble forms. Those from Sibuluhan Sihaporas B and Sarudik are dominantly present as crystalline Fe-oxide, from which range from 43 to 93 and 6 to 42 ppm, respectively (Table 8.1).

The ΣLREE extracted from the weathered crust of granitoids from Sibuluhan Sihaporas A, sibuluhan Sihaporas B, Sarudik and Sibolga Julu are significantly higher than ΣHREE as shown in Figure 8.16.

8.5 Mass Balance

Material balance is that assuming immobile element such as Ti, Al, Zr, Yb, Nb is no quantitative change and is constant even after alteration, mobile element indicating quantitatively the extent of increase and decrease when fresh rock altered. The value of the mass balance is not only the amount of of mass movement. Volume of rock itself is changed and density of rock is also changed by changing volume of rock (Humpris et al., 1978).

Mass balance was calculated with respect to REE in the parent granitoids from bedrock from Sibuluhan Sihaporas A (S1), Sibuluhan Sihaporas B (S6), Sarudik (S16), and Sibolga Julu (S17) and their weathered crusts from Sibuluhan Sihaporas A (S1-S4), Sibuluhan Sihaporas B (S5-S8), Sarudik (S9-S12) and Sibolga Julu (S13-S15). Nb, Zr and Yb were used as inert components to establish the volumetric change, εi, given below

$\varepsilon_{i,w} = (\rho_w C_{i,w}/\rho_p C_{i,p})-1$ (Brimhall & Dietrich, 1987)

where ρp and ρw (g/cm^3) refer to the densities of the parent granitoids and their weathered crusts, respectively, while $C_{i,p}$ and $C_{i,w}$ (mol/l) are concentrations of a species in the parent

granitoids and their weathered crust, respectively. If ε_i value= 0 the weathering process that took place was isovolumetric or volume conservative. If ε_i value is higher than 0, the weathering induced expansion (Velde & Meunier, 2008) or dilution (White et al., 2002) while lower than 0 value denotes collapse (Velde & Meunier, 2008) or compaction (White et al., 2002).

Using Zr, and Nb as stable components the induced expansion due to weathering process (Velde & Meunier, 2008) occurred at Sibuluhan Sihaporas A based on positive trend of volume change (ε_i), but trends towards decreasing values suggest increasing trend of expansion (Table 8.2 and Fig. 8.17). On the other hand, the weathering process occured at Sibuluhan Sihaporas B resulted mainly is negative values of volume change. It suggest that the weathering processes is mainly of collapse (Velde & Meunier, 2008) or compaction (White et al., 2002). The values show increasing values from surface to the lower horizon, indicate increasing trend of collapse (Velde & Meunier, 2008) or compaction (White et al., 2002). The weathered crusts of Sarudik show positive trend which denotes expansion or dilution, but trends towards decreasing values suggest decreasing trend of expansion (Table 8.2). On the other hand, the weathering process occured at Sibolga Julu resulted is negative values of volume change. It suggest that the weathering processes is mainly of collapse (Velde & Meunier, 2008) or compaction (White et al., 2002). The values show increasing values from surface to the lower horizon, indicate decreasing trend of collapse (Velde & Meunier, 2008) or compaction (White et al., 2002).

Table 8.2 Volumetric change of major elements of weathered crusts of granitoids in Sibolga and its surrounding areas

Sample	Locality	Depth	Horizon	Density	Volumetric change ($\varepsilon_{i,w}$)									
					Si	Ti	Al	Fe	Mn	Mg	Ca	Na	K	P
S1	Sibuluhan Sihaporas A	50	A	1.81	-0.51	23.31	0.32	14.72	22.50	14.10	2.59	-0.91	-0.79	41.81
S2		240	B	1.51	-0.41	-0.16	-0.03	3.70	1.10	-0.59	0.05	0.45	-0.05	6.01
S3		310	B	1.76	-0.31	-0.12	0.25	-0.41	-0.47	-0.25	1.28	1.71	0.38	5.89
S4		500	B	1.85	-0.28	-0.44	0.14	3.68	0.47	-0.50	7.99	9.55	0.21	4.26
S5	Sibuluhan Sihaporas B	50	A	1.68	-0.40	0.76	0.36	-0.04	-0.68	0.26	-0.99	-0.96	-0.43	0.19
S6		200	B	1.8	-0.40	0.70	0.56	0.57	-0.40	0.58	-1.00	-0.96	-0.15	0.13
S7		350	B	1.59	-0.46	-0.37	0.34	-0.70	-0.70	-0.30	-0.99	-0.93	0.28	-0.26
S8		450	B	1.7	-0.45	0.52	0.43	0.12	2.29	0.09	-0.99	-0.92	0.17	0.48
S9	Sarudik	50	A	1.68	-0.51	9.00	0.91	4.24	-0.52	1.19	-0.99	-0.99	-0.94	2.24
S10		200	B	1.73	-0.40	2.91	0.38	2.03	-0.67	0.27	-0.99	-0.99	-0.94	0.43
S11		500	B	1.58	-0.50	2.15	0.51	1.93	-0.40	0.78	-1.00	-0.99	-0.74	0.57
S12		950	C	1.82	-0.59	3.78	1.90	2.47	-0.31	1.50	-1.00	-0.99	-0.68	2.32
S13	Sibolga Julu	40	A	1.73	-0.26	0.35	-0.06	0.99	0.92	-0.32	-1.00	-0.99	0.16	-0.74
S14		200	B	1.87	-0.14	0.54	-0.02	0.83	-0.21	-0.42	-0.99	-0.99	-0.10	-0.83
S15		360	B	1.92	-0.33	0.07	-0.05	6.23	22.66	-0.10	-1.01	-0.99	-0.37	-0.53

Table 8.3 Elemental changes of major elements of weathered crusts of granitoids in Sibolga and its surrounding areas

Sample	Locality	Depth	Horizon	Density	Elemental change ($\tau j_{,w}$)									
					Si	Ti	Al	Fe	Mn	Mg	Ca	Na	K	P
S1	Sibuluhan Sihaporas A	50	A	1.81	-0.76	590.09	0.75	246.18	551.15	227.06	11.87	-0.99	-0.96	1831.74
S2		240	B	1.51	-0.65	-0.30	-0.07	21.11	3.43	-0.83	0.11	1.11	-0.10	48.19
S3		310	B	1.76	-0.52	-0.23	0.57	-0.65	-0.72	-0.43	4.18	6.34	0.92	46.44
S4		500	B	1.85	-0.48	-0.69	0.30	20.92	1.15	-0.75	79.76	110.24	0.47	26.64
S5	Sibuluhan Sihaporas B	50	A	1.68	-0.64	2.11	0.85	-0.09	-0.90	0.59	-1.00	-1.00	-0.68	0.43
S6		200	B	1.8	-0.64	1.90	1.43	1.47	-0.64	1.49	-1.00	-1.00	-0.28	0.27
S7		350	B	1.59	-0.71	-0.61	0.79	-0.91	-0.91	-0.51	-1.00	-1.00	0.65	-0.46
S8		450	B	1.7	-0.69	1.31	1.06	0.24	9.85	0.20	-1.00	-0.99	0.37	1.20
S9	Sarudik	50	A	1.68	-0.76	98.94	2.65	26.44	-0.77	3.78	-1.00	-1.00	-1.00	9.53
S10		200	B	1.73	-0.64	14.28	0.91	8.21	-0.89	0.60	-1.00	-1.00	-1.00	1.05
S11		500	B	1.58	-0.75	8.92	1.28	7.61	-0.64	2.18	-1.00	-1.00	-0.93	1.48
S12		950	C	1.82	-0.83	21.89	7.41	11.06	-0.52	5.25	-1.00	-1.00	-0.90	10.03
S13	Sibolga Julu	40	A	1.73	-0.45	0.81	-0.12	2.97	2.67	-0.54	-1.00	-1.00	0.35	-0.93
S14		200	B	1.87	-0.27	1.37	-0.03	2.36	-0.37	-0.66	-1.00	-1.00	-0.19	-0.97
S15		360	B	1.92	-0.56	0.15	-0.10	51.24	558.95	-0.19	-1.00	-1.00	-0.60	-0.78

Table 8.4 Elemental change, τj of REE+Y of weathered crusts of granitoids in Sibolga and its surrounding areas

Sample	Locality	Depth	Horizon	Density	Elemental change (Tj,w)														
					La	Ce	Pr	Nd	Sm	Eu	Gd	Tb	Dy	Ho	Tm	Er	Yb	Lu	Y
S1	Sibuluhan Sihaporas A	50	A	1,81	-0.92	2.50	-0.90	-0.88	-0.94	34.25	-0.96	-0.97	-0.97	-0.96	-0.96	-0.96	-0.95	-0.94	-0.99
S2		240	B	1,51	-0.96	4.63	-0.97	-0.97	-0.98	-0.94	-0.98	-0.99	-0.98	-0.97	-0.96	-0.97	-0.95	-0.94	-0.99
S3		310	B	1,76	-0.73	6.26	-0.67	-0.64	-0.69	-0.43	-0.80	-0.83	-0.83	-0.76	-0.69	-0.78	-0.67	-0.57	-0.94
S4		500	B	1,85	-0.96	10.17	-0.95	-0.95	-0.96	-0.96	-0.97	-0.96	-0.94	-0.91	-0.87	-0.90	-0.84	-0.81	-0.98
S5	Sibuluhan Sihaporas B	50	A	1,68	-0.97	-0.35	-0.96	-0.96	-0.97	-0.84	-0.97	-0.95	-0.93	-0.89	-0.82	-0.87	-0.80	-0.75	-0.98
S6		200	B	1,8	-0.96	-0.19	-0.95	-0.95	-0.96	-0.81	-0.97	-0.96	-0.95	-0.91	-0.86	-0.89	-0.83	-0.81	-0.98
S7		350	B	1,59	-0.97	-0.83	-0.96	-0.96	-0.96	-0.83	-0.96	-0.94	-0.92	-0.89	-0.87	-0.89	-0.85	-0.85	-0.99
S8		450	B	1,7	-0.71	4.16	-0.64	-0.65	-0.73	-0.52	-0.83	-0.80	-0.81	-0.77	-0.70	-0.75	-0.66	-0.64	-0.93
S9	Sarudik	50	A	1,68	-0.97	-0.20	-0.98	-0.99	-0.99	-0.74	-0.98	-0.95	-0.89	-0.74	-0.12	-0.46	0.28	0.71	-0.92
S10		200	B	1,73	-0.99	-0.56	-1.00	-1.00	-1.00	-0.97	-1.00	-0.99	-0.98	-0.96	-0.85	-0.92	-0.77	-0.68	-0.99
S11		500	B	1,58	-0.99	-0.46	-0.99	-1.00	-1.00	-0.98	-0.99	-0.98	-0.95	-0.85	-0.44	-0.68	-0.18	0.00	-0.96
S12		950	C	1,82	-1.00	0.06	-1.00	-1.00	-1.00	-0.85	-0.99	-0.98	-0.96	-0.89	-0.64	-0.78	-0.43	-0.21	-0.96
S13	Sibolga Julu	40	A	1,73	-1.00	-0.67	-1.00	-1.00	-1.00	-1.00	-1.00	-1.00	-1.00	-1.00	-0.99	-0.99	-0.98	-0.97	-1.00
S14		200	B	1,87	-0.99	-0.62	-0.99	-0.99	-0.99	-0.99	-0.99	-0.99	-0.98	-0.98	-0.94	-0.97	-0.91	-0.89	-1.00
S15		360	B	1,92	-1.00	-0.85	-1.00	-1.00	-1.00	-1.00	-1.00	-0.99	-0.99	-0.99	-0.98	-0.99	-0.97	-0.97	-1.00

The volume change trend of the weathered granitoids at those study areas show varieties, increase trend of collapse in the weathering process from surface (horizon A) to the bottom of horizon B and C.

Mobility of elemental during the weathering is characterized by the mass transfer coefficient, τj (White et al., 2002) calculated using:

$\tau_{j,w} = (\rho_w C_{j,w})/ \rho_\rho C_{j,p})(\varepsilon_{i,w}+1)-1$ (Brimhall & Dietrich, 1987)

Positive values denote mass addition while negative values denote mass losses (Anderson & Anderson, 2010). Following White et al. (2002), the calculation assume that element j is conservative, thus when τ_j= -1, element j is completely removed during weathering while τ_j=0, means that the element is immobile during weathering with respect to the volume of the parent granitoids.

Elemental change, τj, was calculated for the the parent granitoids from Sibuluhan Sihaporas A (S1), Sibuluhan Sihaporas B(S2), Sarudik (S6) and Sibolga Julu (S17), and their weathered crusts of granitoids from Sibuluhan Sihaporas A (S1-S4), Sibuluhan Sihaporas B (S5-S8), Sarudik (S9-S12) and Sibolga Julu (S13-S15). The τ_j values for those four different granitoids are various from the upper to the lower part of profile for each location. The volume of the weathered granitoids at Sibuluhan Sihaporas A was decreased by the weathering process, while that at Sibuluhan Sihaporas B increased.

The values of elemental change $(\tau_j)_{(Si,\ Ca,\ Na,\ K)}$ of weathered crusts of Sibuluhan Sihaporas B, Sarudik and Sibolga Julu are -1 suggest losses or removal of these elements. On the other hand, $(\tau_j)_{(Al,\ Fe,\ Mn,\ Ca,\ Na,\ K,\ P)}$ in the Sibuluhan Sihaporas A are +1 suggest addition of these elements. The $\tau_{j(REE)}$ for all weathered crusts of granitoids are -1 suggest losses or removal of these elements. These signatures might be related differential fractionation degree of the REE-bearing minerals (e.g. allanite and titanite) during weathering.

CHAPTER 9

DISCUSSION

9.1 Petrochemistry of granitoids in Sibolga and its surrounding areas, North Sumatra, Indonesia

The SiO_2 contents of syenogranites (75 to 80 wt.%) and alkali feldspar syenite (73 wt.%) from Sarudik range narrowly among the granitic rocks from the Sibolga area (75 wt.%), Those granitoids at Sarudik with high SiO_2 and low P_2O_5 contents with high Rb/Sr ratios are highly differentiated. Negative correlations between Al_2O_3, CaO, P_2O_5, MgO, FeO_{tot}, MnO, TiO_2 and SiO_2 contents suggest that the granitic magmas likely underwent fractional crystallization during magmatic differentiation. The decrease in P_2O_5, MgO and FeO_{tot} indicates removal of apatite and mafic minerals (such as biotite and hornblende) during differentiation. The fractional crystallization is also suggested by the Eu negative anomalies which indicate fractionation of feldspars during differentiation (Fig. 9.1).

Quartz alkali feldspar syenite, quartz syenite, and alkali feldspar granite were found at Tanjung Jae - Panyabungan. SiO_2 and REE content of quartz alkali feldspar syenite are 70 wt% and 365 ppm, respectively, those of alkali feldspar granite are 72.3 wt.% and 223 ppm while those of quartz syenite are 74.7 wt% and 107 ppm. P_2O_5 contents of three granitoids are 0.08 wt.%. SiO_2 and ΣREE contents are negatively correlated. Quartz alkali feldspar syenite and alkali feldspar granite were found at Pintu Padang Julu. SiO_2 and ΣREE contents of quartz alkali feldspar syenite at Pintu Padang Julu are 66.8 wt.% and 219 ppm, while those of alkali feldspar

granite are 71.6% and 439 ppm. P_2O_5 contents of alkali feldspar granite from Pintu Padang Julu are 0.33 wt. % and 0.15 wt.%. SiO_2 and ΣREE are positively correlated while P_2O_5 and SiO_2 are negatively correlated. The SiO_2 content of alkali feldspar syenite from Tano Tombangan range from 55 to 58 wt.%, P_2O_5 contents range from 0.01 to 0.02 wt.% and ΣREE range from 35 to 90 ppm.

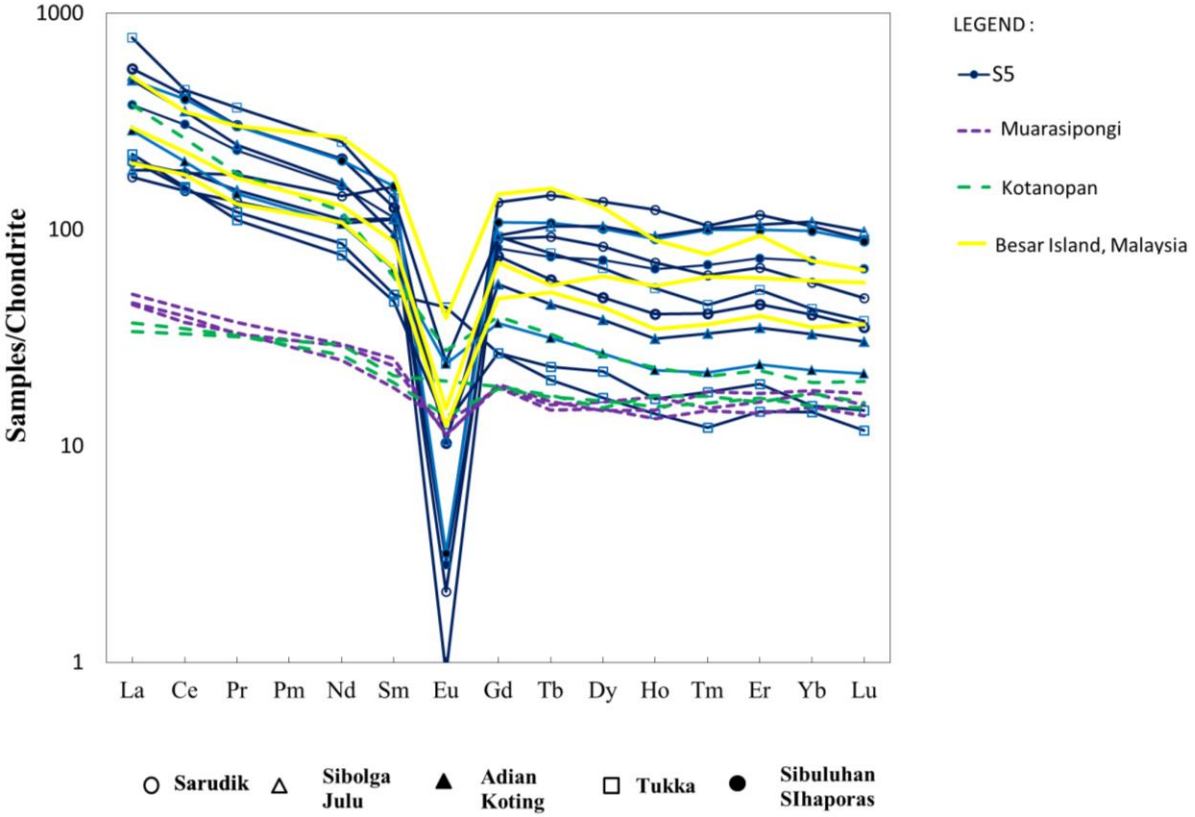

Fig. 9.1 Chondrite normalized REE patterns (normalizing values of chondrite are from McDonough & Sun, 1995).

SiO_2 content of monzogranites and quartz monzonite at Muara Sipongi ranges from 63.9 to 67.6 wt.%, and 61.5 wt.%, respectively. P_2O_5 contents ranges from 0.09 to 0.12 wt% and is 2.35 wt % respectively, while ΣREE content ranges from 66 to 75 ppm and is 71 ppm, respectively.

SiO_2 contents are negatively correlated with ΣREE contents. Zircon and apatite are accessories minerals.

SiO_2 content of monzogranite from Tolung is 71 wt%, P_2O_5 is 0.11 wt.%, and ΣREE content is 359 ppm, while that of quartz monzonite is 63.6 wt. % and that of monzodiorite is 66.5 wt.%, those of P_2O_5 of granitoids contents are 0.11 and 0.12 wt.%, respectively and those of ΣREE contents of granitoids are 63.6 to 63.8 ppm, respectively. SiO_2, P_2O_5, and ΣREE contents suggest that magma source of Kotanopan granitoids are different than that of Tolung. ΣREE content is positively correlated with SiO_2. Zircon occurs as an accessory mineral of monzogranite, zircon and apatite were occurred in quartz monzonite.

The alkali feldspar syenite, quartz syenite, syenite and syenogranites from Sibolga and the surrounding areas are composed mainly of K-feldspar, quartz, plagioclase, biotite and hornblende. Common accessory minerals are zircon, allanite, apatite, and titanite.

Quartz monzonite from Tarutung, quartz alkali feldspar syenites from Tukka and Sibuluhan Sihaporas, and alkali feldspar syenite from Sarudik contain allanite and apatite, thus their chondrite normalized REE patterns show enrichment in both of LREE and HREE, while quartz syenite from Adian Koting and quartz alkali feldspar syenite from Tukka contain only zircon and they are relatively depleted both in LREE and HREE.

REE were enriched in the quartz monzonite from Tarutung and quartz alkali feldspar syenite from Sibuluhan Sihaporas, and alkali feldspar syenite from Sarudik presumably due to the accumulation of allanite and titanite, correlated to the low P_2O_5 content. The P_2O_5 content decrease as SiO_2 and ΣREE contents increase (Fig. 9.2). Average ΣREE content of the quartz syenite and monzogranite from Sibolga Julu is 704 ppm, average ΣREE content of quartz syenite

and quartz monzonite from Tarutung is 797 ppm, average ΣREE content of quartz alkali feldspar syenite, quartz alkali feldspar syenite and syenogranite from Sibuluhan Sihaporas is 539 ppm, and average ΣREE content of alkali feldspar syenite and syenogranites from Sarudik is 413 ppm.

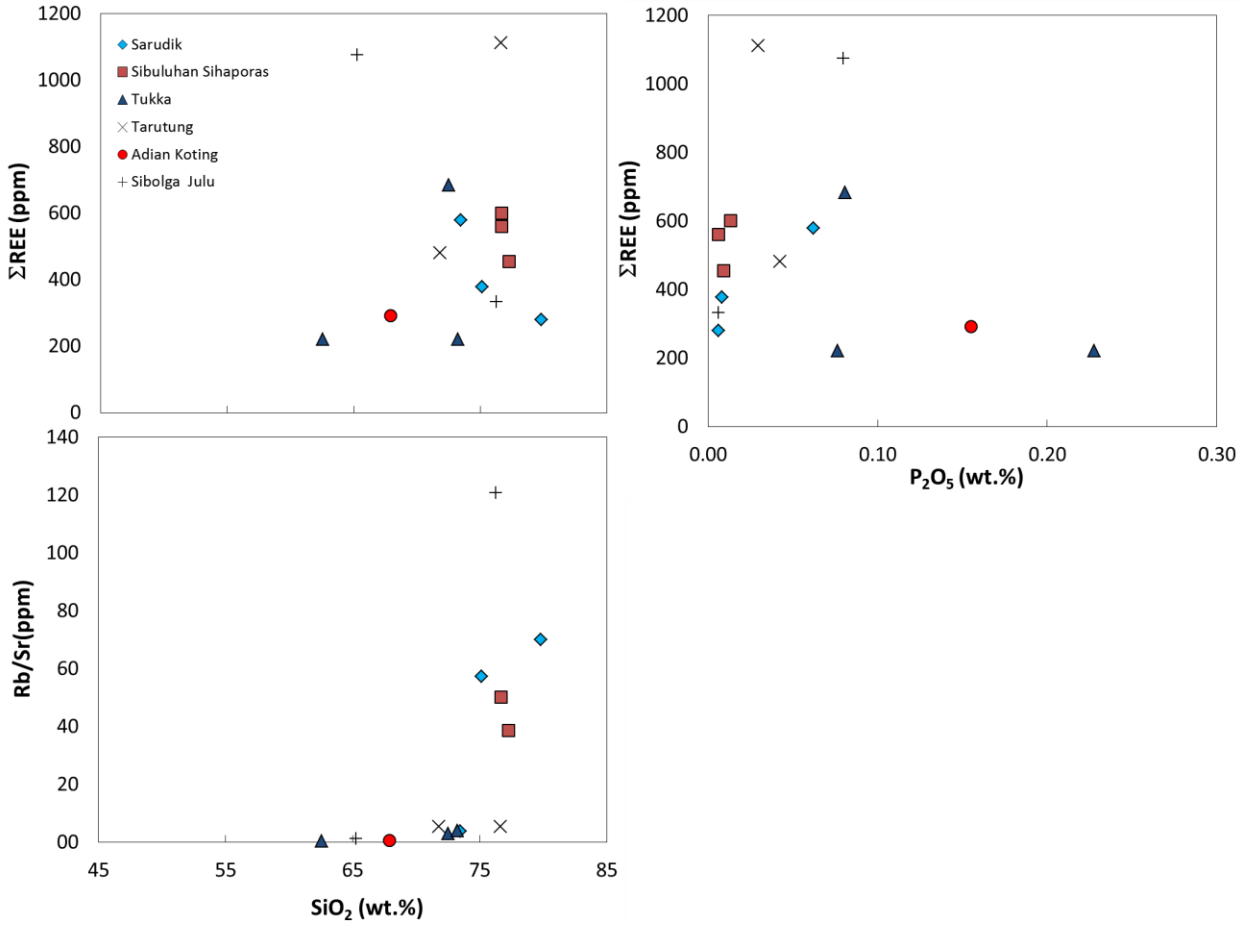

Fig.9.2 Plots of a. SiO_2 versus ΣREE b. SiO_2 versus P_2O_5 and c. SiO_2 versus Rb/Sr.

On the other hand, REE are not enriched in the granitoids which formed in volcanic arc setting. ΣREE contents of quartz alkali feldspar syenite from Tukka range from 203 to 205 ppm. Cordierite and corundum coexist with biotite, hornblende, zircon and apatite in the quartz syenite at Adian Koting (S21, SB2, and SB3). In the syenogranite from Sarudik, corundum is associated with zircon, apatite, titanite. ΣREE of granitoids that contain corundum and cordierite are

relatively low due to removal of apatite which is consistent with a decrease of P_2O_5 during magmatic differentiation. Low P_2O_5 contents prohibit saturation of REE phosphate. The allanite and titanite are the main host of REE. Apatite, monazite and xenotime are rarely present in the granitoids in Sibolga.

SiO_2 and ΣREE of granitoids from Panyabungan in general are positively correlated, but in each group of the sample, they do not show clear patterns, ΣREE contents are different at the same SiO_2 content in granitoids at Padang Julu. ΣREE content and SiO_2 in the granitoids from Tano Tombangan and Tanjung are negatively correlated (Fig. 9.3). Relation between SiO_2 and Rb/Sr of granitoids from Tano Tombangan are unclear. At the same SiO_2 contents, two of three samples from Tano Tombangan have different Rb/Sr ratios. SiO_2 and Rb/Sr of granitoids from Tanjung are negatively correlated (Fig.9.3). P_2O_5 and ΣREE, in general are negatively correlated. P_2O_5 contents are low when ΣREE are high. P_2O_5 and ΣREE are positively correlated in the granitoids at Tanjung Jae, while negatively correlated in granitoids at Pintu Padang Julu. These unclear patterns of Harker diagram and wide variation of SiO_2 and ΣREE, P_2O_5 contents and Rb/Sr ratio suggest heterogeneous magma sources (Fig.9.3). ΣREE contents of quartz syenite, alkali feldspar granite and quartz alkali feldspar syenite range from 85 to 356 ppm, P_2O_5 contents are 0.08 wt.%.

SiO_2 contents of quartz syenite and alkali feldspar granite from Tanjung are 74.7 wt% and 72.3wt.%, respectively. Both have P_2O_5 0.08 wt%, ΣREE from 85 and 198 ppm, respectively. Allanite and apatite occur as the accessory mineral in quartz alkali feldspar syenite suggesting that REE are accomodated in allanite and apatite. The SiO_2 contents are negatively correlated

with REE content. SiO_2 contents of alkali feldspar granite and quartz alkali feldspar syenite from Pintu Padang Julu are 66.4 and 72 wt.%.

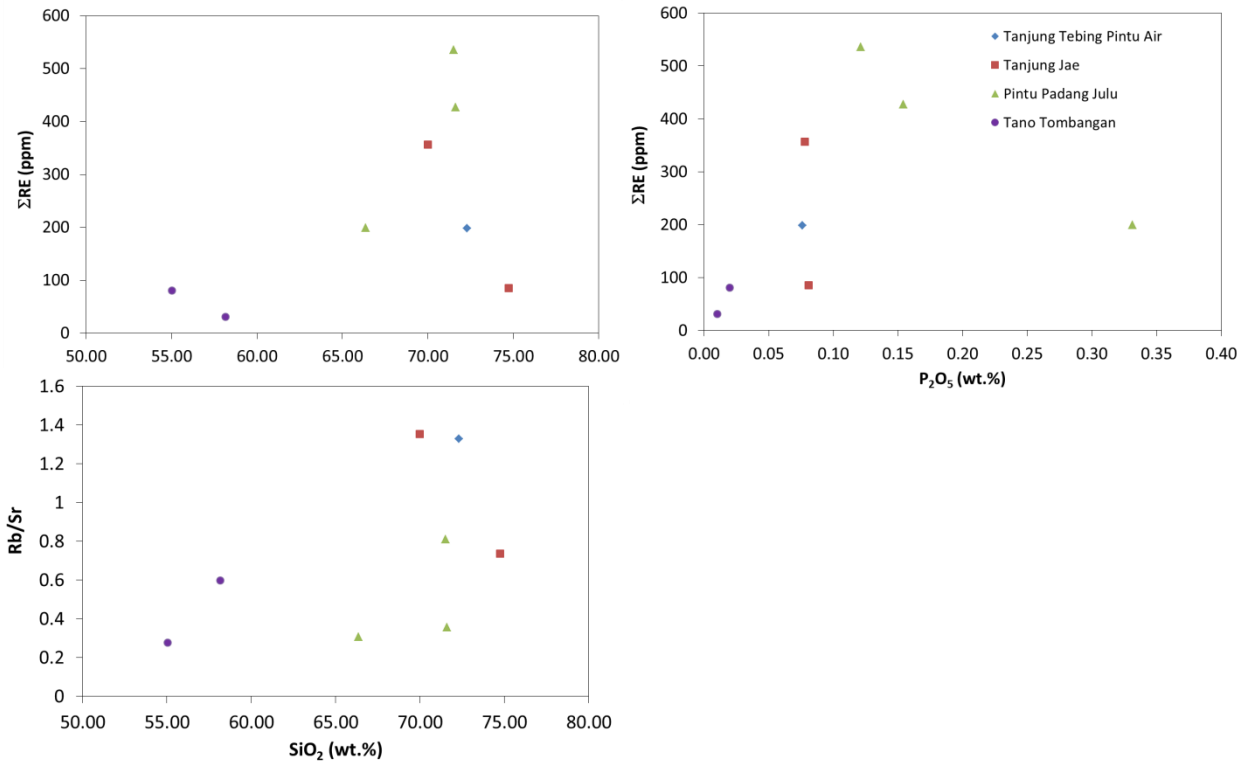

Fig. 9.3 SiO_2 and ΣREE, SiO_2 and Rb/Sr, and P_2O_5 and ΣREE of granitoids from Panyabungan.

P_2O_5 contents are 0.33 and 0.15 wt%, respectively, and ΣREE are 200 and 427 ppm. In general, they are ferroan, peraluminous characteristic and formed in the volcanic arc setting. Apatite and allanite are accessory minerals. SiO_2 contents of alkali feldspar syenite from Tano Tombangan range from 55 to 58 wt.%, P_2O_5 contents range from 0.01 to 0.02 wt.%, and REE contents range from 31 to 81 ppm. They have ferroan, metaluminous and formed in volcanic arc environment.

ΣREE contents of granitoids from Muara Sipongi are low contrasting to that of Sibolga, Panyabungan and Kotanopan. REE was not enriched in granitoids at Muara Sipongi. SiO_2

contents of monzogranite range from 64 to 68 wt%, P_2O_5 0.09 to 012 wt.% and ΣREE 66 to 75 ppm. While SiO_2 content of quartz monzonite is 62 wt.%, P_2O_5 is 0.14 wt.% and ΣREE is 71 ppm. They have magnesian, calcic and mostly metaluminous affinity.

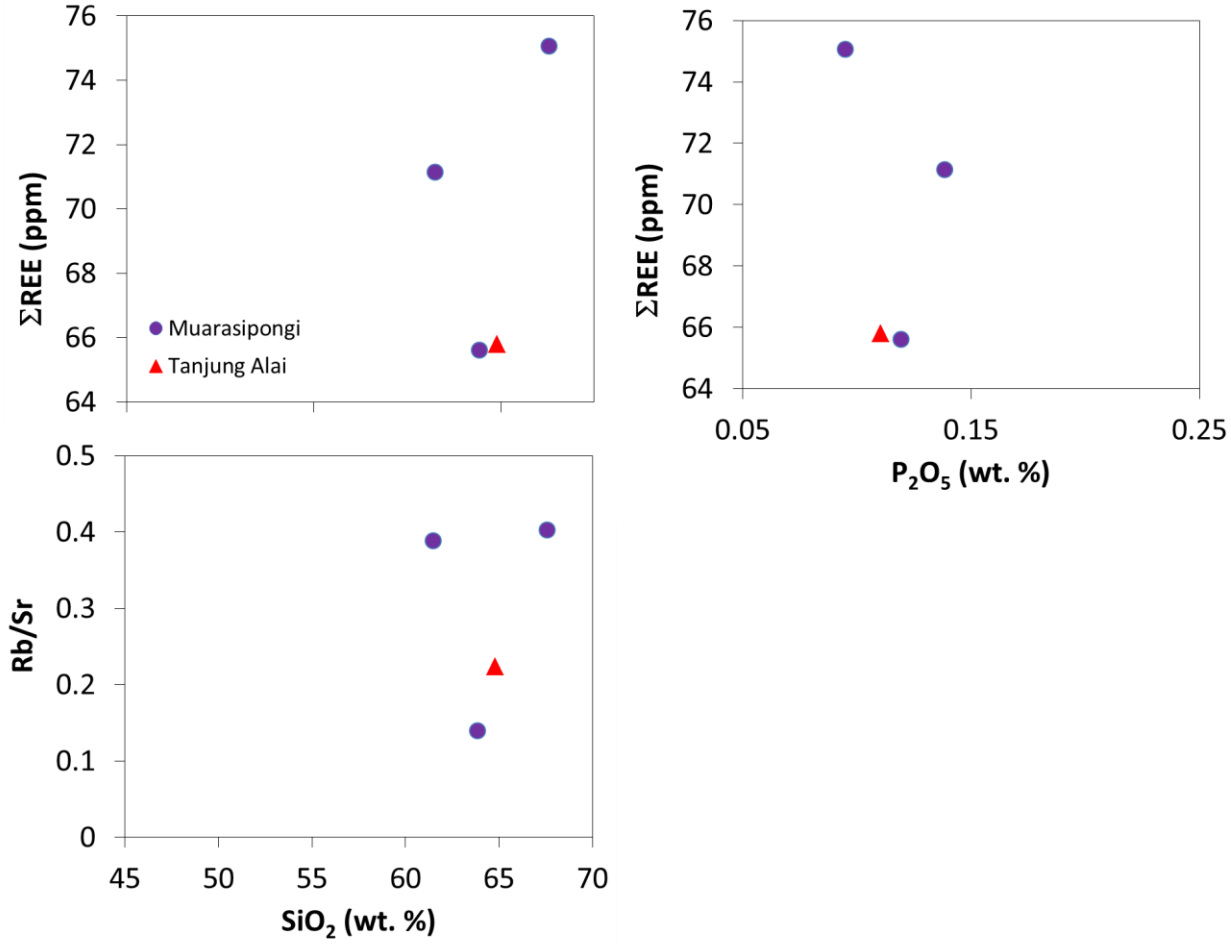

Fig. 9.4 SiO_2 and ΣREE, SiO_2 and Rb/Sr, and P_2O_5 and ΣREE of granitoids at Muara Sipongi.

ΣREE and Rb/Sr are positively correlated with SiO_2, while P_2O_5 and ΣREE are negatively correlated in monzogranite and quartz monzonite (MS 6 and MS 12) from Muara Sipongi (Fig. 9.4). SiO_2 and ΣREE are positively correlated while SiO_2 and Rb/Sr, P_2O_5 and ΣREE are negatively correlated in monzogranite and quartz monzonite from Kotanopan (Fig. 9.5).

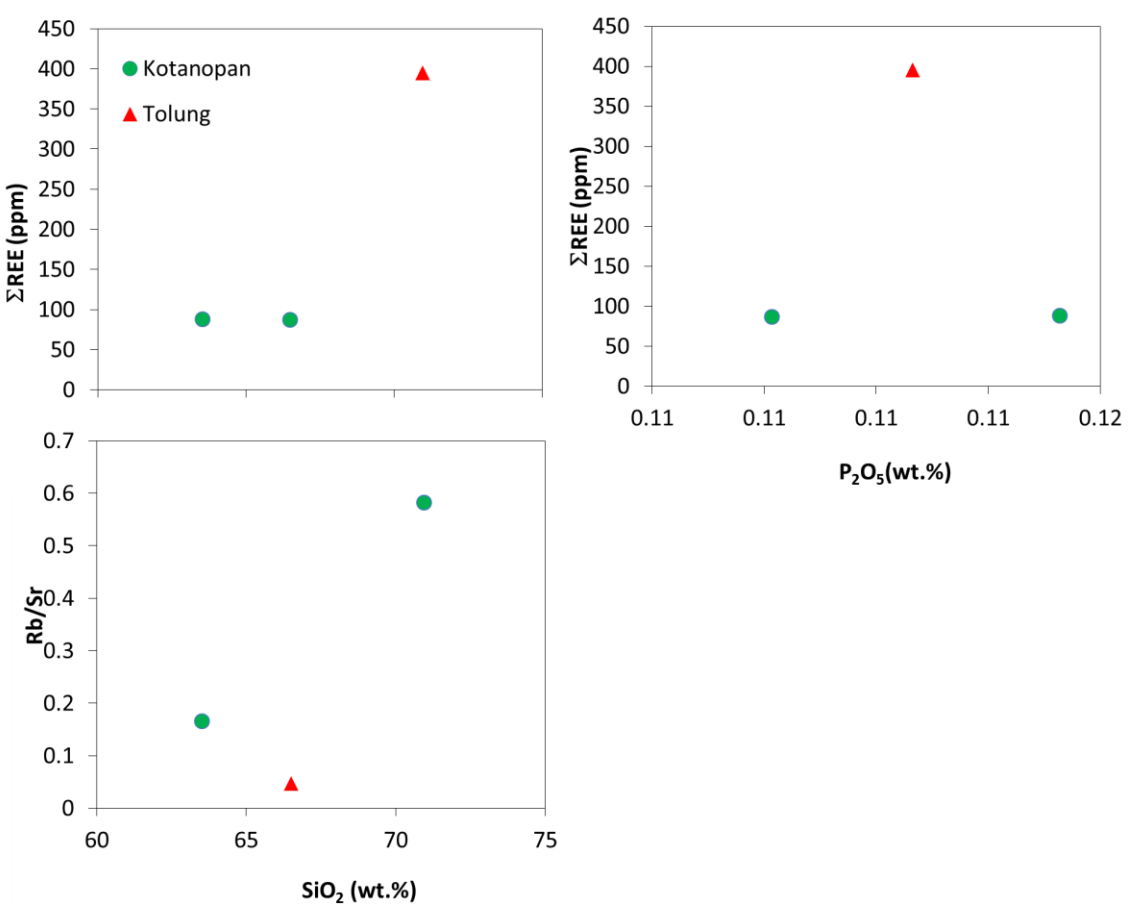

Fig. 9.5 Plots of SiO_2 and ΣREE, b. P_2O_5 and ΣREE, and SiO_2 and Rb/Sr of granitoids at Kotanopan.

The negative correlation of P_2O_5 and ΣREE of granitoids from Muara Sipongi and Kotanopan suggests low ΣREE due to a removal of REE phosphate-bearing minerals. ΣREE content of granitoids which were formed in volcanic arc setting and that have I-type character is very low compared to those granitoids that were formed within plate setting and that have ferroan magma affinity.

Granitoids from Sibolga which are A-type, ilmenite-series and those from Panyabungan which are S-type ilmenite-series have significantly higher ΣREE than those from Muara Sipongi and Kotanopan. SiO_2 content of monzogranite from Tolung is 71 wt%, P_2O_5 0.11 wt.%, and

ΣREE is 359 ppm. The monzogranite was formed in volcanic arc environment, with ferroan and peraluminous characters. SiO_2 contents of quartz monzonite and monzodiorite are 64 and 67 wt.%, P_2O_5 contents are 0.11 and 0.12 wt.%, and ΣREE range from 63.6 to 63.8 ppm. Chondrite normalized REE patterns of monzonite and monzodiorite show cogenetic relationship, magnesian, and metaluminous character. Based on Rb-(Y+Nb) and Nb-Y discriminant diagrams (Pearce et al, 1984), granitoids from Muara Sipongi and Kotanopan were formed in the volcanic arc environment (Chapter 6).

The relation of SiO_2 and P_2O_5 with ΣREE contents of monzogranite and quartz monzonite at Kotanopan and Tolung are not clear, however, SiO_2 and Rb/Sr of both granitoids are positively correlated (Fig. 9.5). In the case of granitoids at Kotanopan, the ΣREE contents are higher than those of Muara Sipongi. The high REE content occurs in the peraluminous granitoids formed in the volcanic arc environment.

9.2 Geochemistry and Sr-Nd isotopic signatures of granitoids in the western part of North Sumatra, Indonesia

Summary of SiO_2, Rb/Sr, Sr, Rb, Sm, Nd concentration and ∑REE content is depicted in Table 9.1. Table of age reference show in Table 9.2

The studied granitoids of Sibolga do not have age data. The ages were obtained from the previous study in the Sibolga and Panyabungan and their surroundings. The ages are from Hehuwat (1975, 1976, 1977), Aspden et al. (1982), Beckinsale (in Aspden 1982), Wikarno et al. (1988, 1993), and Fontaine & Gafoer (1989).

Table 9.1 Summary of initial ratio of SiO_2 contens, Rb/Sr ratio, Rb, Sr, Sm, and Nd contents, $^{87}Sr/^{86}Sr$ ratios based on calculation

No	Location	Sample name	SiO_2 (wt %)	Rb (ppm)	Sr (ppm)	Rb/Sr	Sm (ppm)	Nd (ppm)	ΣREE
1	Tanjung Jae	PYB4D	74.74	92.6	457	0.2	4.66	17	106.49
2	Tanjung Jae	P4	72.8	226	283	0.8	10.15	65.2	382.75
3	Pintu Padang Julu	P7	66.37	173	668	0.26	7.28	36.8	219.32
4	Tano Tombangan	P8C	54.97	117	262	0.45	10.35	53.6	306.17
5	Adian Koting	S21_2	67.9	200	274	0.73	9.72	48.6	327.48
6	Adian Koting	SB3	67.92	204	264	0.77	8.47	47.8	317.53
7	Sibolga (Sarudik)	SR1	75.14	752	13.1	57.4	23.4	65.5	575.58
8	Sibolga (Tukka)	S8	72.5	257	83.5	3.08	20.7	116	773.22
9	Sibolga (Sihobuk)	S24B	65.96	208	427	0.49	10.45	61.6	428.85

Correlation diagram of Rb/Sr ratios with the present $^{87}Sr/^{86}Sr$ of granitoids from each sample from Panyabungan and those from Sibolga do not have a linear correlation suggesting that they do not have a genetic relationship among each other.

The calculation of initial Sr isotope ratios (Sr_i) are using the present-day (measured) $^{87}Sr/^{86}Sr$ (Sr_p) and the age obtained from the references (Table 9.2). The equation is as follow:

$^{87}Sr/^{86}Sr\ (Sr_p) - {}^{87}Sr/^{86}Sr\ (Sr_i) = {}^{87}Rb/^{86}Sr\ (Sr_p)\ (e^{\lambda t-1})$ (Rasskazov et al., 2010)

Nicolaysen (1961) used this equation for calculating Sr (i) using isochrones method,

Where:

$y = mx + b$

y = measured $^{87}Sr/^{86}Sr\ (Sr_p)$,

m slope $= e\ \lambda t-1$, $x = {}^{87}Rb/^{86}Sr_p$ (calculated using the Sr_p)

b= unknown Sr (Sr_i)

For slope measurement, the age (t) is referring to the age obtained by the previous study (Table 9.2). Ages of collected granitoids are referring to the nearest and most similar characteristics of granitoids.

Table 9.2 Summary of age dating result of Sibolga and Panyabungan area

Location	Inferred location	Isotopic method mineral	Age (Ma)	References
Sibolga granite complex	Unspecified area	K/Ar on biotite	206.1+2.5	1
Sibolga	Unspecified area	K-Ar on biotite	211±3	2
Sibolga	Unspecified area	K-Ar on hornblende	219±4	2
Sibolga	Unspecified area	Sr-Rb	257±24	3
Sibolga (near city)	Sarudik (?)		**264**	4
	Unspecified area	K-Ar on biotite	211+5	5
Sibolga	Unspecified area	Rb-Sr on biotite	211,5±2,6	6
Sibolga	Unspecified area	Rb-Sr on biotite	217,4±4,4	6
Padang Sidempuan	Panyabungan (?)	K-Ar, on biotite	202±2	7
Sibolga granite complex (Mpisl)	Unspecified area	Rb/Sr whole rock	**264+6**	7
Tarutung	Adian Koting (?)	Rb-Sr on hornblende	206,1±2,5	6
Tarutung	Tarutung	Rb-Sr on biotite	218,8±3,9	6
Sibolga	Unspecified area	K-Ar on biotite	206±2	8
Satelit Sibolga	Unspecified area	K-Ar on biotite	212±3	8
Sibolga	Unspecified area	K-Ar on biotite	216±3	8
Satelit Sibolga	Unspecified area	K-Ar on biotite	217±4	8
Sibolga	Unspecified area	K/Ar on hornblende	144+2.4	8
Sibolga	Unspecified area	K/Ar on biotite	147+2.4	8
Sibolga	Unspecified area	K/Ar on biotite	211+2.6	8
Sibolga	Unspecified area	K/Ar on biotite	217.4+4	8
Sibolga	Unspecified area	K/Ar on hornblende	218.8+3.9	8

Reference :
1) Hehuwat, 1975; 2) Hehuwat 1976; 3) Hehuwat, 1977; 4) Aspden et al., 1982; 5) Beckinsale (in Aspden 1982); 6) Wikarno dkk. (1988); 7 Wikarno dkk. (1993); 8) Fontaine & Gafoer (1989).

The result shows that initial $^{87}Sr/^{86}Sr$ (Sr_i) isotopic value of granitoids from Panyabungan and Sibolga ranges widely (Table 9.3). The initial isotopic value (Sr_i) of Tanjung – Panyabungan ranges from 0.719129 to 0.712104 at 202 Ma, that of Pintu Padang Julu ranges from 0.709382 to

0.713683 at 202 Ma, while that of granitoids from Tano Tombangan is 0.711030 at 257 Ma. Sr_i of granitoids from Sibolga ranges from 0.724526 to 0.723730 (Sarudik) at 211 Ma, that of granitoids from Adian Koting ranges from 0.710729 to 0.710769 at 219 Ma, that of granitoid from Tukka is 0.710700 at 264 Ma, and that of granitoid from Sihobuk is 0.714956 at what 264 Ma (Table 9.3).

The average Sr_i of syenogranite from Sarudik is high (0.724128), which suggests that the syenogranite magma was resulted from partial melting of granitic crusts and was probably contaminated with metasedimentary rocks in the upper crust. Thus, the Sr_i of syenogranite from Sarudik is similar with the Sr_i of granitoids from Belinyu, and Penangas of the Klabat Suite, Bangka region ranging from 0.7270 to 07163 (Cobbing, 1992; Aspden et al., 1982), suggesting a genetic relationship between the granitic rocks from Sarudik and Klabat Suite of Bangka region. Sr_i of quartz syenites from Adian Koting (SB3 and SB21) (0.710729 and 0.710769) are similar with those of granitoids from Langkawi, West Malaysia (0.7107) (Kwan et al., 1992) and Malacca of Peninsular Malaysia (0.711) (Hutchison, 1977), suggesting that they have similar source and formed by partial melting of upper crust. Sr_i of the granitoids from Tanjung Jae ranging from 0.712104 to 0.719129 and average of the granitoids from Pintu Padang Julu (Panyabungan) 0.710812 suggest that they were likely resulted from partial melting of a various of sources crustal materials rocks. Sr_i of quartz alkali feldspar syenite from Sihobuk is high (0.714956). Quartz alkali feldspar syenites from Tukka and Sihobuk, and quartz syenites from Adian Koting are probably contaminated with the alumina-rich rocks. Sr_i of quartz alkali feldspar syenite from Sihobuk is relatively close to that of Hatapang granite at the northeast of Sibolga ($Sr_{i=}$ 0.7151) (Clarke & Beddoe-Stephens, 1987). These suggest a genetic relationship

between quartz syenite from Tanjung Jae and Hatapang granites, which were derived from upper crusts.

The Sibolga granitoids were most probably formed by partial melting of granodioritic crust and was contaminated by metasedimentary rocks, while the Panyabungan magmas were generated from a partial melting of metasedimentary rock sources.

The initial isotopic values (Sr_i) of granitoids from Panyabungan and Sibolga are lower than that of granitoids from Bebulu and Klabat suite from Bangka Island. The average Sr_i of quartz alkali feldspar syenite from Pintu Padang Julu (P7) (0.710812), and Tukka (S8) (0.710700) are most probably belong to the Main Range Belt based on assumed initial ratio for the Main Range Belt 0.711 to 0.710 (Hutchison, 1978). Age of emplacement was referred to 202 Ma (Wikarno, 1993) for Pintu Padang Julu-Panyabungan and 264 Ma for granitoids from Tukka-Sibolga (Aspden et al., 1982). Hutchison (1994) suggested the age of the Main Range by Rb/Sr range from Late Late Triassic to Carbonaceous.

Plots of $^{87}Sr/^{86}$ Sr (p) and Rb/Sr concentration on isochron diagram show random distribution, especially plots of Panyabungan (Fig. 9.6). These suggest that magma sources are multiple and not cogenetic.

SiO_2 vs $^{87}Sr/^{86}$ Sr of granitoids from Sibolga and Panyabungan show unclear correlation. $^{87}Sr/^{86}$ Sr vs P_2O_5 of granitoids from Sibolga and Panyabungan show slightly negative correlation. $^{87}Sr/^{86}$ Sr vs ΣREE of granitoids from Sibolga show slightly positive correlation, while those from Panyabungan is negatively correlated. These suggest that most of the granitoids from Sibolga and Panyabungan do not have genetic relationship among each other. They most probably derived from different sources.

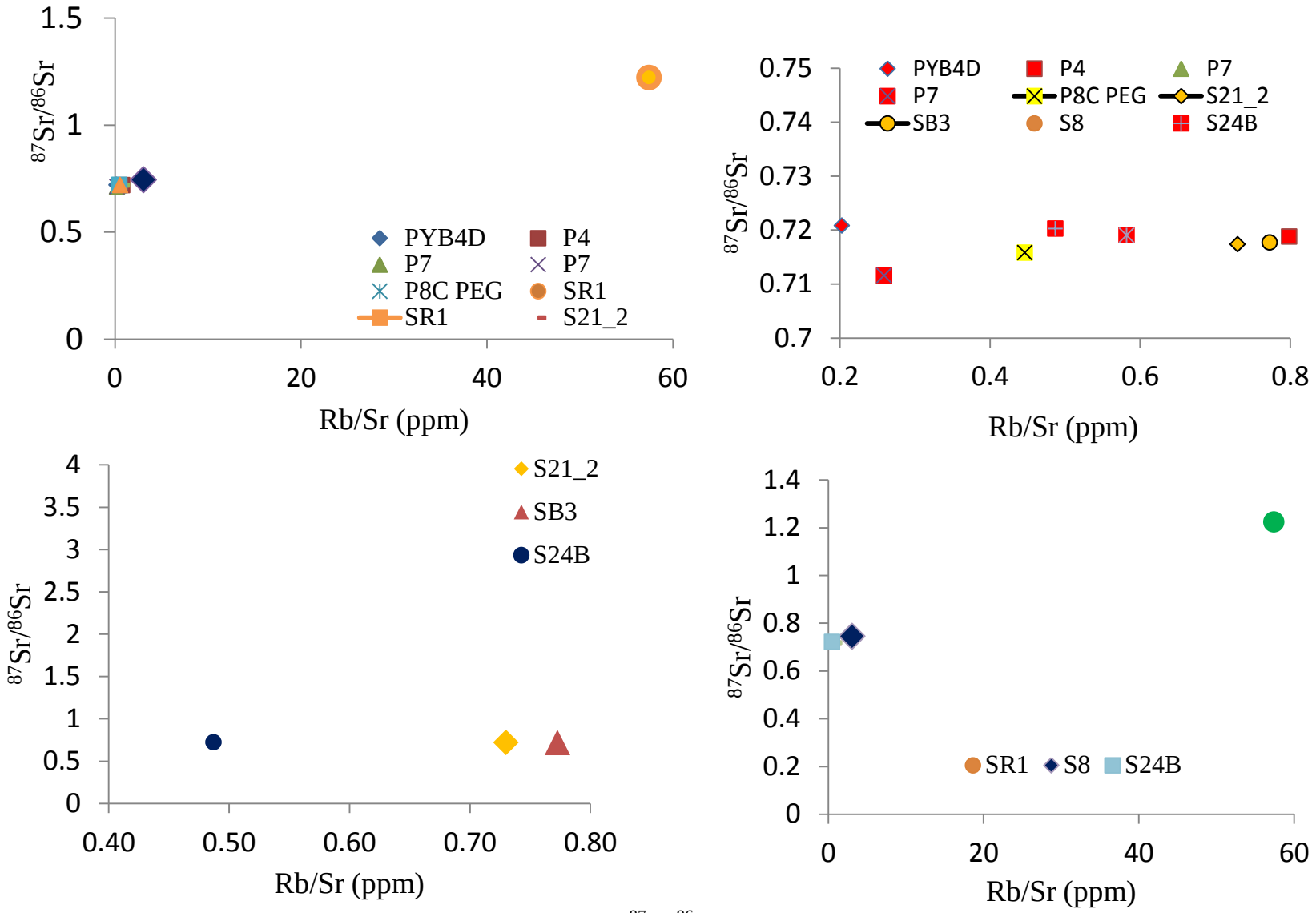

Fig. 9.6 Correlation diagram of Rb/Sr ratios with the present $^{87}Sr/^{86}Sr$ of Panyabungan and Sibolga granitoids do not have a linier correlation.

Table 9.3 Summary of Rb/Sr and Sm/Nd measurement (TIMS) result of granitoids from Sibolga

No	Location	Sample code	$^{87}Rb/^{86}Sr$ (p)	$^{87}Sr/^{86}Sr$ (p)	Mean Sr atomic	Age (reference)	$^{87}Sr/^{86}Sr$ (initial)	^{143}Nd / ^{144}Nd (p)	Correction
1	Tanjung Jae	PYB4D	0.587	0.720814	87.560426	202(*1)	0.719129	-	-
2	Tanjung Jae	P4	2.312	0.718746	87.576753	202(*1)	0.712104	0.512217	0.000017
3	Pintu Padang Julu	P7	0.750	0.711523	87.719627	202(*1)	0.709369	-	-
		P8	0.750	0.711536	87.719627	202(*1)	0.709382	0.512251	0.000013
		P9	0.750	0.711530	87.719627	202(*1)	0.713683	-	-
4	Tano Tombangan	P8C	1.293	0.715757	87.574875	257(*2)	0.711030	-	-
5	Adian Koting	S21_2	2.113	0.717345	87.574875	219(*4)	0.710769	0.512193	0.000011
6	Adian Koting	SB3	2.237	0.717691	87.589328	219(*4)	0.710729	0.512215	0.000007
7	Sibolga	SR1	166.193	1.223221	83.443984	211(*3)	0.724526	-	-
	Sibolga		166.193	1.222425	83.443984	211(*3)	0.723730	-	-
	Sibolga		166.193	1.222823	83.443984	211(*3)	0.724128	-	-
8	Sibolga (Tukka)	S8	8.911	0.744167	87.358640	264(*5)	0.710700	0.512018	0.000007
9	Sibolga (Sihobuk)	S24B	1.410	0.720253	87.560426	264(*5)	0.714956	0.511929	0.000003

Age reference:

*[1] : K-Ar, Wikarno et al. (1993)

*[2] : Sr-Rb, Hehuwat (1977)

*[3] : Sr-Rb on biotite, Wikarno et al. (1998)

*[4] : K-Ar on hornblende, Wikarno et al. (1988)

*[5]: Sr-Rb on whole rock, Aspden et al. (1982)

ΣREE content of granitoids from Sibolga (SR1, S8, S21, and S24B) are higher that that from Panyabungan (PYB 4D, P4, and P7) (Fig. 9.7, Table 9.4).

The result of the initial ^{143} Nd/^{144} Nd isotopic values have a wide range (Table 9.3). The initial isotopic value of Tanjung Jae (P4) is 0.512217 at 202 Ma, that of Pintu Padang Julu (P4) 0.512251 at 202 Ma. ^{143} Nd/^{144} Nd of Adian Koting range from 0.512215 to 0.512193 at 219 Ma, that of from Tukka is 0.512018 at 264 Ma, and that of Sihobuk 0.511929 at 264 Ma. Initial strontium for S-type granite (initial $^{87}Sr/^{86}Sr$) is >0.708 because their source rocks had been through an earlier sedimentary cycle while that of I-type have initial $^{87}Sr/^{86}Sr$ ratios in the range from 0.704 to 0.706 (Huthison, 1978; Chappel & White, 1974).

Table 9.4 Summary of ΣREE and $^{87}Sr/^{86}Sr$ and P_2O_5 contents of granitoids from Sibolga and Panyabungan

Sample code	Locality	Rock name	SiO_2	P_2O_5	ΣREE	$^{87}Sr/^{86}Sr$ (initial)
SR1	Sarudik	Syenogranite	75.14	0.01	378	0.724128
S8	Tukka	Qtz.alk.fel.sye	72.5	0.08	684	0.710700
S21	Adian Koting	Qquartz syenite	67.9	0.16	292	0.710769
SB3	Adian Koting	Quartz syenite	67.92	0.16	292	0.710729
S24B	Sihobuk	Qtz.alk.fel.sye	65.96	0.14	283	0.714956
PYB4D	Tanjung Jae	quartz syenite	74.74	0.08	85	0.719129
P4	Tanjung Jae	Alk.fel.sye	72.80	0.10	368	0.710736
P7	Pintu Padang Julu	Qtz.alk.fel.sye	66.37	0.33	200	0.711533
P8C	Tano Tombangan	Alk.fel.sye	54.97	0.01	275	0.711030

Isochrons of I-types granitoids from Sibolga show a regular straight set of points whereas those of S-types granitoids from Panyabungan are scattered, reflecting variations in the initial $^{87}Sr/^{86}Sr$ within a single pluton as a consequence of more heterogeneous source materials.

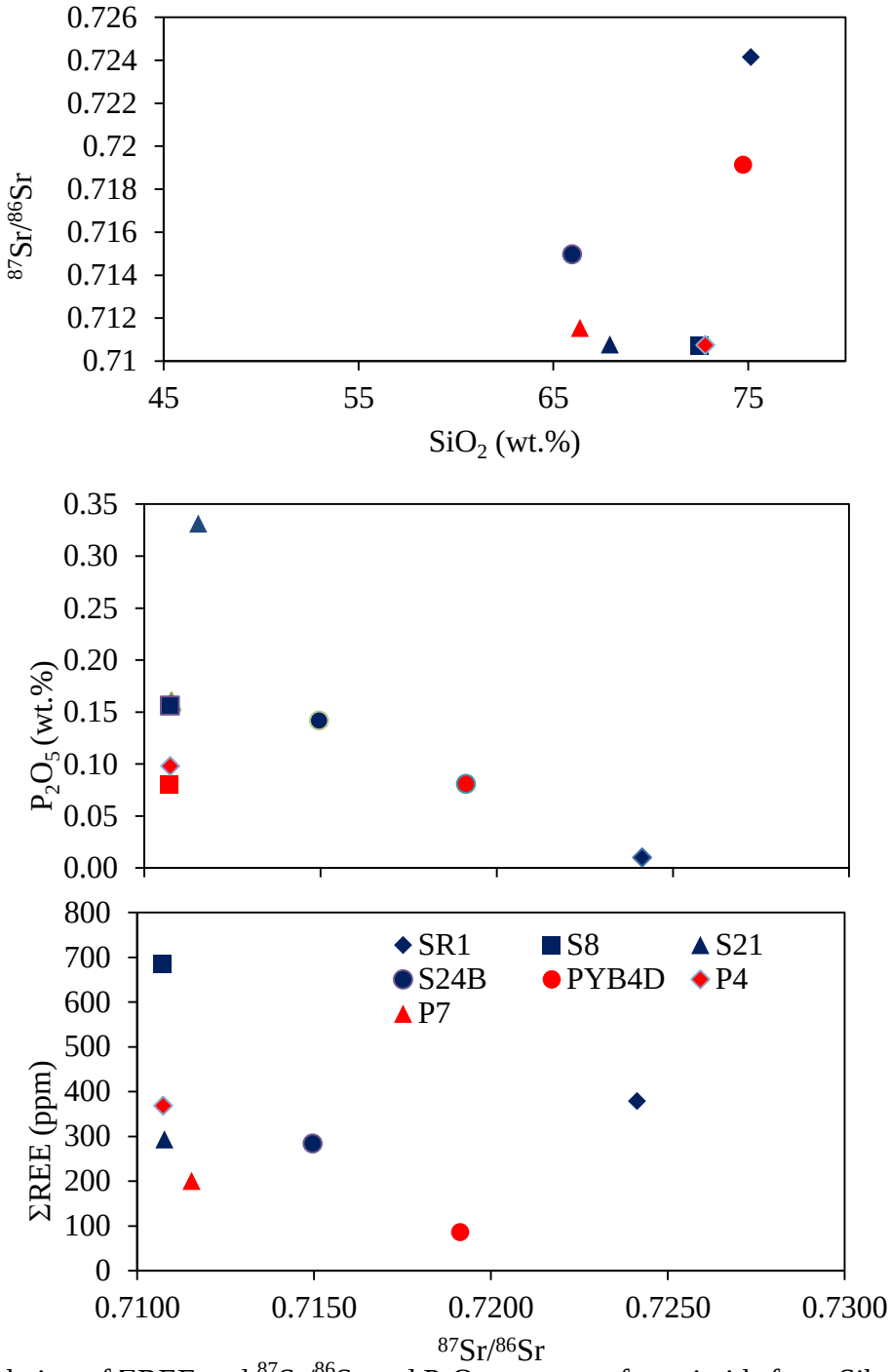

Fig. 9.7 Relation of ΣREE and $^{87}Sr/^{86}Sr$ and P_2O_5 contents of granitoids from Sibolga (SR1, S8, S21, and S24B) and Panyabungan (PYB 4D, P4, and P7).

9.3 Tectonic Evolution and Petrogenetic Model

9.*3.1 Tectonic evolution*

Granitoids from Sibolga were classified as ilmenite-series based on magnetic susceptibility (e.g. Ishihara, 1977). Based on SiO_2 versus $FeO_{tot}/(FeO_{tot}+MgO)$, SiO_2 versus Na_2O+K_2O-CaO and alumina saturation index (ASI) versus molar $Al_2O_3/ (Na_2O +K_2O)$ the granitoids are mainly of alkali to alkali-calcic, and peraluminous (Frost et al., 2001) (Chapter 6). However based on the occurrence of hornblende in the syenogranite and quartz alkali feldspar syenite from Sarudik, quartz syenite from Tarutung, quartz syenite from Adian Koting, these granitoids exhibit I-type ilmenite-series in character (Gill, 2010; Chappel & White, 1974, 2001). The occurrence of ilmenite-series I-type granitoids in the Sibolga area may be explained by an interaction of originally I-type granitic magma with sedimentary basement rocks as a reducing agent, which eventually reduced the magma (Ishihara, 1998). Cordierite as xenocrysts and corundum as inclusions in K-feldspar coexist with biotite, hornblende, zircon and apatite in the quartz syenite at Adian Koting, while corundum coexists with zircon, apatite, titanite in the syenogranite from Sarudik. These evidence suggest assimilation of metasedimentary or pelitic basement rocks beneath Sibolga. The formation of the syenogranite and quartz alkali feldspar syenite from Sarudik, quartz syenite from Tarutung, quartz syenite from Adian Koting of I-type granitoids is possibly related with the subduction which have initiated during the Late Permian at the west coast of Sumatra (Aspden, 1982).

Nb-Y and Rb-(Y+Nb) discrimination diagrams (Pearce et al., 1984) suggest that the quartz alkali feldspar syenite, and syenogranites from Sarudik, quartz alkali feldspar syenite, and monzogranite from Sibolga Julu, quartz alkali feldspar syenite, quartz syenite and syenogranite from Sibuluhan Sihaporas, quartz alkali feldspar syenite from Tukka, quartz alkali feldspar syenite, and quartz syenite from Tarutung, and quartz syenite from Adian Koting were formed within plate setting, while the quartz alkali feldspar syenite and alkali feldspar syenite from Tukka were formed in volcanic arc setting (Pearce et al., 1984) (Figs. 9.15). This coexistence of two differences tectonic environments suggests a change in tectonic setting in Sibolga during Permian to Late Triassic. The change was presumably from subduction related granitoids with characters of metaluminous, I-type and magnetite-series granitoids to peraluminous, A-type and ilmenite-series granitoids (Hutchison, 1994, 2014; Searle, 2012; Metcalfe, 2000; Subandrio, 2012).

Gravitational collapse during Late Paleozoic to Triassic of the inactive slab resulted in the production of large amounts of granitoids and basaltic dyke swarm (Kadir et al., 1997; Subandrio et al., 1997; Subandrio, 2012). The formation of A-type granitoids at Sibolga and its surroundings within plate setting was a consequence of the regional extensional stress during that time. Sibolga and its surrounding areas were part of West Sumatra Block (WSB) (Hutchison, 1994, 2014; Searle et al., 2012; Metcalfe, 2000; Subandrio, 2012) which were moved to recent positions at the west of Sibumasu by tectonic translation of strike-slip mechanism (Metcalfe, 2000) along the Medial Sumatra Tectonic Zone (MSTZ) from Early Permian to Early Triassic. A dip slip component resulted by the movement associated with the translation mechanism caused a block stretching (Mc Caffrey, 2009) and possibly created spaces occupied by the granitoids (Gill, 2010). Subandrio (2012) proposed a change of tectonic setting from subduction during

Permian to continental rifting in Triassic. The formation of I-type granitoids in volcanic arc setting is supposed to have been followed by A-type granitoids formed within plate setting. However, two metaluminous alkali feldspar granites show ferroan characters, on the other side quartz syenite from Tanjung Jae and quartz alkali feldspar syenite from Pintu Padang Julu are peraluminous and magnesian characters. Those granitoids were formed in volcanic arc environment (Chapter 6).

Plots of SiO_2 versus (FeO_{tot}/[FeO_{tot}+MgO]) and SiO_2 versus (Na_2O+K_2O-CaO) and Aluminium Saturation Index (ASI) versus molecular ratio (Al/[Na+K]) discrimination diagrams show that most of the granitoids from Muara Sipongi and Kotanopan were fall in within magnesian, calcic-alkali and metaluminous affinity based on the classification diagram of Frost et al. (2001) (Fig. 9.14), which were formed in volcanic arc environment (Chapter 6).

Plots of SiO_2 versus (FeO_{tot}/[FeO_{tot}+MgO]), and SiO_2 versus (Na_2O+K_2O-CaO) and Aluminium Saturation Index (ASI) versus molecular ratio (Al/[Na+K]) discrimination diagrams show that most of the granitoids from Panyabungan fall within ferroan and peraluminous-type granites based on the classification diagram of Frost et al. (2001) (Chapter 6). According to Kanao et al. (1971), Hehuwat & Sopaheluwakan (1978) and Aspden et al. (1984), Muara Sipongi and Kotanopan granitoids were probably formed during the Late Triassic to Early Jurassic, ranging from 197 to 186 Ma and from 182 to 142 Ma. During that time, Meso-Tethys oceanic floor was subducted beneath amalgamated West Sumatra Block and Sibumasu continent (Barber et al., 2005). Igneous activities involved the intrusions of granitoids in Muara Sipongi, and Kotanopan lasted from Jurassic through Cretaceous to Neogene.

9.3.2 Petrogenetic models

The SiO_2 contents of Sibolga granites are high ranging from 66 to 75 wt%, indicating that these parental magmas experienced extensive magmatic differentiation (Whalen et al., 1987). The SiO_2 contents of granitic rocks at Panyabungan range from 66 to 75 wt%, and they have lower Na_2O+K_2O contents and FeO total/MgO ratios. TiO_2, Al_2O_3, FeO total, MnO, CaO and P_2O_5 contents decrease as SiO_2 contents increase.

The magmas of syenogranites at Sarudik, and quartz-alkali feldspar syenites at Tukka and Sihobuk were probably derived from different sources. Magmas of quartz syenite and alkali feldspar syenite magma at Tanjung Jae and quartz alkali feldspar syenite at Pintu Padang Julu magma were also probably derived from different sources.

Syenogranite from Sarudik has strong negative Ba, Sr, HREE and Eu anomalies, which suggests fractionation of K-feldspar and plagioclase either in magma chambers or during magma ascent (Wilson, 1989). These evidences also support negative correlations between CaO, Al_2O_3, and SiO_2. Decreases of TiO_2 and P_2O_5 with increasing SiO_2 content would be attributed to fractionation of titanite and apatite, respectively. The fractionation of accessory phases such as zircon, allanite, and titanite can account for depletion in zirconium and yttrium (SR1) (e.g. Romick et al., 1992; Hoskin et al., 2000).

The present $^{87}Sr/^{86}Sr$ (1.222823) of syenogranite at Sarudik is very high and distinctly different with other granitoids from Sibolga and Panyabungan. These suggest that magma source might be modified with crustal materials. Petrography suggests the contamination of primary magma with metasedimentary rocks.

Relationships among $^{87}Sr/^{86}Sr$ and P_2O_5 with ΣREE contents for granitoids from Sibolga and that from Panyabungan suggest magma source from lower crust contain more REE

compared to upper crust. Modification with surrounding upper crust material such as metasedimentary rocks possibly reduces the REE content.

Initial Sr isotopic ratio of Sibolga granitoids ranges from 0.710700 to 0.724100, those from Panyabungan ranges from 0.709382 to 0.712104, those initial isotopic ratios are lower than those granitoids from Klabat Suites and Bebulu from Bangka Island have range from 0.7163 to 0.7270 and 0.7123 to 0.7171, respectively. The $^{87}Sr/^{86}Sr$ of quartz alkali feldspar syenite from Pintu Padang Julu (P7) (0.710812), and Tukka (S8) (0.710700) suggest that those granitoids from the two areas most probably belong to the Main Range, assumed by initial ratio of the Main Range, which ranges from 0.711 to 0.710 (Hutchison, 1978). Age of emplacement was referred to 202 Ma (Wikarno, 1993) for Pintu Padang Julu-Panyabungan and 264 for granitoids from Tukka-Sibolga (Aspden et al., 1982). Hutchison (1994) suggested the age of the Main Range by Rb/Sr range from Late Late Triassic to Carbonaceous

Whole-rock Nd initial isotopic value ($^{\varepsilon i}Nd$) of Sibolga and Panyabungan granitoids are negative, and initial Sr (Sr_i) are high.

The Sr_i of syenogranite from Sarudik is high (0.724128), which suggests that the syenogranite magma has resulted from partial melting of granitic crusts and was probably contaminated with metasedimentary rocks in the upper crust. Thus, the Sr_i of syenogranite from Sarudik is similar with the Sr_i of granitoids from Belinyu, and Penangas of the Klabat Suite, Bangka region ranging from 0.7270 to 07163 (Cobbing, 1992; Aspden et al., 1982), suggesting a genetic relationship between the granitic rocks from Sarudik and Klabat Suite of Bangka region. Sr_i of quartz syenites from Adian Koting (SB3 and SB21) (0.710769 and 0.710729) are similar with those of granitoids from Langkawi, West Malaysia (0.7107) (Kwan et al., 1992) and Malacca of Peninsular Malaysia (0.711) (Hutchison, 1977), suggesting that they have similar

source and formed by partial melting of upper crust. Sr_i of the granitoids from Tanjung Jae and Pintu Padang Julu (Panyabungan) ranging from 0.710736 to 0.719129 suggest that they have likely resulted from partial melting of a various of sources crustal materials rocks. Sr_i of quartz alkali feldspar syenite from Sihobuk is high (0.714956) (Fig. 9.8).

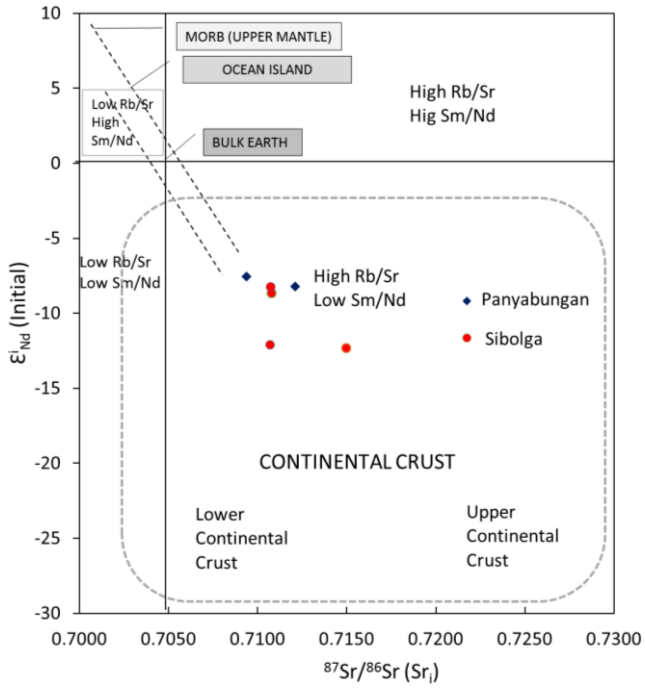

Fig. 9.8 $^{\varepsilon i}$Nd initial values vs Sr_i isotopic ratios of granitoids from Sibolga and Panyabungan (modified after DePaolo & Wasserburg, 1979).

Quartz alkali feldspar syenites from Tukka and Sihobuk, and quartz syenites from Adian Koting are probably contaminated with the alumina-rich rocks. Sr_i of quartz alkali feldspar syenite from Sihobuk is relatively close to that of Hatapang granite at the northeast of Sibolga (0.7151) (Clarke & Beddoe-Stephens, 1987). These suggest a genetic relationship between quartz syenite from Tanjung Jae and Hatapang granites, which were derived from the upper crust (Fig. 9.16).

9.4 REE geochemistry of weathered crusts of granitoids at Sibolga and its surrounding areas

Fifteen samples of weathered granitoids and four samples of parent granitoids were collected from four weathered profiles of 5 to 12 m height at Sibuluhan Sihaporas A and Sibuluhan Sihaporas B, Sarudik and Sibolga Julu. The weathered profiles consist of horizon A, horizon B, horizon C and bedrocks. Parent rocks of the granitic rocks around Sibolga are differentiated ilmenite-series and I-/A-type granite which are composed mainly of K-feldspar, quartz, plagioclase, and biotite. Zircon, allanite, apatite, titanite, monazite and xenotime are accessory minerals. The total REE (ΣREE) content of the weathered crust of granitoids from Sibuluhan Sihaporas A ranges from 265 to 479 ppm, ΣREE extracted by sequential extraction ranges from 151 to 263 ppm, and percentage of extracted REE ranges from 55 to 74%, while those of Sibuluhan Sihaporas B range from 302 to 634 ppm, 82 to 198 ppm, and 28 to 44% respectively. ΣREE content of weathered granitoids crusts from Sarudik ranges from 135 to 219 ppm, ΣREE extracted by sequential extraction ranges from 21 to 82 ppm, and percentage of extracted REE ranges from 11 to 50 %, while those of Sibolga Julu range from 191 to 304 ppm, 111 to 138 ppm, and 27 to 44%, respectively.

The ΣREE content of weathered crusts of granitoids from Sibuluhan Sihaporas B is higher than that of weathered crusts of granitoids from Sibuluhan Sihaporas A, but the ΣREE extracted from weathered crusts of granitoids from Sibuluhan Sihaporas B is lower than that of weathered crusts of granitoids from Sibuluhan Sihaporas A. Halloysite and gibbsite are present in the horizon B of both the weathered crusts, and they contain monazite, allanite, and apatite. Titanite and allanite occur in the weathered crusts of granitoids from Sibuluhan Sihaporas A. Chondrite-

normalized REE patterns of bedrock and extracted fraction of weathered crusts of granitoids from Sibuluhan Sihaporas A show negative Ce anomaly. ΣREE content of weathered rocks and extracted fraction from Sarudik is the lowest.

The degree of chemical weathering of granitic rocks is represented by the Chemical Index of Alteration (CIA) proposed by Nesbitt & Young (1982). The CIA values are mostly over 90% in the upper part of the profile at Sibuluhan Sihaporas A, Sarudik and Sibolga Julu, and less than 90% in the lower part except for Sibuluhan Sihapoas A and Sibuluhan Sihaporas B. The weathered sample from Sibuluhan Sihaporas B has low CIA at both upper part and lower part (Fig. 9.9). CIA of weathered crusts of granitoids from Sibuluhan Sihaporas A, Sibuluhan Sihaporas B, Sarudik, and Sibolga Julu range from 72 to 95%, 70 to 74%, 93 to 99%, and 92 to 96%, respectively, suggesting the occurrence of clay minerals. The weathered granitoids from Sibolga Julu with whitish in color show the highest CIA among the various sample from Sibuluhan Sihaporas A, Sibuluhan Sihaporas B, and Sarudik suggest the occurrence clay minerals.

Ce was predominantly accumulated in the upper part of profile due to oxidation of Ce^{3+} to Ce^{4+}, while most of the REE^{3+} moved to the lower part by acidic soil water and they were adsorbed onto clay minerals. Therefore, most of the REE was present as ion exchangeable state. In the Sibuluhan Sihaporas A, allanite was decomposed while in the Sibuluhan Sihaporas B monazite was refractory to retain REE.

The P_2O_5 contents of the weathered crust of granitoids from Sibuluhan Sihaporas A and Sibuluhan Sihaporas B tend to be higher than the parent rocks, suggesting the occurrence of secondary phospate in the weathered crusts. ΣREE content in the weathered crusts in Sibolga are lower than those of their parent rocks suggesting that REEs were leached out during weathering.

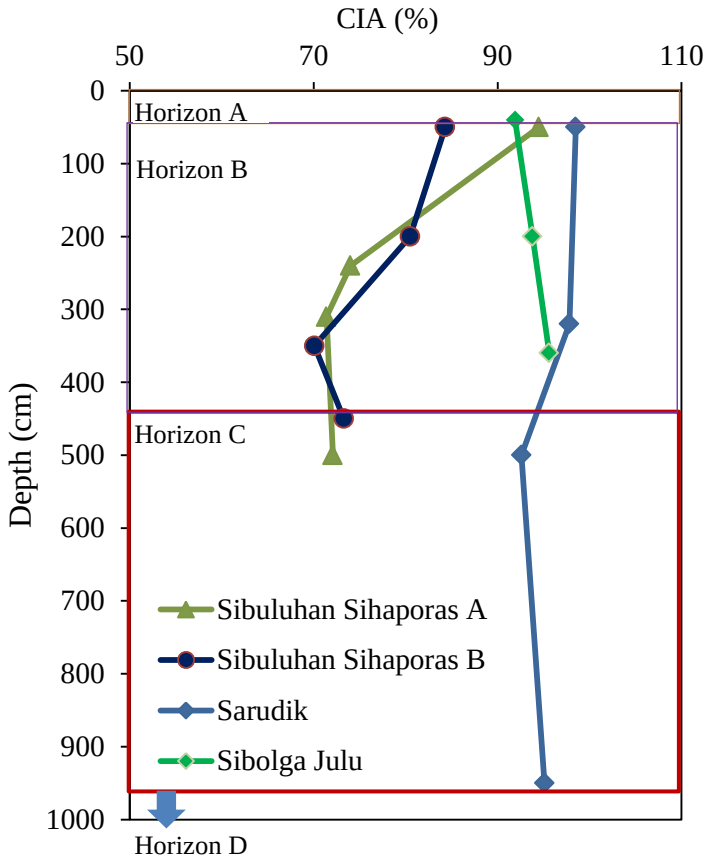

Fig. 9.9 Chemical index of alteration(CIA) of weathered granitoids from Sibuluhan Sihaporas A, Sibuluhan Sihaporas B, Sarudik and Sibolga Julu.

CHAPTER 10

CONCLUSIONS

Granitoids in Sibolga, Panyabungan, Muara Sipongi and Kotanopan are I-/A-types, S-type, and I-types granitoids, respectively. The Sibolga Granitoids are calk-alkaline, ilmenite-series, and mainly peraluminous. Cordierite and corundum occur as xenocrysts and inclusions in K-feldspar in syenogranite from Sarudik at Sibolga. Ganitoids in Panyabungan is calk-alkaline to alkali calcic, ilmenite- and magnetite-series, metaluminous to peraluminous. Coexistence of metaluminous, I-type and magnetite-series quartz alkali feldspar syenites and peraluminous, S-type and ilmenite-series granites at Tano Tombangan suggests that those granitoids were derived from different sources. LREE are enriched in alkali feldspar syenite from Pintu Padang Julu and quartz alkali feldspar syenite from Tanjung Jae. ΣREE contents are high in the S-type and ilmenite-series granitoids than the magnetite-series granitoids, which contain allanite and apatite. Granitoids in Kotanopan are calk-alkaline, magnetite- and ilmenite-series, slightly peraluminous to peraluminous, and I-type.

The present Sr isotopic ratios, $^{87}Sr/^{86}Sr$ (p), of granitoids from Tanjung Jae ranges from 0.720814 to 0.718746, those from Pintu Padang Julu ranges from 0.711523 to 0.711536, and that from Tano Tombangan ranges from 0.715757. The $^{87}Sr/^{86}Sr$ (p) of granitoids from Sarudik, 1.223221 to 1.222425, are the highest among all the samples even with those from Panyabungan. Those from Adian Koting ranges from0.717345 to 0.717691, and those from Sibolga Julu ranges from 0.744167 to 0.720253. The $^{87}Sr/^{86}Sr$ (p) of granitoids from Sarudik is the highest, calculated value average is 1.222823.

The ε^{143}Nd value is estimated approximately -8.2 and -7.5 assuming an age of 202 Ma for granitoids from Tanjung Jae and Pintu Padang Julu, respectively. The ε^{143}Nd value is estimated approximately -8.7 and -8.2 assuming an age of 219 Ma for the granitoids from Adian Koting, that of -12.1 and -12.3 assuming an age of 264 Ma for granitoids from Tukka and Sihobuk (Sibolga), respectively.

10.1 Petrochemistry of granitoids in Sibolga and its surrounding areas, North Sumatra, Indonesia

SiO_2, Th, Nb, Ta, HREE, and Na_2O+ K_2O contents of the syenogranites, A-type granite at Sarudik are high, while Eu, CaO, Ba and Sr contents of the syenogranites at Sarudik are low compared to those of quartz alkali feldspar syenites from Tukka and Sihobuk. Quartz syenites from Adian Koting are I-type and were formed within plate setting (WPG). Quartz alkali feldspar syenite from Pintu Padang Julu, and quartz syenite and alkali feldspar syenite from Tanjung Jae are S-type and were formed in the volcanic arc setting (VAG). Sibolga granitoids are highly fractionated I-type and A-type granitoids.

The A-type granitoids of Sibolga are highly differentiated and their ΣREE contents are high, while that of granitoids from Muara Sipongi and Kotanopan, are metaluminous, I-type, and magnetite-series, and they have low ΣREE content.

Negative correlations between Al_2O_3, CaO, P_2O_5, MgO, FeO_{tot}, MnO, TiO_2 and SiO_2 contents suggest that the granitic magmas likely underwent fractional crystallization during magmatic differentiation. The decrease in P_2O_5, MgO and FeO_{tot} indicates removal of apatite and mafic minerals (such as biotite and hornblende) during differentiation.

SiO_2 and REE contents at Sibolga and Panyabungan are positively correlated while P_2O_5 and REE are negatively correlated. Allanite and titanite are possibly the sources of REE of granitoids

from Sibolga and Panyabungan, and there is no significant ΣREE concentration in the granitoids at Muara Sipongi and Kotanopan where titanite and allanite were absent.

Cordierite and corundum occur as xenocrysts and inclusions in K-feldspar which coexist with biotite and hornblende in the quartz syenite at Adian Koting. Corundum is associated with zircon, apatite, titanite in the syenogranite from Sarudik. The coexistence of these minerals suggests assimilation by aluminous rock, i.e. metasedimentary or pelitic basement rocks beneath Sibolga. The ΣREE contents of granitoids associated with corundum and cordierite are low due to removal of apatite during magmatic differentiation suggested by a decrease of P_2O_5.

ΣREE contents of granitoids from four out of six locations in Sibolga and its surrounding areas are high. A-type ilmenite-series, peraluminous granitoids at Sibolga were formed in within plate setting, S- and I-type, ilmenite- and magnetite-series, peraluminous to metaluminous granitoids at Panyabungan were formed in volcanic arc setting, while I-type, magnetite-series and metaluminous granitoids at Muara Sipongi and Kotanopan were formed in a volcanic arc setting. REE enrichment occurred in A-type and or S-type granitoids which have ilmenite-series and peraluminous characters. The granitoids contaminated with metasedimentary rocks and formed in volcanic arc setting have low ΣREE content. The alkali feldspar syenite and quartz alkali feldspar syenite at Tukka were formed in volcanic arc setting, while the rest of the granitoids at Sarudik, Sibuluhan Sihaporas and Adian Koting were formed within plate setting. The former formed metaluminous, I-type granitoids and the latter produced peraluminous, A-type and ilmenite-series granitoids. The ΣREE contents of the granitoids that formed in the volcanic arc setting are low.

The Sr_i of syenogranite from Sarudik is high (0.724128), which suggests that the syenogranite magma was resulted from partial melting of granitic crusts and was probably

contaminated with metasedimentary rocks in the upper crust. Sr_i of granitoids from Panyabungan and Sibolga are lower than that of granitoids from Bebulu and Klabat suite from Bangka Island. However $^{87}Sr/^{86}Sr$ of quartz alkali feldspar syenite from Pintu Padang Julu (P7) (0.710812), and Tukka (S8) (0.710700) suggest that those granitoids most probably belong to the Main Range Belt. Age of emplacement was referred to 202 Ma for granitoids from Pintu Padang Julu-Panyabungan and 264 Ma for granitoids from Tukka-Sibolga. Hutchison (1994) suggested that the age of granitoids from the Main Range by Rb/Sr range from Late Triassic to Late Cretaceous.

10.2 Tectonic evolution and petrogenetic model

The evidence of coexistence magnetite-series with ilmenite-series and overlapping tectonic environment between volcanic arc and within plate settings indicate a change in tectonic setting occurred in the study area. The change was presumably related to the Early Permian subduction of Paleo-Tethys beneath amalgamated Western Sumatra Block, East Malaya and Indochina which formed metaluminous, I-type and magnetite-series granitoids and translation tectonics which resulted in an extensional condition and produced peraluminous, A-type and ilmenite-series granitoids in Sibuluhan Sihaporas, Sibolga Julu, Sarudik and Tarutung. At Panyabungan, the granitoids were associated with deformation which recorded as foliation, and brecciation. At the Muara Sipongi and Kotanopan, the granitoids are apparently formed due to subduction, which were possibly related with the Early Triassic to Early Jurrasic subduction of Meso- Tethys beneath the Southeastern margin of amalgamated Western Sumatra Block with Sibumasu.

10.3 REE geochemistry of weathered crusts of granitoids at Sibolga and its surrounding areas

Highly differentiated ilmenite-series I-/A-type granitoids are the parent rock of the weathered crusts in Sibolga. Titanite and allanite occur in syenogranite at Sibuluhan Sihaporas A. Chondrite-normalized REE patterns of bedrock and weathered granitoids from Sibuluhan Sihaporas A show negative Ce anomaly. ΣREE content of leachate from Sarudik is the lowest. Chemical Index of Alteration (CIA) of weathered crusts of granitoids from Sibuluhan Sihaporas A, Sibuluhan Sihaporas B, Sarudik, and Sibolga Julu range from 72 to 95%, 70 to 74%, 93 to 99%, and 92 to 96%, respectively, suggesting the occurrence of halloysite group minerals and gibbsite.

Ce was predominantly accumulated in the upper part of profile due to oxidation of Ce^{3+} to Ce^{4+}, while most of the REE^{3+} moved to the lower part by acidic soil water and they were adsorbed mainly onto halloysite group minerals and gibbsite. Most of the REE was present as ion exchangeable form. At Sibuluhan Sihaporas A, allanite was decomposed while at Sibuluhan Sihaporas B monazite was refractory to retain REE. The P_2O_5 contents of the weathered crust of granitoids from Sibuluhan Sihaporas A and Sibuluhan Sihaporas B tend to be higher than the parent rocks, suggesting the occurrence of secondary phospate in the weathered crusts. ΣREE contents in the weathered crusts in Sibolga are lower than those of their parent rocks suggesting that REEs were leached out during weathering.

The values of elemental change $(\tau_j)_{(Si, Ca, Na, K)}$ of weathered crusts of Sibuluhan Sihaporas B, Sarudik and Sibolga Julu are -1 suggest losses or removal of these elements. On the other hand, $(\tau_j)_{(Al, Fe, Mn, Ca, Na, K, P)}$ in the Sibuluhan Sihaporas A are +1 suggest addition of these elements. The $\tau_{j(REE)}$ for all weathered crusts of granitoids are -1 suggest losses or removal of these elements.

REFERENCES

Amiruddin (2011) Tectonic rifting of Upper Paleozoic – Mesozoic Intra-Cratonic Basins in the southeastern Gondwanaland and its economic aspects: with refference to the geology of north Sumatra and West Australia, Geodynamics, Jurnal Sumberdaya Geologi, Badan Geologi, Indonesia, 21, 249-255.

Aspden, J.A., Kartawa, W., Aldiss, D.T., Djunuddin, A., Whandoyo R., Diatma, D., Clarke, M.C.G. and Harahap, H. (1982) Geologic Map of the Padang Sidempuan and Sibolga Quadrangles, Sumatra: Explanatory Notes Geological Research and Development Centre, Bandung, Indonesia.

Aydin A., Ferré E.C., and Aslan Z (2007) The magnetic susceptibility of granitic rocks as a proxy for geochemical composition: Example from the Saruhan granitoids, NE Turkey. Tectonophysics, 441, 85-95.

Barber, A. J. and Crow, M. J. (2005a) Structure and structural history. In: Barber, A.J., Crow, M.J. and Milsom, J.S. (eds.), Sumatra- Geology, Resources and Tectonic Evolution. Geol. Soc. London, Mem., 31, 175-233.

Barber, A. J. and Crow, M. J. (2005b) Pre-Tertiary stratigraphy. In: Barber, A.J., Crow, M.J. and Milsom, J.S. (eds.), Sumatra- Geology, Resources and Tectonic Evolution. Geol. Soc. London, Mem., 31, 24-53.

Bea, F. (1996) Residence of REE, Y, Th and U in granites and crustal protoliths: implication for the chemistry of crustal melts. J. Petrol. 37, 521–552.

Beckinsale, R. D. (1979) Granite magmatism in The Tin Belt of Southeast Asia, In: Atherton, M.P. & Tarney, J., (eds) Origin of the granites batholiths, geochemical evidence, Birkhäuser Boston, 34-44.

Cameron, N. R., Clarke, M. C. G., Aldiss, D. T., Asdpen, J. A. and Djunuddin, A. (1980) The geological evolution of northern Sumatra, Proc. 9th Ann. Conv. IPA., Jakarta, 149-187.

Castor, S. B. and Hedrick, J. B. (2006) Rare earth elements. In Kogel, J. E., Trivedi, N. C., Barker, J. M. and Krukowski, S. T. (eds.) Industrial Minerals & Rocks: Commodities, Markets, and Uses. Society for Mining, Metallurgy, and Exploration (U.S.), 769-792.

Chappel, B.W. and White, A. J. R. (2001) Two contrasting granite types: 25 years later. Australian Journal of Earth Sciences, 48, 489-499.

Chappel, B.W. and White, A.J.R. (1992) I- and S-type granites in the Lachlan Fold Belt. Transactions of the Royal Society of Edinburgh, Earth Sciences, 83, 1–26.

Chappel, B.W. and White, A. J. R. (1974) Two contrasting granite types, Pacific Geol., 8, 173-174.

Charusiri, P., Pungrassami, T. and Sinclair, G. (2006) Classification of rare-earth element (REE) deposits in Thailand: A genetic model. J. Geol. Soc. Thai., 1, 57–66.

Charusiri, P., Clark, A. H., Farrar, E., Archibald, D. and Charusiri, B. (1993) Granite belts in Thailand: Evidences from the $^{40}Ar/^{39}Ar$ geochronological and geological syntheses. J. Southeast Asian Earth Sci., 8, 127–136.

Clarke, M. C. G. and Beddoe-Stephens B. (1987) Geochemistry, Mineralogy and Plate Tectonic Setting of a Late Cretaceous Sn-W Granite from Sumatra, Indonesia. Mineralogical Magazine, 51, 371-387.

Cobbing, E. J. (2005) Granites. In : Barber, A. J., Crow, M. J. and Milsom, J. S., (eds.), Sumatra-Geology, Resources and Tectonic Evolution. Geol. Soc. London, Mem., 31, 54-62.

Cobbing, E. J., Pitfield, P. E. J., Darbyshire, D. P. F. and Mallick, D. I. J. (1992) The Granites of the Southeast Asian Tin Belt. British Geological Survey Overseas Memoir, 10, 369p.

Cobbing, E. J., Mallick, D. I. J., Pitfield, P. E. J. and Teoh, L. H. (1986) The granites of the SE Asian Tin Belt. J. Geol. Soc. London, 143, 537–550.

Collins, W. J., Beams, S. D., White, A. J. R. and Chappell, B. W. (1982) Nature and origin of A-type granites with particular reference to southeastern Australia. Contributions to Mineralogy and Petrology, 80**,** 189–200.

Cox, K. G., Bell, J. D. and Pankhurst, R. J. (1979). The Interpretation of Igneous Rocks. Boston, George Allen and Unwin, London.

Creaser, R.A. and White, A.J.R. (1991) Yardea Dacite—Large-volume, high-temperature felsic volcanism from the Middle Proterozoic of South Australia. Geology, 19, 48-51.

Creaser, R. A., Price, R. C. and Wormald, R. J. (1991) A-type granites revisited: assessment of a residual-source model. Geology, 19, 163–166.

De Paolo, D.J., and Johnson, R.W. (1979) Magma genesis in the New Britain island arc: constraints from Nd and Sr isotopes and trace element patterns. Contrib. Mineral. Petrol, 70, 367-379.

DePaolo, D.J. and Wasserburg, G.J. (1979) Petrogenetic mixing models and Nd-Sr isotopic patterns. Geochimica et Cosmochimica Acta, 43, 615-627.

Dickson, J. S. (2015) Rare earth elements: Global market overview. In: Simandl, G. J. and Neetz, M., (eds.), Symposium on Strategic and Critical Materials Proceedings, November 13-14, 2015, Victoria, British Columbia. British Columbia Ministry of Energy and Mines, British Columbia Geological Survey Paper, 5-11.

Faure, G. (1986) Principles of Isotope Geology, 2nd edition Wiley, New York, 466 pp.

Fitch, T. J. (1972) Plate convergence, transcurrent faults and internal deformation adjacent to Southeast Asia and the western Pacific. J. Geophys. Res. 77, 4432–4460.

Fontaine, H. and Gafoer, S. (1989) The Pre-Tertiary Fossils of Sumatra and their Environments. CCOP Technical Papers, United Nations, Bangkok, 19, 31-40.

Frost, B.R., Barnes, C.G., Collins, W.J., Arculus, R.J., Ellis, D.J., and Frost, C.D. (2001) A geochemical classification of granitic rocks, Journal of Petrology, 42, 2033-2048.

Gardiner, N.J., Searle M.P., Morley C.K., Whitehouse M.P., Spenser C.J., and Robb L.J. (2015) The closure of Palaeo-Tethys in Eastern Myanmar and Northern Thailand: New insights from zircon U–Pb and Hf isotope data, Gondwana Research, http://dx.doi.org/10.1016/j.gr.2015.03.001.

Ghani A A, Searle M, Robb L and Chung S-L (2013) Transitional I-S type characteristics in the Main Range Granite, peninsular Malaysia; J. Asian Earth Sci. 76, 225–240.

Gill, R. (2010) Igneous rocks and processes: A practical guide. Wiley-Blackwell, Chichester, UK, 440 p.

Hamilton, W. (1979) Tectonic of Indonesian regions, United States Geological Survey Profesional Paper, 1078p.

Harjanto, S., Virdhian S., and Afrilinda (2013) Characterization of Indonesia rare earth minerals and their potential processing techniques. Proceedings of The ^{52}nd Conference of Metallurgists (Com), Hosting by Materials Science Technology Conference (Ms&T), October 27 to 31, 2013, Montréal, Québec, Canada.

Hehuwat, F. and Sopaheluwakan, J. (1978) Geologic Map of Central Sumatra, 1: 250.000. Unpublished compilation by National Institute of Geology and Mining (LIPI), Bandung.

Hehuwat, F. (1976) Isotopic age determinations in Indonesia, the state of art. Proc. Seminar on Isotopic Dating, CCOP, Bangkok, 3, 135-155.

Hillier, S. and Ryan, P.C. (2002) Identification of halloysite (7 Å) by ethylene glycol salvation 'MacEvans effect'Clays Clay Miner., 7, pp. 487-496

Hoskin, P.W.O., Kinny, P.D., Wyborn, D., and Chappell, B.W. (2000) Identifying accessory mineral saturation during differentiation in granitoid magmas: An integrated approach. Journal of Petrology, 41, 1365–1395.

Hotson, M.D., Khin Zaw, Oliver, G.H.J., Meffre, S., Manaka, T. (2011) U–Pb zircon geochronology of granitoids from Singapore: Implications for tectonic setting. Abstracts for 8th meeting. Asia Oceania Geological Society, Taipei, Taiwan.

Humphris, S.E. and Thompson, G. (1978): Hydrothermal alteration of oceanic basalt by seawater, Geochim Cosmochim Acta, 42, pp. 107-125.

Hutchison, C. S. (2014) Tectonic evolution of Southeast Asia. Bulletin of the Geological Society of Malaysia, 60, 1 – 18.

Hutchison, C.S. (2007) Geological Evolution of South-East Asia, 2nd ed. Kuala Lumpur, Geological Society of Malaysia, Oxford University Press, 433 p.

Hutchison, C. S. (1996) South-East Asian oil, gas, coal and mineral deposits. Oxford Monographs on Geology and Geophysics, 36, Oxford University Press, Oxford, 265p.

Hutchison, C.S. (1994) Gondwanaland and Cathaysian blocks, Palaeotethys sutures and Cenozoic tectonics in South-East Asia. Geologisches Rundschau, 82, 388–405.

Hutchison, C. S. (1988) The tin metallogenic provinces of S.E. Asia and China: A Gondwanaland inheritance. Hutchison, C. S. (eds.), Geology of Tin Deposits in Asia and the Pacific. Springer Verlag, Heidelberg, 225-234.

Hutchison, C. S. and Taylor, D. (1978) Metallogenesis in SE Asia. Journal of Geological Society, London, 135, 407–428.

Hutchison, C.S. (1977) Granite emplacement and tectonic subdivision of Peninsular Malaysia. Geological Society of Malaysia, 9, 187-207.

Imai, A., Yonezu, K., Sanematsu, K., Ikuno, T., Ishida, S., Watanabe, K., Pisutha-Arnond, V., Nakapadungrat, S. and Boosayasak, J. (2013) Rare earth elements in hydrothermally altered granitic rocks in the Ranong and Takua Pa tin-field, southern Thailand. Resour. Geol., 63, 84–98.

Ishihara, S. (1998) Granitoid series and mineralization in the Circum-Pacific Phanerozoic granitic belts. Resour. Geol., 48, 219–224.

Ishihara, S. (1981) The granitoid series and mineralization. Econ. Geol. 75th Ann., 458-484.

Ishihara, S. (1977) The magnetite-series and ilmenite-series granitic rocks. Mining Geology, 27, 293-305.

Japan International Cooperation Agency (JICA) and Metal Mining Agency of Japan (MMAJ), (1985) Report on the cooperative mineral exploration of Northern Sumatra: consolidated report.

Kadir, W. G. A., Zen, M.T., Hendraja, L., Santoso, D. and Sukmono, S. (1997) Anomali gayaberat negatif sekitar daerah Sumatra Utara dan model penipisan keraknya. Prosiding Himpunan Ahli Geofisika Indonesia, Pertemuan Ilmiah Tahunan ke-22, Bandung, 16-17 Oktober 1997. (in Indonesian).

Kanao, N.E.A. (1971) Summary Report on the Survey of Sumatra, Block 5, Japanese Overseas Mineral Development Company Limited. Unpublished manuscript.

Koesoemadinata, R. P. and Sastrawiharjo, S. (1987) Uranium prospects in Tertiary sediments in The Sibolga Area, North Sumatra, In: Metallogenesis of Uranium Deposits. Proc. Tech. Meet. 543, Vienna, IAEA, 121-140.

Kwan, T. S., Kraehenbuehl, R., and Jaeger, E. (1992) Rb-Sr, K-Ar and fission track ages for granites from Penang Island, West Malaysia: an interpretation model for Rb-Sr whole-rock and for actual and experimental mica data. Contributions to Mineralogy and Petrology, 4, 527-542.

Le Bas, M. J. and Streckeisen, A. L. (1991) The IUGS systematic igneous rocks. Journal of Geological Society, London, 148, 825-833.

Liu, C. and Evett, J. B (1984) Soil properties: testing, measurement and evaluation. Prentice Hall, Inc, Englewood Cliffs, New Jersey, USA, 315 p.

Loiselle M.C., and Wones D.R. (1979) Characteristics and origin of anorogenic granites. Geological Society of America Abstract Program, 11, 468.

Long, K. R., Van Gosen, B. S., Foley, N. K. and Cordier, D. (2010) The principal rare earth elements deposits of the United States—A summary of domestic deposits and a global perspective. U.S. Geological Survey Scientific Investigations Report 2010–5220, 96p. http://pubs.usgs.gov/sir/2010/5220/.

McCaffrey, R. (2009) The Tectonic Framework of the Sumatra Subduction Zone. An. Rev. Earth Planet. Sci., 37, 345-66.

McDonough, W. F. and Sun, S. (1995) Composition of chondrite, the composition of the Earth. Chem. Geol., 120, 223–253.

Metcalfe, I. (2000) The Bentong–Raub Suture Zone. J. Asian Earth Sci. 18, 691–712.

Mitchell, A.H.G. (1977) Tectonic settings for emplacement of Southeast Asian tin granites. Geological Society of Malaysia Bulletin, 9, 123–140.

Moore, D.M. and Reynolds, R.C., Jr. (1997) X-ray Diffraction and the Identification and Analysis of Clay Minerals. Oxford University Press, Oxford, 378 pp

Nasdala, L., Wenzel, M., Vavra, G., Irmer, G., Wenzel, T. and Kober, B. (2001) Metamictisation of natural zircon: accumulation versus thermal annealing of radioactivity-induced damage. Contributions to Mineralogy and Petrology, 141, 125–144.

Ng, S.W.-P., Chung, S.-L., Robb, L.J., Searle, M.P., Ghani, A.A., Whitehouse, M.J., Oliver, G.J.H., Sone, M., Gardiner, N.J., and Roselee, M.H. (2015) Petrogenesis of Malaysian granitoids in the Southeast Asian tin belt: Part 1. Geochemical and Sr-Nd isotopic characteristics. Geological Society of America Bulletin, 127, 1209-1237.

Ngadenin (2013) Geologi dan potensi terbentuknya mineralisasi uranium tipe batupasir di daerah Hatapang, Sumatera Utara. Eksplorium, 34, 1–10. (in Indonesian)

Ni, Y., Hughes, J. M. and Mariano, A. N. (1995) Crystal chemistry of the monazite and xenotime structures. American Mineralogist 80, 21-26.

Nishimura, S. and Suparka, S. (1997) Tectonic approach to the Neogene evolution of Pacific-Indian Ocean Seaways, Tectonophysics, 281, 1-16

Orris, Greta J., and Grauch, Richard I. (2002) Rare Earth Element Mines, Deposits, and Occurrences: U.S. Geological Survey Open-File Report 02-189, U.S. Geological Survey, Tucson, AZ.

Pearce, J.A., Harris, N.B.W. and Tindle, A.G. (1984) Trace elements discrimination diagrams for the tectonic interpretation of granitic rocks. Journal of Petrology, 25, 956-983.

Pecht, M. G., Kaczmarek, R. E., Song, X., Hazelwood, D. A., Kavetsky, R. A., and Anand, D. K. (2012) Rare Earth Materials: Insights and Concerns. Energetic Science and Technology Series, University of Maryland, CALCE ESPC Press, 125p.

Pulunggono, A. and Gumilar, B. (2000) Sumatra. In: Darman H. and Sidi, F.H. (eds.), An Outline of the Geology of Indonesia. Indonesian Association of Geologists, 11-36.

Pulunggono, A. and Cameron N. R. (1984) Sumatran microplates, their characteristics and their role in the evolution of the Central and South Sumatra Basin, Proceedings Indonesian Petroleum Association, 13th Annual Concention.

Romick, J.D., Kay, S.M., and Kay, R.W. (1992) The influence of amphibole fractionation on the evolution of calc-alkaline andesite and dacite tephra from the central Aleutians, Alaska. Contribution to Mineralogy and Petrology, 112, 101–118.

Sainsbury, C.L. (1969) Tin Resources of the World: A Description of the Types of Tin Deposits and Main Tin-producing Areas of the World. Geological Survey Bulletin 1301, U.S. Govt. Printing Office, Washington, 53p.

Sanematsu, K., Kon, Y. and Imai, A. (2015) Influence of phosphate on mobility and adsorption of REEs during weathering of granites in Thailand, Journal of Asian Earth Sciences 111, 14-30.

Sanematsu, K., Kon, Y., Imai, A., Watanabe, K. and Watanabe, Y. (2013) Geochemical and mineralogical characteristics of ion-adsorption type REE mineralization in Phuket, Thailand. Miner. Deposita, 48, 437-451.

Schwartz, M. O., Rajah, S. S., Askury, A. K., Putthapiban, P. and Djaswadi, S. (1995) The Southeast Asian Tin Belt. Earth-Science Reviews, 38, 95-293.

Salvi, S., and Williams-Jones, A.E. (2005) Alkaline granite-syenite deposits. In: Linnen, R.L., Samson, I.M. (eds.), Rare-element geochemistry and mineral deposits. Geological Association of Canada, 315-336.

Searle, M. P., Whitehouse, M. J., Robb, L. J., Ghani, A. A., Hutchison, C. S., Sone, M., Ng, S. W.-P, Roselee, M. H., Chung, S.-L. and Oliver, G. J. H. (2012) Tectonic evolution of the Sibumasu–Indochina terrane collision zone in Thailand and Malaysia: Constraints from new U–Pb zircon chronology of SE Asian Tin granitoids. J. Geol. Soc., 169, 489-500.

Shives, R.B.K. (2015) Using gamma ray spectrometry to fi nd rare metals. In: Simandl, G.J. and Neetz, M. (eds.), Symposium on Strategic and Critical Materials Proceedings, November 13-14, 2015, Victoria, British Columbia. British Columbia Ministry of Energy and Mines, British Columbia Geological Survey Paper 2015-3, 199-209.

Streckeisen, A. (1976) To each plutonic rock its proper name. Earth Science Reviews, 12, 1–33.

Subandrio, A. S. (2012) Evolution of Magmatic Rock and Metalogenesis of Sibolga Granitoid Complex, North Sumatra, PhD Dissertation, Padjadjaran University, Unpublished, 280p. (in Indonesian)

Subandrio, A.S., Gatzweiler, R. and Friedrich, G. (2007) Relationship between magnetite-ilmenite series and porphyry copper-tin metallogenic province of Sumatra Islands – with special aspect of Sibolga and Bangka Granitoid Complex, Proceed PIT IAGI 36th, Nusadua, Bali, 334-354.

Suprapto, S. J. (2009) Tinjauan tentang unsur tanah jarang, Buletin Sumberdaya Geologi, 4, 1-11. (in Indonesian)

Suwimonprecha, P., Cerny, P. and Friedrich, G. (1995) Rare metal mineralization related to granites and pegmatites, Phuket, Thailand. Econ. Geol., 90, 603–615.

Suparka, S. and Asikin, S. (1981) Pemikiran perkembangan tektonik Pra-Tersier di Sumatra Bagian Tengah. Riset Geologi dan Pertambangan LIPI, 4, 1-13. In Indonesian

Suprapto, S. J. (2009) Tinjauan tentang unsur tanah jarang, Buletin Sumberdaya Geologi, 4, 1-11. (in Indonesian)

Suwargi, E., Pardianto, B. and Ishlah, T. (2010) Potensi logam tanah jarang di Indonesia. Buletin Sumberdaya Geologi, 5, 131-141. (in Indonesian)

Tjokrokardono, S. and Ngadenin (2004) Peluang Kedapatan Cebakan uranium di Daerah Hatapang dan Sekitarnya, Sumatera Utara. Prosiding Seminar Geologi Nuklir dan Sumberdaya Tambang, Pusat Pengembangan Bahan Galian dan Geologi Nuklir, BATAN, 31-44. (in Indonesian)

Whalen, J.B., Currie, K.L. and Chappell, B.W. (1987) A-type granites: Geochemical characteristics, discrimination and petrogenesis. Contributions to Mineralogy and Petrology, 95, 407-419.

Whalen, J. B., Currie, K.L., Chappell, B. W. (1987) A-type granites: descriptive and geochemical data. Geological Survey of Canada. Open-File, 1411, 33p.

White, A.J.R. and Chappell, B.W. (1983) Granitoid types and their distribution in the Lachlan Fold Belt, southeastern Australia. Geological Society of America Memoir 159, 21-34.

Wilson, M. (1989) Igneous Petrogenesis. Unwin Hyman, London, 466 p.

Winter, J. D. (2001) An introduction to igneous and metamorphic petrology, 343-361

Wu, C. Y. and Ishihara, S. (1994) REE geochemistry of the Southern Thailand granites. J. SE Asian Earth Sci., 10, 81-94.

Yamamoto, M., Kagami H., Narita A., Maruyama T., Kondo A., Abe S., Takeda R. (2013) Sr and Nd isotopic compositions of mafic xenoliths and volcanic rocks from the Og a Peninsula,

Northeast Japan Arc: Genetic relationship between lower crust and arc magmas, Lithos, vol 162-163: p 88-106

Yamamoto, M.and Maruyama,T. (1996) The Sr and Ndisotopic analysis and the quantitative analysis of Rb and Sr by using MAT261. Memoir Faculty of Mining, Akita University, 61,17-30 (in Japanese with English abstract).

Zaw, K.L., Setijadji, L. D., Warmada, I. W., Watanabe, K. (2011) Petrogenetic interpretation of granitoid rocks using multicationic, parameters in the Sanggau area, Kalimantan Island, Indonesia, J. SE. Asian Appl. Geol., 3, 45-53

Zulkarnain, I. (2009) Geochemical signature of mesozoic volcanic and granitic rocks in Madina regency area, North Sumatra, Indonesia, and its tectonic implication, Jurnal Geologi Indonesia, 4, 117-131

Acknowledgements

First of all I am very thankful to Allah Almighty, who gave me the courage to fulfill this target.

I would like to express my sincere gratitude to my supervisor Prof. Akira Imai and Co-supervisor Dr. Ryohei Takahashi for their invaluable guidance and support throughout this doctoral course program.

I am very thankful to my mentor Prof. Yasushi Watanabe for helpful discussions. I acknowledge Dr. Hinako Sato for the assistance in ICP-MS preparation and analysis of the sample, Dr. Takashi Hoshide for helpful discussions during the microscopic analyses, and Dr. Takeyuki Ogata for helpful assistance during SEM-EDS analysis. I also acknowledge my lab mates especially Ms. Padrones for many helpful discussions during the experiments.

I gratefully acknowledge Prof. Iskandar Zulkarnain (RIP) and Dr. Haryadi Permana, Head of Indonesian Institute of Sciences and Head of Geotechnology Research Center, who allowed me to continuing the study and support the fieldwork.

I am grateful to New Frontier Leader Program for Rare-metal and Resources, Leading Program of Akita University and members of the staff at the Akita University.

Appendix 1.

List of sample from Sibolga and its surrounding areas

No	Sample Code	Location	Coordinates		
			N	S	Rock Name
1	SR-01	Sarudik	479178	191326	Biotite granite
2	SR-02	Sarudik	479147	191470	Biotite granite
3	SB-01	Adian Koting	487686	203691	Biotite granite
4	SB-02	Adian Koting	488184	205017	Biotite granite
5	SB-03	Tarutung	491653	207528	Biotite granite
6	S.1 bedrock	Sarudik	480693	190117	Biotite granite
7	S.1A	Sibuluhan sihaporas	480693	190117	Basaltic/diabasic
8	S.2	Sibuluhan sihaporas	480757	190480	Biotite granite
9	S2.A	Sibuluhan sihaporas	480757	190480	Altered basaltic rock
10	S3	Sibuluhan sihaporas	481657	190974	Altered biotite granite
11	S4	Sibuluhan sihaporas	482103	191528	Biotite granite
12	S5	Sibuluhan sihaporas	483677	189669	Biotite granite
13	S5A	Sibuluhan sihaporas	483808	189649	Kaolinit
14	S5B	Sibuluhan sihaporas	483808	189649	Biotite granite
15	S6 Bedrock	Sibuluhan sihaporas	481549	191179	Biotite granite
16	S7	Sipan sibuluhan	481549	191179	Biotite granite
17	S8	Tukka	485643	186068	Biotite granite
18	S9	Tukka	487978	186318	Biotite granite
19	S10A	Tukka	488223	185767	Biotite granite
20	S10B	Tukka	488223	185767	Biotite granite
21	S11	Tukka	483560	179094	Andesite lava
22	S12	Tukka	482104	181957	Tuffaceous sandstone
23	S13	Tukka	480450	183784	Tuffaceous sandstone
24	S14	Sarudik	479214	191837	Biotite granite
25	S15	Sarudik	479097	191228	Biotite granite
26	S17	Sibolga Julu	477791	192185	Biotite granite
27	S17 Bedrok	Sibolga Julu	477791	192185	Biotite granite
28	S18A	Tarutung-Sibolga	477069	193717	Biotite granite
29	S18B	Tarutung-Sibolga	477069	193717	Biotite granite
30	S19	Tarutung-Sibolga	477570	194170	Biotite granite
31	S20	Tarutung-Sibolga	491801	207307	Biotite granite
32	S21	Tarutung-Sibolga	491689	207743	Biotite granite
33	S22	Parambunan	477465	192743	Biotite granite
34	S23	Parambunan	477947	191418	Biotite granite
35	S24A	Sihobuk	480634	191166	Biotite granite
36	S24B	Sihobuk	480634	191166	Biotite granite
37	S25	Sarudik	478660	190442	Biotite granite

38	S26	Sibuluhan Coastal river	479222	186912	Biotite granite
39	MS-02	Muarasipongi	602260	66732	Altered granodiorite
40	MS-03	Muarasipongi	601348	67370	Granite-pegmatite
41	MS-04	Muarasipongi	597827	67718	Granodiorite
42	MS-05	Muarasipongi	597571	66946	Granite-granodiorite
43	MS-06	Muarasipongi	594922	68476	Altered granodiorite
44	MS-07	Muarasipongi	595799	67603	Biotite granite
45	MS-08	Muarasipongi	591471	71474	Altered mikrodiorite
46	MS-09	Tanjung Alai	591471	71474	Biotite granite
47	MS-10	Tanjung Alai	596501	67634	Biotite granodiorite
48	MS-11	Muarasipongi	594528	68865	Altered granodiorite
49	MS-12	Muarasipongi	591969	70720	Biotite granite
50	MS-13	Muarasipongi	588264	71763	Biotite granite
51	M.1	muarasipongi	589755	71523	Granite Biotite
52	M.1 A	muarasipongi	589755	71523	Altered aplite granite
53	M.1	muarasipongi	589755	71523	Weathered rock
54	M.2	muarasipongi	601565	67262	Silisified andesite-basaltic lava
55	M.3	pekantan	596354	65972	Hornblende-muscovite granodiorite
56	M.4	muarasipongi	581802	71916	Granite Biotite
57	M.4A	muarasipongi	581802	71916	Altered basaltic andesite/diabasic
58	M.4B	muarasipongi	581802	71916	Basaltic/diabasic
59	M5	kotanopan	581802	71916	Aplit granite (M1A)
60	M6	kotanopan	592793	70644	Biotite- hornblende granodiorite
61	M7	Hutadangka, Ms	583775	71717	Granodiorite
62	M7A	hutadangka	583775	71717	Magnetite sand
63	KNP-01	Kotanopan	583684	71652	Granit
64	KNP-02	Kotanopan	581794	71907	Biotite granite
65	KNP-03	Kotanopan	589755	71523	Altered granidiorite
66	KNP-04	Kotanopan	588259	71760	Altered biotite granite
67	KNP-05	Tolung	583280	66768	Altered granite
68	KNP-06	Tolung	582756	65502	Altered biotite granite
69	KNP-07	Tolung	581543	71181	Altered biotite granite
70	KNP-08	Kotanopan	581192	70870	Altered biotite granite
71	KNP-09	Kotanopan	581299	70989	Altered biotite granite
72	PYB-01	Muarasoma	545854	74319	Altered granit
73	PYB-02	Muarasoma	547803	74020	Altered biotite granit
74	PYB-03	Tebing Tinggi	568497	90841	Biotite granite
75	PYB-04A	Tanjung	571474	88408	Granit - pegmatite
76	PYB-04B	Tanjung	571474	88408	Granit - pegmatite
77	PYB-04C	Tanjung	571420	88387	Granit - pegmatite
78	PYB-04D	Tanjung	571420	88387	Granit - pegmatite

79	PYB-04E	Tanjung	571420	88387	Granit - pegmatite
80	PYB-05	Tanjung	573043	87251	Granit - pegmatite
81	PYB-06	Tebing Tinggi	568721	90780	Biotite granite
82	PYB-07	Pintupadang Julu	559619	109515	Biotite granite
83	PYB-08A	Pintupadang Julu	560742	109662	Biotite granite
84	PYB-08B	Pintupadang Julu	560742	109662	Biotite granite
85	PYB-08C	Pintupadang Julu	560742	109662	Biotite granite
86	PYB-08D	Pintupadang Julu	560742	109662	Biotite granite
87	PYB-08E	Pintupadang Julu	560742	109662	Biotite granite
88	PYB-09A	Tano Tombangan	545703	120004	Biotite granite
89	PYB-09B	Tano Tombangan	545703	120004	Biotite granite
90	PYB-10	Aek Nangali	545703	120004	Granodiotite
91	P1	Hutasiantar	545703	120004	Conglomeratic breccia
92	P2	Parmompang-timur	458203	4466142	Biotite granite
93	P3	Parmompang-timur	459839	4465193	Biotite granite
94	P3A	Parmompang-timur	459839	4465193	Biotite granite
95	P3B	Parmompang-timur	459839	4465193	Biotite granite
96	P3C	Parmompang-timur	459839	4465193	Biotite granite
97	P3D	Parmompang-timur	459839	4465193	Biotite granite
98	P3E	Parmompang-timur	459839	4465193	Biotite granite
99	P3F	Parmompang-timur	459839	4465193	Sand
100	P4	Tanjung Jae	459839	4465193	Biotite granite
101	P4A	Tanjung Jae	459839	4465193	Biotite granite
102	P5	Tanjung Jae	573041	573041	Biotite granite
103	P6	Tebing Tinggi	568595	908080	Biotite granite
104	P7/PYB 9	Pintu padang Julu	559767	109709	Altered basaltic-andesite and granite
105	P8/PYB 9	Tano Tombangan	545684	120040	Biotite- hornblende granite
106	P8A/PYB 9	Tano Tombangan	545684	120040	Biotite- hornblende granite
107	P8B/PYB 9	Tano Tombangan	545684	120040	Biotite- hornblende granite
108	P8C/PYB 9	Tano Tombangan	545684	120040	Biotite- hornblende granite
109	P8D/PYB 9	Tano Tombangan	545684	120040	Granite and basalt
110	P8E/PYB 9	Tano Tombangan	545684	120040	Basalt
111	P9	Tano Tombangan	545609	120417	Biotite- hornblende granite
112	P5	Tanjung Jae	545609	120417	Biotite granite
113	P8A	Si Tumba, Tano Tombangan	545609	120417	Biotite granite
114	P8B	Si Tumba, Tano Tombangan	545609	120417	Biotite granite
115	P8C	Si Tumba, Tano Tombangan	545609	120417	Biotite granite
116	P8D	Si Tumba, Tano Tombangan	545609	120417	Biotite granite

Appendix 2

List of weathered rock samples and horizons at Sibolga and its surrounding areas

No	Sample	Parent rock	Location	Horizon	Coordinates	
					N	S
	Sibuluhan Sihaporas A					
1	S1.0	Weathered rock	Sibuluhan sihaporas	A horizon	480693	190117
2	S1.50	Weathered rock	Sibuluhan sihaporas	B horizon	480693	190117
3	S1.100	Weathered rock	Sibuluhan sihaporas	B horizon	480693	190117
4	S1.160	Weathered rock	Sibuluhan sihaporas	B horizon	480693	190117
5	S1.240	Weathered rock	Sibuluhan sihaporas	B horizon	480693	190117
6	S1.310	Weathered rock	Sibuluhan sihaporas	B horizon	480693	190117
7	S1.370	Weathered rock	Sibuluhan sihaporas	B horizon	480693	190117
8	S1.450	Weathered rock	Sibuluhan sihaporas	B horizon	480693	190117
9	S1.500	Weathered rock	Sibuluhan sihaporas	B horizon	480693	190117
10	S1	Biotite granite	Sibuluhan sihaporas	Bedrock	480693	190117
Sibuluhan Sihaporas B						
1	S6 top	Weathered rock	Sibuluhan sihaporas	A horizon	481549	191179
2	S6.0	Weathered rock	Sibuluhan sihaporas	A horizon	481549	191179
3	S6.50	Weathered rock	Sibuluhan sihaporas	A horizon	481549	191179
4	S6.100	Weathered rock	Sibuluhan sihaporas	B horizon	481549	191179
5	S6.150	Weathered rock	Sibuluhan sihaporas	B horizon	481549	191179
6	S6.200	Weathered rock	Sibuluhan sihaporas s	B horizon	481549	191179
7	S6.250	Weathered rock	Sibuluhan sihaporas	B horizon	481549	191179
8	S6.300	Weathered rock	Sibuluhan sihaporas	B horizon	481549	191179
9	S6.350	Weathered rock	Sibuluhan sihaporas	B horizon	481549	191179
10	S6.400	Weathered rock	Sibuluhan sihaporas	B horizon	481549	191179
11	S6.450	Weathered rock	Sibuluhan sihaporas	B horizon	481549	191179
12	S6.500	Weathered rock	Sibuluhan sihaporas	B horizon	481549	191179
13	S6 Bedrock	Weathered rock	Sibuluhan sihaporas	B horizon	481549	191179

	Sarudik					
1	S16.0	Biotite granite	Sarudik	A horizon	479108	191133
2	S16.50	Biotite granite	Sarudik	A horizon	479108	191133
3	S16.100	Biotite granite	Sarudik	B horizon	479108	191133
4	S16.150	Biotite granite	Sarudik	B horizon	479108	191133
5	S16.200	Biotite granite	Sarudik	B horizon	479108	191133
6	S16.250	Biotite granite	Sarudik	B horizon	479108	191133
7	S16.300	Biotite granite	Sarudik	B horizon	479108	191133
8	S16.350	Biotite granite	Sarudik	B horizon	479108	191133
9	S16.400	Biotite granite	Sarudik	B horizon	479108	191133
10	S16.450	Biotite granite	Sarudik	B horizon	479108	191133
11	S16.500	Biotite granite	Sarudik	B horizon	479108	191133
12	S16.550	Biotite granite	Sarudik	B horizon	479108	191133
13	S16.600	Biotite granite	Sarudik	B horizon	479108	191133
14	S16.650	Biotite granite	Sarudik	B horizon	479108	191133
15	S16.700	Biotite granite	Sarudik	B horizon	479108	191133
16	S.16.900	Biotite granite	Sarudik	B horizon	479108	191133
17	S.16.950	Biotite granite	Sarudik	B horizon	479108	191133
18	S.16.1000	Biotite granite	Sarudik	B horizon	479108	191133
19	S.16.1050	Biotite granite	Sarudik	B horizon	479108	191133
20	S.16.1100	Biotite granite	Sarudik	B horizon	479108	191133
21	S.16.1150	Biotite granite	Sarudik	B horizon	479108	191133
22	S.16. Bedrock up	Biotite granite	Sarudik	C horizon	479121	191195
23	S.16.Bedrock down	Biotite granite	Sarudik	C horizon	479121	191195
Parombunan-Sibolga Julu						
2	S17 Top surface	Biotite granite	Sibolga Julu	A horizon	477791	192185
3	S17.40	Biotite granite	Sibolga Julu	B horizon	477791	192185
4	S17.90	Biotite granite	Sibolga Julu	B horizon	477791	192185
5	S17.150	Biotite granite	Sibolga Julu	B horizon	477791	192185
6	S17.200	Biotite granite	Sibolga Julu	B horizon	477791	192185
7	S17.250	Biotite granite	Sibolga Julu	B horizon	477791	192185
8	S17.310	Biotite granite	Sibolga Julu	B horizon	477791	192185
9	S17.360	Biotite granite	Sibolga Julu	B horizon	477791	192185
10	S17.420	Biotite granite	Sibolga Julu	B horizon	477791	192185
11	S17.540	Biotite granite	Sibolga Julu	B horizon	477791	192185
12	S17.580	Biotite granite	Sibolga Julu	B horizon	477791	192185
13	S17.600	Biotite granite	Sibolga Julu	B horizon	477791	192185
14	S17 Bedrock up	Biotite granite	Sibolga Julu	Bed rock	477791	192185
15	S17 Bedrock down	Biotite granite	Sibolga Julu	Bed rock	477791	192185

Appendix 3

Magnetic susceptibility of Sibolga and its surroundings

No	Sample Code	Rock Name	Location	Granite Series	Value x 10^{-3} (SI)									
1	SR-01	Biotite granite	Sarudik	ilmenite-series	0.005	0.01	0.021	0.005	0.006	0.015	0.008	0.012	0.009	
2	SR-02	Biotite granite	Sarudik	ilmenite-series	0.607	0.591	0.584	0.466	0.306	0.63				
3	SB-01	Biotite granite	Adian Koting	ilmenite-series	0.113	0.195	0.099	0.115	0.135	0.087	0.126			
4	SB-02	Biotite granite	Adian Koting	ilmenite-series	0.107	0.106	0.092	0.055						
5	SB-03	Biotite granite	Tarutung	ilmenite-series	0.14	0.121	0.109	0.107	0.121	0.128	0.122	0.128	0.089	0.03
6	S.1 bedrock	Biotite granite	Sarudik	ilmenite-series	0.00	0.01								
7	S.1A	Basaltic/diabasic	Sibuluhan sihaporas	ilmenite-series	0.01	0.01	0.00							
8	S.2	Biotite granite	Sibuluhan	ilmenite-series	0.01	0.01	0.00							
9	S2.A	Altered basaltic rock	Sibuluhan	ilmenite-series	0.00	0.00	0.01							
10	S3	Altered biotite granite	Sibuluhan	ilmenite-series	0.05	0.01	0.00							
11	S4	Biotite granite	Sibuluhan	ilmenite-series	0.01	0.00								
12	S5	Biotite granite	Sibuluhan	ilmenite-series	0.01	0.01	0.01							
13	S5B	Biotite granite	Sibuluhan	ilmenite-series	0.17	0.16								
14	S6 Bedrock	Weathered rock	Sibuluhan sihaporas	ilmenite-series	0.08	0.08	0.04							
15	S7	Biotite granite	Sipan sibuluhan	ilmenite-series	0.00	0.01	0.01							
16	S8	Biotite granite	Tukka	ilmenite-series	0.06	0.05								
17	S9	Biotite granite	Tukka	ilmenite-series	0.10	0.09		0.09						
18	S10B	Biotite granite	Tukka	ilmenite-series	0.11	0.16	0.13							
19	S13	Tuffaceous sandstone	Tukka	-	0.25									
20	S14	Biotite granite	Sarudik	-	0.60	0.53	0.58							
21	S15	Biotite granite	Sarudik	-	0.02	0.01								
22	S18A	Biotite granite	Tarutung-Sibolga	ilmenite-series	0.03	0.01								
23	S18B	Biotite granite	Tarutung-Sibolga	ilmenite-series	0.01	0.06								
24	S19	Biotite granite	Tarutung-Sibolga	ilmenite-series	0.24	0.24	0.24							

25	S20	Biotite granite	Adian	ilmenite-series	0.16	0.14	0.11							
26	S21	Biotite granite	Adian	ilmenite-series	0.11	0.11	0.07							
27	S22	Biotite granite	Parambunan	ilmenite-series	0.70	0.43	0.66	0.43						
28	S23	Biotite granite	Parambunan	ilmenite-series	0.00	0.02	0.01							
29	S24A	Biotite granite	Sihobuk	ilmenite-series	0.09	0.08	0.12	0.07						
30	S24B	Biotite granite	Sihobuk	ilmenite-series	0.14	0.19	0.19							
31	S25	Biotite granite	Sarudik	ilmenite-series	0.07	0.08	0.05	0.06						
32	S26	Quartz sand	Sibuluhan	ilmenite-series	0.11	0.13	0.13	0.13						
33	PYB-01	Altered granite	Muarasoma	ilmenite-series	0.615	0.604	0.597	0.6	0.465	0.591	0.603			
34	PYB-02	Altered biotite granit	Muarasoma	ilmenite-series	7.78	7767.00	7854.00	7128.00	15.08	13.14	8532.00	16.28		
35	PYB-03	Biotite granite	Huta Siantar/T. Tinggi	ilmenite-series	0.058	0.018	0.016	0.014	0.018	0.075	0.081	0.09	0.087	0.085
36	PYB-04A	Granit - Pegmatite	Tanjung	ilmenite-series	0.084	0.084	0.013	0.08	0.017					
37	PYB-04B	Granit - Pegmatite	Tanjung	ilmenite-series	0.054	0.012	0.054	0.01	0.058	0.007	0.006	0.055	0.058	
38	PYB-04C	Granit - Pegmatite	Tanjung	ilmenite-series	0.085	0.061	0.089	0.077	0.068					
39	PYB-04D	Granit - Pegmatite	Tanjung	ilmenite-series	0.183	0.191	0.183	0.18						
40	PYB-04E	Granit - Pegmatite	Tanjung	ilmenite-series	0.088	0.077	0.078	0.08						
41	PYB-05	Granit - Pegmatite	Tanjung Dae	ilmenite-series	0.077	0.079	0.073	0.066	0.071					
42	PYB-06	Biotite granite	Tebing Pintu Air	ilmenite-series	0.015	0.02	0.016	0.016	0.056	0.061	0.063	0.07		
43	PYB-07	Biotite granite	Pintupadang Julu	ilmenite-series	0.01	0.156	0.059	0.013	0.153	0.139	0.083	0.14	0.124	
44	PYB-08A		Pintupadang Julu	ilmenite-series	0.108	0.053	0.017	0.058	0.013					
45	PYB-08B	Hornblende	Pintupadang Julu	ilmenite-series	0.065	0.075	0.088	0.084	0.075	0.099	0.077	0.088		
46	PYB-08C		Pintupadang Julu	ilmenite-series	0.056	0.075	0.075	0.058	0.069	0.063	0.086	0.063	0.082	
47	PYB-08D		Pintupadang Julu	ilmenite-series	0.096	0.094	0.092	0.098	0.041	0.105				
48	PYB-08E		Pintupadang Julu	ilmenite-series	0.01	0.006	0.007	0.012	0.01	0.043				
49	PYB-09A	Biotite granite	Tano Tombangan - Angkola	ilmenite-series	0.447	0.443	0.31	0.468	0.446	0.482				
50	PYB-09B		Tano Tombangan - Angkola	ilmenite-series	0.986	0.621	0.967	0.63	0.454	0.983				
51	PYB-10	Granit granodiotite	Aek Nangali	ilmenite-series	14.2	13.5	13.28	14.27	14.43	14.17	15.15			
52	P2	Biotite granite	Parmompang-timur	Ilmenite	0.02	0.01	0.00	0.02						

53	P3	Biotite granite	Parmompang-	Ilmenite	0.06	0.08	0.07							
54	P3A	Biotite granite	Parmompang-	Ilmenite	0.13	0.11	0.08	0.10						
55	P3B	Biotite granite	Parmompang-	Ilmenite	0.06	0.46	0.07	0.08						
56	P3C	Biotite granite	Parmompang-	Ilmenite	0.07	0.02	0.06							
57	P3D	Biotite granite	Parmompang-	Ilmenite	0.38	0.27	0.31							
58	P3E	Biotite granite	Parmompang-	Ilmenite	0.17	0.14	0.10	0.18						
59	P3F	sand	Parmompang-	Ilmenite	0.19	0.18	0.19							
60	P4	Biotite granite	Tanjung Jae	Ilmenite	0.09	0.06	0.08							
61	P4A	Biotite granite	Tanjung Jae	Ilmenite	0.06	0.06	0.06							
62	P5	Biotite granite	Tanjung Jae	Ilmenite	0.11	0.09	0.09	0.10						
63	P6	Biotite granite	Tebing Tinggi	Ilmenite	0.04	0.06	0.06							
64	P7/PYB 9	Altered basaltic andesite. and granite	Pintu Padang	Ilmenite	0.21	0.16	0.32							
65	P8/PYB 9	Biotite- hb granite	Tano Tombangan	Ilmenite	0.64	0.57	0.87	0.74						
66	P8A/PYB 9	Biotite- hb granite	Tano Tombangan	Ilmenite	0.46	0.47	0.44	0.47						
67	P8B/PYB 9	Biotite- hb granite	Tano Tombangan	Magnetite	7.71	9.66	5.02							
68	P8C/PYB 9	Biotite- hb granite	Tano Tombangan	Magnetite	1.45	1.54	1.61							
69	P8D/PYB 9	Granite and basalt	Tano Tombangan	Ilmenite	0.28	0.25	0.21							
70	P8E/PYB 9	Basalt	Tano Tombangan	Ilmenite	0.68	0.64								
71	P9	Quartz hornblende Biotite - granite	Tano Tombangan	Ilmenite	0.46	0.38	0.34							
72	P5	Biotite granite	Tanjung Jae	Ilmenite	0.07	0.08	0.09							
73	P8A	Biotite granite	Si Tumba. tanotumbangan	Magnetite	22.24	24.38	28.24							
74	P8B	Biotite granite	Si Tumba. tanotumbangan	Ilmenite	0.71	0.69	0.63							
75	P8C	Biotite granite	Si Tumba. tanotumbangan	Ilmenite	1.42	1.98	1.54							
76	P8D	Biotite granite	Si Tumba. tanotumbangan	Magnetite	22.14	20.81	21.08							
77	MS-02	Altered granodiorite	Muarasipongi	Magnetite	25.78	3864.00	25.27	25.17	27.87	28.57	25.97	28.63	28.9	
78	MS-03	Granit-Pegmatite	Muarasipongi	Magnetite	16.72	16.03	14.87	14.33	13.76	15.64	15.79			
79	MS-04	Granodiorite	Muarasipongi	Magnetite	6.843	7.162	8.995	6.67	6.998					

80	MS-05	Granit-Granodiorite	Muarasipongi	Magnetite	15.28	15.18	15.59	15.31	12.92	14.96	16.05	16.1		
81	MS-06	Altered granodiorite	Muarasipongi	Magnetite	9.681	9.874	10.74	9.6	11	6.83	6.606	11.27	11.8	
					13.53	14.15	8.61	10.79						
82	MS-07	Biotite granite	Sungai Cibadak	Magnetite	9.487	9.681	9.252	9.609	9.833	9.821	9.538			
83	MS-08	Altered mikrodiorite	Muarasipongi	Magnetite	1.178	1.253	1.47	1.536	1.622	1.536	1.633	1.579		
84	MS-09	Biotite granite	Tanjung Alai	Magnetite	17.18	15.8	15.77	11.08	17.44	18.22	12.07			
85	MS-10	Biotit granodiorite	Tanjung Alai	Magnetite	6.147	7.749	8.469	5.989	11.53	7.703				
86	MS-11	Altered granodiorite	Muarasipongi	Magnetite	19.6	7.833	3.285	4.03	7.508	12.52	10.72			
87	MS-12	Biotite granite	Muarasipongi	Magnetite	8.377	6.752	5.99	8.305	7.658	7.176				
88	M.1	Biotite granite	Muara Sipongi	Magnetite	7.38	17.59								
89	M.1 A	Altered aplite granite	Muara Sipongi	Magnetite	17.59	7.38	15.41	13.71						
90	M.1	Weathered rock	Muara Sipongi	Magnetite	4.26	4.76	4.95							
91	M.3	Hornblende-biotite granodiorite	Pekantan	Magnetite	24.39	23.92	22.50							
92	M.4	Biotite granite	Muara Sipongi	Magnetite	9.08	11.14	6.18							
93	M.4A	Altered basaltic andesite/diabasic	Muara Sipongi	Magnetite	0.49	1.27	0.67	0.68						
94	M5	Aplite granite (M1A)	Kotanopan	Magnetite	4.55	6.35	4.70							
95	M6	Hornblende-biotite granodiorite	Kotanopan	Magnetite	11.12	12.68	14.03							
96	M7	Granodiorite	Hutadangka. Ms	Magnetite	4.04	5.70	6.28							
97	KNP-01	Granite	Kotanopan	Magnetite	1.072	0.889	0.937	0.668	0.712	1.678	1.467	0.468		
					3.141	2.502	1.942							
98	KNP-02	Biotit granite	Kotanopan	Magnetite	8.612	6.246	9.014	8.716	6.987	7.986				
99	KNP-03	Altered granidiorite	Kotanopan	Magnetite	16.35	17.89	17.89	14.84	17.76	20.69	18.06	18.07		
100	KNP-04	Altered biotite granite	Kotanopan	Magnetite	10.8	10.22	11.62	5.298	20.57	15.64	10.67	10.49		
101	KNP-05	Altered granite	Tolung	Magnetite	0.541	0.99	0.544	0.476	1.259	0.925	0.937			
102	KNP-06	Altered biotite granite	Tolung	Magnetite	0.107	0.332	0.224	0.104	0.171	0.134				
103	KNP-07	Altered biotite	Tolung	Magnetite	13.83	13.14	13.85	9.171	12.38	13.88	11.81			

		granite												
104	KNP-08	Altered biotite granite	Kotanopan	Magnetite	16.55	15.78	15.99	16.61	16.11	15.6	17.17			
105	KNP-09	Altered biotite granite	Kotanopan	Magnetite	12.51	11.25	13	12.25	13.41	20.31	18.75	24.73		

Appendixs 4

Gamma radioactivity of Sibolga and its surroundings

		Rock name	Location	Radioactivity											
1	SR1	Biotite granite	Sarudik	0.093	0.1	0.108	0.115	0.115	0.115	0.115	0.122	0.122	0.122	0.122	0.129
				0.136	0.165										
2	SB3	Biotite granite	Tarutung	0.059	0.066	0.066	0.073	0.073	0.08	0.08	0.08	0.08	0.087	0.087	0.093
				0.093	0.1	0.115	0.122								
3	SB 1	Biotite granite	Adian Koting	0.07	0.08	0.09	0.1	0.1	0.115	0.115	0.122	0.122	0.122	0.122	0.122
				0.136	0.136	0.136	0.143	0.143	0.143	0.151	0.151	0.151	0.158	0.158	0.158
				0.173	0.173	0.18	0.18	0.196	0.129	0.129	0.129	0.158	0.165	0.165	0.129
				0.173											
4	SB 4			0.129	0.129	0.122	0.122	0.122	0.122	0.115	0.115	0.115	0.108	0.108	0.1
				0.073	0.052	0.052	0.046								
5	S.1 BEDROCK	Biotite-muscovite granite	Sibuluhan sihaporas	0.3	0.349	0.374	0.383								
6	S.1A	Basaltic/diabasic	Sibuluhan sihaporas	0.465	0.474										
7	S.2	Biotite muscovite granite	Sibuluhan sihaporas	0.483	0.465	0.502									
8	S2.A	Altered basaltic rock	Sibuluhan sihaporas	0.581	0.612	0.601									
9	S3	Altered biotite muscovite granite	Sibuluhan sihaporas	0.612	0.601	0.581	0.642								
10	S4	Biotite muscovite granite	Sibuluhan sihaporas	0.551	0.502	0.392	0.323								
11	S5	Biotite muscovite granite	Sibuluhan sihaporas	0.465	0.446	0.428	0.446								
12	S5B	Biotite muscovite granite	Sibuluhan sihaporas	0.581	0.501	0.405									
13	S7	Biotite granite	Sipan sibuluhan	0.551	0.541	0.5	0.591								
14	S8	Biotite muscovite granite	Tukka	0.541	0.57	0.551	0.521								
15	S9	Biotite muscovite granite	Tukka	0.392	0.357	0.274	0.34								
16	S10B	Biotite muscovite granite	Tukka	0.165	0.226	0.136									

17	S13	Tuffaceous sandstone		0.541	0.502	0.483	0.512								
18	S14	Biotite muscovite granite	Sarudik	0.57	0.56	0.622	0.638								
19	S15	Biotite muscovite granite	Sarudik	0.707	0.798	0.821									
20	S17 BEDROCK UP	Biotite muscovite granite	Sibolga Julu	0.56	0.465	0.428									
21	S17 BEDROK DOWN	Biotite muscovite granite	Sibolga Julu	0.653	0.612	0.601	0.622	0.642	0.729						
22	S18A	Biotite muscovite granite	Tarutung-Sibolga	0.653	0.674	0.664									
23	S18B	Biotite muscovite granite	Tarutung-Sibolga	0.63	0.607	0.622									
24	S19	Biotite muscovite granite	Tarutung-Sibolga	0.56	0.751	0.798									
25	S20	Biotite muscovite granite	Adian Koting	0.664	0.621	1,042	1,075	0.645							
26	S21	Biotite muscovite granite	Adian Koting	0.541	0.622	0.57									
27	S22	Biotite muscovite granite	Parambunan	0.721	0.85	0.775	0.633								
28	S23	Biotite muscovite granite	Parambunan	0.29	0.315	0.332	0.374								
29	S24A	Biotite muscovite granite	Sihobuk waterfall	0.551	0.541	0.581	0.57								
30	S24B	Biotite muscovite granite	Sihobuk waterfall	0.633	0.612	0.601	0.581								
31	S25	Biotite muscovite granite	Sarudik	0.2741	0.306	0.29	0.266								
32	S26	Quartz sand	Sibuluhan coastal river	0.234	0.211	0.219	0.226								
33	P2	Biotite granite	Parmompang-Ptimur	0.173	0.196	0.185	0.188								
34	P3	Biotite granite	Parmompang-Ptimur	0.185	0.188	0.203	0.211								
35	P3A	Biotite granite	Parmompang-Ptimur	0.282	0.266	0.242	0.25								
36	P3B	Biotite granite	Parmompang-Ptimur	0.306	0.266	0.282	0.274								
37	P3C	Biotite granite	Parmompang-Ptimur	0.29	0.266	0.274	0.258								
38	P3D	Biotite granite	Parmompang-Ptimur	0.219	0.203	0.226	0.25								
39	P3E	Biotite granite	Parmompang-Ptimur	0.188	0.173	0.165	0.18								
40	P3F	Sand	Parmompang-Ptimur	0.18	0.165	0.196	0.15								

41	P4	Biotite granite	Tanjung Jae	0.383	0.366	0.374	0.34								
42	P4A	Biotite granite	Tanjung Jae	0.336	0.299	0.29	0.315	0.323	0.34						
43	PYB-04A	Granit - Pegmatite	Tanjung	0.084	0.084	0.013	0.08	0.017							
44	PYB-04B	Granit - Pegmatite	Tanjung	0.054	0.012	0.054	0.01	0.058	0.007	0.006	0.055	0.058			
45	PYB-04C	Granit - Pegmatite	Tanjung	0.085	0.061	0.089	0.077	0.068							
46	PYB-04D	Granit - Pegmatite	Tanjung	0.183	0.191	0.183	0.18								
47	PYB-04E	Granit - Pegmatite	Tanjung	0.088	0.077	0.078	0.08								
48	PYB-05	Granit - Pegmatite	Tanjung Jae	0.077	0.079	0.073	0.066	0.071							
49	P5	Biotite granite	Tanjung Jae	0.203	0.241	0.196									
50	P5	Biotite granite	Tanjung Jae	0.323	0.34	0.349	0.332								
51	P6	Biotite granite	Tebing Tinggi	0.196	0.226	0.18	0.211	0.258	0.274						
52	PYB-03	Biotite granite	Huta Siantar/T. Tinggi	0.058	0.018	0.016	0.014	0.018	0.075	0.081	0.09	0.087	0.085		
53	PYB-06	Biotite granite	Tebing Pintu Air	0.015	0.02	0.016	0.016	0.056	0.061	0.063	0.07				
54	P7	Altered basaltic andesite+ granite	Pintu padang julu	0.465	0.521	0.428	0.465								
55	PYB-07	Biotite granite	Pintupadang Julu	0.01	0.156	0.059	0.013	0.153	0.139	0.083	0.14	0.124			
56	PYB-08A		Pintupadang Julu	0.108	0.053	0.017	0.058	0.013							
57	PYB-08B	Hornblende	Pintupadang Julu	0.065	0.075	0.088	0.084	0.075	0.099	0.077	0.088				
58	PYB-08C		Pintupadang Julu	0.056	0.075	0.075	0.058	0.069	0.063	0.086	0.063	0.082			
59	PYB-08D		Pintupadang Julu	0.096	0.094	0.092	0.098	0.041	0.105						
60	PYB-08E		Pintupadang Julu	0.01	0.006	0.007	0.012	0.01	0.043						
61	PYB-09A	Biotite granite	Tano Tombangan - Angkola	0.447	0.443	0.31	0.468	0.446	0.482						
62	PYB-09B	Biotite granite	Tano Tombangan - Angkola	0.986	0.621	0.967	0.63	0.454	0.983						
63	P8	Biotite- hb granite	Tano Tombangan	0.29	0.323	0.306									
64	P8A	Biotite- hb granite	Tano Tombangan	0.41	0.383	0.392	0.374								
65	P8B	Biotite- hb granite	Tano Tombangan	0.437	0.446	0.374	0.36								
66	P8C	Biotite- hb granite	Tano Tombangan	0.322	0.282	0.299	0.274								
67	P8D	Granite and basalt	Tano Tombangan	0.323	0.34	0.349	0.357								
68	P8E	Basalt	Tano Tombangan	0.383	0.258	0.165	0.052								
69	P9	Quartz hb- biotite granite	Tano Tombangan	0.392	0.41	0.428	0.349								

70	P8A	Biotite granite	Si Tumba. tanotumbangan	0.323	0.34	0.332									
71	P8B	Biotite granite	Si Tumba. tanotumbangan	0.332	0.306	0.315	0.288								
72	P8C	Biotite granite	Si Tumba. tanotumbangan	0.242	0.234	0.274	0.266								
73	P8D	Biotite granite	Si Tumba. tanotumbangan	0.25	0.234	0.242	0.258	0.29							
74	KNP 2	Biotite granite	Kotanopan	0.087	0.1	0.11	0.115	0.122	0.129	0.129	0.136	0.143	0.151		
75	KNP 3	Altered granidiorite	Kotanopan	0.08	0.087	0.093	0.093	0.1	0.1	0.108	0.108	0.115	0.115		
76	KNP 8	Altered biotite granite	Kotanopan	0.087	0.115	0.122	0.129	0.136	0.143	0.143	0.143	0.143	0.151	0.151	0.165
				0.173											
77	KNP 7	Altered biotite granite	Tolung	0.073	0.073	0.08	0.108	0.122	0.129	0.151	0.155	0.18	0.196		
78	KNP 9	Altered biotite granite	Kotanopan	0.073	0.08	0.08	0.087	0.093	0.093	0.1	0.108	0.108	0.115	0.122	0.122
				0.136											
79	KNP 4	Altered biotite granite	Kotanopan	0.093	0.093	0.1	0.1	0.108	0.108	0.115	0.122	0.129	0.129	0.136	0.136
				0.158	0.143	0.143	0.151	0.151							
80	KNP 1	Biotite granite	Kotanopan	0.052	0.066	0.087	0.093	0.093	0.1	0.108	0.108	0.108	0.115	0.122	0.122
				0.136	0.151	0.151	0.165	0.173	0.18	0.18	0.323	0.428	0.122	0.129	0.136
81	MS1		Muarasipongi	0.087	0.093	0.1	0.115	0.122	0.122	0.129	0.129	0.136			
82	MS 2	Altered granodiorite	Muarasipongi	0.108	0.115	0.115	0.122	0.129	0.129	0.129	0.136	0.143	0.143	0.143	0.143
				0.151	0.165										
83	MS3	Granite-Pegmatite	Muarasipongi	0.1	0.108	0.115	0.115	0.115	0.122	0.122	0.122	0.122	0.129	0.129	0.129
				0.129	0.136										
84	MS4	Granodiorite	Muarasipongi	0.165	0.173	0.173	0.173	0.18	0.188	0.188	0.188	0.188	0.196	0.196	0.203
				0.203	0.211	0.211	0.219	0.226	0.211						
85	MS 5	Granite-Granodiorite	Muarasipongi	0.143	0.143	0.151	0.165	0.173	0.173	0.18	0.18	0.18	0.188	0.188	0.188
				0.211											
86	MS6	Altered granodiorite	Muarasipongi	0.129	0.136	0.143	0.143	0.151	0.151	0.151	0.158	0.158	0.165	0.165	0.173
				0.173	0.18										
87	MS 7	Biotite granite	Sungai Cibadak	0.115	0.122	0.122	0.129	0.136	0.136	0.143	0.143	0.143	0.151	0.151	0.158
				0.158	0.173	0.18									

88	MS10	Biotite granodiorite	Tanjung Alai	0.158	0.158	0.165	0.165	0.173	0.18	0.188	0.188	0.196	0.196	0.196	0.196
				0.203	0.203	0.211									
89	MS 11	Altered granodiorite	Muarasipongi	0.08	0.087	0.093	0.1	0.108	0.122	0.129	0.136	0.143	0.143	0.143	0.151
				0.158											
90	MS12	Biotite granite	Muarasipongi	0.136	0.136	0.151	0.158	0.165	0.165	0.173	0.173	0.18	0.18	0.18	0.188
				0.203											
91	M.1	Biotite granite	Muara Sipongi	0.152	0.228	0.289	0.205								
92	M.1 A	Altered aplite granite	Muara Sipongi	0.158	0.173	0.165									
93	M.1	Weathered rock	Muara Sipongi	0.15	0.158	0.165	0.18								
94	M.3	Hornblende-biotite granodiorite	Pekantan	0.108	0.115	0.1	0.043	0.122	0.115						
95	M.4	Biotite granite	Muara Sipongi	0.115	0.108	0.087	0.093								
96	M.4A	Altered basaltic andesite/diabasic	Muara Sipongi	0.136	0.143	0.173	0.166								
97	M5	Aplite granite (M1A)	Kotanopan	0.158	0.203	0.136	0.211	0.188	0.181						
98	M6	Hornblende-biotite granodiorite	Kotanopan	0.087	0.093	0.108	0.122	0.129	0.136						
99	M7	Granodiorite	Hutadangka. Ms	0.188	0.18	0.203	0.211	0.196	0.226						
100	M7A	Magnetite sand	Hutadangka	0.219	0.226	0.203	0.18	0.188							